

**London South Bank**  
University

**Catalytic conversion of carbon dioxide (CO<sub>2</sub>)  
into value added chemicals**

**By**  
**Rim Saada**

**A Doctoral Thesis submitted in partial fulfilment of  
the requirements for the award of the degree of  
Doctor of Philosophy in Chemical Engineering**

**School of Engineering**  
**September 2015**

*To the loving memory of my precious mother,*

*Huda Zaabouti.*

*Though you passed away, I always remember and cherish  
your unflinching commitment to my education. I miss you  
terribly. I love you mum. Love you always....*

## **ACKNOWLEDGEMENTS**

I owe my deepest gratitude to my supervisor Prof. Saha for his continuous support. He has dedicated his time to support me. I am very grateful for his invaluable input. I really would not be able to do this research without his help. I cannot express enough thanks to Dr. Samuel Larkai for his enormous encouragement and support in various ways throughout my journey at London South Bank. His continued motivation and truly personal guidance helped me to keep going and not to give up. I am indebted to him more than he knows.

I would like to thankfully acknowledge London South Bank University for awarding me a scholarship to complete my PhD. Special thanks goes to Prof. Maidment, your generosity has allowed me to be a step closer to my goal. I express my warm thanks to Dr. Patel for his amazing support, advice and guidance throughout this research work. He has been incredibly supportive and assisted me whenever I needed help. Many thanks and appreciations also go to the staff members at London South Bank University especially to Dr. Kellici for her outstanding support and help with catalyst preparation and characterisation. I would like to thank Mr. Jones who was always available when I required his assistance. A lot of hours were saved thanks to his presence and availability.

The completion of this research would not have been possible without the support of my precious family. I am beholden to my dear father who provided all the moral support and given me the strength to strive in order to achieve all this. My gorgeous sister, Ferial you should know that your support and was more than I can express on paper. My brother, Maxi Mo for all his love and motivation. I would like to thank my adorable son and daughter who were patient and always proud of my achievements and my precious husband, Monir for his support and encouragement. I strongly believe it would have not been an easier task to complete my thesis without his love and moral support. I would like to also express my special gratitude to the best Zohra Chadha and Aaliyah Siddiqui for their ongoing love and motivation. Many thanks to all my friends especially Tan and Sami for their sincere support and prayers throughout my research.

Last but not least, I dedicate this work to my late mother. Your dream was to see me successful in my studies and I hope that today I have fulfilled your dream.

## ABSTRACT

Atmospheric concentrations of carbon dioxide (CO<sub>2</sub>) are significantly increasing since the industrial revolution at an accelerating rate causing environmental impact such as global warming and climate change. Projections indicate that CO<sub>2</sub> concentrations will continue to rise to unsustainable levels. This highlights the scale of the challenge our scientists are facing in order to reduce CO<sub>2</sub> emissions and underpins the importance of promoting green process engineering for the utilisation of CO<sub>2</sub> as a valuable commodity in the process industry. The transformation of CO<sub>2</sub> to value-added chemicals such as organic carbonates provides a promising technological advancement aimed at reducing CO<sub>2</sub> atmospheric concentrations to sustainable levels.

Dimethyl carbonate (DMC) is a promising green compound that exhibits versatile and excellent chemical properties and therefore finds applications as an intermediate in the chemical and pharmaceutical industries. DMC has a high oxygen content and can be used as an oxygenate additive to gasoline to improve its performance and reduce exhaust emission. The conventional method for DMC synthesis involves the utilisation of phosgene as a toxic feedstock. Thus, greener and more sustainable synthetic processes for the synthesis of DMC are required. Recently, non-toxic synthetic routes have been explored; these include, oxidative carbonylation of carbon monoxide (CO), oxygen (O<sub>2</sub>) and MeOH, direct synthesis from MeOH and CO<sub>2</sub> and the transesterification of cyclic carbonates and methanol (MeOH). The oxidative carbonylation route suffers from the use of expensive raw materials and corrosive reagents as well as being hazardous due to the explosive potential of CO. The direct production of DMC from MeOH and CO<sub>2</sub> offers an attractive and green synthetic route for DMC synthesis. Also, the synthesis of DMC *via* the transesterification of cyclic carbonates and MeOH, where cyclic carbonates can be synthesised from their corresponding epoxides and CO<sub>2</sub>, makes the synthesis of DMC *via* transesterification route more environmentally friendly and desirable in terms of green chemistry and sustainable development. Therefore, in this research new greener catalytic processes for DMC synthesis *via* addition of MeOH to CO<sub>2</sub> route and transesterification route have been explored.

In this work, several commercially available heterogeneous catalysts such as ceria and lanthana doped zirconia (Ce–La–Zr–O), ceria doped zirconia (Ce–Zr–O), lanthana doped zirconia (La–Zr–O), lanthanum oxide (La–O) and zirconium oxide (Zr–O) have been extensively assessed for the synthesis of DMC. Strongly coupled graphene based inorganic nanocomposites represent an exciting and new class of functional materials and therefore the utilisation of graphene oxide (GO) as a suitable support for metal oxide catalysts has been explored. Ceria doped zirconia graphene nanocomposites (Ce–Zr/GO) have been synthesised using conventional wet impregnation methods. Samples of Ce–Zr/GO have been subjected to heat treatment at various temperatures (773 K, 873 K, 973 K and 1073 K) in an attempt to enhance their catalytic performance. As-prepared Ce–Zr/GO sample and the corresponding heat treated samples have been assessed for the direct synthesis for DMC from MeOH and CO<sub>2</sub>. Furthermore, a new innovative approach has been employed for synthesising advanced, highly efficient and active heterogeneous catalysts *via* utilisation of a continuous hydrothermal flow synthesis (CHFS) reactor. Tin doped zirconium oxide (Zr–Sn–O) and tin doped zirconia/graphene nanocomposite (Zr–Sn/GO) have been assessed as suitable heterogeneous catalysts for the synthesis of DMC *via* the transesterification route. The catalysts were characterised using various analytical techniques such as scanning electron microscopy (SEM), transmission electron microscopy (TEM), powder X-ray diffraction (XRD), X-ray photoelectron spectroscopy (XPS), Raman spectroscopy and Brunauer-Emmett-Teller (BET) surface area measurement.

A heterogeneous catalytic process for the synthesis of DMC has been investigated using a high pressure reactor. The effect of various reaction parameters such as the reactant molar ratio, catalyst loading, reaction temperature, CO<sub>2</sub> pressure, reaction time and the use of a dehydrating agent was studied for the optimisation of DMC synthesis. Reusability studies were conducted to evaluate the long term stability of the heterogeneous catalysts by recycling and reusing the catalyst several times for the synthesis of DMC. Tin doped zirconia graphene oxide (Sn–Zr/GO) nanocomposite catalyst has been found to be the best performed catalyst for the synthesis of DMC as compared to other catalysts evaluated in this research work. This can be attributed to the phase composition and crystallinity of the catalyst along with the defects on the

graphene sheet such as, holes, acid/basic groups and presence of residual which can provide additional active catalytic sites. Catalyst reusability studies evidently showed that Sn–Zr/GO nanocomposite can be easily recovered and reused without any significant reduction in the catalytic performance.

Response Surface Methodology (RSM) has track record in helping researchers in modeling and optimisation of the experimental design for various applications in food industry, catalysis and chemical reaction engineering. Therefore, it has been employed to evaluate the relationship between multiple process variables in order to optimise a specified response (i.e. yield of DMC). RSM using Box-Behnken design (BBD) was carried out for process modeling and optimisation, with an aim to better understand the relationship between five operating variables (i.e. MeOH:PC molar ratio, catalyst loading (w/w), reaction temperature, reaction time and stirring speed) and their impact on the yield of DMC. A model for the synthesis of DMC by transesterification of PC and MeOH has been developed using BBD to compare the experimental data and the predicted results by the BBD model. Furthermore, regression analysis was applied to establish the optimum reaction conditions for a maximising DMC synthesis. The BBD model predicted values are in good agreement with the experimental results.

Keywords: Carbon dioxide (CO<sub>2</sub>) utilisation, dimethyl carbonate (DMC), methanol (MeOH), propylene carbonate (PC), heterogeneous catalysts, tin doped zirconia graphene oxide (Sn–Zr/GO), ceria-zirconia oxide/graphene (Ce–Zr/GO) nanocomposite, ceria and lanthana doped zirconia (Ce–La–Zr–O), continuous hydrothermal flow synthesis (CHFS) reactor, supercritical CO<sub>2</sub> (scCO<sub>2</sub>).

### *List of Abbreviations*

$\text{Al}_2\text{O}_3$	Aluminium oxide
$\text{AlCl}_3$	Aluminium chloride
$\text{AlI}_3$	Aluminium iodide
$\text{AlO}_4$	Tetrahedra of alumina
$\text{AlO}_4$	Alumina
ANOVA	Analysis of variance
BBD	Box-Behnken design
BET	Brunauer-Emmett-Teller
CaO	Calcium oxide
$\text{Ce}(\text{NO}_3)_3 \cdot 6\text{H}_2\text{O}$	Cerium(III) nitrate hexahydrate
Ce–La–Zr–O	Ceria and lanthana doped zirconia
$\text{CeO}_2$	Cerium oxide
Ce–Zr	Ceria-zirconia
Ce–Zr/GO	Ceria doped zirconia graphene nanocomposites
Ce–Zr–O	Ceria doped zirconia
$\text{CH}_2\text{Cl}_2$	Dichloromethane
$(\text{CH}_3)_4\text{NOH}$	Tetramethylazanium hydroxide
$\text{CH}_2\text{O}$	Formaldehyde
$\text{CH}_3\text{I}$	Methyl iodide
$\text{CH}_3\text{OH}$	Methanol
$\text{CH}_3\text{OK}$	Potassium methoxide
$\text{CH}_3\text{ONa}$	Sodium methoxide
CHC	Cyclohexene carbonate
CHFS	Continuous hydrothermal flow synthesis
CM	Ceria-zirconia oxide/graphene nanocomposite synthesised using conventional method
CM500	CM catalyst heat treated at 773 K
CM700	CM catalyst heat treated at 973 K
CM900	CM catalyst heat treated at 1173 K
CO	Carbon monoxide
$\text{CO}_2$	Carbon dioxide
$\text{COCl}_2$	Phosgene
Cs–P–Si oxide	Caesium–phosphorous–silicon mixed oxide
$\text{CuCl}_2$	Copper chloride

Cu-Ni	Copper-nickel
DEC	Diethyl carbonate
DMAP	4-dimethylaminopyridine
DMC	Dimethyl carbonate
DME	Dimethyl ether
DMF	<i>N,N</i> -dimethylformamide
Et <sub>4</sub> NBr	ethyl-ammonium bromide
Fe <sub>2</sub> O <sub>3</sub>	Iron oxide
FID	Flame ionisation detector
GC	Gas chromatography
GEP	General Electric Plastics
GO	Graphene oxide
Gt/y	Gigatonne per year
H <sub>2</sub>	Hydrogen
H <sub>2</sub> O	Water
H <sub>2</sub> O <sub>2</sub>	Hydrogen peroxide
H <sub>2</sub> SO <sub>4</sub>	Sulphuric acid
H <sub>3</sub> PMo <sub>12</sub> O <sub>40</sub> /ZrO <sub>2</sub>	Heteropoly acid on zirconium oxide
H <sub>3</sub> PO <sub>4</sub>	Phosphoric acid
H <sub>3</sub> PW <sub>12</sub> O <sub>40</sub>	Tungstophosphoric heteropoly acid
HCl	Hydrochloric acid
HEPrIMBr	3-(2-hydroxyl-ethyl)-1-propylimidazolium bromide
HEPrIMBr	3-(2-hydroxyl-ethyl)-1-propylimidazolium bromide
HPLC	High performance liquid chromatography
HTR	Ceria-zirconia oxide/graphene nanocomposite synthesised using CHFS reactor
HTR500	HTR catalyst heat treated at 773 K
HTR600	HTR catalyst heat treated at 873 K
HTR700	HTR catalyst heat treated at 973 K
IPA	<i>isopropyl</i> alcohol
ITQ-2	Type of zeolite
K <sub>2</sub> CO <sub>3</sub>	Potassium carbonate
K <sub>2</sub> CO <sub>3</sub>	Calcium carbonate
K <sub>3</sub> PO <sub>4</sub>	<i>tripotassium</i> phosphate

KMnO <sub>4</sub>	Potassium permanganate
KOH	Potassium hydroxide
La <sub>2</sub> O <sub>3</sub>	Lanthanum oxide
La–O	Lanthanum oxide
La–Zr–O	Lanthana doped zirconia
MCM-41	Molecular sieve
MCR	Membrane catalytic reactors
Me <sub>4</sub> NBr	<i>Tetra</i> -methyl-ammonium bromide
(MeO) <sub>2</sub> ClSi(CH <sub>2</sub> ) <sub>3</sub> S	Organotin compound
nCl <sub>3</sub>	
MeOH	Methanol
Mg	Magnesium oxide
Mg-Al oxide	Magnesium- aluminium mixed oxide
MgO	Magnesium oxide
MoO <sub>3</sub>	Molybdenum trioxide
Mt	Mega tonne
Mt/y	Megatonne per year
MTBD	7 methyl-1,5,7-triazabicyclo[4.4.0]dec-5-ene
NaNO <sub>3</sub>	Sodium nitrate
Nb	Niobium
Nb <sub>2</sub> O <sub>5</sub>	Niobium pentoxide
<i>n</i> -Bu <sub>4</sub> NBr	<i>Tetra-n</i> -butyl ammonium bromide
<i>n</i> -Bu <sub>4</sub> NBr	Butyl-ammonium bromide
NGP	Natural graphite powder
NiCl <sub>2</sub>	Nickel chloride
<i>n</i> -Pr <sub>4</sub> NBr	propyl-ammonium bromide
O <sub>2</sub>	Oxygen
OFAT	One-factor at a time analysis
OH	Hydroxide ion
P <sub>2</sub> O <sub>5</sub>	Phosphorous pentoxide
P <sub>2</sub> O <sub>5</sub>	Phosphorus pentoxide
PC	Propylene carbonate
PO	Propylene oxide
ppm	Parts per million
ppmv	Parts per million by volume

PVC	Polyvinyl chloride
Rh	Rhodium
RS	Raman spectroscopy
RSM	Response Surface Methodology
SBA-15	Mesoporous silica
SC	Styrene carbonate
scCO <sub>2</sub>	Supercritical CO <sub>2</sub>
SEM	Scanning electron microscopy
SiO <sub>2</sub>	Silica
SiO <sub>4</sub>	silica
SmOCl	Samarium oxychloride
SnC <sub>2</sub> O <sub>4</sub>	Tin (II) oxalate
SnO <sub>2</sub>	Tin oxide
SO	Styrene oxide
TBAB	Tetra- <i>n</i> -butyl ammonium bromide
TBD	1,5,7-triazabicyclo[4.4.0]dec-5-ene
TEM	Transmission electron microscopy
TiO <sub>2</sub>	Titanium oxide
TMM	1,1,1, trimethoxymethane
UV	Ultraviolet
V <sub>2</sub> O <sub>5</sub>	Vanadium oxide
XPS	X-ray photoelectron spectroscopy
XRD	Powder X-ray diffraction
Zn	Zinc
ZnCl <sub>2</sub>	Zinc chloride
ZnO	Zinc oxide
ZnO-SiO <sub>2</sub>	Zinc oxide particles loaded on silica
Zn-Si	Zinc-silicon oxide
Zr-O	Zirconium oxide
ZrO(NO <sub>3</sub> ) <sub>2</sub> .6H <sub>2</sub> O	Zirconium (IV) oxynitrate hydrate
ZrO <sub>2</sub>	Zirconium oxide
Zr-Sn/GO	Tin doped zirconia/ graphene nanocomposite
Zr-Sn-O	Tin doped zirconium oxide
ZSM-5	Zeolite International

*List of Nomenclature*

$A_i$	Area for the $i^{\text{th}}$ component
$A_{is}$	Area of internal standard
AR	Area ratio
$C_i$	Concentration of the $i^{\text{th}}$ component
$C_{is}$	Concentration of the internal standard
CR	Concentration ratio
RF	Response factor

## TABLE OF CONTENTS

<b>ACKNOWLEDGEMENTS</b> .....	<b>II</b>
<b>ABSTRACT</b> .....	<b>III</b>
<b>LIST OF FIGURES</b> .....	<b>XIV</b>
<b>LIST OF TABLES</b> .....	<b>XXI</b>
<b>CHAPTER 1</b> .....	<b>1</b>
<b>1. INTRODUCTION</b> .....	<b>2</b>
1.1. Motivation .....	2
1.1.1. Sources of CO <sub>2</sub> .....	3
1.2. Sources of Carbon Dioxide and Environmental Impact .....	4
1.2.1. Atmospheric Concentrations of CO <sub>2</sub> and Global Warming .....	4
1.2.2. Controlling CO <sub>2</sub> Levels .....	5
1.3. CO <sub>2</sub> Conversion and Utilisation .....	6
1.3.1. Potential for CO <sub>2</sub> Utilisation .....	6
1.3.2. Barriers and Challenges for CO <sub>2</sub> Utilisation .....	7
1.3.3. Research Strategies for CO <sub>2</sub> Utilisation .....	8
1.3.3.1. Development of new processes .....	9
1.3.3.2. Replacement of hazardous chemicals .....	9
1.4. Sustainability .....	10
1.5. Research Aims and Objectives .....	11
1.6. Structure of Thesis .....	13
<b>CHAPTER 2</b> .....	<b>16</b>
<b>2. LITERATURE REVIEW</b> .....	<b>17</b>
2.1. Introduction .....	17
2.2. What is Carbon Dioxide? .....	17
2.2.1. Properties of Carbon Dioxide .....	17
2.2.2. Reactivity of CO <sub>2</sub> .....	19
2.3. Transformation of Carbon Dioxide (CO <sub>2</sub> ) .....	20
2.3.1. Industrial Applications of CO <sub>2</sub> .....	20
2.3.2. Industrial Syntheses from CO <sub>2</sub> .....	20
2.3.2.1. Conversion to fuel .....	21
2.3.2.2. Conversion to urea .....	22

2.3.2.3. Conversion to carboxylic acid .....	23
2.3.2.4. Conversion to organic carbonates .....	23
2.4. Synthesis of Cyclic Carbonates .....	24
2.4.1. Cycloaddition of CO <sub>2</sub> to Epoxides .....	24
2.4.2. Metal Oxide Catalysts .....	25
2.4.3. Zeolite and Smectite Catalysts .....	27
2.4.4. Supported Catalysts.....	29
2.4.4.1. Supported organic base catalysts.....	29
2.4.4.2. Supported organometallic complexes catalysts.....	31
2.4.4.3. Supported ionic liquid catalysts .....	32
2.4.5. Other Heterogeneous Catalysts.....	34
2.5. Dimethyl Carbonate (DMC) .....	34
2.5.1. Properties of Dimethyl Carbonate (DMC) .....	34
2.5.2. Industrial Applications of Dimethyl Carbonate .....	35
2.5.2.1. Intermediate for polycarbonate synthesis .....	35
2.5.2.2. DMC as a methylating agent .....	36
2.5.2.3. DMC for the production of carbamates and isocyanates.....	37
2.5.2.4. DMC as a solvent .....	37
2.5.2.5. DMC as a fuel additive.....	37
2.6. Synthesis Routes of DMC .....	38
2.6.1. Methanolysis of Phosgene (COCl <sub>2</sub> ) .....	38
2.6.2. Oxidative Carbonylation.....	38
2.6.3. Transesterification of Carbonates or Urea .....	39
2.6.4. Direct Transformation of CO <sub>2</sub> to DMC.....	41
2.6.4.1. Direct synthesis of DMC from methanol and CO <sub>2</sub> .....	41
2.6.4.2. Synthesis of DMC from epoxides and CO <sub>2</sub> .....	42
2.6.4.3. Synthesis of DMC from acetals and CO <sub>2</sub> .....	43
2.7. Catalysts used for DMC Synthesis .....	43
2.7.1. Catalytic Processes for DMC Synthesis .....	43
2.7.2. Homogeneous Catalysts.....	44
2.7.2.1. Organic metal compound catalysts.....	45
2.7.2.2. Base catalysts.....	46
2.7.2.3. Acetate catalysts.....	46
2.7.2.4. Reaction mechanism for homogeneous catalytic process.....	47
2.7.3. Heterogeneous Catalysts.....	48

2.7.3.1. Single metal oxide catalyst .....	48
2.7.3.2. Modified metal oxide catalysts .....	50
2.7.3.3. Heteropoly acid catalysts .....	52
2.7.3.4. Supported catalysts .....	53
2.7.3.5. Photocatalyst .....	56
2.7.4. Dehydrating Agents .....	56
2.7.5. Novel Techniques .....	57
2.8. Conclusions .....	58
<b>CHAPTER 3 .....</b>	<b>60</b>
<b>3. DIRECT SYNTHESIS OF DMC USING COMMERCIALY AVAILABLE CATALYSTS .....</b>	<b>61</b>
3.1. Intoduction .....	61
3.2. Experimental Method.....	63
3.2.1. Materials .....	63
3.2.2. Addition Reaction of MeOH to CO <sub>2</sub> .....	63
3.2.3. Method of Analysis.....	66
3.2.3.1. Internal standardisation .....	67
3.2.3.2. Calibration method.....	68
3.2.3.3. Chromatogram and calibration curves .....	69
3.2.3.4. Determination of MeOH conversion and DMC yield .....	72
3.2.4. Catalyst Characterisation Techniques .....	73
3.3. Results and Discussion .....	73
3.3.1. Catalyst Characterisation.....	73
3.3.2. Reaction Mechanism .....	82
3.3.3. Effect of Different Catalysts .....	85
3.3.4. Effect of Catalyst Loading .....	86
3.3.5. Effect of Reaction Temperature .....	87
3.3.6. Effect of CO <sub>2</sub> Pressure.....	89
3.3.7. Effect of Reaction Time.....	91
3.3.8. Effect of Mass Transfer in Heterogeneous Catalytic Process.....	92
3.3.9. Catalyst Reusability Studies .....	93
3.4. Conclusions .....	94
<b>CHAPTER 4 .....</b>	<b>96</b>

<b>4. DIRECT SYNTHESIS OF DMC FROM CO<sub>2</sub> AND MEOH USING METAL OXIDE/ GRAPHENE NANOCOMPOSITE CATALYSTS .....</b>	<b>97</b>
4.1. Introduction.....	97
4.2. Experimental Method.....	100
4.2.1. Materials .....	100
4.2.2. Catalyst Preparation .....	101
4.2.2.1. Preparation of graphene oxide .....	101
4.2.2.2. Ceria-zirconia oxide/graphene nanocomposite synthesis <i>via</i> conventional method.....	103
4.2.2.3. Ceria-zirconia oxide/graphene nanocomposite synthesis <i>via</i> CHFS route .....	104
4.2.2.4. Ceria-zirconia oxide/graphene nanocomposite heat- treatment	105
4.2.3. Addition Reaction of Methanol and CO <sub>2</sub> .....	106
4.2.4. Catalyst Characterisation Techniques .....	107
4.2.5. Method of Analysis.....	108
4.3. Results and Discussion .....	108
4.3.1. Catalyst Characterisation.....	108
4.3.2. Batch Studies.....	119
4.3.2.1. Effect of different catalysts.....	119
4.3.2.2. Effect of catalyst loading .....	121
4.3.2.3. Effect of reaction temperature .....	122
4.3.2.4. Effect of CO <sub>2</sub> pressure .....	124
4.3.2.5. Effect of reaction time .....	125
4.3.2.6. Effect of dehydrating agent.....	127
4.3.2.7. Effect of mass transfer in heterogeneous catalytic process .....	128
4.3.2.8. Reusability studies .....	130
4.4. Conclusions .....	131
<b>CHAPTER 5 .....</b>	<b>133</b>
<b>5. TRANSESTERIFICATION OF PROPYLENE CARBONATE (PC) USING COMMERCIALY AVAILABLE CATALYSTS .....</b>	<b>134</b>
5.1. Introduction.....	134
5.2. Experimental Method.....	135
5.2.1. Materials .....	135
5.2.2. Catalytic Reactions .....	135

5.2.3. Method of Analysis.....	136
5.2.4. Catalyst Characterisation.....	138
5.3. Results and Discussion .....	139
5.3.1. Reaction Mechanism .....	139
5.3.2. Effect of Different Catalysts .....	142
5.3.3. Effect of Reactant Molar Ratio .....	143
5.3.4. Effect of Catalyst Loading .....	145
5.3.5. Effect of Reaction Temperature .....	146
5.3.6. Effect of Reaction Time.....	148
5.3.7. Effect of Mass Transfer in Heterogeneous Catalytic Process.....	149
5.3.8. Catalyst Reusability .....	151
5.4. Conclusions .....	152
<b>CHAPTER 6 .....</b>	<b>154</b>
<b>6. TRANSESTERIFICATION OF PC WITH MEOH USING METAL OXIDE/GRAPHENE NANOCOMPOSITE CATALYSTS .....</b>	<b>155</b>
6.1. Introduction.....	155
6.2. Experimental Method.....	157
6.2.1. Materials .....	157
6.2.2. Catalyst Preparation .....	157
6.2.3. Tin Doped Zirconia Graphene Nanocomposite Heat-Treatment ....	159
6.2.4. Catalyst Characterisation Techniques .....	160
6.2.5. Transesterification of Propylene Carbonate with MeOH.....	161
6.2.6. Method of Analysis for Transesterification Reactions .....	162
6.2.7. One-Factor-at-a-Time Analysis (OFAT).....	162
6.2.8. Experimental Design.....	163
6.2.9. Statistical Analysis .....	165
6.3. Results and Discussion .....	166
6.3.1. Catalyst Characterisation.....	166
6.3.2. Model Development.....	174
6.3.3. Statistical Analysis .....	175
6.3.4. Model Validation .....	178
6.3.5. Batch Experimental Results.....	178
6.3.5.1. Effect of different catalysts.....	179
6.3.5.2. Effect of reactant molar ratio.....	180

6.3.5.3. Effect of catalyst loading .....	182
6.3.5.4. Effect of reaction temperature .....	183
6.3.5.5. Effect of reaction time .....	185
6.3.5.6. Effect of mass transfer in heterogeneous catalytic process .....	186
6.3.5.7. Catalyst reusability studies .....	188
6.3.6. Optimisation of DMC synthesis.....	189
6.4. Conclusions .....	193
<b>CHAPTER 7 .....</b>	<b>195</b>
<b>7. CONCLUSIONS AND RECOMMENDATIONS FOR FUTURE WORKS.....</b>	<b>196</b>
7.1. Conclusions .....	196
7.2. Recommendation for Future Work .....	197
7.2.1. Development of New Innovative Catalysts with Higher Catalytic Performance .....	197
7.2.2. Extensive Catalyst Characterisation .....	198
7.2.3. Utilisation of Waste CO <sub>2</sub> for the Synthesis of DMC .....	198
7.2.4. Investigating Different Routes for the Synthesis of DMC.....	199
7.2.5. Syntheses of Other Organic Carbonates .....	199
7.2.6. Continuous Flow Synthesis of DMC .....	199
7.2.7. Aspen HYSYS Simulation.....	199
7.2.8. Economic Feasibility Study of the Current Process .....	200
<b>CHAPTER 8 .....</b>	<b>201</b>
<b>8. REFERENCES .....</b>	<b>202</b>
<b>CHAPTER 9 .....</b>	<b>245</b>
<b>9. APPENDIX .....</b>	<b>246</b>
9.1. Research Publications.....	246
9.1.1. Journal Papers.....	246
9.1.2. Conference Papers .....	246
9.2. News and Awards.....	247
9.3. Risk Assessment .....	247
9.4. Training Sessions .....	247
9.4.1. Postgraduate Certificate in Research Skills Key Skills Development Programme Training .....	247
9.4.2. Additional Training Sessions.....	248

## List of Figures

Figure 1.1. Methods for CO <sub>2</sub> management. ....	5
Figure 1.2. Potential applications of CO <sub>2</sub> .....	7
Figure 2.1. Methanolysis of phosgene. ....	38
Figure 2.2. Oxidative carbonylation of MeOH. ....	39
Figure 2.3. Direct synthesis of DMC via the carboxylation of methanol. ....	42
Figure 2.4. Two-step process for DMC production utilising CO <sub>2</sub> as a raw material. .....	43
Figure 2.5. Mechanism for the synthesis of DMC over methoxy magnesium catalyst (Cao <i>et al.</i> , 2012). ....	47
Figure 2.6. Synthesis of DMC in the presence of an alkali catalyst (Fang <i>et al.</i> , 1996). ....	48
Figure 2.7. Possible reaction mechanism for the synthesis of DMC over ZrO <sub>2</sub> catalyst as proposed by Jung and Bell (2001). ....	49
Figure 3.1. Schematic representation of the experimental set-up for DMC synthesis using a high pressure reactor. Key: CC, CO <sub>2</sub> cylinder; SCFP, supercritical fluid pump; GIV, gas inlet valve; SV, sampling valve; PG, pressure gauge; SM, stirring motor; TC, thermocouple; GOV, gas outlet valve; R, reactor; RC, reactor controller. ....	64
Figure 3.2. Batch experimental set-up for DMC synthesis. ....	65
Figure 3.3. A Shimadzu gas chromatography (GC–2014) used for analysis of experimental samples. ....	66
Figure 3.4. A typical chromatogram from Shimazu-2014 gas chromatograph (GC).....	70
Figure 3.5. Calibration curve for response factor determination of MeOH using IPA as an internal standard. ....	71
Figure 3.6. Calibration curve for response factor determination of DMC using IPA as an internal standard. ....	72
Figure 3.7. Photographic images of commercially available catalysts used in this work .....	74
Figure 3.8. Scanning electron microscopy (SEM) image of ceria and lanthana doped zirconia (Ce–La–Zr–O) catalyst.....	76
Figure 3.9. Scanning electron microscopy (SEM) image of ceria doped zirconia (Ce–Zr–O) catalyst. ....	77

Figure 3.10. Scanning electron microscopy (SEM) image of lanthanum oxide (La–O) catalyst. ....	78
Figure 3.11. Scanning electron microscopy (SEM) image of lanthana doped zirconia (La–Zr–O) catalyst. ....	78
Figure 3.12. Scanning electron microscopy (SEM) image of zirconium oxide (Zr–O) catalyst. ....	79
Figure 3.13. Raman spectra of ceria and lanthana doped zirconia (Ce–La–Zr–O), ceria doped zirconia (Ce–Zr–O), lanthanum oxide (La–O), lanthana doped zirconia (La–Zr–O) and zirconium oxide (Zr–O) catalysts. ....	80
Figure 3.14. X-ray diffraction (XRD) patterns of ceria and lanthana doped zirconia (Ce–La–Zr–O), ceria doped zirconia (Ce–Zr–O), lanthanum oxide (La–O), lanthana doped zirconia (La–Zr–O) and zirconium oxide (Zr–O) catalysts. ....	81
Figure 3.15. Reaction scheme for the synthesis of DMC from MeOH and CO <sub>2</sub> . .	82
Figure 3.16. Proposed reaction mechanism for the synthesis of DMC from MeOH and CO <sub>2</sub> . ....	84
Figure 3.17. Effect of different heterogeneous catalysts on the direct synthesis of DMC. Experimental conditions: catalyst loading, 15% (w/w); reaction temperature, 393 K; CO <sub>2</sub> pressure, 290 bar; reaction time, 20 h and stirring speed, 300 rpm. ....	85
Figure 3.18. Effect of catalyst loading on MeOH conversion and yield of DMC. Experimental conditions: catalyst, Ce–Zr–O; reaction temperature, 393 K; CO <sub>2</sub> pressure, 290 bar; reaction time, 20 h and stirring speed 300 rpm. ....	87
Figure 3.19. Effect of reaction temperature on MeOH conversion and yield of DMC. Experimental conditions: catalyst, Ce–Zr–O; catalyst loading, 15% (w/w); CO <sub>2</sub> pressure, 290 bar; reaction time, 20 h and stirring speed, 300 rpm. ....	88
Figure 3.20. Effect of CO <sub>2</sub> pressure on MeOH conversion and yield of DMC. Experimental conditions: catalyst, Ce–Zr–O; catalyst loading, 15% (w/w); reaction temperature, 393 K; reaction time, 20 h and stirring speed, 300 rpm. ....	90
Figure 3.21. Effect of reaction time on MeOH conversion and yield of DMC. Experimental conditions: catalyst, Ce–Zr–O; catalyst loading, 15% (w/w); reaction temperature, 393 K; CO <sub>2</sub> pressure, 290 bar and stirring speed 300 rpm. ....	91
Figure 3.22. Effect of stirring speed on MeOH conversion and yield of DMC. Experimental conditions: catalyst, Ce–Zr–O; catalyst loading, 15% (w/w); reaction temperature, 393 K; CO <sub>2</sub> pressure, 290 bar and reaction time, 20 h. ....	93

Figure 3.23. Catalyst reusability studies for synthesis of DMC. Experimental conditions: catalyst, Ce–Zr–O; catalyst loading, 15% (w/w); reaction temperature, 393 K; CO<sub>2</sub> pressure, 290 bar; reaction time, 20 h and stirring speed, 300 rpm. 94

Figure 4.1. Experimental set-up for the preparation of graphene oxide (GO)... 102

Figure 4.2. A schematic representation of graphite powder transformation to graphene oxide (GO)..... 102

Figure 4.3. A schematic representation of the synthesised Ce–Zr/GO nanocomposite catalyst..... 103

Figure 4.4. A schematic of a CHFS reactor set up used for the synthesis of Ce–Zr/GO nanocomposite catalyst..... 105

Figure 4.5. Photographic images of Ce–Zr/GO nanocomposite samples: (a) as-prepared sample synthesised using CHFS route labelled as HTR and (b) the corresponding heat-treated (973 K) sample labelled as HTR700; (c) sample CM synthesised *via* wet impregnation route and (d) the corresponding heat treated (973 K) sample labelled as CM700. .... 106

Figure 4.6. Transmission Electron Microscopy (TEM) image of Ce–Zr/GO nanocomposite as-prepared sample synthesised using CHFS route labelled as HTR. .... 109

Figure 4.7. Transmission Electron Microscopy (TEM) image of Ce–Zr/GO nanocomposite heat-treated (973 K) sample labelled as HTR700..... 110

Figure 4.8. Transmission Electron Microscopy (TEM) image of Ce–Zr/GO nanocomposite sample synthesised *via* wet impregnation route labelled as CM. .... 111

Figure 4.9. Transmission Electron Microscopy (TEM) image of Ce–Zr/GO nanocomposite sample synthesised *via* wet impregnation route, heat-treated (973 K) and labelled as CM700. .... 112

Figure 4.10. X-ray powder diffraction (XRD) patterns of different ceria–zirconia oxide/graphene nanocomposites. .... 114

Figure 4.11. X-ray photoelectron spectroscopy (XPS) spectra showing the deconvoluted C(1s) region of Ce–Zr/GO samples synthesised *via* continuous hydrothermal flow reactor and conventional wet impregnation route. .... 116

Figure 4.12. X-ray photoelectron spectroscopy (XPS) spectra showing the Ce(3d) region of Ce–Zr/GO samples synthesised *via* continuous hydrothermal flow reactor and conventional wet impregnation route. .... 117

Figure 4.13. X-ray photoelectron spectroscopy (XPS) spectra showing the Zr (3d) region for of Ce–Zr/GO samples synthesised *via* continuous hydrothermal flow reactor and conventional wet impregnation route. .... 118

Figure 4.14. Effect of different Ce–Zr/GO nanocomposite catalysts on the direct synthesis of DMC. Experimental conditions: catalyst Loading, 10% (w/w); reaction temperature, 383 K; CO<sub>2</sub> pressure, 275 bar; reaction time, 16 h; TMM:MeOH ratio, 1:1 (w/w) and stirring speed, 300 rpm. .... 120

Figure 4.15. Effect of catalyst loading on MeOH conversion and yield of DMC. Experimental conditions: catalyst, Ce–Zr/GO - HTR700; reaction temperature, 383 K; CO<sub>2</sub> pressure, 275 bar; reaction time, 16 h; TMM: MeOH ratio, 1:1 (w/w) and stirring speed, 300 rpm..... 122

Figure 4.16. Effect of reaction temperature on MeOH conversion and yield of DMC. Experimental conditions: catalyst, Ce–Zr/GO - HTR700; catalyst Loading 10% (w/w); CO<sub>2</sub> pressure, 275 bar; reaction time, 16 h; TMM:MeOH ratio, 1:1 (w/w) and stirring speed, 300 rpm. .... 123

Figure 4.17. Effect of CO<sub>2</sub> pressure on MeOH conversion and yield of DMC. Experimental conditions: catalyst, Ce–Zr/GO - HTR700; catalyst Loading 10% (w/w); reaction temperature, 383 K; reaction time, 16 h; TMM:MeOH ratio, 1:1 (w/w) and stirring speed, 300 rpm. .... 125

Figure 4.18. Effect of reaction time on MeOH conversion and yield of DMC. Experimental conditions: catalyst, Ce–Zr/GO - HTR700; catalyst Loading 10% (w/w); reaction temperature, 383 K; CO<sub>2</sub> pressure, 275 bar; TMM:MeOH ratio, 1:1 (w/w) and stirring speed, 300 rpm. .... 126

Figure 4.19. Effect of TMM: MeOH (w/w) on MeOH conversion and yield of DMC. Experimental conditions: catalyst, Ce–Zr/GO - HTR700; catalyst Loading 10% (w/w); reaction temperature, 383 K; CO<sub>2</sub> pressure, 275 bar; time, 16 h and stirring speed, 300 rpm. .... 128

Figure 4.20. Effect of stirring speed on MeOH conversion and yield of DMC. Experimental conditions: catalyst, Ce–Zr/GO - HTR700; catalyst Loading 10% (w/w); reaction temperature, 383 K; CO<sub>2</sub> pressure, 275 bar; time, 16 h and TMM:MeOH, 1:1 (w/w). .... 129

Figure 4.21. Catalyst reusability for synthesis of DMC. Experimental conditions: catalyst, Ce–Zr/GO - HTR700; catalyst loading 10% (w/w); reaction temperature, 383 K; CO<sub>2</sub> pressure, 275 bar; time, 16 h; TMM:MeOH ratio, 1:1 (w/w) and stirring speed, 300 rpm..... 131

Figure 5.1. Calibration curve for response factor determination of PC using IPA as an internal standard. ....	137
Figure 5.2. A typical chromatogram from Shimadzu-2014 gas chromatograph (GC) for the components present in PC transesterification reaction mixture. ...	138
Figure 5.3. Reaction scheme for the synthesis of DMC from PC and MeOH. ..	140
Figure 5.4. Proposed reaction mechanism for the synthesis of DMC from MeOH and CO <sub>2</sub> . ....	141
Figure 5.5. Effect of different heterogeneous catalysts for synthesis of DMC. Experimental conditions: MeOH:PC molar ratio, 10:1; catalyst loading, 5% (w/w); reaction temperature, 443 K; reaction time, 6 h and stirring speed, 300 rpm. .	143
Figure 5.6. Effect of different reactant molar ratio (i.e. MeOH:PC) for synthesis of DMC. Experimental conditions: catalyst, Ce–La–Zr–O; catalyst loading, 5% (w/w); reaction temperature, 443 K; reaction time, 6 h and stirring speed, 300 rpm. ....	144
Figure 5.7. Effect of varying catalyst loading on the direct synthesis of DMC. Experimental conditions: catalyst, Ce–La–Zr–O; MeOH:PC molar ratio, 10:1; reaction temperature, 443 K; reaction time, 6 h and stirring speed, 300 rpm. .	146
Figure 5.8. Effect of reaction temperature on the direct synthesis of DMC. Experimental conditions: catalyst, Ce–La–Zr–O; MeOH:PC molar ratio, 10:1; catalyst loading, 5% (w/w); reaction time, 6 h and stirring speed, 300 rpm. ....	147
Figure 5.9. Effect of reaction time on the synthesis of DMC. Experimental conditions: catalyst, Ce–La–Zr–O; MeOH:PC molar ratio, 10:1; catalyst loading, 5% (w/w); reaction temperature, 443 K and stirring speed, 300 rpm. ....	149
Figure 5.10. Effect of different stirring speed on the synthesis of DMC. Experimental conditions: catalyst, Ce–La–Zr–O; MeOH:PC molar ratio, 10:1; catalyst loading, 5% (w/w); reaction temperature, 443 K and reaction time, 6 h. ....	150
Figure 5.11. Catalyst reusability for the synthesis of DMC. Experimental conditions: catalyst, Ce–La–Zr–O; MeOH:PC molar ratio, 10:1; catalyst loading, 5% (w/w); reaction temperature, 443 K; reaction time, 6 h and stirring speed, 300 rpm. ....	152
Figure 6.1. A schematic representation of the synthesised tin doped zirconia graphene nanocomposite catalyst. ....	158
Figure 6.2. A schematic of a CHFS reactor set up used for the synthesis of Zr–Sn/GO nanocomposite catalyst. ....	159

Figure 6.3. Photographic images of tin doped zirconia samples: (a) pure tin doped zirconia as-prepared sample synthesised using CHFS route labelled as Zr–Sn–O; tin doped zirconia graphene nanocomposite as-prepared sample synthesised using CHFS route labelled as Zr–Sn/GO; (c) Zr–Sn/GO heat-treated (773 K) sample labelled as HT500 and (d) Zr–Sn/GO heat-treated (973 K) sample labelled as HT700..... 160

Figure 6.4. Transmission Electron Microscopy (TEM) image of Sn–Zr–O catalyst. .... 167

Figure 6.5. Transmission Electron Microscopy (TEM) image of Sn–Zr/GO nanocomposite catalyst..... 168

Figure 6.6. Transmission Electron Microscopy (TEM) image of graphene oxide. .... 169

Figure 6.7. X-ray powder diffraction (XRD) patterns of (a) tin doped zirconia graphene (Zr–Sn/GO) and (b) tin doped zirconia (Sn–Zr–O) samples synthesised *via* continuous hydrothermal flow reactor..... 170

Figure 6.8. X-ray photoelectron spectroscopy (XPS) spectra showing the Sn (3d) region of tin doped zirconia (Sn–Zr–O) and tin doped zirconia graphene (Zr–Sn/GO) samples synthesised *via* continuous hydrothermal flow reactor. .... 171

Figure 6.9. X-ray photoelectron spectroscopy (XPS) spectra showing the Zr (3d) region of tin doped zirconia (Sn–Zr–O) and tin doped zirconia graphene (Zr–Sn/GO) samples synthesised *via* continuous hydrothermal flow reactor. .... 172

Figure 6.10. X-ray photoelectron spectroscopy (XPS) spectra showing the O (1s) region of graphene oxide (GO), tin doped zirconia (Sn–Zr–O) and tin doped zirconia graphene (Zr–Sn/GO) samples..... 173

Figure 6.11. X-ray photoelectron spectroscopy (XPS) spectra showing the deconvoluted C(1s) region of graphene oxide (GO) and tin doped zirconia graphene (Zr–Sn/GO) samples..... 174

Figure 6.12. Model predicted DMC yield vs experimentally obtained DMC yield. .... 178

Figure 6.13. Effect of different heterogeneous catalysts for synthesis of DMC. Experimental conditions: MeOH:PC molar ratio, 10:1; catalyst loading, 2.5% (w/w); reaction temperature, 433 K; reaction time, 4 h and stirring speed, 300 rpm. .... 180

Figure 6.14. Effect of different reactant molar ratio (i.e. MeOH:PC) on the PC conversion and yield of DMC. Experimental conditions: catalyst, Zr–Sn/GO;

catalyst loading, 2.5% (w/w); reaction temperature, 433 K; reaction time, 4 h and stirring speed, 300 rpm.....	181
Figure 6.15. Effect of varying catalyst loading on the PC conversion and yield of DMC. Experimental conditions: catalyst, Sn–Zr/GO; MeOH:PC molar ratio, 10:1; reaction temperature, 433 K; reaction time, 4 h and stirring speed, 300 rpm. .	183
Figure 6.16. Effect of reaction temperature on the PC conversion and yield of DMC. Experimental conditions: catalyst, Sn–Zr/GO; MeOH:PC molar ratio, 10:1; catalyst loading, 2.5% (w/w); reaction time, 4 h and stirring speed, 300 rpm. .	185
Figure 6.17. Effect of reaction time on the PC conversion and yield of DMC. Experimental conditions: catalyst, Sn–Zr/GO; MeOH:PC molar ratio, 10:1; catalyst loading, 2.5% (w/w); reaction temperature, 433 K and stirring speed, 300 rpm. ....	186
Figure 6.18. Effect of different stirring speed on the PC conversion and yield of DMC. Experimental conditions: catalyst, Sn–Zr/GO; MeOH:PC molar ratio, 10:1; catalyst loading, 5% (w/w); reaction temperature, 443 K and reaction time, 6 h. ....	187
Figure 6.19. Effect of catalyst reusability on the PC conversion and yield of DMC. Experimental conditions: catalyst, Sn–Zr/GO; MeOH:PC molar ratio, 10:1; catalyst loading, 2.5% (w/w); reaction temperature, 433 K; reaction time, 4 h and stirring speed, 300 rpm.....	189
Figure 6.20. Response surface graph: Effect of MeOH:PC molar ratio and catalyst loading (w/w) on DMC yield. ....	191
Figure 6.21. Response surface graph: Effect of reaction temperature and stirring speed on DMC yield. ....	192
Figure 6.22. Response surface graph: Effect of catalyst loading (w/w) and reaction time on DMC yield. ....	193

## LIST OF TABLES

Table 1.1. Global CO <sub>2</sub> sources and their yearly emissions (Gale <i>et al.</i> , 2006). ....	4
Table 1.2. Annual rate of increase of CO <sub>2</sub> emissions (Mikkelsen <i>et al.</i> , 2010).....	5
Table 2.1. Properties of CO <sub>2</sub> . .....	18
Table 2.2. Current and future predicted annual use of CO <sub>2</sub> in Mt (Mikkelsen <i>et al.</i> , 2010). .....	21
Table 2.3. Catalytic performance of various metal oxide catalysts for the synthesis of cyclic carbonates. ....	26
Table 2.4. Properties of DMC. ....	35
Table 3.1. Physical and chemical properties of ceria and lanthana doped zirconia (Ce–La–Zr–O), ceria doped zirconia (Ce–Zr–O), lanthanum oxide (La–O), lanthana doped zirconia (La–Zr–O), and zirconium oxide (Zr–O) catalysts. ....	75
Table 4.1. Physical and chemical properties of Ce–Zr/GO nanocomposite catalysts. ....	113
Table 6.1. Independent variables and their levels used in the response surface design. ....	163
Table 6.2. Experimental results of the response surface methodology. ....	164
Table 6.3. ANOVA for response surface quadratic model analysis of variance. ....	177

# **Chapter 1**

## **Introduction**

## 1. INTRODUCTION

### 1.1. MOTIVATION

Atmospheric levels of carbon dioxide (CO<sub>2</sub>) are rising significantly from approximately 315 parts per million (ppm) in 1959 to a current ~401 ppm in 2015 (Dlugokencky and Tans, 2015). Current projections estimate CO<sub>2</sub> atmospheric concentrations to continue to rise to as much as 882 ppm by 2100 (NOAA, 2014). This increase is thought to cause global warming, which is considered as the biggest environmental challenge our scientists are facing nowadays.

Carbon dioxide is an important organic molecule. It is recognised as an abundant, cheap, recyclable and non-toxic carbon source (Dienes *et al.*, 2012). The utilisation of this renewable carbon source is a prerequisite for sustainable society. CO<sub>2</sub> can be used to synthesise value added chemicals for the chemical industry. For instance, organic carbonates are produced *via* the coupling reaction of CO<sub>2</sub> and epoxides (Lu *et al.*, 2004, Adeleye, 2015). Organic carbonates have many chemical applications such as solvents, selective reagents, fuel additives, and monomers for polymers and intermediates in the production of pharmaceuticals and fine chemicals (Sun *et al.*, 2004a; 2004b).

There has been a considerable amount of academic work published on the synthesis of carbonates such as propylene carbonate (PC) (Peng and Deng, 2001; Yasuda *et al.*, 2006; Bu *et al.*, 2007; Shiels and Jones, 2007; Murugan *et al.*, 2010; Adeleye *et al.*, 2014), styrene carbonate (SC) (Kawanami and Ikushima, 2000; Sun *et al.* 2004a; 2004b; 2005; Fujita *et al.*, 2010), dimethyl carbonate (DMC) (Ballivet-Tkatchenko *et al.*, 2003; Wang *et al.*, 2010; Mikkelsen *et al.*, 2010) and cyclohexene carbonate (CHC) (Aresta *et al.*, 2003a; Darensbourg *et al.*, 2003). Different catalytic systems have been investigated such as salen aluminium complex (Alvaro *et al.*, 2005), transition metal catalysts (De Pasquale, 1973), organic catalysts (Yasuda *et al.*, 2002) and metal catalysts (Kim *et al.*, 2003). While advances have been made, the catalysts known so far for the epoxidation of CO<sub>2</sub> suffer from the complexity of reaction system, the need of a toxic organic solvent and the requirement for high CO<sub>2</sub> pressure, high reaction temperature and long reaction time (Sun *et al.*, 2005).

In this research, several heterogeneous catalysts such as metal oxide and mixed metal oxides have been synthesised and studied for the effective synthesis of organic carbonates such as DMC. Heterogeneous catalysts are preferred in the industry to homogeneous catalysts due to their stability and ease of separation, purification, handling and reusability. Hence, there is a reduction in the production cost if heterogeneous catalyst is used (Dai *et al.*, 2009).

### 1.1.1. Sources of CO<sub>2</sub>

There are numerous sources for atmospheric CO<sub>2</sub>. Table 1.1 shows different global CO<sub>2</sub> sources and their yearly emissions. Almost all CO<sub>2</sub> emissions come from fossil fuels use. When fossil fuels are combusted, the carbon stored in them is emitted mostly as CO<sub>2</sub>. Many manufacturing and industrial processes produce large amounts of CO<sub>2</sub> mainly for two reasons:

- ❖ Use of fossil fuels to generate heat and steam needed at various stages of production.
  
- ❖ Their energy intensive activities use more electricity than any other sector so unless they are using renewable sources the energy that they use is responsible for vast amount of CO<sub>2</sub> emissions.

Table 1.1. Global CO<sub>2</sub> sources and their yearly emissions (Gale *et al.*, 2006).

<b>Process</b>	<b>Emissions (Mt of CO<sub>2</sub>/yr)</b>
Fossil Fuels	
Power (coal, gas, oil and others)	10539
Cement production	932
Refineries	798
Iron and steel industry	646
Petrochemical industry	379
Oil and gas processing	50
Other sources	33
Biomass	
Bioethanol and bioenergy	91
Total	13466

## 1.2. SOURCES OF CARBON DIOXIDE AND ENVIRONMENTAL IMPACT

Since the industrial revolution in the early 1900's there has been a steady increase in the amount of CO<sub>2</sub> in the atmosphere resulting in a gradual increase in the atmospheric temperature over the decades.

### 1.2.1. Atmospheric Concentrations of CO<sub>2</sub> and Global Warming

The levels of CO<sub>2</sub> have changed over the earth's history, e.g. atmospheric concentrations of CO<sub>2</sub> have changed from 280 parts per million by volume (ppmv) in 1000 to 295 ppmv in 1900 based on Antarctic ice core data. (NOAA, 2008). CO<sub>2</sub> has further increased significantly from 315 ppm in 1958 to 401 ppm in 2014 based on actual figures from Hawaii (NOAA, 2014). Table 1.2 shows that the annual rate of increase in atmospheric CO<sub>2</sub> concentrations in 2011 has more than doubled since 1962.

Carbon dioxide (CO<sub>2</sub>) is the primary greenhouse gas and therefore is the main contributor to global warming. This has become a critical phenomenon which concerns both the scientists and the public community and considered as the most serious problem our civilisation faces. It is expected that CO<sub>2</sub> levels will continue to increase over the coming years especially with plans to shut down 50 nuclear power stations in Japan (Samseth, 2012). If other countries follow the

same route then there will be a greater demand to generate thermal power from coal burning resulting in higher CO<sub>2</sub> emissions.

Table 1.2. Annual rate of increase of CO<sub>2</sub> emissions (Mikkelsen *et al.*, 2010).

Decade	Total increase (ppm)	Annual rate of increase (ppm)
2002-2011	20.72	2.07
1992-2001	16.00	1.60
1982-1991	15.10	1.51
1972-1981	13.95	1.40
1962-1971	8.99	0.89

### 1.2.2. Controlling CO<sub>2</sub> Levels

CO<sub>2</sub> emissions could be managed by three methods as shown in Figure 1.1. Reducing CO<sub>2</sub> emissions could be carried out on a personal and global scale. It could be done by using less fossil fuel power, increased usage of renewable energy and designing processes with higher efficiency. However, due to increased population, higher agriculture and transportation demands, political and economical factors a substantial decrease in CO<sub>2</sub> emissions have not been achieved.

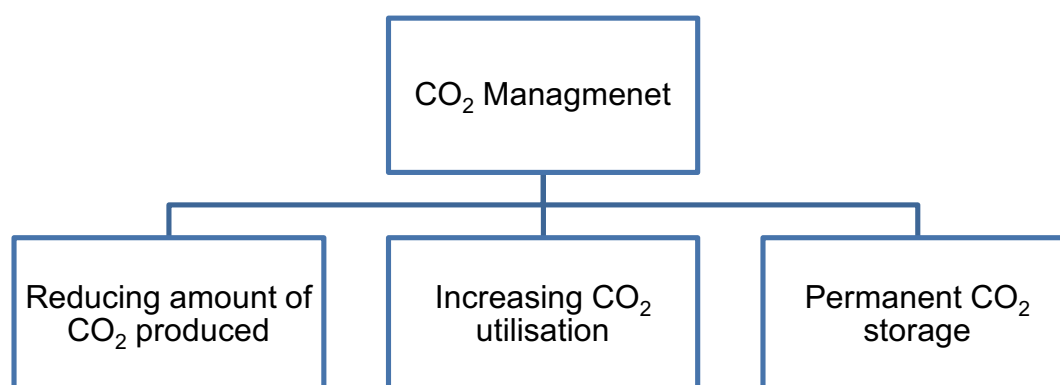


Figure 1.1. Methods for CO<sub>2</sub> management.

One way of reducing CO<sub>2</sub> emissions is by carbon capture and storage which involves capturing CO<sub>2</sub> released from power plants and injecting them at high pressures into an underground for permanent storage (Gibbins and Chalmers, 2008). This method can make a significant contribution to the control and reduction of CO<sub>2</sub> levels in the atmosphere. However, there are few limitations in following this path such as the maximum annual allowable injection rate of CO<sub>2</sub>, development of carbon capture technologies, public acceptance and political barriers. Utilisation of CO<sub>2</sub> could be a potential alternative due to the following reasons:

- ❖ Accelerated growth in the consumption of carbon-based energy worldwide.
- ❖ Decline in the carbon-based energy resources (oil and gas).
- ❖ Low efficiency in current energy systems.
- ❖ Continuous rise in atmospheric CO<sub>2</sub> concentrations.

### **1.3. CO<sub>2</sub> CONVERSION AND UTILISATION**

The utilisation of CO<sub>2</sub> is an integral part of carbon management. Successful utilisation of CO<sub>2</sub> has the potential to reduce CO<sub>2</sub> emissions by 3.7 Gt/y which is equivalent to about 10% of the world's annual CO<sub>2</sub> emissions (Sneeden, 2011). This approach for carbon management can result in the production of value added products and the creation of new jobs for additional economical benefits.

#### 1.3.1. Potential for CO<sub>2</sub> Utilisation

CO<sub>2</sub> is commonly used in the food and beverage industries, however, a new and innovative approach for CO<sub>2</sub> utilisation is required. It has been estimated that by 2035 the world will produce 15 Gt/y of CO<sub>2</sub> only from burning fuels (Sneeden, 2011). Therefore, developing new processes where captured CO<sub>2</sub> from industries and power plants is reused in a beneficial way will achieve multiple goals; reducing CO<sub>2</sub> atmospheric concentrations and hence reducing the effect of global warming as well as creating jobs and revenues that can contribute to the cost of

CO<sub>2</sub> capture. Various current and potential applications for CO<sub>2</sub> utilisation are shown in Figure 1.2.

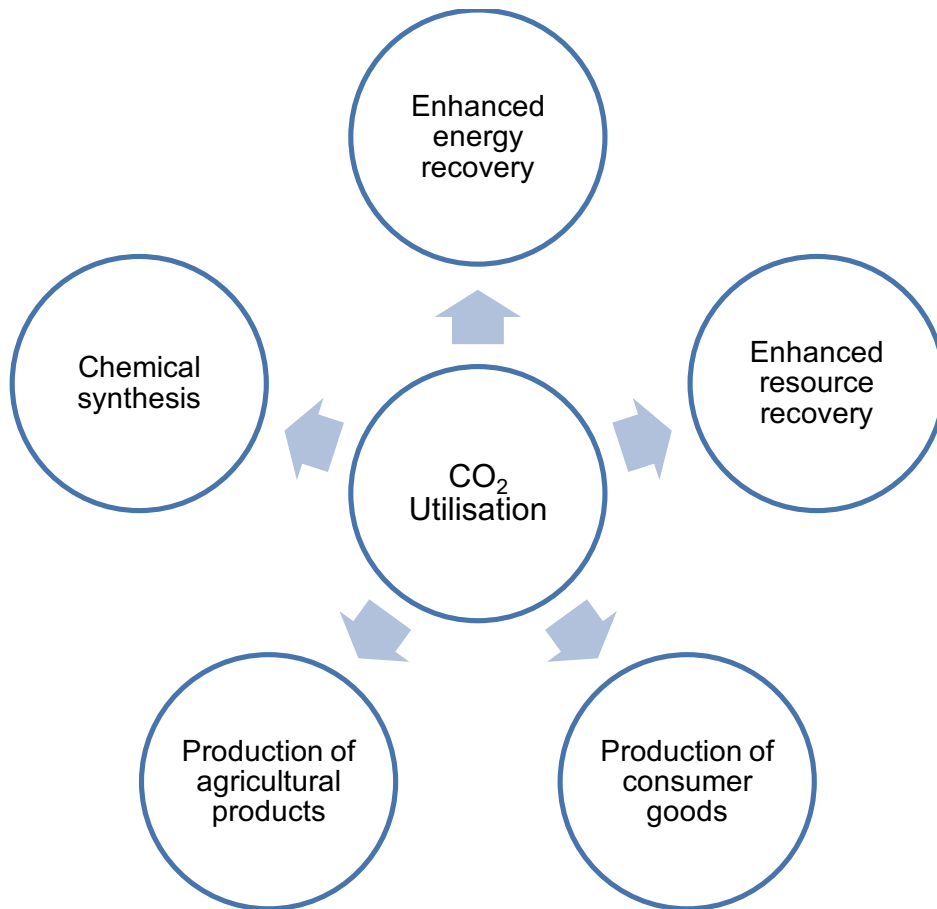


Figure 1.2. Potential applications of CO<sub>2</sub>.

### 1.3.2. Barriers and Challenges for CO<sub>2</sub> Utilisation

The idea of carbon dioxide utilisation is not new and scientists have been conducting research on a variety of products where CO<sub>2</sub> can be used either as a raw product or an intermediate to a value added end product. However, there are some challenges for CO<sub>2</sub> conversion and utilisation and therefore the implementation of carbon dioxide utilisation has been rather slow so far. Global challenges related to CO<sub>2</sub> utilisation include, policy regulations, energy economics and environmental protection. In addition to these, there are key issues and barriers for CO<sub>2</sub> conversion, which include:

- ❖ Economical challenges: costs of CO<sub>2</sub> capture, separation, purification and transportation to the utilisation site (Song, 2006).
- ❖ Energy requirements: CO<sub>2</sub> is low in energy content and therefore is thermodynamically very stable. Hence, transformation of CO<sub>2</sub> requires a large energy input or high energy starting material such as epoxides and hydrogen. Furthermore, catalysts are usually required to overcome high kinetic energy barriers, e.g. in polymerisation reactions (Whipple and Kenis, 2010).
- ❖ Market Limitations: some industrial processes are already well established and the utilisation of CO<sub>2</sub> will require modifications/upgrades for their process. There are size and investment limitations, lack of incentives and industrial commitment for enhancing CO<sub>2</sub> utilisation.
- ❖ Driving force: there is a lack of socio-economical driving forces for enhanced CO<sub>2</sub> utilisation (Song, 2006).

It is apparent that no single new technology will be the solution for CO<sub>2</sub> utilisation. Extensive research for new technologies/processes that will overcome the barriers and challenges for CO<sub>2</sub> utilisation with enhanced potential industrial interest is required.

### 1.3.3. Research Strategies for CO<sub>2</sub> Utilisation

The unique physical and chemical properties of carbon dioxide molecule should be considered when conducting research on the utilisation of carbon dioxide. The targets for our scientists are:

- ❖ To utilise CO<sub>2</sub> as an environmentally benign building block to produce industrially value added chemicals/products.
- ❖ To incorporate CO<sub>2</sub> to physical/chemical processing that adds a value to the process.

- ❖ To apply CO<sub>2</sub> as a beneficial medium in chemical process for energy recovery and removal of impurities specifically using its unique physical properties as a supercritical fluid.
- ❖ To develop efficient and low energy intensity processes for the separation and purification of CO<sub>2</sub>.
- ❖ To develop biochemical or geologic formulation to convert CO<sub>2</sub> into new fossil energy.

There are various catalytic/non catalytic processes where CO<sub>2</sub> can be used as a reactant or a co-feed. Chemical, biochemical, photochemical, photo-catalytic reduction and electro-catalytic conversion are among processes subject to extensive research in recent years. Carbon dioxide can be used as a whole molecule, carbon source or/and as an oxygen source in chemical reactions (Creutz and Fujita, 2000).

### 1.3.3.1. Development of new processes

The development of new innovative processes for chemicals/products with large market demand is essential and effective way to enhance CO<sub>2</sub> utilisation. The challenge in development of such processes is the ability to have the right balance of safety, reliability, economic feasibility and product quality. For example, the production of methanol using CO<sub>2</sub>-rich synthesis gas instead of H<sub>2</sub>/CO rich synthesis gas as a raw material increases the utilisation of CO<sub>2</sub> (Song *et al.*, 2002). Expanding the market potential for products/chemicals from CO<sub>2</sub> is a key to increasing CO<sub>2</sub> application and utilisation. Increasing the commercial applications for CO<sub>2</sub> end products will increase the demand for these products thus increasing the demand for CO<sub>2</sub> as a raw material.

### 1.3.3.2. Replacement of hazardous chemicals

In some chemical processes where the raw material used is poisonous, toxic or not environmentally friendly, carbon dioxide can be used in chemical processes as a green substitute (Darensbourg *et al.*, 2010; Leino *et al.*, 2010; Omae, 2012; Adeleye *et al.*, 2014; Dienes *et al.*, 2012; Honda *et al.*, 2014). This does not only eliminate toxic and hazardous chemicals, but also encourages and increases

utilisation of carbon dioxide. CO<sub>2</sub> can be used to replace poisonous/hazardous phosgene, isocyanates and dimethyl sulphate (Bian *et al.*, 2009a; Honda *et al.*, 2010). The synthesis of DMC is an excellent example of this where, CO<sub>2</sub> can react with MeOH to produce DMC instead of phosgene and carbon monoxide. In conventional Friedel-Crafts reactions carbon groups are introduced to benzene rings using halides, alcohols and alkenes in the presence of aluminium chloride as a catalyst (Hitzler *et al.*, 1998; Hepworth *et al.*, 2002). This route produces undesired wastes and destroys the catalyst. Employing supercritical CO<sub>2</sub> allows the utilisation of heterogeneous catalyst (which can be easily recycled and reused) and minimises waste generation (Hitzler *et al.*, 1998; Komoto and Kobayashi, 2002).

### 1.4. SUSTAINABILITY

Sustainable development is the concept of achieving the balance between three pillars (people, planet and profit) to thrive. In modern life it is almost impossible to imagine our life without products from the process industry and therefore, for sustainable development in the process industries, an additional 'product' pillar exists and is taken into account. Most of the products synthesised in the chemical/process industries generate waste or undesired chemicals leading to an increase in greenhouse emissions thus affecting the human health and the environment. These are major concerns for our planet and society and therefore, there has been great emphasis on the development of environmentally friendly approaches for greener and more sustainable synthesis of chemicals and products (Centi and Perathoner, 2003; Beckman, 2004).

The increase in atmospheric concentrations of CO<sub>2</sub> has an adverse effect on achieving sustainability, therefore, many companies are working on ways to reduce their carbon footprint and have targets set in an attempt to reduce CO<sub>2</sub> emissions. Kyoto protocol is an important international treaty adopted in Kyoto in 1997. The objective of this protocol is to reduce atmospheric concentrations of greenhouse gases by setting various targets for different countries among the developed and developing nations (Wigley, 1998). This is considered as a step forward for a more sustainable environment, however, this on its own is not the solution.

Green process engineering is a key tool that could significantly contribute towards making hazardous processes more innovative and sustainable for the benefit of society, environment and economy (Diwekar, 2005; Patel *et al.*, 2014). Green process engineering is defined as “the design, commercialization, and use of processes and products, which are feasible and economical while minimising (a) generation of pollution at the source and (b) risk to human health and the environment”. In the past, minimising cost and increasing profits were the main objectives of process engineering. Assessment on long-term impacts on society and planet used to be neglected (Patel *et al.*, 2014). Therefore, scientists and engineers need to develop new greener technologies and products in an environmentally friendly manner in order to save the planet.

### 1.5. RESEARCH AIMS AND OBJECTIVES

The aims and objectives of this research work are:

- ❖ To study the utilisation of CO<sub>2</sub> as a raw material for the synthesis of a value added chemical, such as dimethyl carbonate (DMC). To develop and design a greener and sustainable process for the synthesis of DMC. This has been achieved by systematically investigating various reaction routes for the production for DMC using solvent free heterogeneous catalytic processes.
  
- ❖ To investigate the catalytic performance of commercially available metal oxides/mixed metal oxides as suitable heterogeneous catalysts for the synthesis of DMC. The catalysts include ceria and lanthana doped zirconia (Ce–La–Zr–O), ceria doped zirconia (Ce–Zr–O), lanthana doped zirconia (La–Zr–O), lanthanum oxide (La–O) and zirconium oxide (Zr–O). Also, to prepare inorganic graphene based nanocomposite catalysts using continuous hydrothermal flow synthesis (CHFS) reactor such as ceria-zirconia oxide/graphene nanocomposite (Ce–Zr/GO) and tin doped zirconia/graphene oxide (Zr–Sn/GO). A thorough investigation has been carried out to investigate the catalytic performance of the inorganic graphene based nanocomposite for the synthesis of DMC.

- ❖ To investigate various reaction routes for the synthesis of DMC to maximise the yield of DMC. These routes include, direct synthesis from methanol (MeOH) and CO<sub>2</sub> and transesterification of propylene carbonate (PC) with MeOH. The reactions have been carried out using a high pressure reactor with a solvent free heterogeneous catalyst.
- ❖ To extensively characterise different heterogeneous catalysts such as Ce–La–Zr–O, Ce–Zr–O, La–Zr–O, La–O, Zr–O, GO, Ce–Zr/GO and Zr–Sn/GO using various analytical characterisation techniques to study the molecular structure, morphological and physico-chemical properties of the catalysts. The techniques include Raman spectroscopy (RS), scanning electron microscopy (SEM), transmission electron microscopy (TEM), X-ray photoelectron spectroscopy (XPS) Brunauer-Emmett-Teller (BET) surface area and X-ray powder diffraction (XRD).
- ❖ To investigate the effect of various parameters such as heat-treatment temperature, reactant molar ratio, catalyst loading, reaction temperature, CO<sub>2</sub> pressure, reaction time and stirring speed to determine the optimum reaction conditions for the synthesis of DMC.
- ❖ To investigate the long term stability of the heterogeneous catalysts for the synthesis of DMC. Reusability studies have been carried out in a high pressure reactor where the fresh catalyst was reused up to six times for DMC synthesis to investigate the long term stability of the catalyst.
- ❖ To reduce the process complexity of conventional homogeneous catalytic processes with an effective single step solvent free heterogeneous catalytic process. This was achieved using effective experimental procedures and simple reaction mixture/catalyst separation method.
- ❖ To replace the conventional complex homogeneous catalytic processes with an effective solvent free heterogeneous catalytic process. This was achieved by using highly active, stable and inexpensive heterogeneous catalysts.

## 1.6. STRUCTURE OF THESIS

The thesis is structured as follows:

**Chapter 1: Introduction:** In this chapter the motivation for carrying out this research study is presented. A detailed overview of atmospheric concentrations of CO<sub>2</sub> and its environmental impact is presented to provide background information about the research work. Different approaches for CO<sub>2</sub> utilisation, challenges and barriers as well as research strategies for the development of sustainable and green process engineering are discussed. Moreover, the aims and objectives of the research work are highlighted and organisation of the thesis is introduced.

**Chapter 2: Literature Review:** A detailed literature review about carbon dioxide, its properties and industrial applications are presented. The chapter provides a general perspective on the different approaches for transformation of CO<sub>2</sub>. Also, a detailed review about DMC, its properties and important applications in the process industry is covered. The different routes for DMC synthesis are discussed in the subsequent section. This is followed by a broad overview on the main types of catalysts employed for the direct synthesis of DMC.

**Chapter 3: Direct synthesis of DMC using commercially available catalysts:** This chapter covers detailed description of materials, experimental procedure and characterisation of heterogeneous catalysts used in this research i.e. ceria and lanthana doped zirconia (Ce–La–Zr–O), ceria doped zirconia (Ce–Zr–O), lanthana doped zirconia (La–Zr–O), lanthanum oxide (La–O) and zirconium oxide (Zr–O). Extensive characterisation of the catalysts to determine their molecular structure, morphological and physico-chemical properties is presented. Batch addition reactions of methanol and CO<sub>2</sub> catalysed by Ce–Zr–O are presented in this chapter. The method used for the analysis of experimental samples is also explained. The effect of various reaction parameters on methanol conversion and yield of DMC is presented and discussed in this chapter.

**Chapter 4: Direct synthesis of DMC using metal oxide/graphene nanocomposite catalysts:** In this chapter, the detailed description of procedures followed for the preparation and characterisation of ceria zirconia oxide/graphene

nanocomposite catalysts for the direct synthesis of DMC is highlighted. Furthermore, the results for catalysts characterisation such as powder X-ray diffraction (XRD), scanning electron microscopy (SEM), transmission electron microscopy (TEM), Brunauer-Emmett-Teller (BET) surface area measurement and X-ray photoelectron spectroscopy (XPS) analysis are discussed. The general descriptions of the set-up and procedure developed for the addition reaction experiments in the presence of 1,1,1, trimethoxymethane (TMM) as a dehydrating agent are provided. The effect of catalyst heat treatment, catalyst loading, reaction temperature, CO<sub>2</sub> pressure, reaction time and TMM:MeOH ratio on the catalyst performance are explained. Catalyst stability and reusability studies carried out as a part of the batch studies are explained.

**Chapter 5: Transesterification of propylene carbonate using commercially available catalysts:** This chapter presents the efficiency of various metal oxide catalysts in the transesterification of propylene carbonate with MeOH at atmospheric pressure. The plausible reaction mechanism for the esterification reaction is discussed in this chapter. This is followed by discussion of batch studies results that were carried out in order to optimise reaction conditions. Furthermore, the long term stability of Ce–Zr–O investigated by carrying out reusability studies at optimum reaction conditions is presented.

**Chapter 6: Transesterification of propylene carbonate using metal oxide/graphene nanocomposite catalysts:** This chapter provides a detailed description of a green, rapid, highly efficient and continuous hydrothermal flow synthesis of tin doped zirconia/graphene nanocomposites, which were used as heterogeneous catalysts for the transesterification of PC with MeOH. This is followed by detailed discussion of catalyst characterisation results. The description of experimental set-up and procedure developed for the transesterification reaction are provided. The effect of catalyst heat treatment, reactant molar ratio, catalyst loading, reaction temperature, reaction time and stirring speed were extensively evaluated to maximise the yield of DMC. Furthermore, catalyst stability and reusability studies carried out at the optimised reaction conditions are explained.

**Chapter 7: Conclusions and recommendations for future work:** The general conclusions relating to the overall research findings and suggestions for future work in the field are presented in this chapter.

**Chapter 8: References:** This chapter lists all the references to the literature materials used and cited in this research work.

**Chapter 9: Appendices:** Some helpful explanations and supporting materials that are relevant to the research work are provided in this chapter.

# **Chapter 2**

## **Literature Review**

## 2. LITERATURE REVIEW

### 2.1. INTRODUCTION

Carbon dioxide (CO<sub>2</sub>) is the most important anthropogenic greenhouse gas and therefore it is considered as the most important cause for global warming. CO<sub>2</sub> can be used as a raw material for the syntheses of value added chemicals using a suitable catalyst.

This chapter provides an overview about the utilisation of CO<sub>2</sub> as a raw material in the syntheses of organic carbonates. It reviews the different routes of dimethyl carbonate (DMC) synthesis. It analyses and reviews different catalytic systems reported for the direct synthesis of DMC. This chapter compares advantages and disadvantages of using heterogeneous and homogeneous catalysts.

### 2.2. WHAT IS CARBON DIOXIDE?

Carbon dioxide is a chemical compound naturally occurs in the earth's atmosphere. It is composed of two oxygen atoms covalently bonded to a single carbon atom. Depending on the temperature and pressure, the physical properties of CO<sub>2</sub> change from subcritical to supercritical. At supercritical conditions (304.1 K, 73.9 bar), CO<sub>2</sub> behaves like a gas while exhibiting a liquid like density (Mikkelsen *et al.*, 2010). CO<sub>2</sub> is considered as a very stable compound because the carbon atom is in its most oxidised form and thermodynamically stable (Omae, 2012). Recently, CO<sub>2</sub> is achieving a great importance as an environmentally benign building block in the chemical industry due to its non-toxic, non-flammable, recyclable and cheap properties (Leino *et al.*, 2010).

#### 2.2.1. Properties of Carbon Dioxide

CO<sub>2</sub> is a linear molecule that is thermodynamically very stable with bond strength measured at 532 kJmol<sup>-1</sup>. The physical properties of CO<sub>2</sub> are summarised in Table 2.1.

Table 2.1. Properties of CO<sub>2</sub>.

Properties of CO <sub>2</sub>	
Molar Mass	44 g mol <sup>-1</sup>
Heat of formation at 298 K	-393.5 kJ mol <sup>-1</sup>
Entropy of formation at 298 K	213.6 JK <sup>-1</sup> mol <sup>-1</sup>
Gibbs free energy at 298 K	-394.3 kJ mol <sup>-1</sup>
Sublimation point at 1 atm	194.7 K
Melting point at 1 atm	216.6 K
Critical temperature	304 K
Critical pressure	73.9 bar
Critical density	0.468 g cm <sup>-3</sup>
Gas density	1.976 kg m <sup>-3</sup>
Liquid density	770 kg m <sup>-3</sup>
Solid density	1560 kg m <sup>-3</sup>
Specific Volume	0.546 m <sup>3</sup> kg <sup>-1</sup>
Latent heat of vaporisation (0 K)	231.3 J g <sup>-1</sup>
Latent heat of vaporisation at 194.5 K	353.4 J g <sup>-1</sup>
Viscosity at 194.5 K and 1 atm	0.07 cP
Solubility in water at 0 K	0.3346 g L <sup>-1</sup>
Solubility in water at 298 K	0.1449 g L <sup>-1</sup>

There are many properties that make carbon dioxide an important molecule in the process industry. CO<sub>2</sub> is an easily available renewable carbon source which increases the number of inexpensive easily available raw material for the process industry. CO<sub>2</sub> is also an oxygen carrier and mild oxidiser and therefore can be used in mild oxidation reactions, which widens the safe operation of some chemical processes.

When CO<sub>2</sub> is at supercritical conditions (scCO<sub>2</sub>), its physical properties change in a way that makes it more valuable for the process industry. The high density and low viscosity of scCO<sub>2</sub> makes it an excellent medium for mass transfer. Supercritical CO<sub>2</sub> has low surface tension which increases the overall rate of reaction when used as a reaction medium. It also prevents catalyst coking and prolongs the interval of catalyst regeneration which in turn makes heterogeneous

catalysis more applicable (Baiker, 1999). The utilisation of scCO<sub>2</sub> in reaction processes results in a single phase operation rather than multiphase operation. This eliminates mass transfer resistance, increases overall rate of reaction and improves the conversion and selectivity (Baiker, 1999; Cao *et al.*, 2002; Du *et al.*, 2005; Wang *et al.*, 2007b). This in turn helps to maintain the product quality and simplifies catalytic processes. Furthermore, CO<sub>2</sub> has a low evaporation temperature and does not leave any harmful traces on the product thus it is recognised as a safe solvent.

The thermo-physical and heat transfer properties of CO<sub>2</sub> allows for high heat transfer and refrigeration capacity. This leads to the reduction of most components in the refrigeration systems and replaces an anthropologically made substance by a benign product leading to cheaper and less complicated refrigeration processes (Fournaison *et al.*, 2004).

### 2.2.2. Reactivity of CO<sub>2</sub>

Carbon dioxide is thermodynamically and kinetically stable molecule and is rarely used to its fullest potential. However, due to the presence of  $\pi$ -electron density of the double bonds, the lone pair of electrons on the oxygen atom and the electron deficiency of the carbonyl carbons, most CO<sub>2</sub> reactions are dominated by nucleophilic attacks at the carbon atom. Since CO<sub>2</sub> is a very stable molecule, there are four different methodologies to transform CO<sub>2</sub> into value added chemicals/products:

- ❖ To supply large energy input such as electricity or light.
- ❖ To remove a particular by-product and thereby shifting the reaction equilibrium to the product side.
- ❖ To choose low energy chemicals as target products such as organic carbonates.
- ❖ To use high energy starting materials i.e. organometallics, hydrogen and unsaturated compounds.

### 2.3. TRANSFORMATION OF CARBON DIOXIDE (CO<sub>2</sub>)

#### 2.3.1. Industrial Applications of CO<sub>2</sub>

The industry uses approximately 110 mega tonnes (Mt) of CO<sub>2</sub> per year for various chemical applications (Aresta and Dibenedetto, 2007). However, the industrial use only accounts to 0.5% of the total CO<sub>2</sub> emissions (36 gega tonnes (Gt) of CO<sub>2</sub> per year) (Mikkelsen *et al.*, 2010). The industrial application of CO<sub>2</sub> is based on utilising the physical properties or chemical properties of the molecule. The physical properties of CO<sub>2</sub> find applications in the beverage industry and enhanced oil recovery (Aresta *et al.*, 2003a). The characteristics of CO<sub>2</sub> at supercritical conditions make it an excellent fluid as a solvent in various reactions and in the synthesis of nanomaterial. The inert properties of CO<sub>2</sub> enable it to be used as a protective gas and as a fire extinguisher (Song, 2006). Furthermore, its physical properties make it a greener substitute for chlorofluorocarbons (CFC's) in refrigeration and much more (Arakawa *et al.*, 2001). The chemical properties of CO<sub>2</sub> make it a valuable reactant for the synthesis of various chemicals such as urea, methanol, salicylic acid and organic carbonates which are discussed in more details in section 2.3.2.

#### 2.3.2. Industrial Syntheses from CO<sub>2</sub>

The catalytic transformation of CO<sub>2</sub> into high value-added chemicals has attracted much attention in recent years. More than 20 reactions involving CO<sub>2</sub> as a starting material have been developed, however, their successful industrialisation is limited. CO<sub>2</sub> can be converted and used as fuel such as hydrocarbons and alcohols. It may also be converted into value added chemicals such as organic carbonates, urea, carboxylic acid, esters and lactones. From Table 2.2, it can be seen that urea, methanol, organic carbonates and carboxylic acid show promising future for CO<sub>2</sub> utilisation.

Table 2.2. Current and future predicted annual use of CO<sub>2</sub> in Mt (Mikkelsen *et al.*, 2010).

<b>Industrial chemical application of CO<sub>2</sub></b>	<b>Current industrial CO<sub>2</sub> usage (Mt/y)</b>	<b>Future predicted CO<sub>2</sub> usage (Mt/y)</b>
Urea	70	100
Methanol	14	1000
Organic carbonates	0.2	100
Salicylic acid	0.02	0.1

The industrial use of CO<sub>2</sub> as a chemical feedstock for syntheses of organic carbonates has been in place since the early 1950's (Mikkelsen *et al.*, 2010). From Table 2.2, it can be seen that future expectation in the use of CO<sub>2</sub> will reach 100 Mt per year. Therefore, this research focuses on the synthesis of organic carbonates such as DMC as an effective method for utilisation of CO<sub>2</sub>.

#### 2.3.2.1. Conversion to fuel

The demand for energy is increasing rapidly due to population and economic growth. For many decades, the combustion of non-renewable fossil feedstock has been the major supply for energy demands, which has resulted in unsustainable increase of CO<sub>2</sub> emissions. As a result, scientists have put much effort in recent years to convert CO<sub>2</sub> from a liability to an asset *via* an attractive approach that involves hydrogenation of CO<sub>2</sub>. The main challenge facing the scientific community is the development of a suitable catalyst which promotes multistep sequence of reduction reactions required to transform CO<sub>2</sub> into MeOH. Copper based catalysts have been reported for the synthesis of MeOH from CO<sub>2</sub> (Saito, 1998; Ushikoshi *et al.*, 1998; Grabow and Mavrikakis, 2011). However, high reaction temperatures are required (523 K), which limits the theoretical yield of the reduction products and leaves the rational tuning of the catalyst challenging (Joó, 2007). Recently, homogeneous catalytic processes operating at lower reaction temperature have been developed (Laitar *et al.*, 2005; Matsuo and Kawaguchi, 2006; Ashley *et al.*, 2009; Menard and Stephen and Erker, 2010; Riduan and Zhang, 2010; Stephen and Erker, 2010) for the effective hydrogenation of CO<sub>2</sub>. However, the applicability of such processes is limited due

to the high cost of hydrogen sources (Tominaga *et al.*, 1993; Riduan *et al.*, 2009; Chakraborty *et al.*, 2010).

### 2.3.2.2. Conversion to urea

Urea synthesis is currently the largest use of CO<sub>2</sub> in organic synthesis (100 million tonnes a year) (Xiang *et al.*, 2012). The synthesis of urea is carried out in two steps at elevated temperatures and pressure (473 K, 250 bar). The first step involves the production of ammonium carbamate from ammonia and CO<sub>2</sub>. The second step involves the dehydration of the carbamate to urea. Various processes have been developed for the synthesis of urea using different techniques for the recovery and recycling of unreacted ammonium carbamate (Sneeden, 2011). The synthesis of urethane derivatives was performed *via* the dehydration of urea using hydrophilic ionic liquids as reaction media (Shi *et al.*, 2003).

On the other hand, amines can react with CO<sub>2</sub> to produce carbamic acids, which upon reaction with electrophiles such as halides, results in the formation of urethanes. A variety of homogeneous and heterogeneous catalysts have been studied for the effective synthesis of urethanes (Aresta and Quaranta, 1992; McGhee *et al.*, 1993; 1995; Salvatore *et al.*, 2001; Yoshida *et al.*, 2000; Srivastava *et al.*, 2004) with mesoporous silica containing ammonium salts being the most effective catalyst without an additional base (Srivastava *et al.*, 2005b; 2006a). Recent studies are carried out to replace the halides by alcohols in an attempt for a greener synthesis of urethanes. If alcohols are used then water is produced as a side product (environmentally friendly) instead of halide based side products. However, yields are very low due to the thermodynamic limitations and catalyst deactivation caused by the coproduced water. Therefore, dehydration of the reaction mixture is vital for higher urethane yields. A variety of dehydrating agents has been tested and Sakakura *et al.* (1999) reported that ketals were working quite effectively. There are still many challenges facing our researchers in order to improve the performance of the catalyst and to propose a catalytic process, which both, meet the criteria for greener chemical syntheses and is economically feasible for production at industrial scale.

#### 2.3.2.3. Conversion to carboxylic acid

Carboxylic acids and their derivatives are important structural units that are often found in various natural products. They are also versatile building blocks for the synthesis of biologically active compounds in the pharmaceutical industry. Salicylic acid is one of the most important carboxylic acids and is used as an intermediate in the synthesis of aspirin (Mikkelsen *et al.*, 2010). The carboxylation of various nucleophiles or unsaturated hydrocarbons and CO<sub>2</sub> is an attractive route to produce carboxylic acids. In most of these reactions, transition metals are used to homogeneously catalyse the reaction under mild conditions (Fujihara *et al.*, 2011; Li *et al.*, 2011a; Takaya *et al.*, 2011; Zhang and Riduan, 2011). Most of these reactions are industrially commercialised, however, due to the importance of CO<sub>2</sub> utilisation, it is anticipated that more reactions using CO<sub>2</sub> as a carboxylative reagent will be developed in the future. Attention to the reaction mechanism of such reactions will help researchers to develop highly efficient and novel catalytic processes for economical production of more carboxylic acid derivatives.

#### 2.3.2.4. Conversion to organic carbonates

CO<sub>2</sub> reacts with epoxides in the presence of suitable catalysts to produce the corresponding carbonates. Commercial synthesis of organic carbonates usually involves utilisation of toxic chemicals i.e. phosgene or involve the production of environmentally unpleasant chemical compounds (Eghbali and Li, 2007; Ulusoy *et al.*, 2011). Alternative routes to organic carbonate synthesis are being pursued in order to eliminate the use of toxic feedstock. The organic carbonates can be divided into acyclic carbonates, cyclic carbonates and polycarbonates. Acyclic carbonates [e.g. DMC and diethyl carbonate (DEC)] find applications in the production of polycarbonate, polyurethane and other fine and intermediate chemicals. DMC's properties, applications and synthetic routes are discussed in detailed in Section 2.5.

Cyclic carbonates such as ethylene carbonate and propylene carbonates are produced from the reaction between CO<sub>2</sub> and ethylene oxide and propylene oxide, respectively. Cyclic carbonates have high boiling points that make them excellent solvents for natural and synthetic polymers such as nylon, lignin and polyvinyl chloride (PVC). Polycarbonates are produced from alternating

copolymerisation of the same epoxide as the synthesis of cyclic carbonates; polymers are kinetic reaction products whereas cyclic carbonates are thermodynamic ones (Coates and Moore, 2004). Polycarbonates have unique properties including excellent toughness, strength, transparency, thermal stability, durability, heat resistance and good electrical insulation. Polycarbonates are amorphous and thereby have excellent mechanical and dimensional stability (Sweileh *et al.*, 2010). Hence, polycarbonates have a wide variety of applications ranging from water bottles to building materials, automobile parts, electrical components, traffic lights, cash dispensers and much more (Darensbourg, 2007).

The synthesis of organic carbonates requires very high energy, either externally provided to the reaction or *via* the utilisation of reactants with high energy content (Zevenhoven *et al.*, 2006). The development of new heterogeneous catalytic systems to replace existing homogeneous catalytic systems for organic synthesis is vital to improve product separation, catalyst recovery and reduce costs.

### 2.4. SYNTHESIS OF CYCLIC CARBONATES

#### 2.4.1. Cycloaddition of CO<sub>2</sub> to Epoxides

Cyclic carbonates can be synthesised *via* the coupling reaction between CO<sub>2</sub> and epoxides in the presence of a suitable catalysts and often at severe reaction conditions (Arakawa *et al.*, 2001; Clements, 2003). This synthesis route benefits from eliminating toxic reagent (phosgene), utilising carbon dioxide and it is 100% atom efficient process which makes it very desirable from the “Green Chemistry” point of view (Du *et al.*, 2005). Cyclic carbonates are valuable organic compounds that can be used as polar solvents, electrolytes in the production of lithium batteries and as important raw material and intermediates for the synthesis of a range of chemicals (Clements, 2003; Du *et al.*, 2005; Omae, 2006; Sakakura *et al.*, 2007; Sakakura and Kohno, 2009).

In the past few years, a variety of catalytic processes have been developed and evaluated for the effective syntheses of cyclic carbonates from CO<sub>2</sub> and epoxides. These include metal oxide (Bhanage *et al.*, 2001; Aresta *et al.*, 2003a; 2003b; Ramin *et al.*, 2006; Yasuda *et al.*, 2006), organometallic complexes (Shen *et al.*, 2003; Lu *et al.*, 2004; Darensbourg *et al.*, 2004; Chen *et al.*, 2007; Jing *et al.*, 2007; Jutz *et al.*, 2008), organic bases (Kawanami and Ikushima, 2000;

Barbarini *et al.*, 2003; Jiang and Hua, 2006), phosphines (Huang and Shi, 2003; Kim *et al.*, 2005; Sun *et al.*, 2006) and ionic liquids (Caló *et al.*, 2002; Kossev *et al.*, 2003; Li *et al.*, 2004; Sun *et al.*, 2008; Zhou *et al.*, 2008; Sun *et al.*, 2009).

### 2.4.2. Metal Oxide Catalysts

Metal oxide catalysts have acidic and basic properties that allow them to interact with polarizable species such as CO<sub>2</sub> and therefore, their catalytic performance has been studied extensively as shown in Table 2.3.

Bhanage *et al.* (2001) prepared and tested several metal oxide such as magnesium oxide (MgO), calcium oxide (CaO), zirconium oxide (Zr<sub>2</sub>O), cerium oxide (CeO<sub>2</sub>), lanthanum oxide (La<sub>2</sub>O<sub>3</sub>), zinc oxide (ZnO) and aluminium oxide (Al<sub>2</sub>O<sub>3</sub>) for the syntheses of cyclic carbonates in the presence of *N,N*-dimethylformamide (DMF). MgO (Table 2.3, entry 8) showed the highest selectivity towards propylene carbonate (92%), whereas La<sub>2</sub>O<sub>3</sub> (Table 2.3, entry 4) exhibited the highest PC yield (54.1%). Yano *et al.* (1997) obtained a higher PC and SC yield (Table 2.3, entries 10 and 11) over MgO compared to Bhanage *et al.*, (2001) (Table 2.3, entries 10 and 11). The discrepancy in the catalytic activity can be attributed to the difference in the reaction condition and the concentration of DMF. Nb<sub>2</sub>O<sub>5</sub> showed even a better catalytic activity in the presence of DMF (Table 2.3, entries 12 and 13) for the cycloaddition of both PO and styrene oxide (SO). When DMF was used alone for the synthesis of styrene carbonate (SC) (Table 2.3, entry 18), SC yield reached 85%. This shows the importance of the basic compound for the cycloaddition reaction as it acts as a co-catalyst besides being a solvent for the reaction.

Table 2.3. Catalytic performance of various metal oxide catalysts for the synthesis of cyclic carbonates.

Entry	Catalyst	Epoxide <sup>a</sup>	Reaction Conditions				Reaction Results		Reference
			Solvent	Pressure (bar)	Temperature (K)	Time (h)	Selectivity (%)	Yield (%)	
1	CaO	PO	DMF	80	423	15	8.1	0.8	(Bhanage <i>et al.</i> , 2001)
2	ZnO	PO	DMF	80	423	15	92.6	8.7	(Bhanage <i>et al.</i> , 2001)
3	ZrO <sub>2</sub>	PO	DMF	80	423	15	50.8	10.9	(Bhanage <i>et al.</i> , 2001)
4	La <sub>2</sub> O <sub>3</sub>	PO	DMF	80	423	15	74.5	54.1	(Bhanage <i>et al.</i> , 2001)
5	CeO <sub>2</sub>	PO	DMF	80	423	15	76.9	17.5	(Bhanage <i>et al.</i> , 2001)
6	Al <sub>2</sub> O <sub>3</sub>	PO	DMF	80	423	15	6.6	6.6	(Bhanage <i>et al.</i> , 2001)
7	DMF	PO	DMF	80	423	15	7.9	7.9	(Bhanage <i>et al.</i> , 2001)
8	MgO	PO	DMF	80	423	15	92.0	32.1	(Bhanage <i>et al.</i> , 2001)
9	MgO	SO	DMF	80	423	15	17.2	15.8	(Bhanage <i>et al.</i> , 2001)
10	MgO	PO	DMF	20	408	12	-	41.0	(Yano <i>et al.</i> , 1997)
11	MgO	SO	DMF	20	408	12	-	60.0	(Yano <i>et al.</i> , 1997)
12	Nb <sub>2</sub> O <sub>5</sub>	PO	DMF	50	423	12	-	88.0	(Aresta <i>et al.</i> , 2003a)
13	Nb <sub>2</sub> O <sub>5</sub>	SO	DMF	50	408	12	-	80.0	(Aresta <i>et al.</i> , 2003a)
14	Mg-Al oxide	PO	DMF	5	393	24	97.7	88.0	(Yamaguchi <i>et al.</i> , 1999)
15	Mg-Al oxide	SO	DMF	5	373	15	97.8	90.0	(Yamaguchi <i>et al.</i> , 1999)
16	Zn-Si oxide	PO	TBAB <sup>b</sup>	45	293	6	100	100	(Ramin <i>et al.</i> , 2006)
17	Cs-P-Si oxide	PO	-	80	473	8	96.0	94.0	(Yasuda <i>et al.</i> , 2006)
18	DMF	SO	-	79	423	15	-	85.0	(Kawanami and Ikushima, 2000)

<sup>a</sup> PO: propylene oxide; SO: styrene oxide; <sup>b</sup> TBAB: Tetra-*n*-butyl ammonium bromide.

The performance of metal oxide catalysts is not yet satisfactory and much higher activities are required before such processes can be used at industrial scale. Mixed metal oxides or mixed metal-non-metal oxides have been studied for the syntheses of cyclic carbonates. Yamaguchi *et al.* (1999) reported that the Mg-Al oxides are effective for the cycloaddition of CO<sub>2</sub> and various epoxides in the presence of DMF (Table 2.3, entries 14 and 15). The catalyst characterisation of Mg-Al showed the acidic sites co-exist with the basic sites on the surface of the catalyst. It has been suggested that the cooperation of both acidic and basic sites contribute to the high catalytic activity of Mg-Al mixed metal oxide. Similarly other acid-base bifunctional catalytic systems have been reported for the synthesis of cyclic carbonates. Zinc oxide particles loaded on silica (ZnO-SiO<sub>2</sub>) showed excellent performance in the presence of tetra-*n*-butyl ammonium bromide (TBAB) as a co-catalyst (Table 2.3, entry 16), where the yield of PC reached 100%. Cs-P-Si was also reported as an effective catalyst for the cycloaddition of CO<sub>2</sub> to PO in the absence of a solvent/co-catalyst (Table 2.3, entry 17). The effect of the bifunctional action of acidic and basic sites is vital for a better catalytic performance of mixed metal/non-metal oxide catalysts (Yamaguchi *et al.*, 1999; Ramin *et al.*, 2006; Yasuda *et al.*, 2006).

Some studies have been carried out to investigate the performance of Zn-containing catalysts (Sankar *et al.*, 2004; Mori *et al.*, 2005; Wu *et al.*, 2008) and reported the importance of Zn<sup>2+</sup> for the activation of epoxide during the cycloaddition reaction. Dai *et al.* (2009) prepared Mg modified Zn-Al mixed oxide catalyst that showed a good catalytic activity for the cycloaddition of CO<sub>2</sub> to propylene oxide under mild conditions in the presence of triethylamine. Catalyst characterisation of Mg-Zn-Al oxide showed the presence of both acidic and basic sites on the surface of the catalyst, which are beneficial for the cycloaddition reaction.

### 2.4.3. Zeolite and Smectite Catalysts

Zeolites are hydrated aluminosilicate minerals that are produced from interlinked tetrahedra of alumina (AlO<sub>4</sub>) and silica (SiO<sub>4</sub>). Zeolites are well defined microporous crystalline solids with a relatively open, three-dimensional crystal structure with large open pores and very regular arrangement. Zeolites are used widely in the process industry as adsorbents and/or catalysts. Zeolites are known

to be very stable and therefore ideal for catalytic processes involving high temperature and pressure. The basicity and reactivity of zeolites can be enhanced *via* the incorporation of alkali metal oxides into the pores of the zeolite (Dorskocil *et al.*, 1999; Davis *et al.*, 2000; Tu and Davis, 2001).

The role of introducing alkali metal oxides into the zeolite pores was reported by Davis *et al.* (2000) who concluded that the presence of the alkali oxide promote and enhance the catalytic activity of the zeolite. Interestingly, an increase in the electropositivity of the alkali metal cations increased the catalytic activity ( $\text{Na}^+ < \text{K}^+ < \text{Cs}^+$ ). Alkali and alkaline-earth-modified Engelhard Titano-Silicate-10 (ETS-10) molecular sieve catalysts have been reported as effective catalyst for the cycloaddition of  $\text{CO}_2$  to PO (Dorskocil, 2004; 2005). The alkali modified catalysts were remarkably more effective compared to alkaline-earth modified catalysts. The presence of a small amount of water during the cycloaddition reaction enhanced the rate of reaction without an increase in the side product formation. This observation is similar to the earlier study carried out by Tu and Davis (2001). Dorskocil (2004, 2005) proposed that the presence of water enhances acidity of the Brønsted sites of the catalyst, produces localised carbonic acid sites that take part in the reaction, enhances the transport of the reactants to the interior active sites of the catalysts and modifies the alkali metal oxide to produce sites with high turnover frequency.

However, despite the attempts to modify zeolites with the addition of alkali metal oxides and small amounts of water, the yield of carbonate is low and only reached a maximum of 55% (Davis *et al.*, 2000). Srivastava *et al.* (2003) evaluated the performance of titanosilicate molecular sieve in the presence of various co-catalysts for the cycloaddition of  $\text{CO}_2$  to epichlorohydrin. A good catalytic activity was reported when dichloromethane ( $\text{CH}_2\text{Cl}_2$ ) was used as a co-catalyst. Highest epichlorohydrin conversion (94.2%) and cyclic carbonate selectivity (97%) were reported when 4-dimethylaminopyridine (DMAP) was used as a co-catalyst at 433 K, 6.9 bar for 4 hours. The study showed that the presence of both catalyst and co-catalysts are vital for an increase in the rate of cycloaddition reactions. Xu *et al.* (2013a) recently reported that the reaction of PO, MeOH and  $\text{CO}_2$  to produce PC and DMC over basic zeolite catalysts that were prepared by loading potassium hydroxide (KOH) on zeolite molecular

sieves. An optimum PO conversion of (~80%) was achieved when the reaction was carried out at 453 K and 20 bar. However, the yield of PC and DMC is still very low.

Smectite is a hexagonal layered clay mineral and its acidic and basic properties can be improved by the incorporation of alkali or transition metal ions into the layered structure (Bhanage *et al.*, 2003a). A series of Mg, Ni, and Mg-Ni containing mesoporous smectites incorporated with various amounts of Na<sup>+</sup>, K<sup>+</sup> and Li<sup>+</sup> have been prepared and employed to catalyse the cycloaddition reaction of PO and CO<sub>2</sub> to produce PC by Fujita *et al.* (2002). The study showed that the elemental composition greatly affects the catalytic performance of the smectite. An increase in the composition of K<sup>+</sup> into the Na-modified Mg-containing smectite increased both conversion of PO and selectivity of PC. The highest PC yield (80.7%) was achieved using high concentrations of Na<sup>+</sup> and K<sup>+</sup> at 423 K and 80 bar. Upon replacement of potassium with lithium and magnesium by nickel, the catalytic activity was unsatisfactory. The application of alkali incorporated smectites as a catalyst for the synthesis of PC have not been studied sufficiently as the number of papers covering this topic is very limited. Therefore, more effort should be dedicated to further study this topic.

#### 2.4.4. Supported Catalysts

Organic bases (Kawanami and Ikushima, 2000; Barbarini *et al.*, 2003; Jiang and Hua, 2006), organometallic complexes (Darensbourg *et al.*, 2004; Chen *et al.*, 2007; Jing *et al.*, 2007, Jutz *et al.*, 2008) and ionic liquids (Li *et al.*, 2004; Sun *et al.*, 2008; Zhou *et al.*, 2008; Sun *et al.*, 2009) usually show a better activity for the cycloaddition reactions compared to metal oxides and modified zeolite catalysts. However, a product/catalyst separation is a major disadvantage due to the homogeneous nature of such catalysts. Therefore, a lot of effort is been put into the immobilisation of effective homogeneous catalysts onto suitable supports in order to avoid separation difficulties.

##### 2.4.4.1. Supported organic base catalysts

Molecular sieves have been used as support of various organic base catalysts. Barbarini *et al.* (2003) investigated the catalytic performance of MTBD (7-methyl-1,5,7-triazabicyclo[4.4.0]dec-5-ene) and its heterogeneous counterpart MCM-41-

TBD that was obtained by covalently bonding 1,5,7-triazabicyclo[4.4.0]dec-5-ene (TBD) to molecular sieve (MCM-41). Catalytic reactions were carried out in the presence of acetonitrile at 413 K and 50 bar resulting in 90% yield of styrene carbonate when MCM-41-TBD was used as a catalyst. The catalyst could be separated and reused easily, however, the reaction time was considerably long (70 h) and is not desirable in the industry.

Srivastava *et al.* (2005a; 2006a; 2006b; 2006c) and Srinivas and Ratnasamy (2007) modified SBA-15 by immobilizing nitrogen based organic molecules such as alkyl amines, adenine and guanine. The studies showed that adenine catalysts showed the highest activity and proposed that the intermediate basicity of the active sites enables CO<sub>2</sub> activation as CO<sub>2</sub> is not held either too weakly or too strongly. Also, the immobilisation of Lewis acidic Al<sup>3+</sup> and Ti<sup>4+</sup> ions were studied in an attempt to enhance the epoxide adsorption and the overall catalytic activity. In a similar study, Shiels and Jones (2007) immobilized DMAP onto SBA-15 for the cycloaddition reaction of CO<sub>2</sub> to PO.

Silica (SiO<sub>2</sub>) has also been reported as a possible support for organic base catalysts. Zhang and co-workers (2006) studied the catalytic performance of silica supported amine catalysts including, NH<sub>2</sub>/SiO<sub>2</sub>, NH(CH<sub>2</sub>)<sub>2</sub>NH<sub>2</sub>/SiO<sub>2</sub> and 1,5,7-triazabicyclo[4,4,0]dec-5-ene/SiO<sub>2</sub> (TBD/SiO<sub>2</sub>). The results showed an increase in the catalytic activity with an increase in the basic strength of the amines (i.e. TBD/SiO<sub>2</sub> > NH(CH<sub>2</sub>)<sub>2</sub>NH<sub>2</sub>/SiO<sub>2</sub> > NH<sub>2</sub>/SiO<sub>2</sub>). A PO conversion of 99.5% was achieved at the optimum reaction conditions (423 K, 20 bar and 20 h) when TBD/SiO<sub>2</sub> was used as a catalyst. Methyl groups were used to remove hydroxyls from the surface of TBD/SiO<sub>2</sub> to study the significance of the hydroxyls for the reaction. The modified catalyst was tested at the optimum conditions and surprisingly the PO conversion decreased to 0.2% showing that surface hydroxyls are vital for the cycloaddition reaction of PO and CO<sub>2</sub>. Jagtap *et al.* (2007) also reported that SiO<sub>2</sub> supported pyridine are effective catalysts for the synthesis of PC.

### 2.4.4.2. Supported organometallic complexes catalysts

Various organometallic complexes of Cr, Co, Al, Ni, Mn, Zn and Ru of various types of salen (Paddock and Nguyen, 2001; Shen *et al.*, 2003; Lu *et al.*, 2004, Darensbourg *et al.*, 2004; Chen *et al.*, 2007; Jing *et al.*, 2007; Jutz *et al.*, 2008), porphyrin (Paddock *et al.*, 2004; Srivastava *et al.*, 2005b; Jin *et al.*, 2007) and others (Jiang *et al.*, 2005; Bu *et al.*, 2007) have been reported to show good catalytic activity for the cycloaddition reaction of PO and CO<sub>2</sub>. However, the homogeneous nature of the catalysts adds extra burden and complexity to the catalytic process. The catalyst is not easy to separate and often is unstable and non-reusable. The immobilization of such complexes into a solid support can be a step forward towards the fabrication of stable and reusable heterogeneous catalysts for the synthesis of cyclic carbonates.

The immobilisation of chromium complexes on aminopropyl functionalised SiO<sub>2</sub>, ITQ-2 (zeolite) and MCM-41 (molecular sieve) has been studied (Baleizao *et al.*, 2002; Alvaro *et al.*, 2004; Ramin *et al.*, 2005). Baleizao *et al.* (2002) found that Cr-salen complexes immobilised on SiO<sub>2</sub>, ITQ-2 and MCM-41 have excellent selectivity for the ring opening and conversion (100%) of cyclohexene oxide. However, a severe leaching of the complex to the solution was observed. The catalysts were then modified so that the Cr complex is attached to the surface of the complex *via* covalent linkage. Results showed that the new modified catalyst was more stable and no leaching was observed, however, the conversion of cyclohexene oxide reduced to less than 70%. Similar results and observations were reported by Alvaro *et al.* (2004) and Ramin *et al.* (2005) when Cr-salen complexes immobilised SiO<sub>2</sub> and ITQ-2 were used as catalysts for the synthesis of cyclic carbonates. In contrast to Baleizao *et al.* (2002) study, Alvaro *et al.* (2004), Ramin *et al.* (2005) and Jutz *et al.* (2008) reported that when manganese complex was attached to the surface of the amino ligand *via* covalent linkage an increased catalytic activity was observed. However, the covalently immobilised catalyst lost its catalytic activity after the first run.

Lu *et al.* (2002) reported that an aluminium phthalocyanine complex covalently immobilised to MCM-41 is an effective catalyst for the cycloaddition reaction in the presence of tetra-*n*-butylammonium bromide (*n*-Bu<sub>4</sub>NBr) as a co-catalyst. The catalyst showed good stability and could be reused up to 10 cycles without a

significant decrease in its performance. Wong and co-workers (2007) also reported that a tricarbonyl Re(I) complex immobilised on ionic liquid (pyrrolidinium moiety) acts as an excellent catalyst in the presence of pyrrolidinium bromide (solvent) for the cycloaddition reaction. Epoxide conversion marginally decreased from 98% to 95% after 10 cycles of catalyst reusability. However, the recycling of the Re complex *via* extraction added to the complexity and cost of the process. Eventhough advances have been made to fabricate new and innovative immobilised complexes, their application in catalysing cycloaddition reactions is still limited due to drawbacks associated with poor reusability, the requirement of a solvent/co-catalyst and expensive separation techniques.

### 2.4.4.3. Supported ionic liquid catalysts

Ionic liquids are widely used as solvents and/or catalysts in organic synthesis. Peng and Deng (2001) were the first to report the use of ionic solvent in cycloaddition reactions. Many researches followed similar steps and studied the use of various ionic liquids such as quaternary ammonium, phosphonium, imidazolium and pyridinium as suitable catalysts for the syntheses of cyclic carbonates (Caló *et al.*, 2002; Kossev *et al.*, 2003; Li *et al.*, 2004; Sun *et al.*, 2008; Zhou *et al.*, 2008; Sun *et al.*, 2009)

The separation and reusability of ionic liquids in catalysis can be challenging and therefore, the immobilization of ionic liquids on solid supports can improve the catalyst recyclability and reusability. Xiao *et al.* (2006) reported the efficiency of ionic liquid (3-*n*-butyl-1-propyl-imidazolium) grafted silica for the cycloaddition of CO<sub>2</sub> and epoxide in the presence of metal salts as co-catalysts such as zinc chloride (ZnCl<sub>2</sub>), nickel (II) chloride (NiCl<sub>2</sub>) and aluminium chloride (AlCl<sub>3</sub>). Highest propylene carbonate yield (95%) was achieved when the reactions were carried out over ionic liquid (3-*n*-butyl-1-propyl-imidazolium), grafted silica and ZnCl<sub>2</sub> at 383 K and 15 bar for 1 h. When the catalyst was recovered and reused for a second run the PC yield dropped to 86% due to the loss of ionic liquid.

Silica supported quaternary ammonium and imidazolium salts have been reported effective for the propylene synthesis with yield > 95% (Wang *et al.*, 2006b; 2007b). Unsupported quaternary ammonium salts are also active for the synthesis of PC and their activity is dependent on the anions (i.e. order of activity:

$n\text{-Bu}_4\text{NBr} > n\text{-Bu}_4\text{NI} > n\text{-Bu}_4\text{Cl} > n\text{-Bu}_4\text{NF}$ ). However, this order of activity is absent among  $\text{SiO}_2$ -supported counterparts (Wang *et al.*, 2006b). Wang *et al.* (2006b) also reported that the length of the alkyl chain of supported quaternary ammonium bromides has some effect on the cycloaddition reactions. Tetra-methyl-ammonium bromide ( $\text{Me}_4\text{NBr}$ ), tetra-ethyl-ammonium bromide ( $\text{Et}_4\text{NBr}$ ), tetra-propyl-ammonium bromide ( $n\text{-Pr}_4\text{NBr}$ ) and tetra-butyl-ammonium bromide ( $n\text{-Bu}_4\text{NBr}$ ) were tested alone for the synthesis of PC at identical conditions. All compounds except  $\text{Me}_4\text{NBr}$  (which was completely inactive) were highly active for the synthesis of PC.

Similar combined effect of the support and catalyst were observed over chitosan immobilised 2-hydroxypropyl trimethylammonium chloride (Takahashi *et al.*, 2006; Zhao *et al.*, 2007) and over  $\text{SiO}_2$ -immobilised phosphonium halides (Sakai *et al.*, 2008). It is clear that  $\text{SiO}_2$  and chitosan play a vital role in the synthesis of cyclic carbonates over catalysts of supported ionic liquids, however, the mechanism of these roles are still unclear.

Ionic liquids can also be incorporated onto solid materials *via* copolymerising the ionic liquid into the monomer of the solid material of interest. Xie *et al.* (2007) reported that 3-butyl-1-vinylimidazolium chloride was copolymerised with divinylbenzene and the ionic liquid was successfully covalently immobilised on the polymer matrix. Similarly Zhu *et al.* (2007) and Udayakumar *et al.* (2008) reported that molecular sieves can be used as effective material support material for ionic liquids. Dai *et al.* (2009) prepared mesoporous silica (SBA-15) and Al-SBA-15 which have been grafted with hydroxyl ionic liquid (3-(2-hydroxyl-ethyl)-1-propylimidazolium bromide) (HEPrIMBr). When tested for the cycloaddition reaction between PO and  $\text{CO}_2$  at 413 K and 20 bar, a PC yield of 98.6% was achieved, which was higher than other supported ionic liquids reported in the literature for the synthesis of PC.

Various other supported catalysts have been studied for the syntheses of cyclic carbonates from  $\text{CO}_2$  and corresponding epoxides. These include poly(4-vinylpyridine)-supported  $\text{ZnCl}_2$  (Kim *et al.*, 2002),  $\text{ZrO}_2$ -supported samarium oxychloride ( $\text{SmOCl}$ ) (Yasuda *et al.*, 2003), resin-supported gold (Xiao *et al.*, 2005) and ion exchange resins (Du *et al.*, 2005). A good catalytic activity for the

syntheses of cyclic carbonates was reported for supported catalyst, however, the catalyst stability and reusability is a major limitation for commercialisation of such catalytic processes.

### 2.4.5. Other Heterogeneous Catalysts

Zinc based catalysts have been reported for the effective cycloaddition of CO<sub>2</sub> to epoxides. Sankar *et al.* (2004) reported that Zn-substituted sandwich type polyoxometalate Na<sub>12</sub>[WZn<sub>3</sub>(H<sub>2</sub>O)<sub>2</sub>(ZnW<sub>9</sub>O<sub>34</sub>)<sub>2</sub>].46H<sub>2</sub>O along with DMAP and CH<sub>2</sub>Cl<sub>2</sub> as a solvent was effective for the conversion of PO at 413 K and 40 bar in 3 h. In another study, Mori *et al.* (2005) prepared a zinc based hydroxyapatite catalyst by exchanging the hydroxyapatite (Ca<sub>10</sub>(PO<sub>4</sub>)<sub>6</sub>(OH)<sub>2</sub>) with zinc nitrate and it showed a good catalytic activity in the presence of an organic base as a co-catalyst. This is attributed to the effect of Zn which acts as Lewis acid and activates the epoxide while organic base which attacks the less hindered carbon atom and open the epoxide ring. Most studies about cycloaddition reaction of CO<sub>2</sub> and epoxides proposed that the epoxide and CO<sub>2</sub> are activated by acidic and basic site respectively and therefore, acid-base bifunctional catalysts are usually effective for the synthesis of cyclic carbonates. Thus, research into the development of heterogeneous catalysts with both acidic and basic properties is a key step towards an improved and efficient cyclic carbonates syntheses route.

## 2.5. DIMETHYL CARBONATE (DMC)

DMC is a promising environmentally benign compound that exhibits versatile and excellent chemical properties. It has low toxicity and high biodegradability which makes it a green reagent and a safer alternative to poisonous dimethyl sulphate and phosgene (Sato and Souma, 2000). DMC can be used as a good precursor material for the production of polycarbonates (Bian *et al.*, 2009a; 2009b) and as an important carbonylation and methylation agent (Sato *et al.*, 1999). DMC can be also used as an oxygenate additive to gasoline to improve its performance and reduce exhaust emission (Zhang *et al.*, 2011).

### 2.5.1. Properties of Dimethyl Carbonate (DMC)

Most of the properties of DMC make it a green reagent particularly if compared to conventional methylating and alkylating agents such as phosgene, methyl halides and dimethyl sulphate. DMC is classified as a flammable liquid, however, it is a

non-toxic compound. DMC smells like methanol and does not have an irritating effect upon contact or inhalation and therefore can be handled safely without special precautions (Tundo and Esposito, 2008). It is not corrosive and has high biodegradability (>90%). Some of the physiochemical properties of DMC are listed in Table 2.4.

Table 2.4. Properties of DMC.

Properties of DMC	
Molar Mass	90.08 g mol <sup>-1</sup>
Melting point	275 K
Boling point	363 K
Relative density	1.069 g cm <sup>-3</sup>
Viscosity	0.625 cP
Solubility in water	130 g L <sup>-1</sup>
Dielectric constant	3.087

DMC has tuneable chemical properties and reactivity that largely depends on the reaction conditions. DMC can react as a methylating or methoxycarbonylating agent in the presence of a nucleophile. At reflux temperature (363 K), DMC primarily acts as a methoxycarbonylating agent, where the nucleophile attacks the carbonyl carbon of DMC leading to esterification reactions. At higher temperature (433 K), DMC tend to act as a methylating agent, where a nucleophile attacks the methyl group of the DMC (Tundo, 1991).

### 2.5.2. Industrial Applications of Dimethyl Carbonate

#### 2.5.2.1. Intermediate for polycarbonate synthesis

By far the most prominent application of DMC is its use as an intermediate in the synthesis of polycarbonate, which currently accounts for just over half of DMC's total consumption (Coker, 2012). In 2002, General Electric Plastics (GEP) installed a technology for the production of polycarbonates *via* DMC (Delledonne *et al.*, 2001) and eliminated the use of toxic phosgene as a toxic feedstock (Rivetti *et al.*, 2000). The GEP process for the DMC based route to polycarbonates was based on the reaction of diphenyl carbonate with bisphenol A. The transesterification reaction between DMC and phenol can be carried out in

the presence of commercially available homogeneous catalysts (Shaikh and Sivaram, 1996). EniChem has developed a process whereby DMC reacts with phenol as a first stage process to produce methylphenyl carbonate, which is then disproportionated to diphenyl carbonate in the presence of titanium alkoxide catalyst. Aliphatic polycarbonates are attractive biodegradable materials that can be used in the production of thermoplastic urethanes, thermoelastomers, paints and adhesives and much more (Park *et al.*, 2013; Xu *et al.*, 2013b). The best method for preparing aliphatic polycarbonates is the condensation polymerisation of DMC and aliphatic diols (Park *et al.*, 2013). Transesterification of DMC with allyl alcohol produced diallylcarbonate, which upon condensation with diethylene glycol produces monomers that can be used for the preparation for optical lenses (Delledonne *et al.*, 2001).

### 2.5.2.2. DMC as a methylating agent

DMC is a versatile reagent that provides a valuable green substitute to typical undesirable reagents used for methylation reactions such as toxic and corrosive phosgene, dimethyl sulphate and methyl halides (Bernini *et al.*, 2011; Glasnov *et al.*, 2012). Among the specific synthetic advantages of using DMC as a methylating agent is its high selectivity to mono-methylation of activated methylene groups in substrates such as arylacetonitriles, which are useful intermediates in the production of anti-inflammatory drugs (Selva *et al.*, 1994; Bomben *et al.*, 1995; Loosen *et al.*, 1996). Methylation of phenols, amines, amides, indoles and benimidazoles with DMC can be achieved in the presence of basic catalysts. This approach provides a practical, efficient and environmentally friendly process for important chemical transformation. The resulting products from this transformation and their derivatives i.e. *p*-phenylenediamine find many applications as precursor to polymers, rubber antioxidants, temporary tattoos, hair dye and much more (Selva *et al.*, 1997; Fu *et al.*, 1998; Shieh *et al.*, 2001). Quaternary ammonium salts can be produced *via* the methylation of aliphatic amines. An important application is the synthesis of these salts from trimethylamine and DMC to produce chlorine free ethyl ammonium hydroxide salts (Yagi and Shimizu, 1993).

### 2.5.2.3. DMC for the production of carbamates and isocyanates

DMC can react with primary or secondary amines to produce carbamates in the presence of a suitable catalyst. Numerous catalysts have been studied in order to achieve the maximum yield of carbamates. Strong bases such as alkali alkoxides, carbon dioxide and Lewis acids such as aluminium chloride ( $\text{AlCl}_3$ ), aluminium iodide ( $\text{AlI}_3$ ) and mercuric salts, zinc acetate and lead oxide have been evaluated as a suitable catalyst for the synthesis of carbamates (Aresta and Quaranta, 1991; Fu and Ono, 1994; Baba *et al.*, 2002; Sima *et al.*, 2002). This provides a promising, green and non-phosgene route for the synthesis of isocyanates and carbamates.

### 2.5.2.4. DMC as a solvent

In 2009, DMC was classified as solvent that is exempt from classification as volatile organic compound and therefore it has grown in popularity and application as a solvent. DMC is considered as a green reagent. DMC is a fast evaporating polar solvent with excellent solubility properties that can dissolve most common coating resins and hence it has been considered as a viable alternative to acetate esters, alcohols and ketones in paints and adhesives industry (Rivetti *et al.*, 2000). DMC is classified as the leader of carbonic esters whose properties can be easily tailored for a specific application e.g. for the production of lubricating oils (Rudnick, 2013). DMC has recently found many applications as an organic solvent in the electronic industry. When DMC is subjected to specific cooling and heating cycles, operating at particular temperature and pressure, a dimethyl product can be obtained not only having a high purity (99.99%), but also a chlorine content of less than 1 ppm. This makes DMC a more useful a solvent for the production of the electrolyte of lithium rechargeable batteries (Tasaki *et al.*, 2009). DMC can be also used to produce isocyanates, which are widely used in the manufacture of foams, fibres, paints, varnishes, elastomers and building insulation materials (Carnaroglio *et al.*, 2013).

### 2.5.2.5. DMC as a fuel additive

DMC is a strong contender as an oxygenate to reduce vehicle emissions and hence reduce environmental and health risks. Also, the utilisation of DMC can help meet the clean Air Act specification for gasoline. DMC has outstanding oxygen content (53%) that is 3 times higher than the oxygen content in methyl

*tert*-butyl ether and is an effective octane enhancer. DMC has good blending properties and does not form a separate phase in a water stream (Pacheco and Marshall, 1997). DMC is low in toxicity, biodegradable and is shown to have a low photochemical ozone creation potential compared to conventional fuels making it an environmentally safe fuel additive (Bruno *et al.*, 2009; Choi *et al.*, 2002). Also, from an economic point of view, studies have shown that it is more economical to use DMC in reformulated gasoline compared to methyl *tert*-butyl ether produced from butane (Pacheco and Marshall, 1997).

## 2.6. SYNTHESIS ROUTES OF DMC

### 2.6.1. Methanolysis of Phosgene (COCl<sub>2</sub>)

Methanolysis of phosgene in the presence of sodium hydroxide is one of the oldest routes for the synthesis of DMC (Shaikh and Sivaram, 1996). However, this process has some shortcomings in regards to safety issues as phosgene is an extremely toxic chemical and hydrochloric acid (HCl) is produced as a side product as shown in Figure 2.1. Therefore, researches have been prompted to investigate new greener routes for the production of DMC.

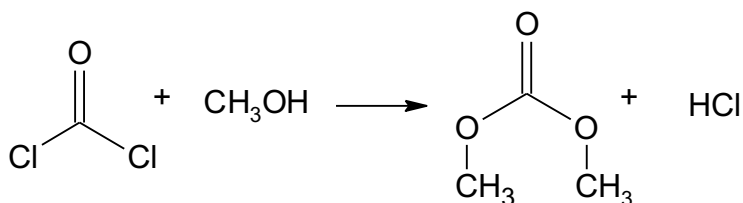


Figure 2.1. Methanolysis of phosgene.

### 2.6.2. Oxidative Carbonylation

In 1983, EniChem developed the first industrial plant for the synthesis of DMC from the reaction of methanol, carbon monoxide and oxygen (Rivetti and Romano, 1992; Delledonne *et al.*, 2001). The reaction shown in Figure 2.2 was carried out using homogeneous copper chloride (CuCl<sub>2</sub>) catalyst at 403 K and 24 bar. The catalytic system has some drawbacks as follows:

- CuCl<sub>2</sub> is soluble in MeOH and therefore reactants cannot react with the catalyst efficiently to form active intermediates.

- $\text{CuCl}_2$  is highly corrosive to reactor vessels/ materials.
- Catalyst deactivation due to loss of  $\text{Cl}_2$  (King, 1996).
- Catalyst short life time in liquid processes (Gongying *et al.*, 2000).

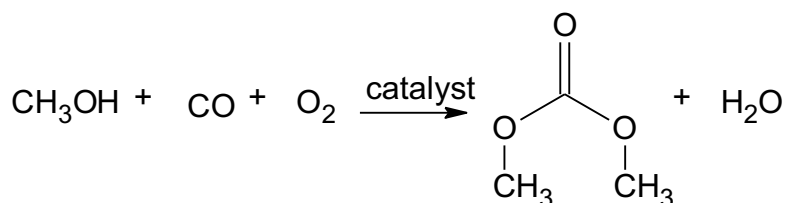


Figure 2.2. Oxidative carbonylation of MeOH.

Delledonne *et al.* (1995) studied the usage of cobalt complexes catalyst for the oxidative carbonylation in an attempt to reduce corrosion and prolong catalyst life for liquid processes. Other attempts to improve catalyst performance were made such as the use of copper chloride/potassium chloride mixture as a catalyst by Kricsfalussy *et al.* (1998) and the introduction of solvents and promoters for example amines, pyridines and immobilised copper salts on supports (Bhattacharya and Nolan, 1987; Sato *et al.*, 2000; Li *et al.*, 2001; Anderson and Root, 2004; Mo *et al.*, 2006; Richter *et al.*, 2007; Tomishige *et al.*, 1999). The use of amine ligands such as pyridine increased the catalytic effectiveness, however, it failed to synthesise DMC due to water sensitivity (Delledonne *et al.*, 2001). The use of dialkyl peroxides have been used to prevent the formation of water in the presence of a copper pyridine complex as the co-catalyst (Morris *et al.*, 1987).

### 2.6.3. Transesterification of Carbonates or Urea

The transesterification of cyclic carbonates i.e. ethylene carbonate and propylene carbonate with methanol is considered as a viable route for the synthesis for DMC (Zhu *et al.*, 1996; Bhanage *et al.*, 2002; Bhanage *et al.*, 2003b; Zhang *et al.*, 2010). Numerous homogeneous catalysts have been evaluated for the transesterification reaction such as alkali metals, ionic liquids and ammonium salts (Darensbourg and Holtcamp, 1996; Bhanage *et al.*, 2002). In addition, numerous heterogeneous catalysts have been proposed for the transesterification reaction, including, molecular sieves (Knifton, 1987) basic metal oxides (Duranleau, 1987), basic salts (Watanabe and Tatsumi, 1998),

metal cyanides (Knifton and Duranleau, 1991), hydrotalcites (Knifton, 1993), anion exchange resins (Leitner, 2002) and silica (Cui *et al.*, 2003). Typically, reactions take place at 373–423 K and at moderate pressures. The addition of a co-catalyst allows for milder reaction conditions i.e. 278–283 K (Knifton, 1987; Delledonne *et al.*, 2001).

Unfortunately, the transesterification reaction of cyclic carbonates with methanol is an equilibrium limited reaction and thermodynamically unfavourable. Therefore, the yield of DMC is still low. Several attempts have been made to improve the yield of DMC. These include the removal of reaction product (DMC) by distillation or by selective solvent extraction of the produced DMC (Delledonne *et al.* 2001). This reaction also suffers from the complications associated with the co-generation of side products, ethylene glycol and propylene glycol when ethylene carbonate and propylene carbonate are used as reactants for the transesterification reaction.

Although great advances have been made (Wei *et al.*, 2003; Cui *et al.*, 2004b; De Filippis *et al.*, 2006; Dhuri and Mahajani, 2006; Fujita *et al.*, 2006; Srivastava *et al.*, 2006b; Wang *et al.*, 2006a; 2006c; Abimanyu *et al.*, 2007; Ju *et al.*, 2007; Stoica *et al.*, 2009) most of the catalytic processes suffer from low catalyst activity (measured in terms of DMC yield), high reaction temperature and pressure and the use of expensive metallic compounds. Therefore, there is a desire for the development of more efficient, easily prepared and cost effective catalytic system for the synthesis of DMC *via* the transesterification of cyclic carbonates (Yang *et al.*, 2010).

DMC can be directly synthesised *via* the transesterification of MeOH and urea. Ammonia is produced as a co-product along with DMC in this reaction but can be recycled for urea synthesis. This makes this route interesting and environmentally friendly process. However, the reaction is thermodynamically unfavourable (Pacheco and Marshall, 1997). During the reaction, urea is converted to methylcarbamate at relatively low temperatures (373–423 K) in the presence of a suitable catalyst (Sun *et al.*, 2004c). Then the carbamate reacts with methanol at slightly higher temperatures (453–463 K) in the presence of a suitable catalyst to produce DMC. These reactions can be carried out in a two separate steps or in

one pot synthesis depending on the catalyst used. The removal of the co-product produced during the reaction i.e. ammonia is a key driving force for higher rates of reactions and therefore, these reactions can be carried out in a reactive distillation column.

Some research advances has been made in an attempt to find a suitable catalytic process for the reaction. Cho *et al.* (1996) studied the application of simple homogeneous catalysts such as potassium carbonate ( $K_2CO_3$ ) and sodium methoxide ( $CH_3ONa$ ) for this reaction, however, DMC yield was  $< 5\%$ . Saleh *et al.* (1996), Suciu *et al.* (1998) and Ryu and co-workers (2002) revealed that organotin derivatives were active catalysts for the synthesis of DMC from urea. Nevertheless, the homogenous nature of the catalysts posed separation and deactivation problems. Also lead, magnesium, zinc, calcium and their compounds have been investigated for urea-based reactions (Bhanage *et al.*, 2003b; Aresta *et al.*, 2004; Wang *et al.*, 2004; Zhao *et al.*, 2004).

Even though this process seems attractive from a “Green” and “Sustainable” point of view, more effort is required in order to develop novel catalytic process. The process should be cost effective, the catalyst should be easy to handle and the product i.e. DMC should be easily separated.

### 2.6.4. Direct Transformation of $CO_2$ to DMC

#### 2.6.4.1. Direct synthesis of DMC from methanol and $CO_2$

The direct synthesis of carbonates *via* the carboxylation of alcohols studied since the 1982 (Hoffman, 1982) and fulfils the “Sustainable Society” and “Green Chemistry” approach (Delledonne *et al.*, 2001). In particular, the direct synthesis of DMC from MeOH and  $CO_2$  has gained much interest recently. Various catalyst have been studied extensively, however, the methanol conversion and DMC yield are still very low. This is due to the equilibrium limited reaction, (see Figure 2.3) and the catalyst deactivation when water is formed as a by-product.

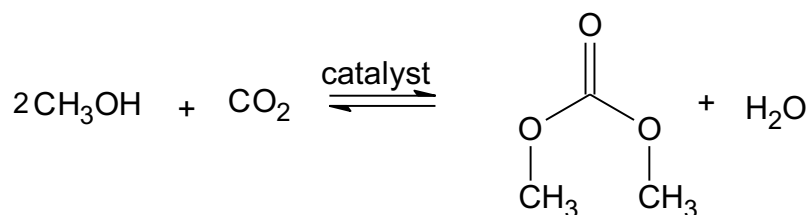


Figure 2.3. Direct synthesis of DMC *via* the carboxylation of methanol.

#### 2.6.4.2. Synthesis of DMC from epoxides and CO<sub>2</sub>

DMC synthesis *via* the transesterification of cyclic carbonates with methanol has attracted much attention from the viewpoint of “green chemistry” and “sustainable development” (Cui *et al.*, 2004a; Jagtap *et al.*, 2008). The two-step reaction process shown in Figure 2.4 is more attractive compared with other process routes such as methanolysis of phosgene and oxidative carbonylation of methanol as it avoids using toxic, corrosive, flammable, and explosive materials (Yang *et al.*, 2010).

The challenge researchers are facing is finding a suitable catalyst which can show high catalytic activity under mild reaction conditions. The performance of different catalysts have been investigated such as metal oxides (Bhanage *et al.*, 2001; Wang *et al.*, 2011a), basic salts (Fang and Fujimoto, 1996; Murugan and Bajaj, 2011), molecular sieves (Aresta and Quaranta, 1997), ionic liquids (Wang *et al.*, 2009; Yang *et al.*, 2010) and polymer resin (Bhanage *et al.*, 2001; Jagtap *et al.*, 2008). However, most of the catalytic systems investigated showed low catalytic activity (Wang *et al.*, 2009), low yields of DMC and high waste generation (Jagtap *et al.*, 2008). Therefore, there is still a need for the development of a suitable catalytic system for the effective and selective synthesis of DMC *via* methanol esterification.

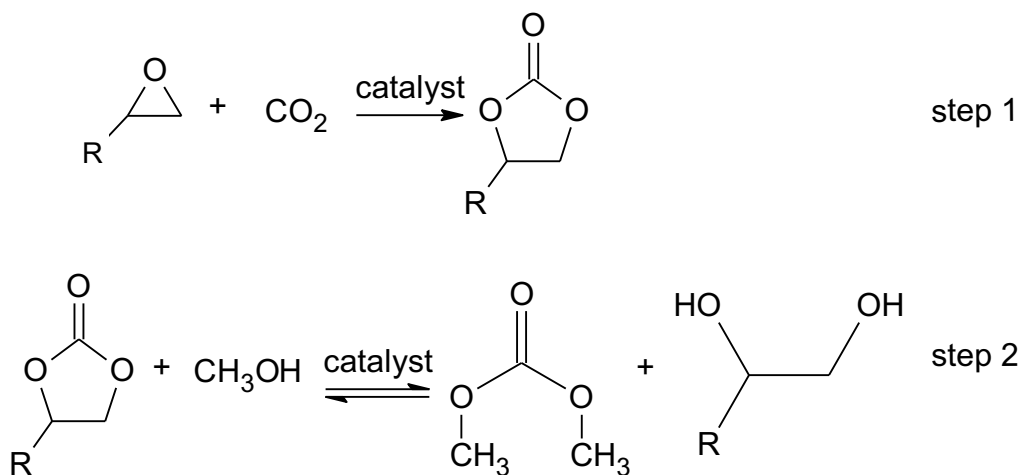


Figure 2.4. Two-step process for DMC production utilising CO<sub>2</sub> as a raw material.

#### 2.6.4.3. Synthesis of DMC from acetals and CO<sub>2</sub>

The direct synthesis of DMC from MeOH and CO<sub>2</sub> faces many challenges such as thermodynamic limitation, catalyst deactivation and DMC hydrolysis due to the formation of water as a by-product (Almusaiteer, 2009; Dai *et al.*, 2009; Bansode and Urakawa, 2014; Honda *et al.*, 2014). Using dehydrated derivatives such as acetals and ortho-esters as a starting material for the synthesis of DMC from CO<sub>2</sub> can eliminate some of those challenges (Choi *et al.*, 2002; 2008). Chu *et al.* (2002) studied the applicability of polymer supported quaternary ammonium iodide as a possible heterogeneous catalyst for the synthesis of DMC from CO<sub>2</sub> and trimethyl orthoesters. However, this approach has drawbacks due to the high cost of the raw material (i.e. trimethyl orthoesters) and the requirement for the addition of phosphorus pentoxide (P<sub>2</sub>O<sub>5</sub>) in order to achieve high yields of DMC.

## 2.7. CATALYSTS USED FOR DMC SYNTHESIS

### 2.7.1. Catalytic Processes for DMC Synthesis

Catalytic processes refer to the utilisation of a catalyst for specific reaction/process. A catalyst is defined as a substance which increases the rate of reaction without itself undergoing a permanent chemical change. Catalysts can be classified as homogeneous (e.g. calcium chloride), heterogeneous (e.g. metal oxides and zeolite) or biological (e.g. enzymes). A catalyst may be classified on the basis of "phase". A phase may be defined as a boundary between two components, even if they exist in the same physical state e.g. a mixture of oil and water consists of two phases. When the catalyst is in the same phase as the

reactants and no phase boundary is existent, it is called homogeneous catalysis (Bond, 1987). Homogeneous catalysis can take place either in the liquid phase or in the gas phase. On the other hand, the catalyst is termed heterogeneous if the phase boundary separates the catalyst from the reactants. In heterogeneous catalysis, one or more of the reactants adsorbed onto the catalyst surface.

Heterogeneous catalysis systems have become popular over homogeneous catalysis because of its advantages over the latter. These advantages include the ease of catalyst separation from the reaction mixture which is more economically viable due to the elimination of complex separation processes. The generation of undesired and toxic by-products could be minimised/eliminated. Also, heterogeneous catalysts have higher stability, longer shelf life and are easier and safer to handle, reuse and dispose compared to the homogenous counterpart.

Even though the advantages of heterogeneous catalysis outweigh the homogeneous catalytic systems, they are still employed in some industrial processes because the heterogeneous catalytic system has a significant impact on the mechanical design and operation of the processes. The main advantage of a homogeneous catalysis system is that the catalyst can be added or withdrawn at any time. However, in the case of a heterogeneous catalyst, there is a need for special mechanical design to accommodate for the replenishment of the catalyst or the catalyst would have to possess a long sustainability in order to avoid constant maintenance.

### 2.7.2. Homogeneous Catalysts

Several homogeneous catalysts have been investigated for the direct synthesis of DMC from MeOH and CO<sub>2</sub> including organic metal-alkoxy compounds, alkaline earth metal-alkoxy compounds, alkali metal-alkoxy, base catalysts and acetate catalysts (Cao *et al.*, 2012). It is well known that metal organic compounds play a key role in the activation of CO<sub>2</sub> due to insertion reaction between metal ions and ligands, which result in the formation of an intermediate product. This intermediate product further reacts with MeOH to form DMC (Shilov *et al.*, 1997; Huang *et al.*, 2011).

### 2.7.2.1. Organic metal compound catalysts

Several organic metal alkoxy compounds have been reported to play an important role in the addition of MeOH to CO<sub>2</sub>. Organotin, titanium alkoxy and Niobium (Nb) alkoxy compounds such as Bu<sub>2</sub>Sn(OEt)<sub>2</sub>, Sn(OMe)<sub>4</sub>, Sn(OBu)<sub>4</sub>, Ti(OMe)<sub>4</sub> and Ti(OBu)<sub>4</sub> have been reported for the direct synthesis of DMC (Ballivet-Tkatchenko *et al.*, 2000; 2006; Aresta *et al.*, 2003; Dibenedetto *et al.*, 2006).

Sakakura *et al.* (2000) investigated the catalytic performance of BuSn(OMe)<sub>2</sub> for the synthesis of DMC and reported that catalytic performance decreased significantly with an increase in the amount of catalyst. In addition, the catalytic performance was directly proportional to the CO<sub>2</sub> pressure. High CO<sub>2</sub> pressures have been reported to accelerate the reaction to proceed (Choi *et al.*, 2008; Kohno *et al.*, 2008). It has been suggested that the acidic-basic sites (–Sn–O–Sn–) enhances MeOH activation when organotin compounds are used as homogeneous catalysts for the synthesis of DMC from MeOH and CO<sub>2</sub> (Ballivet-Tkatchenko *et al.*, 2003).

Niobium alkoxy compounds have been reported to maintain their catalytic activity only in anhydrous reaction medium (Dibenedetto *et al.*, 2006) and therefore, the catalyst deactivates as soon as the water is formed as a by-products. Organic metal compounds supported on a solid matrix (i.e. polystyrene) such as Bu<sub>2</sub>Sn(OMe)<sub>2</sub> and Nb(OMe)<sub>5</sub> have been reported as active catalysts for the direct synthesis of DMC. However, each metal compound behaves in a different way. Tin maintains its catalytic activity whereas niobium loses all catalytic activity in such complexes (Aresta *et al.*, 2008a).

Methoxy metal compounds have also been reported for the direct synthesis of DMC from MeOH and CO<sub>2</sub>. The performance of potassium methoxide as a homogeneous catalyst in the presence of methyl iodide (CH<sub>3</sub>I) as a promoter has been investigated by Cai *et al.* (2005) where they found that 353 K and 20 bar are the optimum reaction conditions for the synthesis of DMC. Cai and co-workers (2005) also reported that potassium methoxide (CH<sub>3</sub>OK) was an efficient and selective catalyst with 16.2% DMC yield 100% selectivity.

### 2.7.2.2. Base catalysts

A series of base catalysts have been studied for the synthesis of DMC such as alkali metal carbonate, alkaline earth carbonate, organic amines, potassium hydroxide and methyl iodide (Fang *et al.*, 1996; Fujita *et al.*, 2001; Wei *et al.*, 2003; Li *et al.*, 2005; Fujita *et al.*, 2006). Base catalysts are inexpensive, have low toxicity. Halogenated hydrocarbons are usually used as co-catalyst for most base catalytic system (Cao *et al.*, 2012). In most cases, the basicity of the catalyst dominated the reaction process rather than the presence of the carbonate ions which explains the catalytic activity of phosphate compounds such as tripotassium phosphate ( $K_3PO_4$ ) and organic base compounds such as tetramethylazanium hydroxide ( $(CH_3)_4NOH$ ). Fang and co-workers (1996) reported that in the presence of  $CH_3I$  as a co-catalyst showed a better performance than other base catalysts studied. They also reported that in the absence of  $CH_3I$  only dimethyl ether was formed instead of DMC. Recent studies are carried out to investigate the application of  $K_2CO_3$  as a catalyst for the synthesis of DMC from ethylene oxide and  $CO_2$  (Choi *et al.*, 2002; Wang *et al.*, 2011b). However, the challenge is the ability to separate ethylene carbonate and DMC as final products.

### 2.7.2.3. Acetate catalysts

The direct synthesis of DMC from MeOH and  $CO_2$  has been studied using acetate catalysts. High DMC selectivity was reported however, the yield of DMC is much lower than that reported using alkoxy metal compounds (Cao *et al.*, 2012). A series of metal acetates were studied by Zhao *et al.* (2000) for the direct synthesis of DMC. These include copper acetate, nickel acetate, magnesium acetate, zinc acetate, cobalt acetate and mercury acetate. Nickel acetate showed the best selectivity for DMC and resulted in the production of the minimum amount of by-products (i.e. methyl acetate). This is due to central metal atom (i.e. nickel) which exhibits high activity due to the strong Lewis acid properties. Cobalt acetate, magnesium acetate and mercury acetate showed a relatively good yield of DMC, whereas copper acetate and sodium acetate only resulted in the formation of methyl acetate without any DMC.

2.7.2.4. Reaction mechanism for homogeneous catalytic process

The reaction mechanism for the synthesis of DMC in the presence of methoxy magnesium catalyst has been proposed as early as 1999 as shown in Figure 2.5 (Cao *et al.*, 2012).

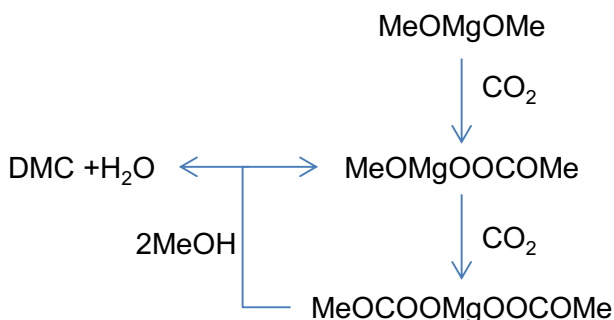


Figure 2.5. Mechanism for the synthesis of DMC over methoxy magnesium catalyst (Cao *et al.*, 2012).

The reaction is initiated by the insertion of  $\text{CO}_2$  on the Mg–O bond of the methoxy magnesium to form first intermediate ( $\text{MeOMgOOCOMe}$ ), which further reacts with another  $\text{CO}_2$  molecule to produce a second intermediate ( $\text{MeOCOOMgOOCOMe}$ ). The second intermediate (with carboxylate structure) reacts with methanol to produce DMC and regenerates the first intermediate in the same time. Also, it has been reported that for organic tin alkoxy catalytic system, the insertion of  $\text{CO}_2$  into the compound catalyst has a key role in the synthesis of DMC.

When an alkali catalyst is used for the direct synthesis of DMC, MeOH is converted into a methoxy anion under the action of an alkali. The methoxy anion then reacts with  $\text{CO}_2$  to produce reaction intermediates that reacts further with methyl iodide to produce DMC and hydrogen iodide. Finally, iodomethane is regenerated through the reaction between hydrogen iodide and methanol as shown in Figure 2.6 (Fang *et al.*, 1996). The basicity of the catalyst is important as it is directly related to the activation of MeOH and the successful regeneration of  $\text{CH}_3\text{I}$  from iodide.

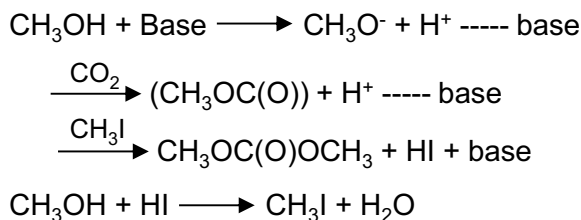


Figure 2.6. Synthesis of DMC in the presence of an alkali catalyst (Fang *et al.*, 1996).

Even though some homogenous catalytic processes are active for the direct synthesis of DMC from MeOH and CO<sub>2</sub>, there are various factors that limit the industrial application of those processes. These include difficulty in catalyst separation and recovery, severe catalyst deactivation, and high CO<sub>2</sub> pressures required for optimum yield of DMC.

### 2.7.3. Heterogeneous Catalysts

#### 2.7.3.1. Single metal oxide catalyst

A variety of metal oxide catalysts have been developed and tested for the effective synthesis of DMC. Cerium oxide (CeO<sub>2</sub>) (Aresta *et al.*, 2010; Tomishige *et al.*, 2001; Yoshida *et al.*, 2006) and zirconium oxide (ZrO<sub>2</sub>) (Tomishige *et al.* 2000; Jung and Bell, 2001; Aymes *et al.*, 2009; Xie and Bell, 2000), titanium oxide (TiO<sub>2</sub>) (La and Song 2006) and tin oxide (SnO<sub>2</sub>) (Aymes *et al.*, 2009) have been investigated over the past few years in an attempt to maximise the catalytic performance and enhance the production rate of DMC.

CeO<sub>2</sub> and ZrO<sub>2</sub> are among the most effective metal oxide catalysts reported so far (Razali *et al.*, 2012). Tomishige *et al.* (1999) reported that the catalytic activity of ZrO<sub>2</sub> is related to the acid-base active sites on the catalyst surface. Jung and Bell (2001) have developed a possible catalytic mechanism based on their Raman studies as shown in Figure 2.7.

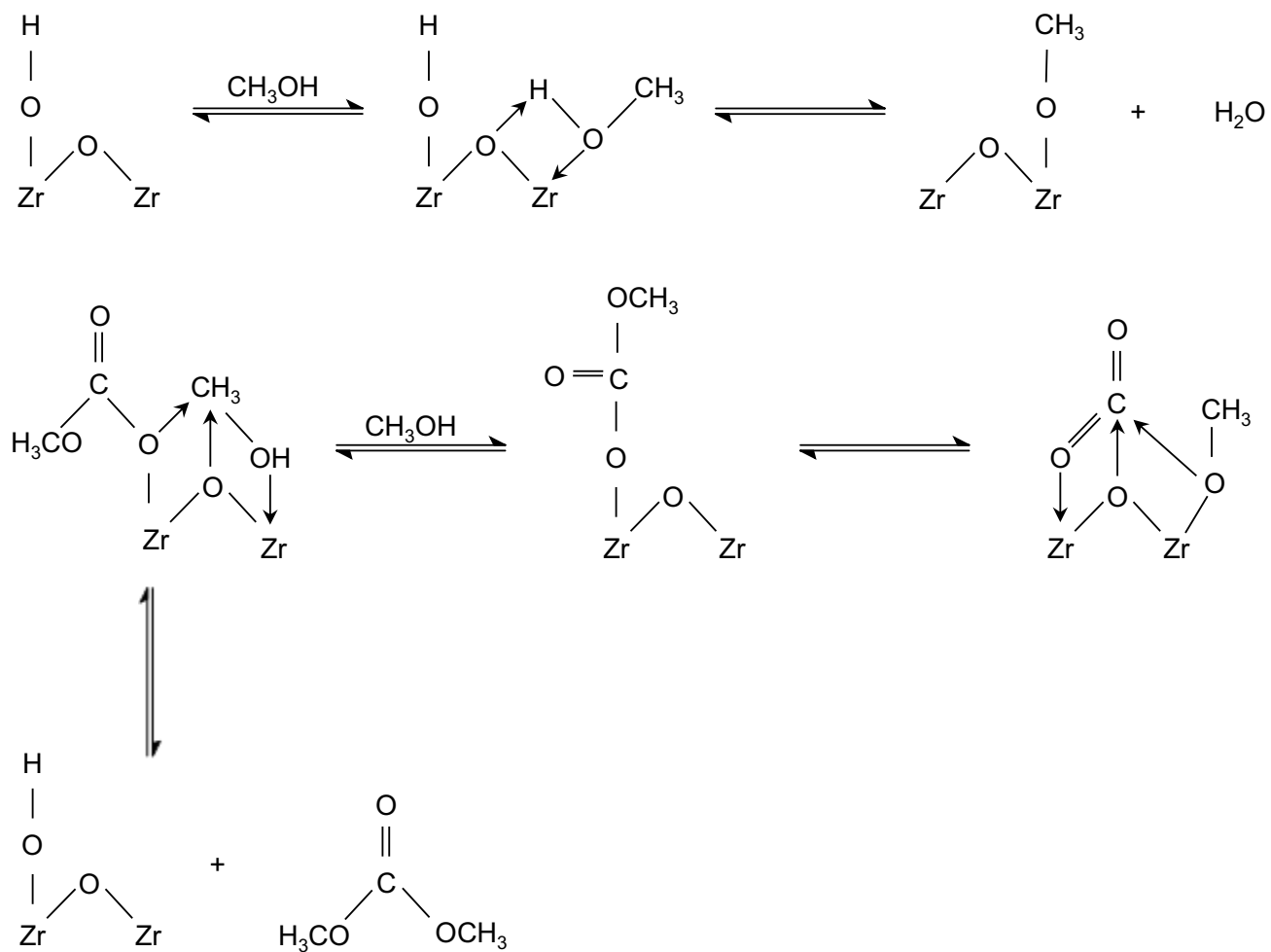


Figure 2.7. Possible reaction mechanism for the synthesis of DMC over ZrO<sub>2</sub> catalyst as proposed by Jung and Bell (2001).

Jung and Bell (2001) proposed that MeOH binds to  $Zr^{4+}$  Lewis acid sites and dissociates to form  $CH_3O-Zr$  releasing an H atom which reacts with a hydroxide ion (OH) to form water. Carbon dioxide is inserted on the Zr–O bond of the  $CH_3O-Zr$  species and forms  $m-CH_3OCOO-Zr$ . The interactions of C and O in the  $CO_2$  molecule with Lewis acid-base active sites of the catalyst are favourable for this reaction. Methyl carbonate intermediates can also be formed due to the reaction of MeOH and  $CO_2$  adsorbed in the form of bicarbonate species. However, this reaction is much slower than the reaction of  $CO_2$  with the methoxide species. Methyl group is transferred to the O atom of the methyl carbonate forming the main product DMC. Tomishige *et al.* (2000) suggested that the activation of methanol on the acidic site of the catalysts is the rate determining step in the direct synthesis of DMC.

#### 2.7.3.2. Modified metal oxide catalysts

Ikeda *et al.* (2000; 2001) attempted to enhance the catalytic activity by modifying  $ZrO_2$  using phosphoric acid ( $H_3PO_4$ ). With the modified catalyst the conversion of MeOH increased up to 4.5%. Wu *et al.* (2005; 2006) found a similar observation on the promoting effect of  $H_3PO_4$  on vanadium oxide ( $V_2O_5$ ) and  $CeO_2$  catalyst. This is due to the formation of Brønsted acid sites on  $ZrO_2/H_3PO_4$  *via* the interaction between the metal (Zr, Ce or V) and P atoms. This suggests that the Brønsted acid sites are more favourable than Lewis acid sites for the activation of MeOH. The acid-base bifunctional properties of  $H_3PO_4/ZrO_2$  along with the catalyst calcination temperatures were reported as the two main parameters that affected the catalytic activity of the modified catalyst by Ikeda *et al.* (2001) and Tomishige *et al.* (2001). It has been reported that the ratio of P:V has a major change on the phase of the catalyst (Wu *et al.*, 2005). When P:V ratio of 0.15 was used in the preparation of  $H_3PO_4/V_2O_5$ , the catalyst from a single orthorhombic phase to a more crystalline combined orthorhombic/tetragonal phase. The crystalline phase of the modified catalyst made it more effective for the DMC synthesis (Wu *et al.*, 2005).

The catalytic performance of mixed metal oxides catalysts was investigated by La and Song (2006) and the catalytic effectiveness was found in the following order:  $Ce_{0.1}Ti_{0.9}O_2 > Ce_xTi_{1-x}O_2$  ( $x = 0.2-0.8$ )  $> ZrO_2 > CeO_2 > TiO_2$ . Upon modification with tungstophosphoric heteropoly acid ( $H_3PW_{12}O_{40}$ ),  $H_3PW_{12}O_{40}/Ce_xTi_{1-x}O_2$

showed a better catalytic activity than the corresponding  $Ce_xTi_{1-x}O_2$  due to the high Brønsted acidic active sites of the compound.  $H_3PW_{12}O_{40}$  has been reported to have much higher acidity than most commonly used solid acid catalysts such as  $H_3PO_4$  (Timofeeva *et al.*, 2005). Some catalyst characterisation was carried out and the SEM images did not show any significant difference in the catalyst morphology before and after the reactions, which illustrate a good stability of the catalyst.

Although some metal oxide/mixed metal oxides have been reported active for the direct synthesis of DMC, these catalysts are prone to deactivation. Aresta *et al.* (2008b) carried out extensive characterisation for  $CeO_2$  and proposed that the reduction of Ce(IV) to Ce(III) changed the catalyst morphology which possibly leads to the catalyst deactivation. Catalyst characterisation also revealed that the particle size has an effect on the catalytic activity of  $CeO_2$  with nano-particles with 15–60 nm particle size being the most favourable for catalysing the reaction. Catalyst doping could inhibit the metal oxide reduction [i.e. reduction of Ce(IV) to Ce(III)] and enhance the catalyst stability. An attempt to improve the stability of  $CeO_2$  was carried out by Aresta and co-workers (2008b) *via* loading of  $Al_2O_3$ ,  $Fe_2O_3$  and  $La_2O_3$  into  $CeO_2$ . The activity of  $CeO_2$  increased after the doping even though when tested alone  $Al_2O_3$ ,  $Fe_2O_3$  and  $La_2O_3$  were not practically active for the activation of MeOH. However, only Al doped  $CeO_2$  showed a good stability and could be used for several runs.

Tomishige and Kunimori (2002) reported that heat treated  $CeO_2-ZrO_2$  is active for the direct synthesis of DMC from MeOH and  $CO_2$ . Catalyst characterisation showed that the surface area decreased at higher calcination temperatures, however, it resulted in better DMC formation. DMP was used as a dehydrating agent to remove water formed during the reaction and that achieved a maximum of 7% MeOH conversion and 97% selectivity towards DMC. The ratio of DMP to MeOH can play an important role in the reaction as any excess of DMP would decrease the formation of DMC and enhance the formation of side product dimethyl ether (DME).

From all the available research on metal oxide catalysts it can be seen that the combination of metal oxide(s) and/or their modification is a promising route and a step forward to heterogeneous catalysis of CO<sub>2</sub>.

### 2.7.3.3. Heteropoly acid catalysts

Heteropoly acid catalyst is an oxygen bridge-containing acid complex with Brønsted acid sites. Its acidic strength is much higher than inorganic acids and therefore has the ability to exhibit high catalytic activity for the direct synthesis of DMC from MeOH and CO<sub>2</sub>. The addition reaction of MeOH and CO<sub>2</sub> over heteropoly compounds was studied by Allaoui and Aouissi (2006). H<sub>3</sub>PMo<sub>12</sub>O<sub>40</sub> was tested for the formation of DMC. The proton of H<sub>3</sub>PMo<sub>12</sub>O<sub>40</sub> was then replaced by copper ions and resultant complex was evaluated for the synthesis of DMC. The study showed that Brønsted sites favoured the formation of DMC at a reaction temperature of 328 K, whereas it favoured the formation of DME higher temperatures. The application of heteropoly acid is however limited due to the small surface area and therefore many researchers tried to load heteropoly acid on metal/mixed metal oxide catalysts in an attempt to improve their performance.

Jiang *et al.* (2003) loaded heteropoly acid on zirconium oxide (H<sub>3</sub>PMo<sub>12</sub>O<sub>40</sub>/ZrO<sub>2</sub>) and used it for the synthesis of DMC. H<sub>3</sub>PMo<sub>12</sub>O<sub>40</sub>/ZrO<sub>2</sub> showed better activity than ZrO<sub>2</sub> due to the formation of weak Brønsted acid sites. This is similar to the modification of ZrO<sub>2</sub> by H<sub>3</sub>PO<sub>4</sub> discussed in section 2.7.3.2. La *et al.* (2007) reported similar findings when they compared the performance of H<sub>3</sub>PW<sub>12</sub>O<sub>40</sub> to the performance of H<sub>3</sub>PW<sub>12</sub>O<sub>40</sub>/Ce<sub>x</sub>Ti<sub>1-x</sub>O<sub>2</sub>. The latter showed better catalytic activity due to the bifunctional catalysis by acidic sites and basic sites provided by H<sub>3</sub>PW<sub>12</sub>O<sub>40</sub> and Ce<sub>x</sub>Ti<sub>1-x</sub>O<sub>2</sub>, respectively.

The acidity/basicity of the catalyst can play an important role in the direct synthesis of DMC. The acidic sites favour MeOH activation to methyl species and the basic sites favour MeOH activation to methoxy species. It also favours the reaction of those species with CO<sub>2</sub> (Jiang *et al.*, 2003). Therefore, there is a need to design new innovative catalysts by loading heteropoly acid on metal/mixed metal oxide catalysts (Cao *et al.*, 2012).

#### 2.7.3.4. Supported catalysts

Using a support can increase the stability of the catalyst and surface area, optimise the dispersion of the active components of the catalyst, and provide important chemical, mechanical, thermal and morphological properties (Dai *et al.*, 1996). The general procedure for preparation of supported catalysts involves the transformation of the precursors into the required active compound and the deposition of the active compound onto the support surface.

Bain *et al.* (2009a) reported a novel copper-nickel (Cu-Ni) bimetallic composite material as an active catalyst for the direct synthesis of DMC. The reaction between MeOH and CO<sub>2</sub> was carried out for 10 h at 383 K and 12 bar using 1 g of the catalyst and resulted in 7.78% conversion of MeOH and a 6.85% DMC yield. Ballivet-Tkatchenko *et al.* (2011a; 2011b) investigated the use of silica as a support for ZrO<sub>2</sub> and SnO<sub>2</sub> catalysts in an attempt to enhance their catalytic performance. It was reported that silica supported ZrO<sub>2</sub> and SnO<sub>2</sub> showed higher activity and selectivity to DMC compared to the unsupported ZrO<sub>2</sub> catalyst. Fan *et al.* (2010) grafted organotin compound on mesoporous silica support [(MeO)<sub>2</sub>ClSi(CH<sub>2</sub>)<sub>3</sub>SnCl<sub>3</sub>] and successfully used it as a suitable catalyst for the synthesis of DMC. The prepared catalyst deactivated mainly by the water produced in the reaction process. A considerable increase in the DMC yield was observed when dehydration agents such as 2,2-dimethoxypropane and 3A molecular sieve were used with the former being more effective water-trapping agent compared to the latter.

Chen *et al.* (2012) prepared molecular sieve supported Cu-Ni bimetal catalyst and applied it for the synthesis of DMC. The catalyst showed good activity (86% selectivity and 5% DMC yield) for 5 h reaction, 393 K and 11 bar CO<sub>2</sub> pressure. Cu-Ni bimetallic catalysts supported on composites were investigated by Zhong *et al.* (2000). Different surface complex supports were investigated such as ZrO<sub>2</sub>-SiO<sub>2</sub>, V<sub>2</sub>O<sub>5</sub>-SiO<sub>2</sub> and molybdenum trioxide-silica (MoO<sub>3</sub>-SiO<sub>2</sub>) and a possible reaction mechanism was proposed. Selectivity of DMC reached 85% and a conversion of 8% was reported over Cu-Ni/ ZrO<sub>2</sub>-SiO<sub>2</sub>. In another study, Wu *et al.* (2006) carried out similar reaction of MeOH and CO<sub>2</sub> over Cu-Ni/V<sub>2</sub>O<sub>5</sub>-SiO<sub>2</sub> catalyst at 413 K and 6 bar. They reported that the crystallinity of the

catalyst has a slight influence on the synthesis of DMC, and a higher crystallinity resulted on higher DMC yield.

The effect of reaction conditions and catalyst supports were evaluated for the synthesis of DMC from CO<sub>2</sub> in the presence of rhodium (Rh) supported catalysts by Almusaiteer (2009). Aluminium oxide (Al<sub>2</sub>O<sub>3</sub>), SiO<sub>2</sub> and ZSM-5 (Zeolite International) were tested as possible supports for the 5% (w/w) Rh catalyst. The studies showed that using a support enhances the catalytic activity; at 393 K the DMC yield was 24.9%, 16.7% and 5.4% for Rh/ZSM-5, Rh/SiO<sub>2</sub>, Rh/ Al<sub>2</sub>O<sub>3</sub>, respectively. In a similar attempt, the influence of Al<sub>2</sub>O<sub>3</sub> on the performance of CeO<sub>2</sub> catalysts was investigated for the carboxylation of MeOH to DMC by Aresta *et al.* (2010). It was reported that the deactivation of CeO<sub>2</sub> catalyst usually occurs due to the surface modification produced by the reduction of Ce(IV) to Ce(III), which is completely eliminated if nanoparticles of ceria loaded with alumina are used as catalysts.

More recently, novel carbonaceous materials such as graphite oxide (GO), activated carbon, thermally expanded graphite and multi-walled carbon nanotubes have been widely used as suitable catalyst supports in recent studies (Bian *et al.*, 2009b). These materials have unique electrical transporting properties, simple preparation techniques and are inexpensive compared to conventional support materials. Bimetallic Cu–Ni catalysts was loaded on thermally expanded graphite as a support and tested for the synthesis of DMC from MeOH and CO<sub>2</sub> (Bian *et al.*, 2009a; 2009b). The catalyst showed a better performance compared to Cu–Ni without any support. At optimum reaction conditions (373 K and 12 bar) a maximum MeOH conversion of 4.97% and DMC selectivity of 89% were obtained. Dimethyl ether (DME), carbon monoxide (CO) and formaldehyde (CH<sub>2</sub>O) were the by-products formed during the addition reaction of MeOH and CO<sub>2</sub>. It has been proposed that the special properties of thermally expanded graphite with various functional groups, loose carbon sheets and the high dispersion of metal atoms on the catalyst surface have played a key role in the DMC synthesis. Also, graphite has a remarkably high ability of electronic transmission and electrical conductivity thus enabling the electron in graphite release easily for enhanced CO<sub>2</sub> activation.

Although there has been a considerable effort dedicated to the use of various supports in heterogeneous catalysis, this area needs to be explored more. As such, strongly coupled graphene based inorganic nanocomposites represent an exciting and new class of functional materials (Bai and Shen, 2012). Unlike other carbon forms, graphene is a unique two-dimensional single layer of carbon in which the atoms are arranged in hexagons (Geim and Novoselov, 2007; Rao *et al.*, 2009). Its unique physical, chemical and mechanical properties including a very high surface area and easy surface modifications allow preparation of nanocomposite materials with novel properties and characteristics (Williams *et al.*, 2008; Dreyer *et al.*, 2010).

The current methods for homogeneously producing graphene-nanocomposites involve homogenisation by mixing of inorganic nanoparticles and grinding, which makes it extremely difficult to get very well dispersed nanoparticles in good electrical contact with the graphene. Thus, improved and innovative approaches are required. In the synthesis of metal oxides (homo, hetero or doped), hydrothermal syntheses in superheated or supercritical water can offer many advantages over conventional preparative methods including fewer synthetic steps and significantly faster reaction times (Darr *et al.*, 1999; Middelkoop *et al.*, 2014). There are currently very few scientific reports utilising hydrothermal routes for decorating graphene with nanoparticles (Liang *et al.*, 2010; Li *et al.*, 2011b; Su *et al.*, 2011; Perera *et al.*, 2012). However, the current hydrothermal syntheses are conducted in batch reactors, which are time consuming and give little control over product properties such as crystallinity, size, etc. Continuous hydrothermal flow synthesis (CHFS) reactors offer many advantages as they have independent control over reaction variables (e.g. pressure and temperature) and hence particle properties (Lin *et al.*, 2010). Generally, the CHFS process involves mixing a flow of supercritical water with a flow of aqueous metal salt(s) to give rapid precipitation and controlled growth of nanoparticles in a continuous manner. The properties of water (such as diffusivity, density, and dielectric constant) change dramatically around the critical temperature and pressure (647 K, 221 bar) leading to its use as an exotic, and tunable reaction solvent/medium. As graphene has a very 2D, platelike structure, it offers an attractive substrate for deposition of inorganic nanoparticles for highly dispersed composites with novel properties.

### 2.7.3.5. Photocatalyst

The addition reaction of MeOH and CO<sub>2</sub> is governed by equilibrium and therefore it has been very challenging to obtain high MeOH conversion and DMC yields. Photo-catalysis can be alternative route to homogeneous and heterogeneous catalysis and to help overcome the equilibrium limitation of the addition reaction. Copper semiconductor complex supported on silica has been investigated in a continuous flow fixed bed reactor. Water was removed continuously during the process (Wang *et al.*, 2007a). Experiments were carried out at (393–413 K) in the presence and absence of ultraviolet (UV) radiation for comparative purposes. UV radiation assisted the reaction, allowed it to occur at low pressure (1 bar) and enhanced the yield of DMC by 57% compared with surface catalytic reactions.

Other studies were carried out on the photo-catalytic synthesis of DMC from CO<sub>2</sub> and MeOH over Cu/NiO–MoO<sub>3</sub>/SiO<sub>2</sub> and Cu/NiO–V<sub>2</sub>O<sub>5</sub>/SiO<sub>2</sub> catalysts (Kong *et al.*, 2005; 2006). Both catalysts showed similar activity for the chemisorption of MeOH and CO<sub>2</sub> and resulted in MeOH conversion of ~13.9% and DMC selectivity of ~90%. Extensive characterisation such as powder X-ray diffraction (XRD) and temperature-programmed reduction (TPR) were carried out to extensively evaluate the properties of the catalyst complex. It was found that the introduction of Cu and NiO improved the even dispersion of the metal oxide (MoO<sub>3</sub> or V<sub>2</sub>O<sub>5</sub>) on the silica support and expanded the absorption region to visible light.

### 2.7.4. Dehydrating Agents

Various catalysts have been studied extensively, however, the methanol conversion and DMC yield are still very low. This is due to the equilibrium limited reaction and the catalyst deactivation when water is formed as a by-product. Different dehydrating agents and additives have been used to minimise the effect of water produced during the reaction and improving the catalytic performance of the catalyst. These systems can be classified as reactive or non-reactive dehydration systems (Honda *et al.*, 2014). These agents include nitrile compounds (Honda *et al.*, 2010; 2011), calcium chloride (Wu *et al.*, 2005), 2,2-dimethoxy propane ((Tomishige and Kunimori, 2002; Honda *et al.*, 2009), molecular sieves (Hou *et al.*, 2002), ketals (Sakakura *et al.*, 2000), aldols (Sakakura *et al.*, 2007) and trimethoxymethane (TMM) (Zhang *et al.*, 2011) and have positively contributed to an increase in MeOH conversion.

### 2.7.5. Novel Techniques

It is essential to develop novel techniques in order to overcome the equilibrium limitation of the reaction between MeOH and CO<sub>2</sub>. The design of new catalytic processes to minimise the effect of water produced and enhance the yield of DMC is required. Among the new techniques are the use of supercritical CO<sub>2</sub>, electrochemical synthesis and the application of membrane catalytic reactors (Yoshida *et al.*, 2009).

In 2000, Zhao *et al.* (2000) reported that near supercritical conditions, DMC was the only product of MeOH and CO<sub>2</sub> reaction over nickel acetate catalyst. They reported that the yield of DMC was 12 times more than the reaction carried out at non-supercritical conditions. Hong *et al.* (2006) had a similar observation and reported that when the reaction between MeOH and CO<sub>2</sub> was carried out over K<sub>2</sub>CO<sub>3</sub>/CH<sub>3</sub>I and in the presence of a DMP as a dehydrating agent, a maximum DMC yield of 12% was achieved. Many other studies were carried out using supercritical carbon dioxide as a reactant and a medium for the synthesis of organic carbonates (Cui *et al.*, 2003; Sun *et al.*, 2005; Ballivet-Tkatchenko *et al.*, 2006; Wang *et al.*, 2006b; Jutz *et al.*, 2008), where all the studies showed a promoting effect on the CO<sub>2</sub> conversion and yield of desired product.

It is clear that CO<sub>2</sub> pressure plays an important role in the addition reaction of MeOH and CO<sub>2</sub>. It is known that physical properties of CO<sub>2</sub> are improved at critical and supercritical state of CO<sub>2</sub>, which in turn enhances the activation of CO<sub>2</sub> molecule to its greatest extent. The reaction between MeOH and CO<sub>2</sub> is governed by equilibrium, however, if CO<sub>2</sub> used is at critical or supercritical state, the mass transfer efficiency of the reactants is improved thus shifting the reaction equilibrium to the product side to overcome the thermodynamic limitations of the reaction (Cao *et al.*, 2012). Also, using CO<sub>2</sub> at supercritical condition is a key to shift the equilibrium to the product side because MeOH and CO<sub>2</sub> reaction mixture is in a single phase compared to two phases when CO<sub>2</sub> is below supercritical conditions.

The development and application of electrochemical technique for the direct synthesis of DMC from MeOH and CO<sub>2</sub> has a great significance and viability. DMC synthesis *via* electrochemical technique can overcome the equilibrium

limitation and enhance the activation of the stable CO<sub>2</sub> molecule. A recent study by Yuan *et al.* (2009) reported using platinum electrodes in ionic liquid–CH<sub>3</sub>OK–methanol electrolyte, in which CH<sub>3</sub>OK acted as a co-catalyst for the synthesis of DMC from CO<sub>2</sub> and MeOH. Electrocatalytic synthesis of organic carbonates from CO<sub>2</sub> has been reported by other researcher groups (Casadei *et al.*, 2000; Zhang *et al.*, 2008). However, the maximum yield of DMC reached 3.9% at 303 K. The yield of DMC is still extremely low and insufficient and impractical for industrial application.

Membrane catalytic reactors (MCR) have been employed for the effective synthesis of DMC (Li and Zhong, 2003). The study proposed that MCR can combine the catalytic reaction and separation process, thus assisting with the removal of water produced, leading to the equilibrium shift in favour of DMC synthesis. However, the study showed that reactants were permeated as well through the membrane reactor. More recently, the application of nitriles as dehydrating agents for the synthesis of DMC has been studied. Honda *et al.* (2009; 2010; 2011) reported that using CeO<sub>2</sub> as a catalyst in the reaction between MeOH and CO<sub>2</sub> has a great effect on the catalytic process. CeO<sub>2</sub> can catalyse the hydration of nitriles to amide thus shifting the equilibrium to the carbonate side and resulting in an enhancement to the yield of DMC. The nitrile hydration techniques can be applied to the synthesis of other dialkylcarbonates from their corresponding alcohols and CO<sub>2</sub>.

### 2.8. CONCLUSIONS

From the literature reviewed it is apparent that the synthesis of DMC from MeOH and CO<sub>2</sub> is a promising route for CO<sub>2</sub> mitigation. Various homogeneous and heterogeneous catalytic processes have been extensively studied and evaluated in the last few years. More attention is focused on heterogeneous catalysis due to its numerous advantages. Therefore, a variety of metal oxide catalysts such as cerium oxide (CeO<sub>2</sub>), zirconium oxide (ZrO<sub>2</sub>), vanadium oxide (V<sub>2</sub>O<sub>5</sub>), titanium oxide (TiO<sub>2</sub>) and tin oxide (SnO<sub>2</sub>) have been developed and assessed for the effective synthesis of DMC. However, MeOH conversion and yields of DMC are very low and unsatisfactory. More effort is required to facilitate the progress in the development of novel heterogeneous catalytic processes that can overcome thermodynamic limitations and provide a step forward towards the industrial

commercialisation of greener and efficient DMC synthesis. The activation of thermodynamically stable CO<sub>2</sub> is a key to the successful conversion of carbon dioxide. Intensive research of different reaction technologies and conditions are desirable in order to achieve high yields of DMC. The properties of the catalyst play an important role in activating both MeOH and CO<sub>2</sub> and therefore the development of new catalysts must be explored. Future work to understand the reaction mechanisms is necessary in order to fully understand and enhance the rate of the reaction.

# **Chapter 3**

## **Direct Synthesis of Dimethyl Carbonate (DMC) using Commercially Available Catalysts**

### 3. DIRECT SYNTHESIS OF DMC USING COMMERCIALY AVAILABLE CATALYSTS

#### 3.1. INTRODUCTION

The utilisation of renewable raw materials in the chemical process industries catalyses a change towards a greener and more sustainable environment. Carbon dioxide (CO<sub>2</sub>) has attracted great interests as a readily available carbon source due to its non-toxic, non-flammable and recyclable properties (Dienes *et al.*, 2012; Honda *et al.*, 2014; Adeleye *et al.*, 2015). However, CO<sub>2</sub> is a very stable compound as the carbon atom is in the most oxidised form and thermodynamically stable (Omae, 2012) and therefore large energy input is required to transform CO<sub>2</sub>.

The synthesis of dimethyl carbonate (DMC) has gained considerable attention in recent years due to the versatile and excellent chemical properties of DMC. DMC has low toxicity and high biodegradability, which makes it a green reagent and a safer substitute to poisonous and undesirable dimethyl sulphate and phosgene in the process industry. It can be used as a good precursor material for the production of polycarbonates (Bian *et al.*, 2009c). DMC is used as a main carbonylation and methylation agent as its significant molecular structure contains methyl, carbonyl and methoxyl active groups. DMC is classified as the leader of carbonic esters whose properties can be easily tailored for a specific application e.g. for the production of lubricating oils (Rudnick, 2013). DMC is a strong contender as an oxygenate to reduce vehicle emissions and hence reduce environmental and health risks. Also, the utilisation of DMC can help meet the clean Air Act specification for gasoline (Pacheco and Marshall, 1997). DMC has outstanding oxygen content (53%) that is 3 times higher than the oxygen content in methyl tert-butyl ether and is an effective octane enhancer (Bruno *et al.*, 2009; Zhang *et al.*, 2011).

Several reaction routes have been known for the synthesis of DMC so far including the methanolysis of phosgene, oxidative carbonylation of methanol, transesterification route and direct synthesis from methanol (MeOH) and CO<sub>2</sub>. The latter being the most attractive route due to the inexpensive raw material, and the avoidance of corrosive reagents such as phosgene and dimethyl sulphate.

Catalyst plays an important role in the design of new greener catalytic process for the synthesis of DMC. The catalyst should not be limited to the enhancement of DMC yield but also should fulfill the requirements for greener and sustainable chemical process (Pescarmona and Taherimehr, 2012). Homogeneous catalysts such as organic metal compounds (Alvaro *et al.*, 2004, Ramin *et al.*, 2005), base catalysts (Zhang *et al.*, 2006; Srinivas and Ratnasamy, 2007; Jagtap *et al.*, 2008) and acetate catalysts (Du *et al.*, 2005) have been the most employed catalysts for the synthesis of various organic carbonates. However, the homogeneous nature of these catalysts posed few drawbacks including high cost of separation of products/catalysts from the reaction mixture, potential production of undesired side products (i.e. HCl), use of co-solvent, challenges in terms of catalyst stability and reusability (Dai *et al.*, 2009).

The development of solvent-less heterogeneous catalytic process for the synthesis of DMC and other organic carbonates is a key aspect for the design of greener chemical synthesis. Heterogeneous catalysts offer numerous advantages including the ease of catalyst separation from the reaction mixture, which is more economically viable due to the elimination of complex separation processes. The generation of undesired and toxic by-products could be minimised/eliminated. Also, heterogeneous catalysts have higher stability, longer shelf life and is easier and safer to handle, reuse and dispose compared to the homogenous counterpart.

Although there has been a considerable effort dedicated to direct synthesis of DMC, there is still a lack in finding a solvent-less heterogeneous catalytic process for the synthesis of DMC from MeOH and CO<sub>2</sub>. Hence in this work, batch addition reactions for the synthesis of DMC from MeOH and CO<sub>2</sub> have been carried out in a high pressure autoclave reactor to evaluate the catalytic performance of several heterogeneous catalysts in the absence of a solvent/dehydrating agent. The catalysts include ceria and lanthana doped zirconia (Ce–La–Zr–O), ceria doped zirconia (Ce–Zr–O), lanthana doped zirconia (La–Zr–O), lanthanum oxide (La–O) and zirconium oxide (Zr–O). The effect of various reaction conditions, such as reaction temperature, CO<sub>2</sub> pressure, catalyst loading and reaction time has been extensively evaluated using the best performed catalyst. An assessment of the

catalyst stability and reusability has been carried out at the optimised reaction conditions.

### 3.2. EXPERIMENTAL METHOD

#### 3.2.1. Materials

A number of chemicals used for this research were purchased from Sigma-Aldrich Co. Ltd (UK). These include methanol (MeOH), isopropyl alcohol (IPA) and dimethyl carbonate (DMC). The liquid CO<sub>2</sub> cylinder (99.9%) equipped with a dip tube was purchased from BOC Ltd, UK. The catalysts including Ce–La–Zr–O, Ce–Zr–O, La–Zr–O and Zr–O were supplied by Magnesium Elektron Ltd. (MEL) Chemicals UK. All chemicals and catalysts were used without any further purification.

#### 3.2.2. Addition Reaction of MeOH to CO<sub>2</sub>

Addition reactions were carried out in a 50 mL autoclave reactor (model 4590, Parr Instrument Company, USA) equipped with a thermocouple (type J), heating mantle, stirring system and a controller (model 4848) as shown in Figures 3.1 and 3.2. The reactor was equipped with a pressure gauge and a thermocouple to monitor the reaction pressure and temperature at all times. In a typical process, 20 g of methanol and the required amount of the heterogeneous catalyst were charged into the reactor vessel. The reactor was continuously stirred and heated to the required temperature. Supercritical fluid pump (model SFT-10, Analytix Ltd., UK.) was used to pump CO<sub>2</sub> at a specified pressure from the cylinder to the reactor *via* the inlet valve. CO<sub>2</sub> was injected at a constant pressure for all the optimised reactions. The reaction was left for the desired reaction time. After the reaction, the reactor was cooled down to room temperature using an ice bath. The reactor was depressurised and the reaction mixture was filtered. The products were analysed using a gas chromatography (GC) equipped with a flame ionisation detector (FID) with a capillary column using isopropyl alcohol as an internal standard. The effect of various reaction parameters were studied for the optimisation of reaction conditions. The stability of the catalyst was assessed by carrying out catalyst reusability studies on the best performed catalyst at the optimum conditions.

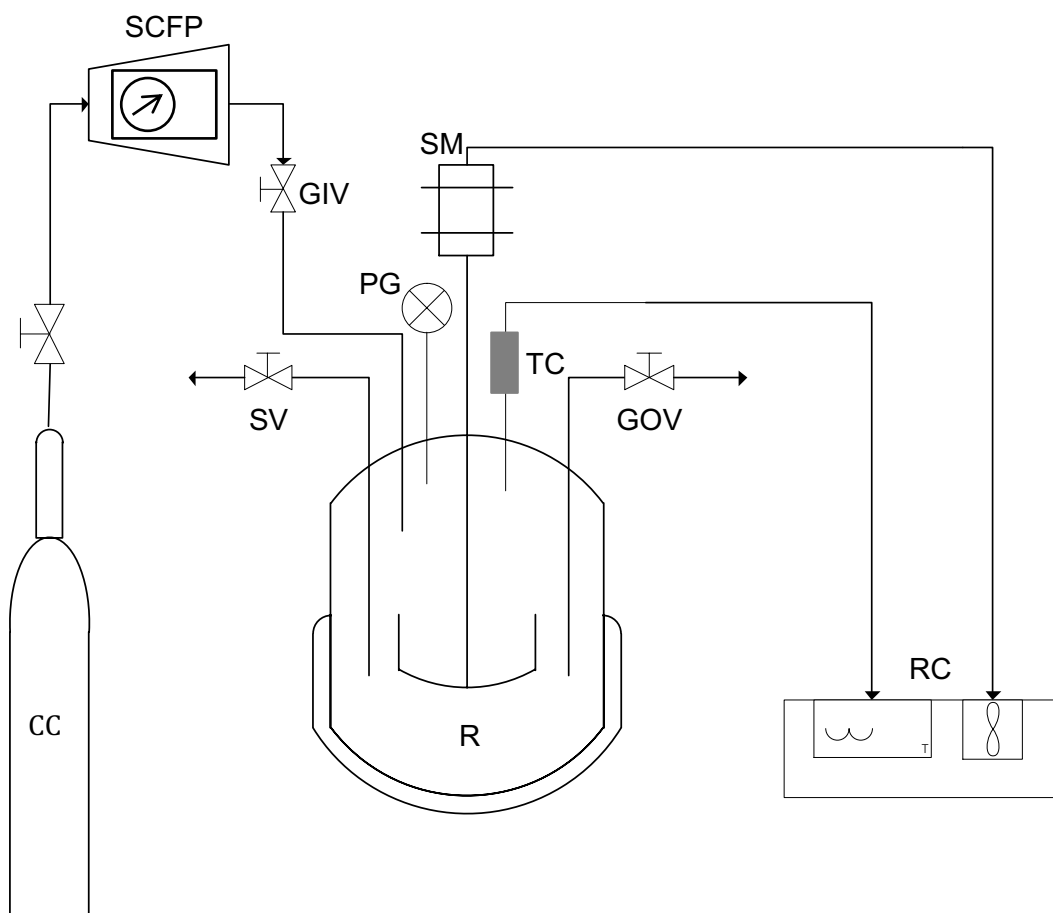


Figure 3.1. Schematic representation of the experimental set-up for DMC synthesis using a high pressure reactor. Key: CC, CO<sub>2</sub> cylinder; SCFP, supercritical fluid pump; GIV, gas inlet valve; SV, sampling valve; PG, pressure gauge; SM, stirring motor; TC, thermocouple; GOV, gas outlet valve; R, reactor; RC, reactor controller.

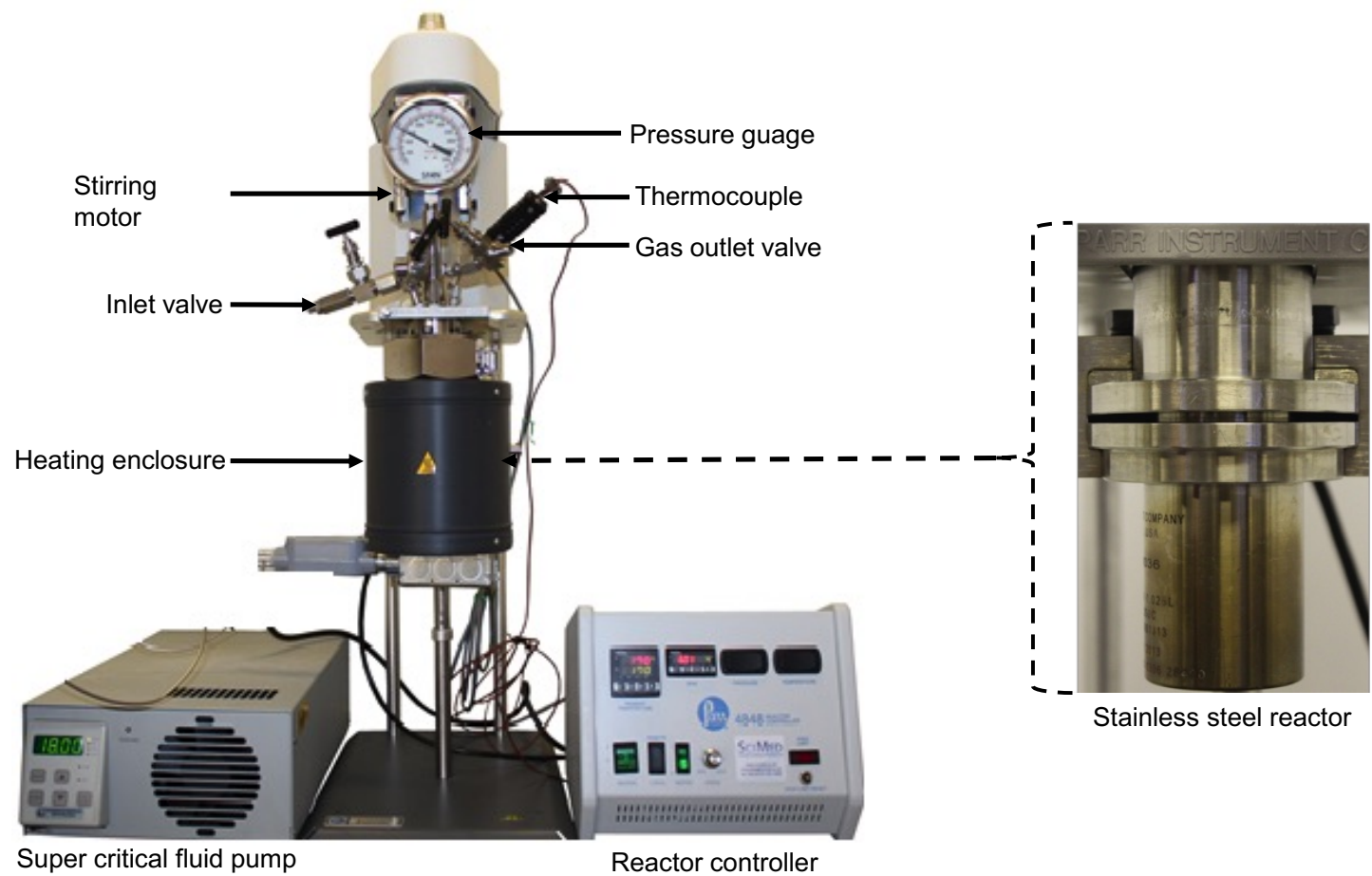


Figure 3.2. Batch experimental set-up for DMC synthesis.

### 3.2.3. Method of Analysis

A Shimadzu gas chromatography (GC-2014) was used to analyse the composition of all experimental samples as shown in Figure 3.3. The GC was equipped with a flame ionisation detector (FID) and helium (99.9%) with a gas flow rate of  $1 \text{ mL min}^{-1}$  was used as the carrier gas for the mobile phase. The stationary phase was a capillary column with length of 30 m, inner diameter of  $320 \mu\text{m}$  and film thickness of  $0.25 \mu\text{m}$ . Oxygen (99.9%) and hydrogen (99.9%) were used as ignition gases. A temperature program was developed and applied for this process where both the detector and injector temperatures were maintained at 523 K. A split ratio of 25:1 and injection volume of  $0.5 \mu\text{L}$  were chosen as part of the GC method.



Figure 3.3. A Shimadzu gas chromatography (GC-2014) used for analysis of experimental samples.

A ramp method was used in order to separate all the compounds present in the sample mixture where the initial temperature of the oven was set at 323 K. The sample was injected by an auto sampler for analysis. The column temperature was held at 323 K for 5 min after the sample had been injected. Afterwards, a temperature ramp was applied that increased the temperature linearly at a rate of 50 K min<sup>-1</sup> to a temperature of 523 K. The total run time for each sample was 12 min. the injection needle was washed twice after the sample injection using *n*-pentane. After each sample run, the column temperature was cooled down to 313 K so that the following sample could be analysed. The component mass fractions were directly calculated from the chromatograms *via* internal standard method using IPA as an internal standard.

### 3.2.3.1. Internal standardisation

Internal standard method was used for the analysis of the sample mixture for batch reactor due to its numerous advantages. Using internal standardisation as an analysis technique allows the result to be expressed as an absolute concentration, i.e. if the units of concentration for the internal standard ( $C_{is}$ ) for both calibration and analysis are the same, the final answer is expressed in the concentration units of calibration ( $C_i$ ). If the units for both  $C_i$  and  $C_{is}$  for the calibration are identical, the response factor is dimensionless and it is possible to obtain the final answer in any desired units by simply adjusting the units of  $C_i$  for the analysis. Also, allowance is made for the response of each component to the detector and the result of each injection is independent of the injection volume.

However, there are some disadvantages associated with using the internal standardisation technique as it is not readily usable for gaseous samples and the need to select a suitable internal standard. For the chosen system, all samples to be analysed are in the liquid phase, which makes the technique suitable.

*iso*-Propyl alcohol (IPA) is chosen as an internal standard for the following reasons:

- ❖ It is miscible with the samples being analysed.
  
- ❖ It is similar in functional group type to the component(s) of interest (i.e. methanol).

- ❖ IPA is stable under the required analytical conditions. It does not react with any of the components or solvents present in the sample.

### 3.2.3.2. Calibration method

It is essential to be able to determine the compositions of the product mixture obtained at the end of the addition experiments. In order to do that, calibration curves must be developed. There are different methods available to develop these curves such as internal standard method and absolute curve method. *iso*-Propyl alcohol was used as the internal standard for DMC analysis.

In order to carry out the calibration, several standard solutions were prepared with known amounts of the reactants, products and internal standard. A constant volume of each standard solution was injected into GC and a chromatogram was obtained for each sample. The ratio of the peak area of each component ( $A_i$ ) to that of the internal standard ( $A_{is}$ ) were calculated as shown in Equation 3.1. The ratio of the concentration of each component ( $C_i$ ) to that of the internal standard ( $C_{is}$ ) were calculated as shown in Equation 3.2. A calibration curve was prepared by plotting the concentration ratio *versus* the area ratio of all components. The response factor ( $RF_i$ ) of individual component was calculated using Equation 3.3. The response factor for each component was used to determine the unknown compositions of the samples collected from the reactor at the end of the reaction as shown in Equation 3.4.

$$\text{Area ratio (AR)} = \frac{\text{Area of the } i^{\text{th}} \text{ component } (A_i)}{\text{Area of internal standard } (A_{is})} \quad (3.1)$$

$$\text{Concentration ratio (CR)} = \frac{\text{Concentration of the } i^{\text{th}} \text{ component } (C_i)}{\text{Concentration of internal standard } (C_{is})} \quad (3.2)$$

Response factor of the  $i^{\text{th}}$  component ( $RF_i$ ) can be calculated using Equation 3.3.

$$R. F. \text{ of the } i^{\text{th}} \text{ component } (RF_i) = \frac{\text{Concentration ratio } (CR_i)}{\text{Area ratio } (AR_i)} \quad (3.3)$$

Equation 3.3 can be rearranged as shown in Equation (3.4) which represents a straight line equation.

$$CR_i = RF_i \times AR_i \quad (3.4)$$

where,

y = concentration ratio of the  $i^{\text{th}}$  component ( $CR_i$ ),

x = area ratio of the  $i^{\text{th}}$  component ( $AR_i$ ), and

gradient (m) = response factor of the  $i^{\text{th}}$  component ( $RF_i$ ).

A plot of concentration ratio *versus* area ratio of all the components were plotted for the determination of response factor. Once the response factor of individual component was determined, the unknown composition of the samples collected from the reactor can be determined by using Equation 3.4.

#### 3.2.3.3. Chromatogram and Calibration curves

Figure 3.4 shows a typical chromatogram from Shimadzu gas chromatography (GC-2014). Methanol peak emerged first followed by IPA and DMC. The total time for a single GC run was about 12 min.

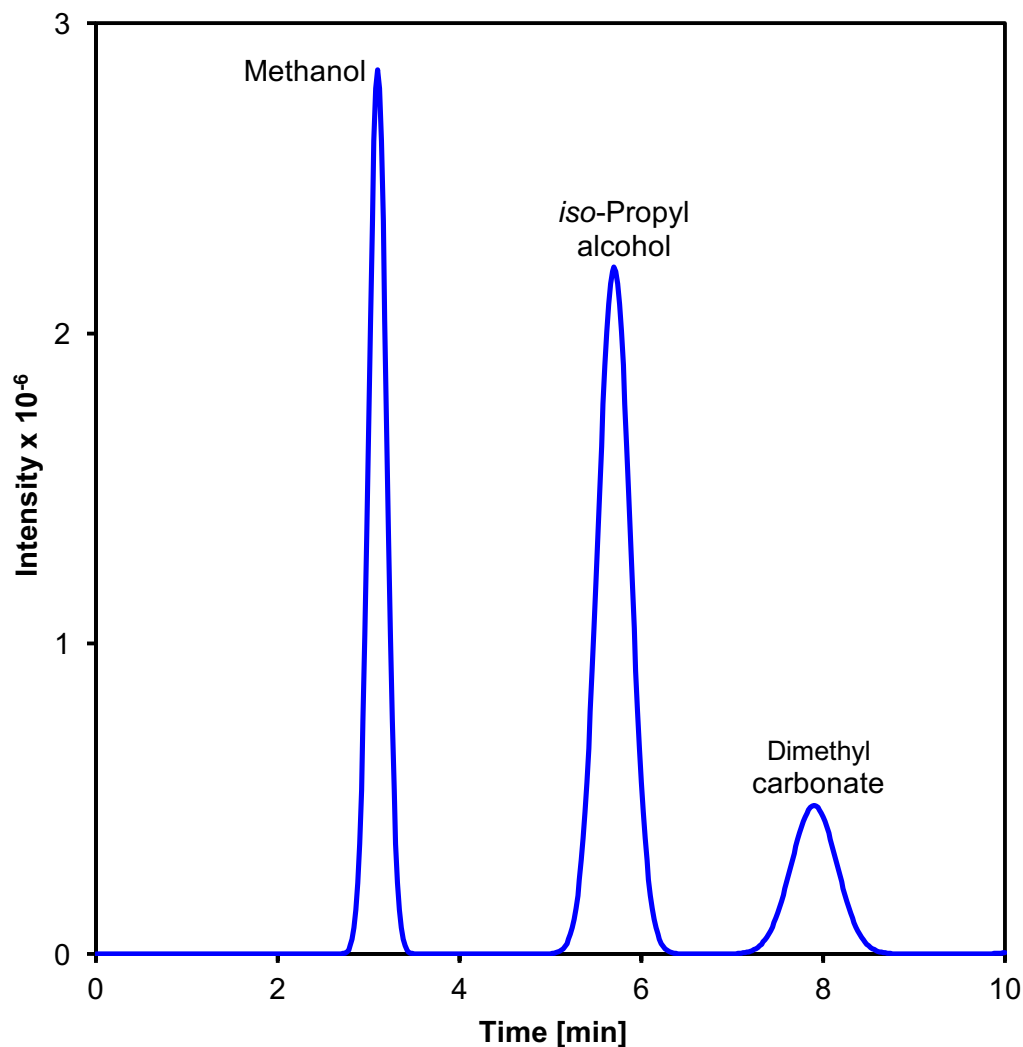


Figure 3.4. A typical chromatogram from Shimadzu-2014 gas chromatograph (GC).

Calibration curves for DMC and MeOH were prepared as shown in Figures 3.5 and 3.6, respectively. Standard solutions containing known concentration of DMC ( $C_{\text{DMC}}$ ), concentration of MeOH ( $C_{\text{M}}$ ) and concentration of IPA ( $C_{\text{IS}}$ ) were prepared. Samples were injected into GC and a chromatogram was obtained for each sample. The peak area of MeOH ( $A_{\text{M}}$ ), peak area of DMC ( $A_{\text{DMC}}$ ) and peak area of IPA ( $A_{\text{IPA}}$ ) were used to calculate the required area ratio. The response factors are 0.6541 and 0.3391 for MeOH and DMC, respectively. The coefficient of determination ( $R^2$ ) value is very close to unity.

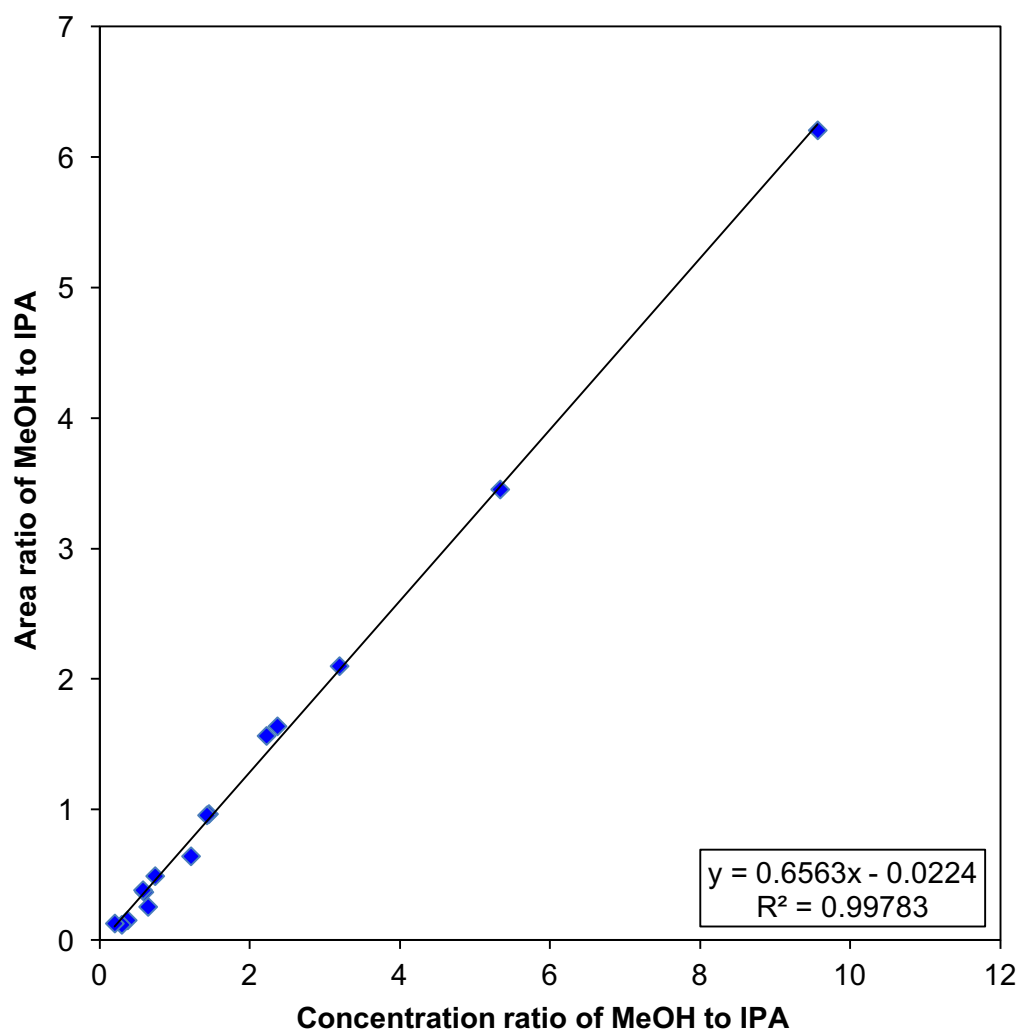


Figure 3.5. Calibration curve for response factor determination of MeOH using IPA as an internal standard.

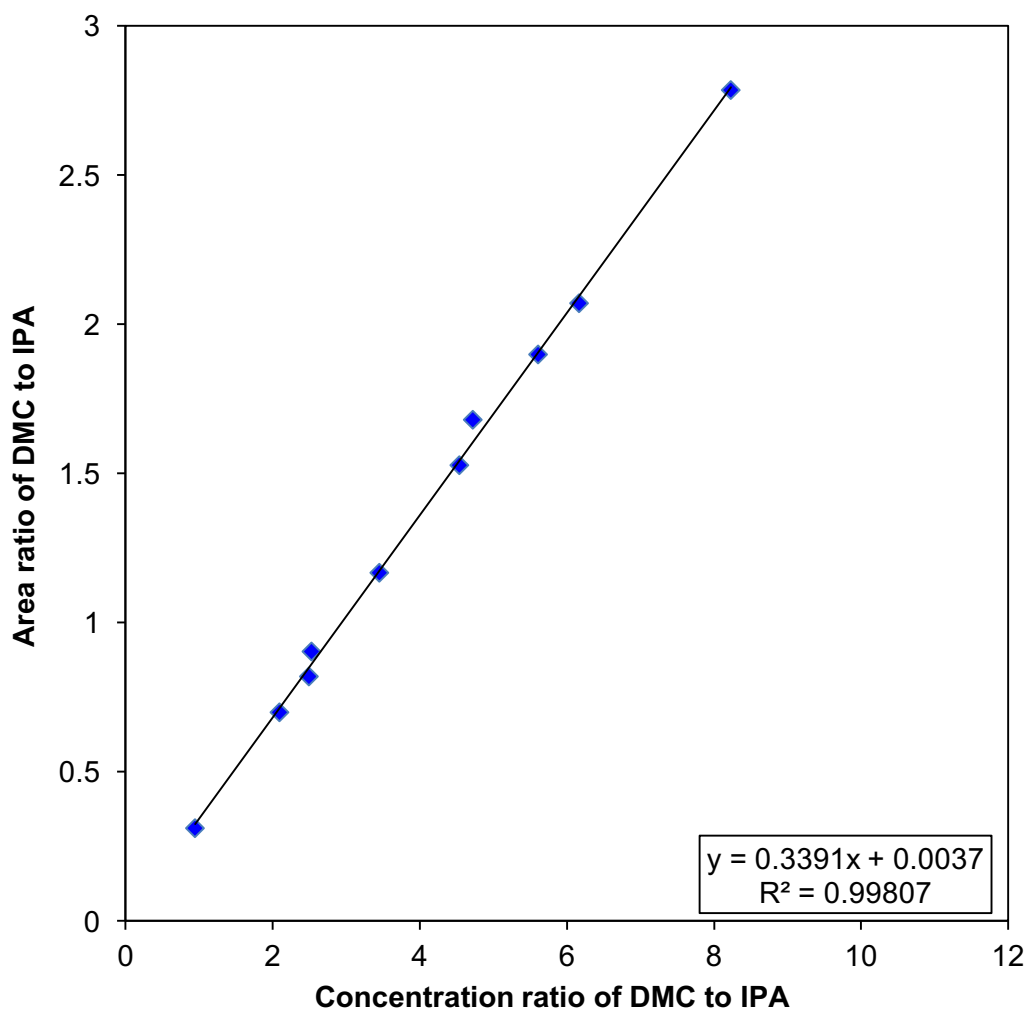


Figure 3.6. Calibration curve for response factor determination of DMC using IPA as an internal standard.

#### 3.2.3.4. Determination of MeOH conversion and DMC yield

MeOH conversion and yield of DMC were calculated using Equations 3.5 and 3.6, respectively.

$$\text{DMC Yield (\%)} = \frac{\text{Moles of products formed}}{\text{Initial moles of Methanol}} \times 100 \quad (3.5)$$

$$\text{MeOH Conversion (\%)} = \frac{\text{Initial moles of MeOH} - \text{moles of MeOH remaining}}{\text{Initial moles of Methanol}} \times 100 \quad (3.6)$$

#### 3.2.4. Catalyst Characterisation Techniques

Heterogeneous catalysts such as metal oxide and mixed metal oxide catalysts are commonly employed for the synthesis of DMC. Several metal oxide and mixed metal oxide catalysts which include La–O, Zr–O and doped zirconia such as Ce–Zr–O, La–Zr–O and Ce–La–Zr–O have been assessed and analysed based on their activity and selectivity towards the production of DMC. The characterisation of heterogeneous catalysts was investigated using scanning electron microscope (SEM), X-ray diffraction (XRD) and Raman spectroscopy.

These oxide catalysts were prepared by proprietary processes developed by MEL Chemicals Ltd., UK that has been optimised to produce specific particle size distributions and different textural properties (pore volume and pore distribution). Morphology of the catalysts was investigated using SEM equipped with FEI Inspect F and Quanta 3D FEG with a gold plated sample holder. XRD patterns were investigated on a Siemens D5000 X-Ray Powder diffractometer analyzer operates in  $\theta/2\theta$  geometry. Raman spectra were recorded using a Renishaw Ramascope 1000 (model 52699) analyser connected to an optical microscope and a modu-laser source. All catalyst characterisation results are presented in detail in section 3.3.1.

### 3.3. RESULTS AND DISCUSSION

#### 3.3.1. Catalyst Characterisation

The photographic images of Ce–La–Zr–O, Ce–Zr–O, La–O, La–Zr–O and Zr–O are shown in Figure 3.7. La–O, Zr–O and La–Zr–O appear as white powder. Ce–Zr–O has a yellow physical appearance due to the presence of cerium oxide. A pale yellow colour can be seen for Ce–La–Zr–O catalyst.

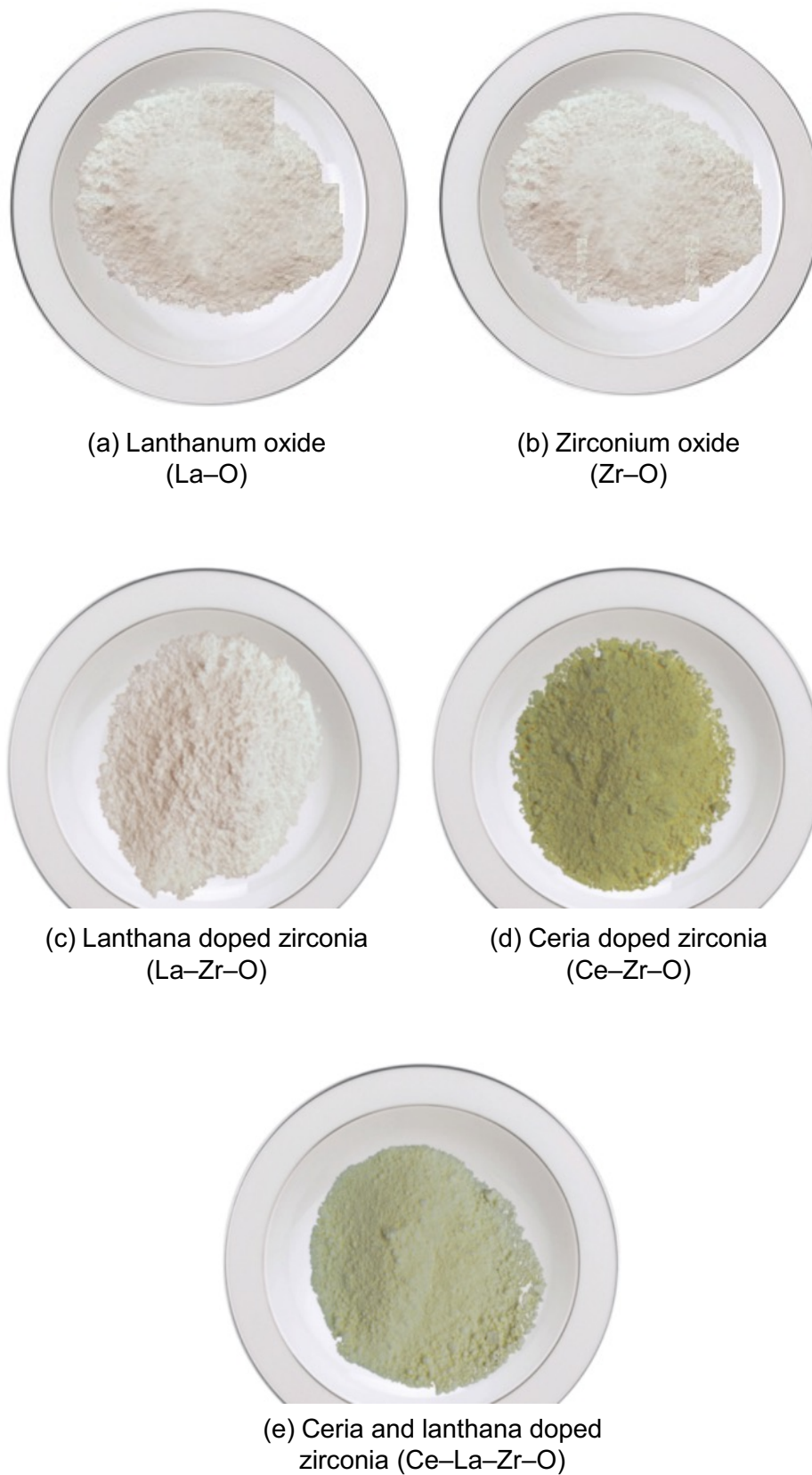


Figure 3.7. Photographic images of commercially available catalysts used in this work .

The physicochemical properties of La–O, Zr–O and doped zirconia catalysts have been presented in Table 3.1. Zr–O catalyst has the largest surface area of  $310 \text{ m}^2\text{g}^{-1}$ . Ce–La–Zr–O, Ce–Zr–O and La–Zr–O catalysts have surface area of  $55 \text{ m}^2\text{g}^{-1}$ ,  $70 \text{ m}^2\text{g}^{-1}$  and  $75 \text{ m}^2\text{g}^{-1}$ , respectively, whilst La–O catalyst showed the least surface area of  $22 \text{ m}^2\text{g}^{-1}$ . It can be seen from Table 3.1 that La–O catalyst has the smallest total pore volume of  $0.015 \text{ cm}^3\text{g}^{-1}$ . Zr–O and Ce–La–Zr–O catalysts exhibited pore volume of  $0.45 \text{ cm}^3 \text{ g}^{-1}$  and  $0.29 \text{ cm}^3 \text{ g}^{-1}$ , while Ce–Zr–O and La–Zr–O catalysts showed similar total pore volume of  $0.2 \text{ cm}^3 \text{ g}^{-1}$  and  $0.22 \text{ cm}^3 \text{ g}^{-1}$ , respectively.

Table 3.1. Physical and chemical properties of ceria and lanthana doped zirconia (Ce–La–Zr–O), ceria doped zirconia (Ce–Zr–O), lanthanum oxide (La–O), lanthana doped zirconia (La–Zr–O), and zirconium oxide (Zr–O) catalysts.

Catalyst Properties	Catalysts				
	Ce–La–Zr–O	Ce–Zr–O	La–O	La–Zr–O	Zr–O
Physical form	Pale yellow powder	Pale yellow powder	White powder	White powder	White powder
Composition (%)	CeO <sub>2</sub> : 17±2 La <sub>2</sub> O <sub>3</sub> : 5±1 ZrO <sub>2</sub> : 78±3	CeO <sub>2</sub> : 18±2 ZrO <sub>2</sub> : 82±2	La <sub>2</sub> O <sub>3</sub> : 100	La <sub>2</sub> O <sub>3</sub> : 10±1 ZrO <sub>2</sub> : 90±1	ZrO <sub>2</sub> : 95±5
Particle size (µm)	1.7	30	0.1	5	5
BET surface area (m <sup>2</sup> g <sup>-1</sup> )	55	70	22	75	310
Pore volume (cm <sup>3</sup> g <sup>-1</sup> )	0.29	0.2	0.015	0.22	0.45
Average pore diameter (nm)	21.1	11.4	2.7	11.7	5.8
Operating Temperature (K) <sup>a</sup>	673	673	2578	673	673

<sup>a</sup>Manufacturer data

The scanning electron microscopy (SEM) images of Ce–La–Zr–O, Ce–Zr–O, La–O, La–Zr–O and Zr–O catalysts are shown in Figures 3.8–3.12. Figure 3.8 shows Ce–La–Zr–O image with well dispersed circular smooth surface, whereas Figure 3.9 gives Ce–Zr–O image with homogeneously aggregated irregular shape surface. Figure 3.10 shows La–O catalyst with rectangular grain-like surface. The SEM image of La–Zr–O catalyst shown in Figure 3.11 has aggregated circular smooth surface, whilst Figure 3.12 shows Zr–O catalyst with irregular grain like surface. Figures 3.8–3.12 clearly depicts that the incorporation of the dopants (lanthana and ceria) have strong influence on the morphology of the catalyst. A decrease in crystal size of Ce–Zr–O, Ce–La–Zr–O and La–Zr–O catalysts were due to the presence of dopants in the catalysts.

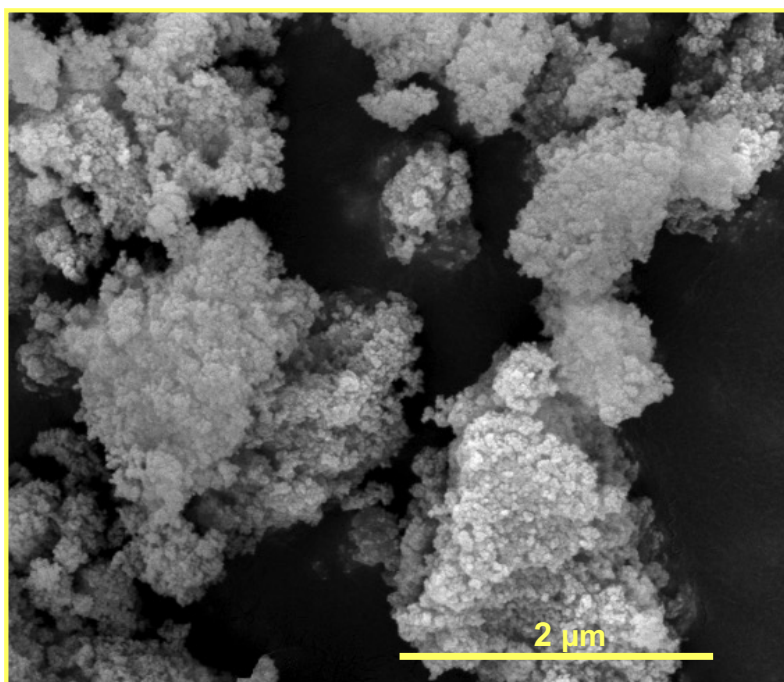


Figure 3.8. Scanning electron microscopy (SEM) image of ceria and lanthana doped zirconia (Ce–La–Zr–O) catalyst.

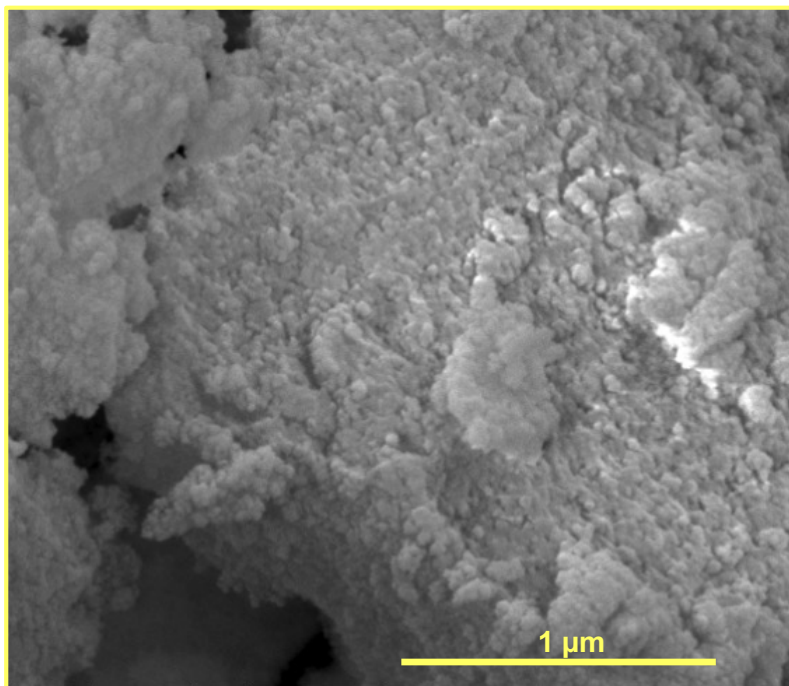


Figure 3.9. Scanning electron microscopy (SEM) image of ceria doped zirconia (Ce-Zr-O) catalyst.

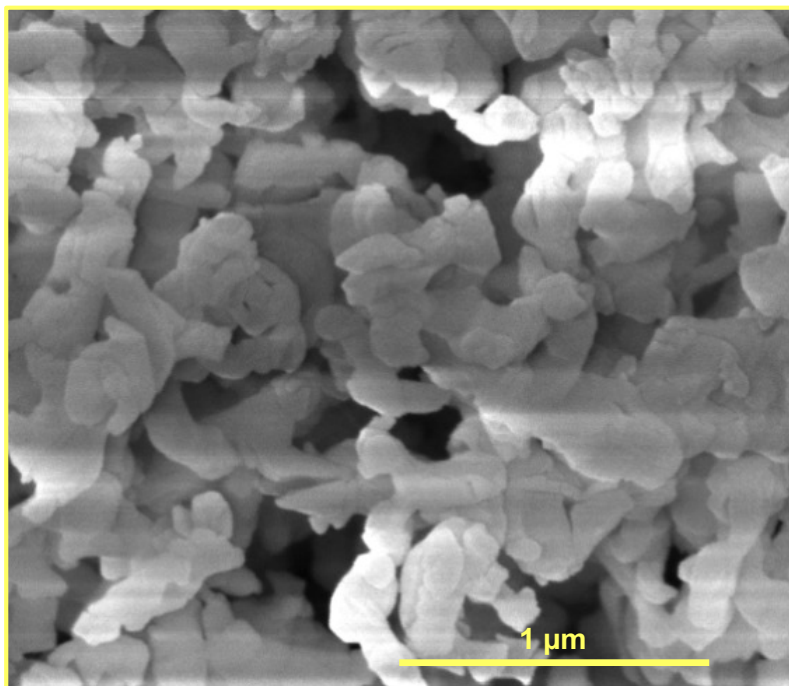


Figure 3.10. Scanning electron microscopy (SEM) image of lanthanum oxide (La-O) catalyst.

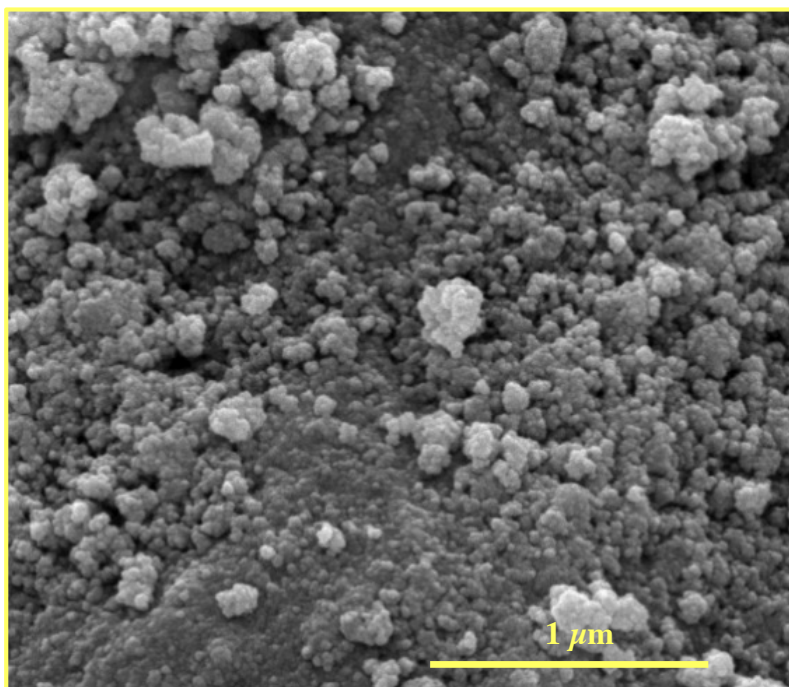


Figure 3.11. Scanning electron microscopy (SEM) image of lanthana doped zirconia (La-Zr-O) catalyst.

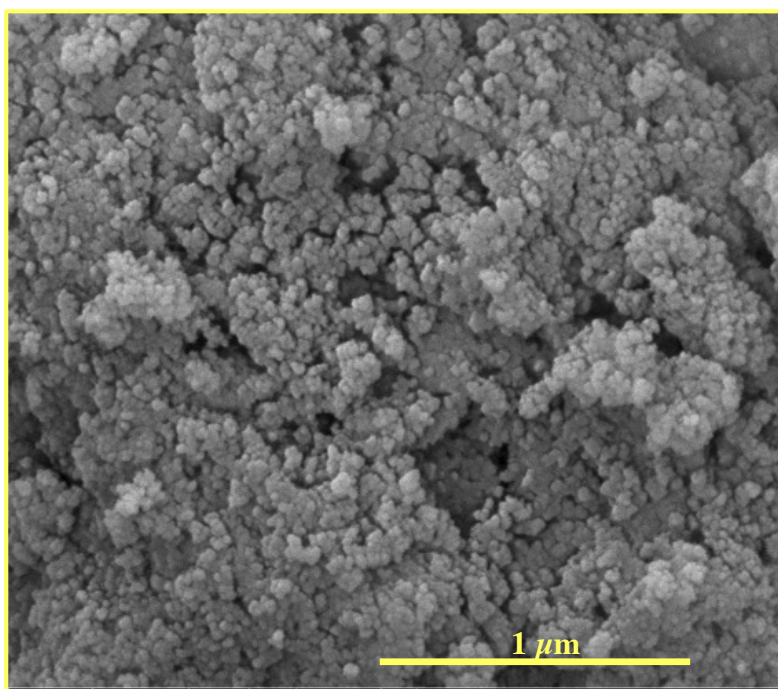


Figure 3.12. Scanning electron microscopy (SEM) image of zirconium oxide (Zr–O) catalyst.

The functional groups of the doped zirconia catalysts were investigated using Raman spectroscopy. Raman spectra of catalysts are presented in Figure 3.13. The parameters that affect the Raman bands include crystal size, structure and stresses (Barberis *et al.*, 1997). High intensity and broad peaks appeared at a wavelength ( $\lambda$ ) of  $620\text{ cm}^{-1}$  and  $1060\text{ cm}^{-1}$ , signifies the presence of Zr–O and La–O respectively, as the major support of the catalysts. Ce–Zr–O showed higher intensity and broader peaks at a wavelength ( $\lambda$ ) of  $620\text{ cm}^{-1}$  as compared to Ce–La–Zr–O and La–Zr–O and Zr–O catalysts. However, La–O catalyst showed no peak at  $\lambda$  value of  $620\text{ cm}^{-1}$  and higher intensity peak of La–O was observed at a  $\lambda$  value of  $1060\text{ cm}^{-1}$ . The broad peaks at a  $\lambda$  value of  $620\text{ cm}^{-1}$  is in accordance with Zr–O reported in the literature (Liu *et al.*, 2010). The intense peaks may be due to an increase in the surface area of Zr–O, which could have been influenced by the incorporation of dopant into the Zr–O.

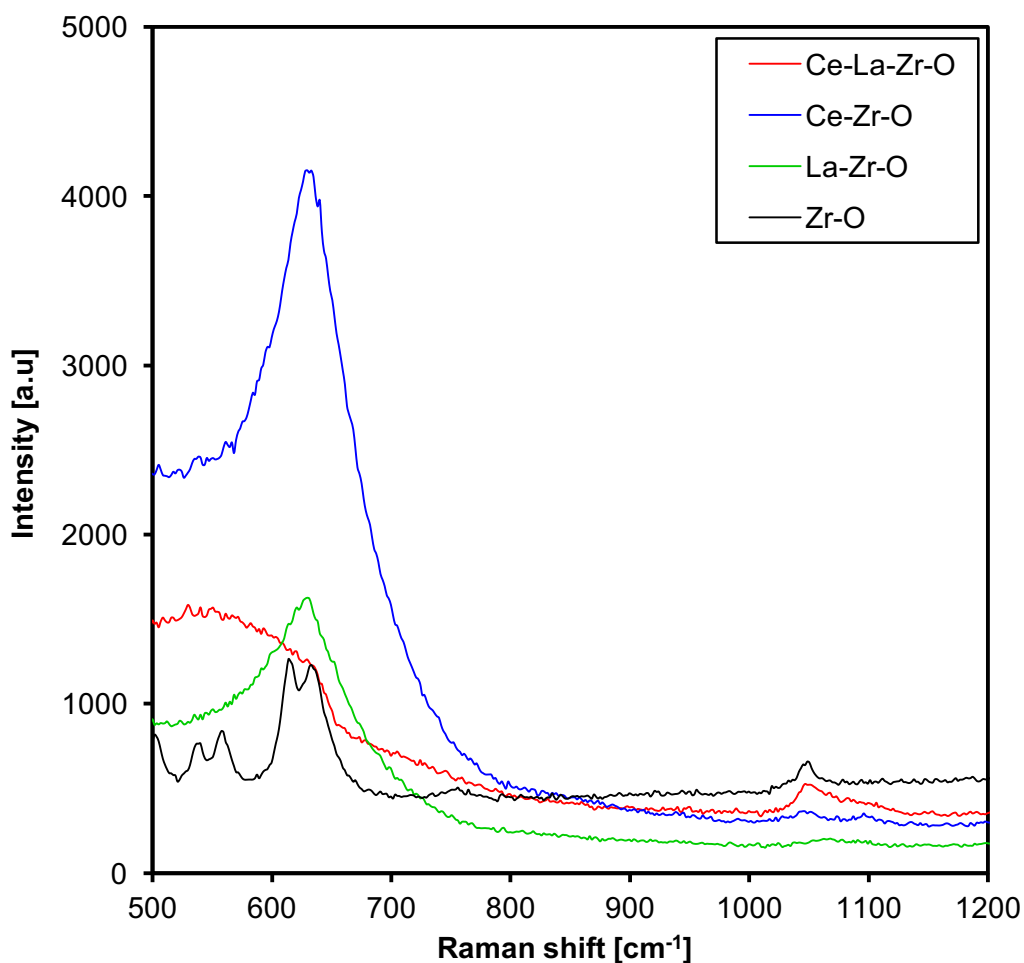


Figure 3.13. Raman spectra of ceria and lanthana doped zirconia (Ce–La–Zr–O), ceria doped zirconia (Ce–Zr–O), lanthana doped zirconia (La–Zr–O) and zirconium oxide (Zr–O) catalysts.

The XRD patterns of the Ce–Zr–O, La–Zr–O, Ce–La–Zr–O and Zr–O catalysts are shown in Figure 3.14. It is clearly shown in Figure 3.14 that the dopants (ceria and lanthana) have stronger interaction with zirconia. The zirconia peaks show low intensity at  $2\theta = 23^\circ, 28^\circ, 30^\circ, 31^\circ, 32^\circ, 50^\circ$  and  $60^\circ$  as compared to Ce–La–Zr–O with higher intensity peaks at  $2\theta = 32^\circ, 54^\circ$  and  $63^\circ$ . Ce–Zr–O and La–Zr–O catalysts have high peaks intensity appeared at  $2\theta = 29^\circ, 32^\circ, 50^\circ$  and  $60^\circ$ .

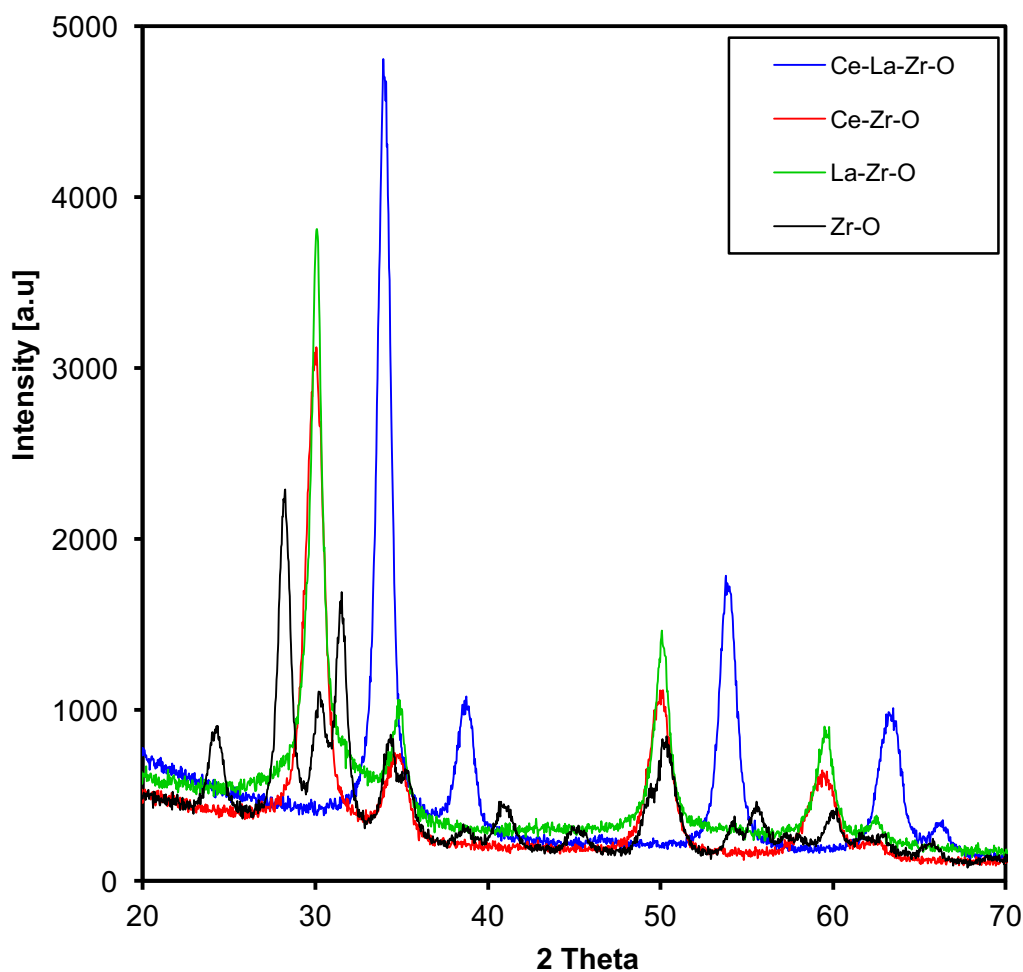


Figure 3.14. X-ray diffraction (XRD) patterns of ceria and lanthana doped zirconia (Ce–La–Zr–O), ceria doped zirconia (Ce–Zr–O), lanthanum oxide (La–O), lanthana doped zirconia (La–Zr–O) and zirconium oxide (Zr–O) catalysts.

These results are in agreement with that reported in the literature (Hu *et al.*, 2007). Zirconia peaks constitute the forms of zirconia (monoclinic and tetragonal zirconia). As a result, the peaks at  $2\theta = 23^\circ$ ,  $28^\circ$  and  $31^\circ$  exhibit monoclinic zirconia and the peaks appear at  $2\theta = 30^\circ$ ,  $32^\circ$ ,  $50^\circ$  and  $60^\circ$  represent tetragonal zirconia. Tetragonal zirconia showed higher thermal stability as compared to monoclinic zirconia. The influence of the dopants, therefore, increases the stability of the catalyst as clearly observed in Figure 3.14. The strong peak intensity of metal oxides doped zirconia was due to a decrease in crystallinity of the zirconia catalyst and therefore the presence of dopants in zirconia increases the surface area and stability of the catalysts.

## 3.3.2. Reaction Mechanism

DMC can be produced *via* the addition reaction of MeOH and CO<sub>2</sub> in the presence of a suitable catalyst as shown in the reaction pathway of Figure 3.15.

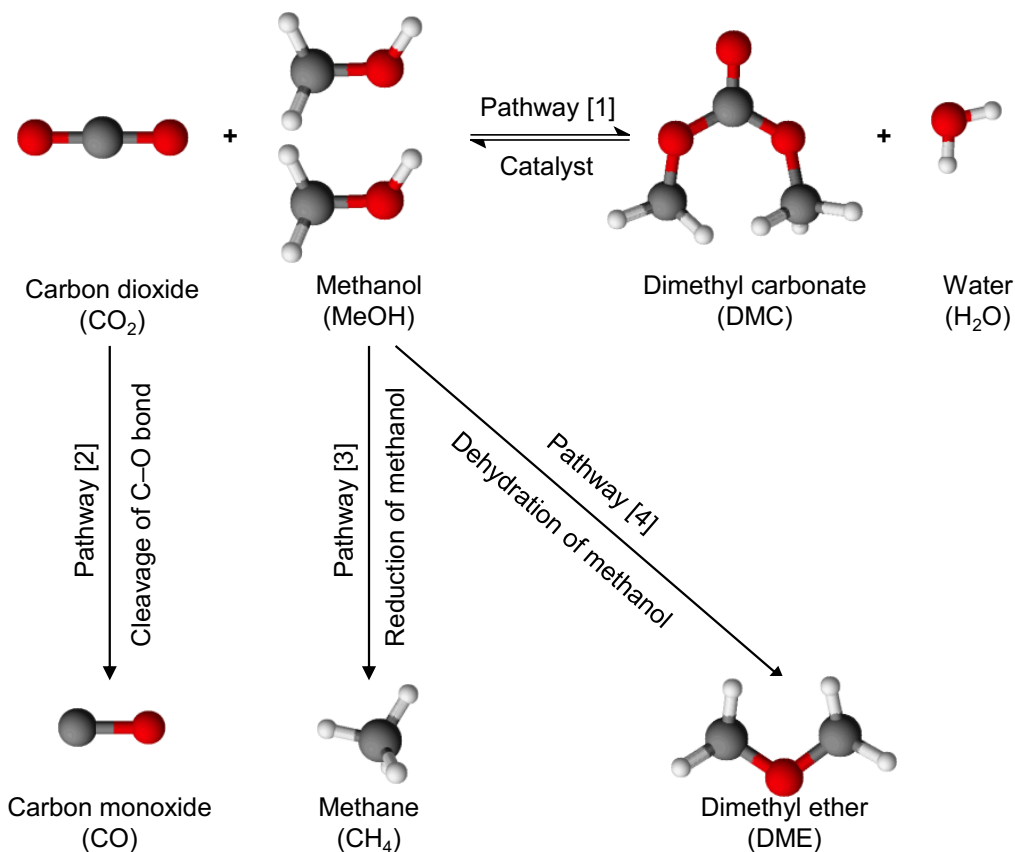


Figure 3.15. Reaction scheme for the synthesis of DMC from MeOH and CO<sub>2</sub>.

Water (H<sub>2</sub>O), carbon monoxide (CO), methane (CH<sub>4</sub>) and dimethyl ether (DME) are expected side products from the reaction of MeOH and CO<sub>2</sub> (Bian *et al.*, 2009a; 2009b; 2009c; 2009d; Zhang *et al.*, 2011). The cleavage of the C-O bond in carbon dioxide results in the production of CO (pathway 2 of Figure 3.15), methane can be produced upon the reduction of methanol (pathway 3 of Figure 3.15) and DME is produced as a result of methanol dehydration (pathway 4 of Figure 3.15) (Bian *et al.*, 2009a; 2009b; 2009c; 2009d; Zhang *et al.*, 2011). CO, CH<sub>4</sub>, H<sub>2</sub>O and DME were below the detection limit of the GC-FID used for the analysis of experimental samples and therefore specific yields of the side products were not calculated. This observation is similar to the work published by Zhang *et al.* (2011).

A proposed reaction mechanism for the synthesis of DMC is shown in Figure 3.16. It consists of four steps; activation of MeOH (step 1), activation of CO<sub>2</sub> (step 2), reaction between the active species to produce DMC (step 3) and finally the desorption of DMC and catalyst regeneration (step 4). In the proposed mechanism, M represents a metal atom that consists of an acidic site; O represents an oxygen atom that consists of a basic site. The reaction is initiated by the chemical adsorption of methanol on the catalyst surface. MeOH is activated and decomposes into methyl and methoxy species bonding on the acidic and basic sites of the catalysts respectively (step 1, Figure 3.16). Then CO<sub>2</sub> is activated by the adsorption on the basic site of the adjacent catalyst to produce carboxylate anion. The oxygen atom from the carboxylate anion (electron rich) coordinates with the methyl species to form a chemical bond (O–C) on the acidic site of the catalyst. The oxygen atom from the methoxy species coordinates with the carbon atom from the carboxylate species to form a chemical bond (O–C) on the basic site of the catalyst. DMC molecule is finally desorbed from the surface of the catalyst. The catalyst is regenerated so another catalytic cycle takes place.

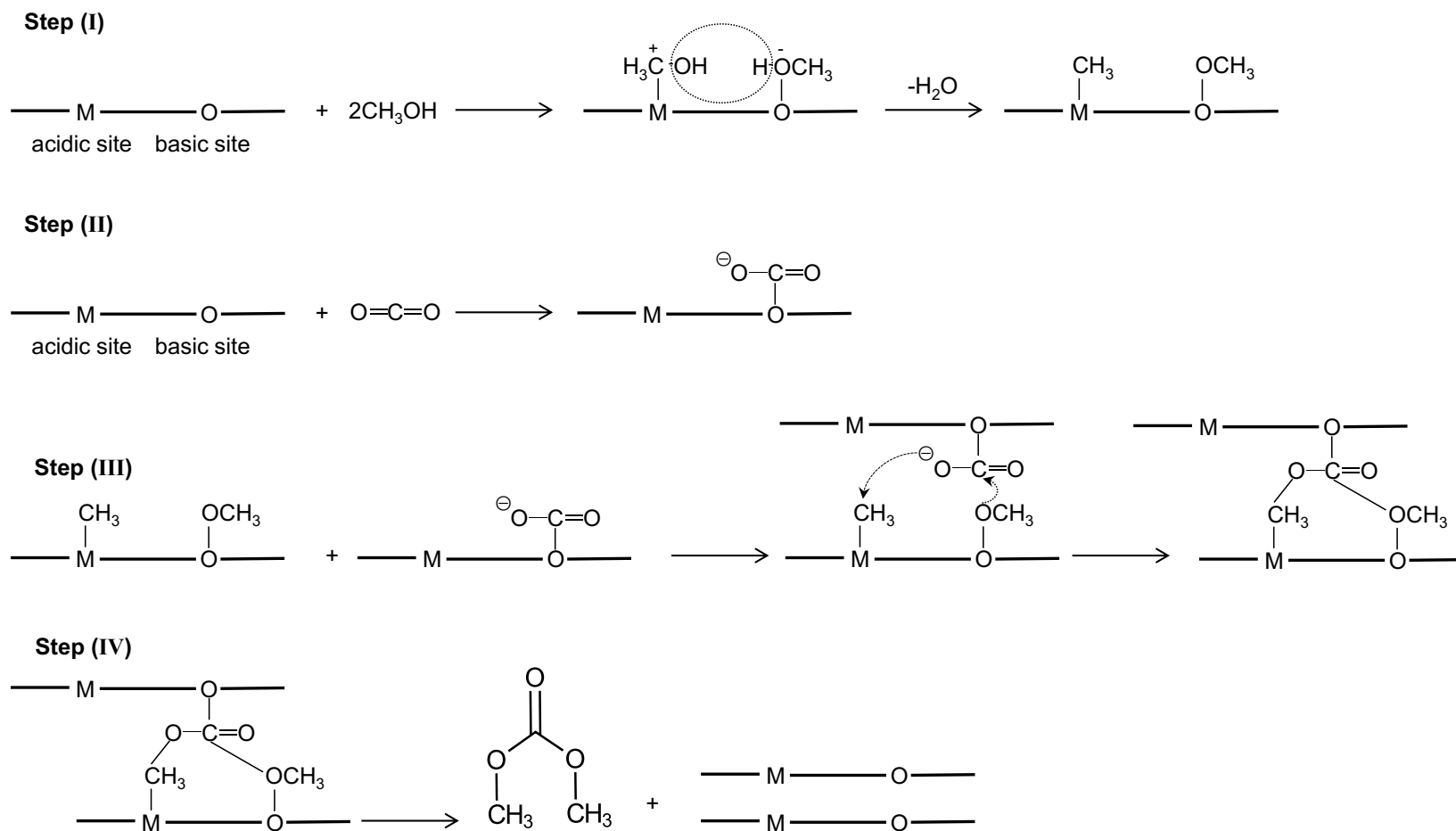


Figure 3.16. Proposed reaction mechanism for the synthesis of DMC from MeOH and CO<sub>2</sub>.

## 3.3.3. Effect of Different Catalysts

The catalytic performance of several heterogeneous catalysts for the synthesis of DMC from MeOH and CO<sub>2</sub> was evaluated in a high pressure reactor. Catalytic performance was indicated by MeOH conversion and DMC yield where two molecules of MeOH are incorporated into DMC. Figure 3.17 shows the effect of different metal oxide and mixed metal oxide catalysts on the conversion of MeOH and yield of DMC.

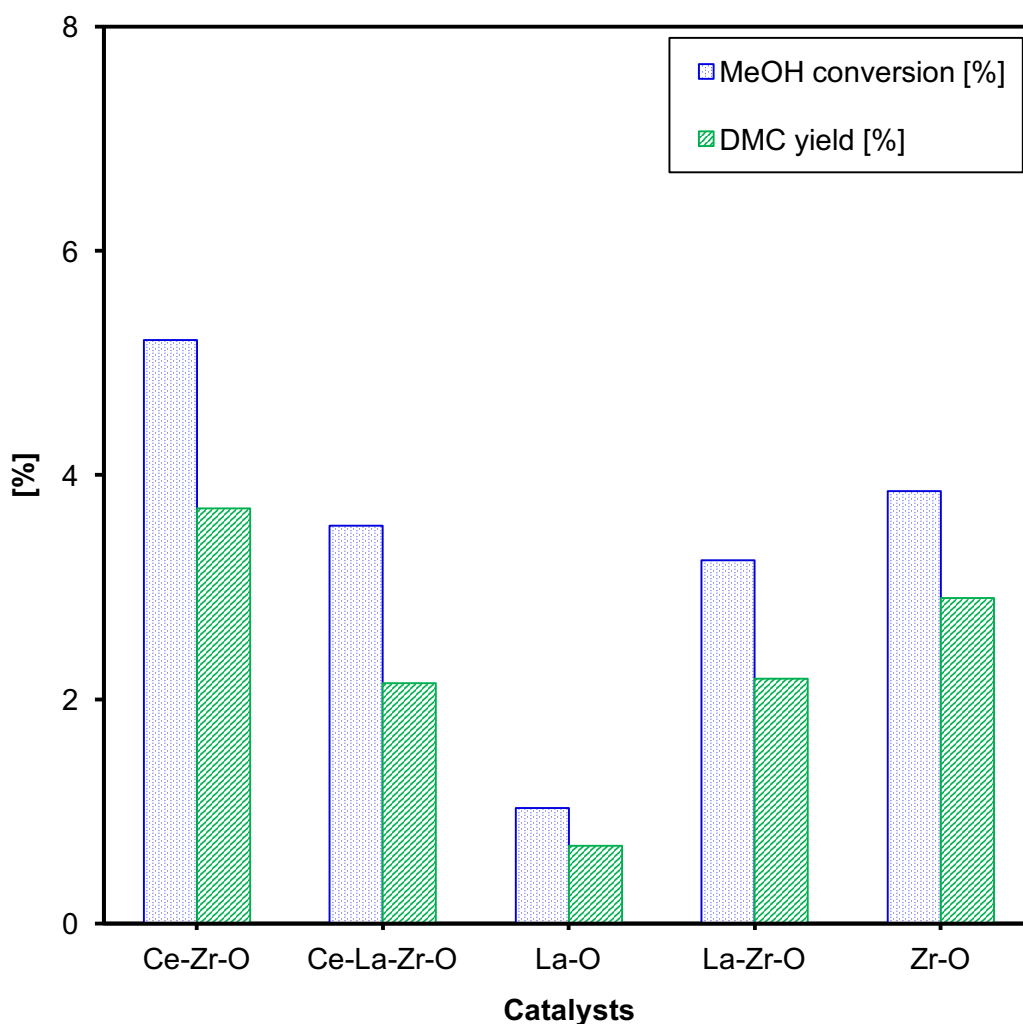


Figure 3.17. Effect of different heterogeneous catalysts on the direct synthesis of DMC. Experimental conditions: catalyst loading, 15% (w/w); reaction temperature, 393 K; CO<sub>2</sub> pressure, 290 bar; reaction time, 20 h and stirring speed, 300 rpm.

The presence of Zr–O has a significant effect on the performance of the catalyst. When Zr–O was tested on its own, the catalyst exhibited a MeOH conversion of ~3.8% and DMC yield of ~2.9%. The good performance of Zr–O catalyst could be attributed to the large surface area that the catalyst exhibits ( $310 \text{ m}^2\text{g}^{-1}$ ). On one hand, when cerium oxide ( $\text{CeO}_2$ ) was incorporated to Zr–O the performance of the resulting catalyst (i.e. Ce–Zr–O) was improved further. It can be seen from Figure 3.17 that Ce–Zr–O catalyst gave the highest MeOH conversion and DMC yield of ~5.2% and ~3.7%, respectively. On the other hand, the addition of lanthanum oxide ( $\text{ZrO}_2$ ) to Zr–O catalyst reduced MeOH conversion to ~3.2% and a DMC yield to ~2.1%. La–O catalyst showed the lowest MeOH conversion (~1%) and DMC yield (~0.69%) The incorporation of all three metal oxides Ce–La–Zr–O gave similar performance to that of La–Zr–O. Based on the catalyst screening tests, Ce–Zr–O was the best performing catalysts for the direct synthesis of DMC from MeOH and  $\text{CO}_2$  and hence it was used for further studies.

### 3.3.4. Effect of Catalyst Loading

In this work, catalyst loading is defined as the percentage ratio of the mass of the catalyst to the mass of the limiting reactant (MeOH). The influence of varying the catalyst loading on the yield of DMC was studied by carrying out a set of addition reactions of MeOH and  $\text{CO}_2$  using different amount of Ce–Zr–O. The results are presented in Figure 3.18. A MeOH conversion of ~1% and DMC yield of ~0.69% were achieved when the reaction was carried out using 2.5% (w/w) catalyst loading. This almost linearly increased to ~5.2% MeOH conversion and ~3.7% yield of DMC when the catalyst loading increased to 15%. Similar MeOH conversion and DMC yield were achieved when the catalyst loading increased to 20% (w/w) and therefore, it was not necessary to increase the catalyst loading above 15% (w/w). In view of the experimental error of  $\pm 3\%$ , it seems that the number of active sites required for MeOH and  $\text{CO}_2$  to react and produce DMC was sufficient at 15% (w/w) catalyst loading. The results show that 15% (w/w) catalyst loading is the optimum amount of catalyst required for this reaction.

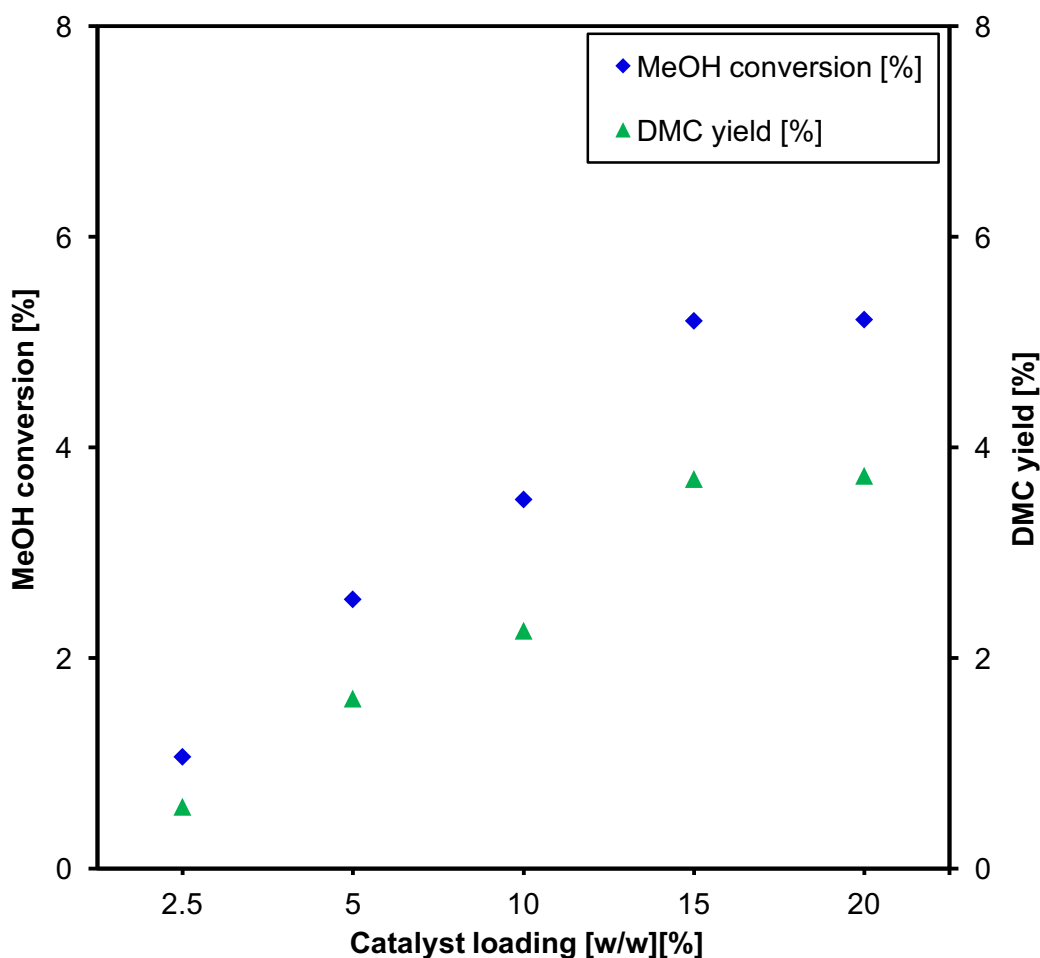


Figure 3.18. Effect of catalyst loading on MeOH conversion and yield of DMC. Experimental conditions: catalyst, Ce–Zr–O; reaction temperature, 393 K; CO<sub>2</sub> pressure, 290 bar; reaction time, 20 h and stirring speed 300 rpm.

### 3.3.5. Effect of Reaction Temperature

The effect of reaction temperature on MeOH conversion and DMC yield was studied in order to optimise reaction conditions. A set of catalytic reactions was conducted at 290 bar within a temperature range of 353 and 413 K for 20 h. The results are summarised and Figure 3.19 shows the temperature dependence of DMC synthesis. It is obvious that reaction temperature has a pronounced effect on the synthesis of DMC. MeOH conversion and DMC yield increased with increasing temperature from 353 K to 393 K. Increasing the temperature beyond 393 K has two opposite effects; an increase in temperature favours the conversion of MeOH and on the other hand favours the decomposition of DMC.

Formaldehyde, carbon monoxide and formic acid are among the side products for the decomposition of DMC at high temperatures (Anderson *et al.*, 2005; Saada *et al.*, 2015). Formaldehyde was not detected during GC analysis and the other side products were under the detection limit of GF-FID used in this study. Therefore, this study indicates that 393 K is the optimised temperature for the reaction between MeOH and CO<sub>2</sub> which agrees well with the published literature (Zhao *et al.*, 2000; Bian *et al.*, 2009a; Zhang *et al.*, 2011).

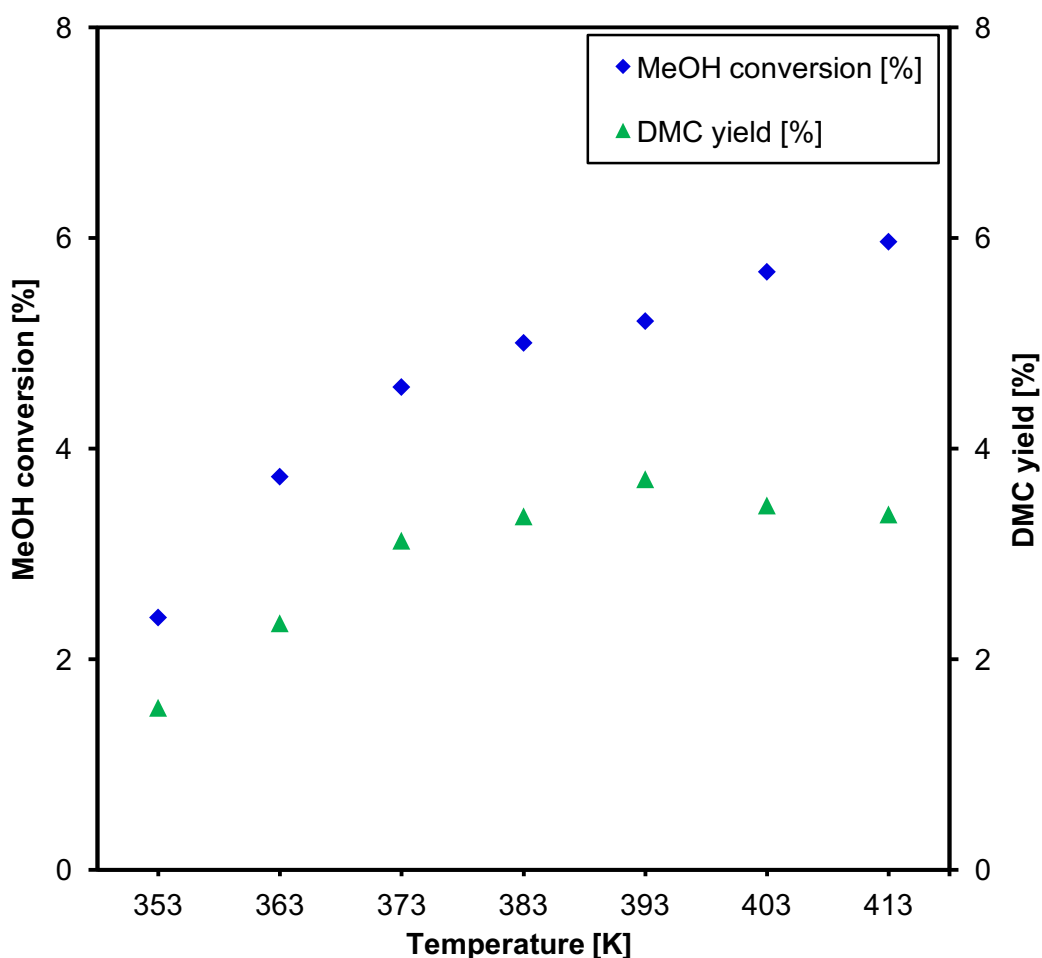


Figure 3.19. Effect of reaction temperature on MeOH conversion and yield of DMC. Experimental conditions: catalyst, Ce–Zr–O; catalyst loading, 15% (w/w); CO<sub>2</sub> pressure, 290 bar; reaction time, 20 h and stirring speed, 300 rpm.

### 3.3.6. Effect of CO<sub>2</sub> Pressure

CO<sub>2</sub> pressure plays an important role in the addition reaction of MeOH and CO<sub>2</sub>. It is known that physical properties of CO<sub>2</sub> are improved at supercritical state of CO<sub>2</sub>, which in turn enhances the activation of the CO<sub>2</sub> molecule to its greatest extent. The reaction between MeOH and CO<sub>2</sub> is governed by equilibrium. Near critical or supercritical state CO<sub>2</sub> reaction system can cause an increase in the mass transfer efficiency of the reactants and shift the reaction equilibrium to overcome the thermodynamic limitation of this reaction (Cao *et al.*, 2012). Also, using CO<sub>2</sub> at supercritical condition is a key to shift the equilibrium to the product side because MeOH and CO<sub>2</sub> reaction mixture is in a single phase compared to two phases when CO<sub>2</sub> is below supercritical conditions. The direct synthesis of DMC *via* the reaction of MeOH and CO<sub>2</sub> was carried out between CO<sub>2</sub> pressure of 170 bar and 290 bar in order to study its effect on the yield of DMC. Figure 3.20 presents the variation of MeOH conversion and DMC yield at different CO<sub>2</sub> pressure.

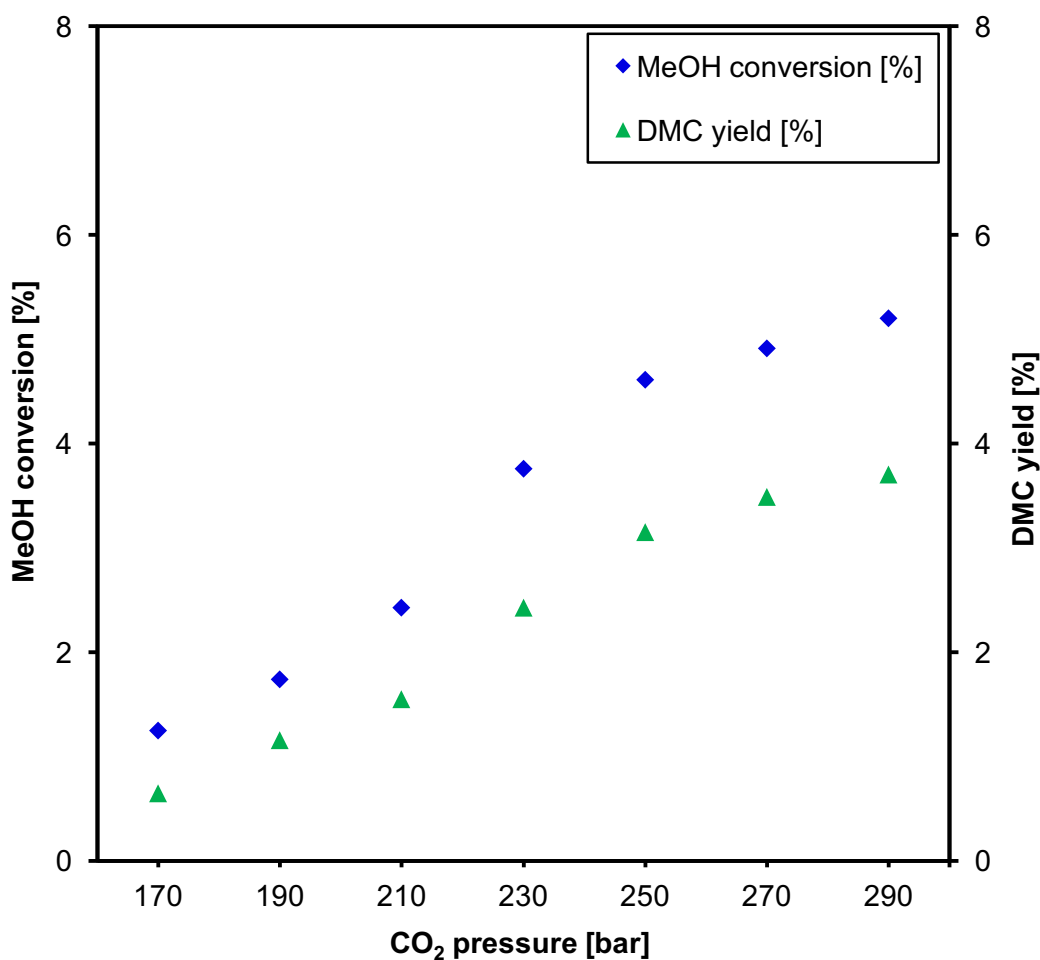


Figure 3.20. Effect of CO<sub>2</sub> pressure on MeOH conversion and yield of DMC. Experimental conditions: catalyst, Ce–Zr–O; catalyst loading, 15% (w/w); reaction temperature, 393 K; reaction time, 20 h and stirring speed, 300 rpm.

From Figure 3.20 it is evident that higher CO<sub>2</sub> pressure gave higher MeOH conversion and yield of DMC at a fixed reaction time for the catalysed reaction. At CO<sub>2</sub> pressure of 170 bar, MeOH conversion and yield of DMC were ~1.2% and ~0.65%, respectively. An increase in CO<sub>2</sub> pressure to 290 bar increased MeOH conversion and DMC yield to a maximum of ~5.2% and ~3.7%, respectively. From this study, it can be concluded that the optimum CO<sub>2</sub> pressure for the reaction of MeOH and CO<sub>2</sub> using Ce–Zr–O is 290 bar.

## 3.3.7. Effect of Reaction Time

A series of experiments were carried out at various reaction time to determine the optimum reaction time for the direct synthesis of DMC using 15% (w/w) Ce–Zr–O to catalyse the reaction. The experiments were carried out at 393 K and 290 bar. The results are presented in Figure 3.21.

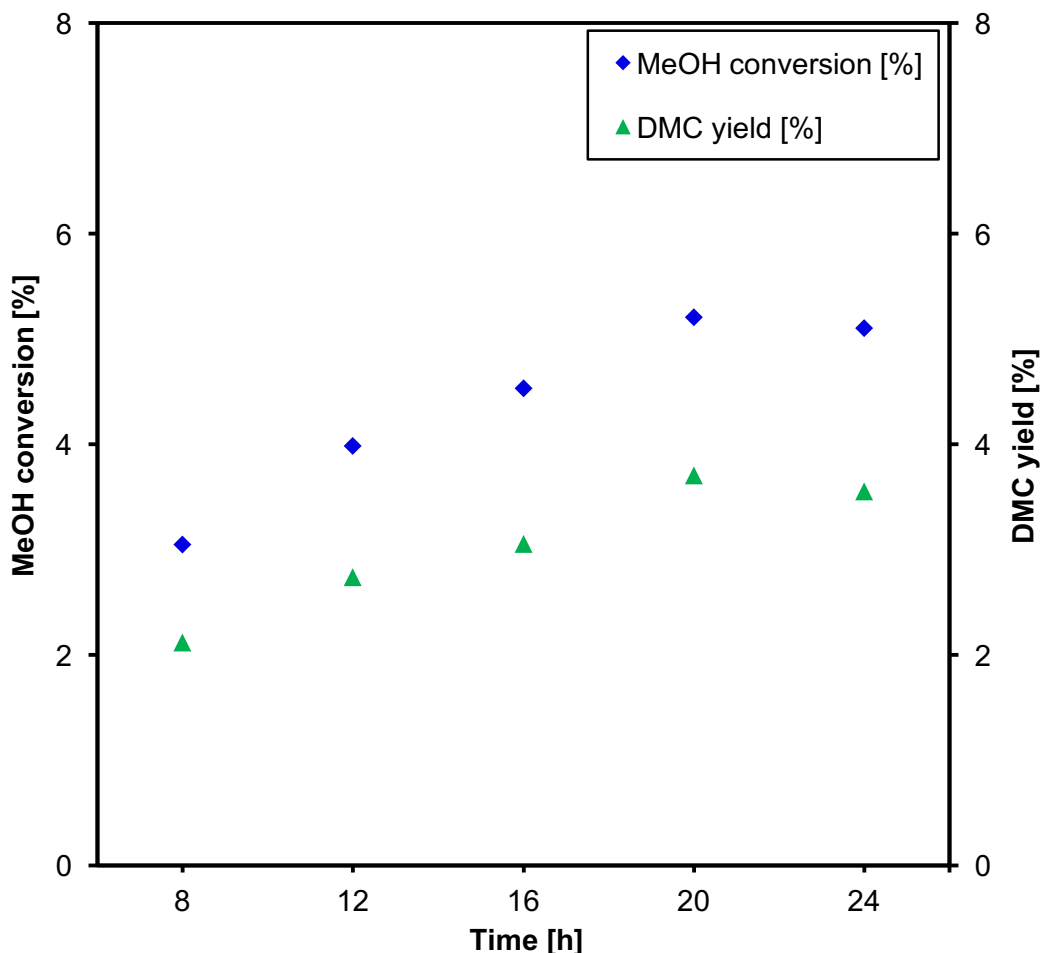


Figure 3.21. Effect of reaction time on MeOH conversion and yield of DMC. Experimental conditions: catalyst, Ce–Zr–O; catalyst loading, 15% (w/w); reaction temperature, 393 K; CO<sub>2</sub> pressure, 290 bar and stirring speed 300 rpm.

Figure 3.21 illustrates that an increase in reaction time increases MeOH conversion as well as the yield of DMC. MeOH conversion of ~3% and ~2.1% yield of DMC were observed for a reaction time of 8 h, whereas ~5.2% conversion of MeOH and ~3.7% yield of DMC were obtained for a reaction time of 20 h. However, when the reaction was carried out for a longer period, i.e.,

24 h, the conversion of MeOH as well as the yield of DMC were similar to that obtained at 20 h. It can be concluded that the reaction reaches equilibrium at 20 h using Ce–Zr–O as a heterogeneous catalyst and 20 h is considered as the optimum reaction time for this study.

### 3.3.8. Effect of Mass Transfer in Heterogeneous Catalytic Process

Mass transfer limitations can be a major factor that affects MeOH conversion and yield of DMC in heterogeneously catalysed process. External and internal mass transfer resistances are the two different types of mass transfer resistances that exist in heterogeneous catalysed reactions. External mass transfer resistance occurs across the solid-liquid interface due to the stirring of the reaction mixture, whereas internal mass transfer resistance occurs in the intra-particle space due to catalyst's physical and chemical structure, particle size, pore size distribution and porosity. The effect of mass transfer resistance on the addition reaction of MeOH and CO<sub>2</sub> using Ce–Zr–O to produce DMC was investigated using a high pressure reactor. The addition reactions were carried out at different stirring speed (300–500 rpm) under otherwise identical conditions as shown in Figure 3.22.

It can be observed that there was negligible difference of MeOH conversion and yield of DMC at different stirring speed, which suggest that there is a homogeneous distribution of catalyst particles in the reaction mixture and hence it can be concluded that external mass transfer resistance is absent in this work. On the other hand, Ce–Zr–O particles are fairly small, uniform and porous (particle size: 30µm and pore diameter 11.4 nm), which eliminates mass transfer limitation (Clerici and Kholdeeva, 2013). Therefore, it can be concluded that internal mass transfer resistance is negligible for Ce–Zr–O catalysed addition reactions due to the nature of the catalyst particles. On the basis of this investigation, all batch experiments were carried at a stirrer speed of 300 rpm using Ce–Zr–O catalysts.

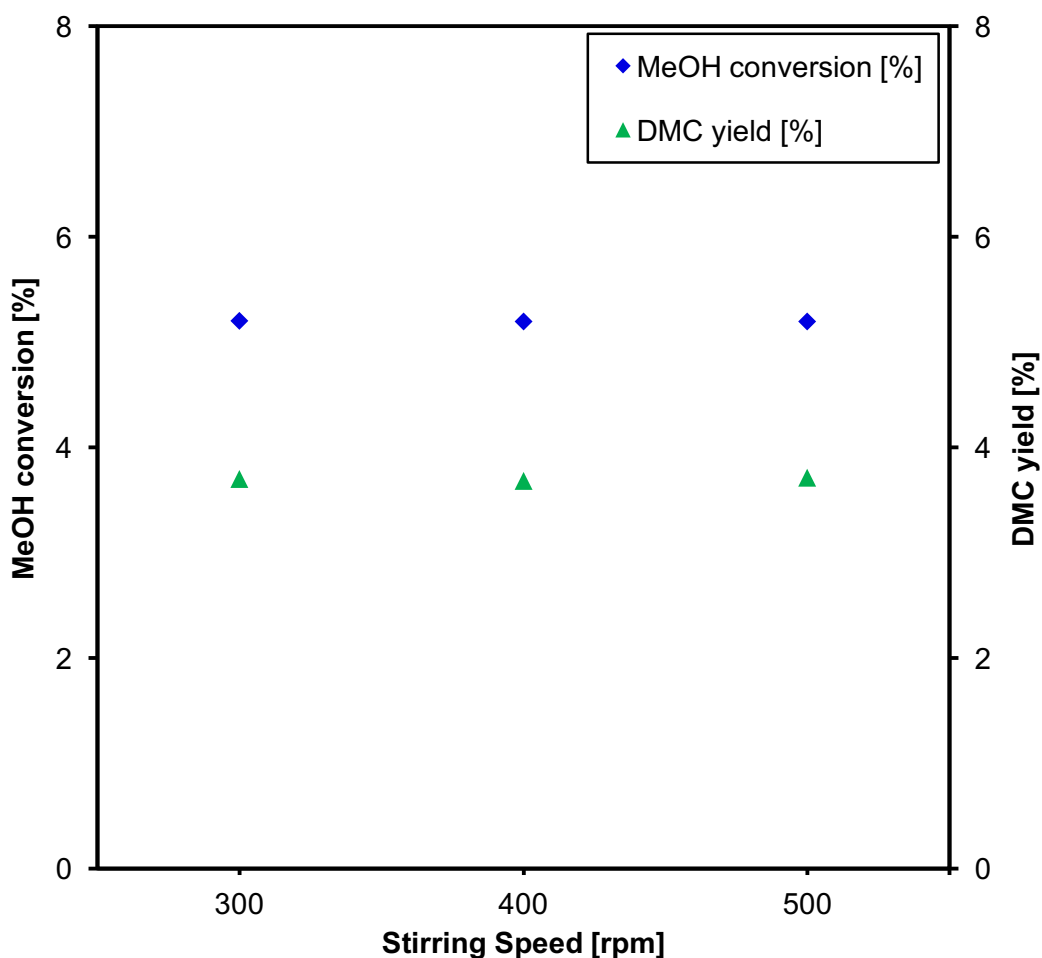


Figure 3.22. Effect of stirring speed on MeOH conversion and yield of DMC. Experimental conditions: catalyst, Ce–Zr–O; catalyst loading, 15% (w/w); reaction temperature, 393 K; CO<sub>2</sub> pressure, 290 bar and reaction time, 20 h.

### 3.3.9. Catalyst Reusability Studies

The reusability of Ce–Zr–O was studied by carrying out a set of experiments at the optimum reaction condition obtained from the batch studies (i.e., reaction temperature 393 K, CO<sub>2</sub> pressure 290 bar, 15% catalyst loading (w/w) and 20 h). The first reaction (labelled as Run 1) was carried out using a fresh batch of catalyst as shown in Figure 3.23. The catalyst was recovered by filtration from the reaction mixture, washed twice with acetone and dried at 333 K for 12 h. The catalyst was then reused for subsequent experiments (labelled as Run 2–Run 6) under the same reaction conditions as shown in Figure 3.23. It can be observed that MeOH conversion and yield of DMC remained comparable even after the 6<sup>th</sup>

Run indicating that Ce–Zr–O exhibits excellent reusability and stability for the synthesis of DMC. It is evident that Ce–Zr–O can be easily recovered and reused without any significant reduction in the catalytic performance.

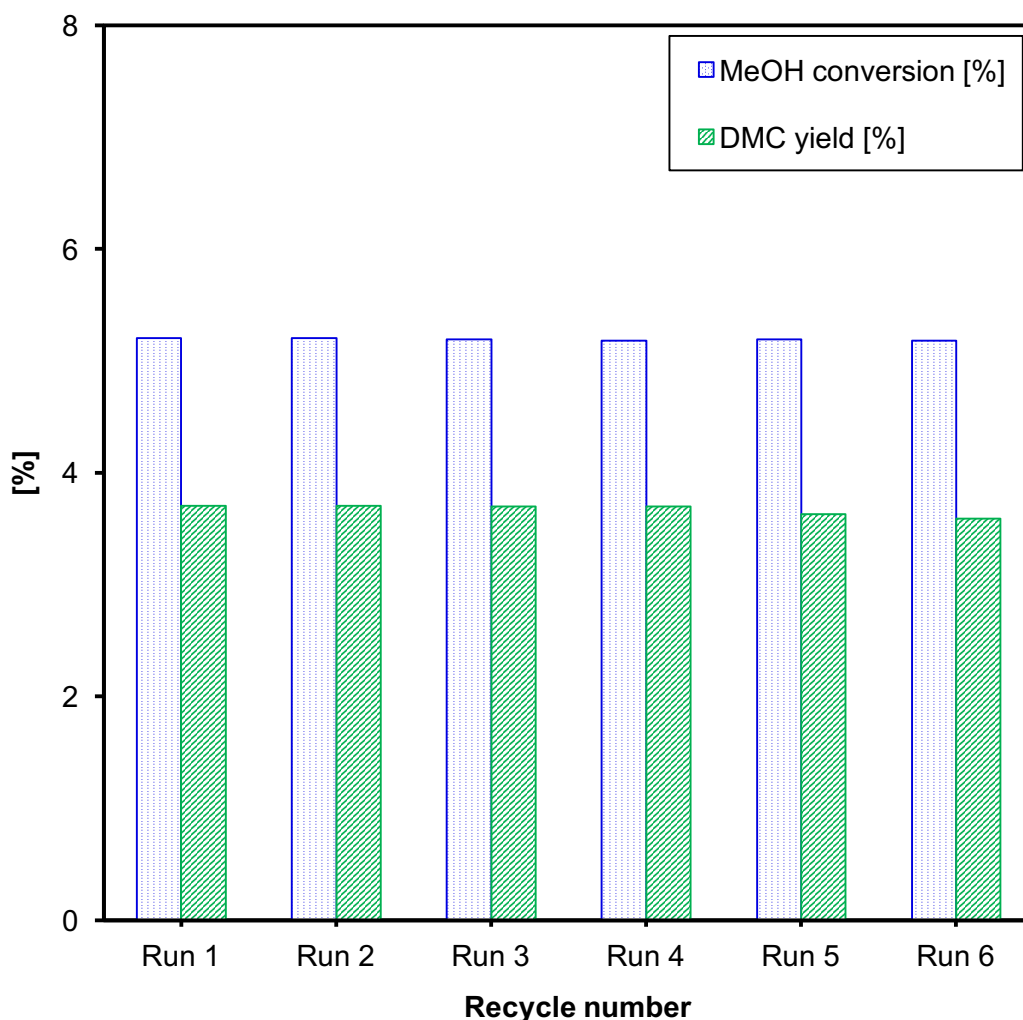


Figure 3.23. Catalyst reusability studies for synthesis of DMC. Experimental conditions: catalyst, Ce–Zr–O; catalyst loading, 15% (w/w); reaction temperature, 393 K; CO<sub>2</sub> pressure, 290 bar; reaction time, 20 h and stirring speed, 300 rpm.

### 3.4. CONCLUSIONS

The addition reaction of MeOH and CO<sub>2</sub> for the direct synthesis of DMC was successfully conducted in a high pressure reactor in the presence of various heterogeneous catalysts in the absence of a solvent. Catalyst characterisation was investigated using scanning electron microscopy, Raman spectroscopy and X-ray diffraction. The effect of various parameters such as catalyst loading,

reaction time, reaction temperature, CO<sub>2</sub> pressure and stirring speed was studied for the optimisation of DMC synthesis. It was found that an increase in CO<sub>2</sub> pressure resulted in an increase in the MeOH conversion and yield of DMC. Ceria doped zirconia (Ce–Zr–O) catalyst was found to be the best performing catalyst for DMC synthesis as compared to other heterogeneous catalysts. The highest MeOH conversion of ~5.2% and DMC yield of ~3.7% were obtained at optimum reaction conditions of 393 K, 290 bar, 300 rpm and 20 h using 15% (w/w) Ce–Zr–O. Reusability studies confirmed that Ce–Zr–O could be easily recycled and reused several times without any reduction in its catalytic performance.

# **Chapter 4**

## **Direct Synthesis of Dimethyl Carbonate (DMC) from Carbon Dioxide (CO<sub>2</sub>) and Methanol (MeOH) using Metal Oxide/ Graphene Nanocomposite Catalysts**

## 4. DIRECT SYNTHESIS OF DMC FROM CO<sub>2</sub> AND MeOH USING METAL OXIDE/ GRAPHENE NANOCOMPOSITE CATALYSTS

### 4.1. INTRODUCTION

Dimethyl carbonate (DMC) is a promising environmentally benign compound that exhibits versatile and excellent chemical properties. It has low toxicity and high biodegradability which makes it a safer alternative to poisonous dimethyl sulphate and phosgene. Several reaction routes have been attempted for DMC production such as oxidative carbonylation and transesterification of cyclic carbonates. However, the direct synthesis of DMC from methanol (MeOH) and carbon dioxide (CO<sub>2</sub>) offers a greener and more sustainable synthetic route for DMC production (Ballivet-Tkatchenko *et al.*, 2006; Bian *et al.*, 2009a).

Various catalysts have been studied extensively; however, the methanol conversion and DMC yield are still very low. This is due to the equilibrium limited reaction and the catalyst deactivation when water is formed as a by-product. Different dehydrating agents and additives have been used to minimise the effect of water produced during the reaction and improving the catalytic performance of the catalyst. These systems can be classified as reactive or non-reactive dehydration systems (Honda *et al.*, 2014). These agents include nitrile compounds (Honda *et al.*, 2010; 2011), calcium chloride (Wu *et al.*, 2005), 2,2-dimethoxy propane (Tomishige and Kunimori, 2002; Honda *et al.*, 2009), molecular sieves (Hou *et al.*, 2002), ketals (Sakakura *et al.*, 2000), aldols (Sakakura *et al.*, 2007) and trimethoxymethane (TMM) (Zhang *et al.*, 2011) and have positively contributed to an increase in MeOH conversion.

A variety of metal oxide catalysts have been developed and assessed for the effective synthesis of DMC. Cerium oxide (CeO<sub>2</sub>) (Aresta *et al.*, 2010; Tomishige *et al.*, 2001; Yoshida *et al.*, 2006), zirconium oxide (ZrO<sub>2</sub>) (Tomishige *et al.* 2000; Jung and Bell, 2001; Aymes *et al.*, 2009; Xie and Bell, 2000), vanadium oxide (V<sub>2</sub>O<sub>5</sub>) (Wu *et al.*, 2005; 2006), titanium oxide (TiO<sub>2</sub>) (La and Song 2006) and tin oxide (SnO<sub>2</sub>) (Aymes *et al.*, 2009) have been investigated over the past few years in an attempt to maximise the catalytic performance and enhancing the production rate of DMC.

The usage of a support can increase the stability of the catalyst, optimise the dispersion of the active components of the catalyst, and provide important chemical, mechanical, thermal and morphological properties (Dai *et al.*, 1996). The general procedure for preparation of supported catalysts involves the transformation of the precursors into the required active compound and the deposition of the active compound onto the support surface. Different materials have been widely used as suitable catalyst supports in recent studies; these include silica (Fan *et al.*, 2010; Ballivet-Tkatchenko *et al.*, 2011a), molecular sieve (Chen *et al.*, 2012), complex supports (Wu *et al.*, 2006) metal oxides (Almusaiteer, 2009), graphene oxide (GO), activated carbon and multi-walled carbon nanotubes (Bian *et al.*, 2009b).

Although there has been a considerable effort dedicated to the use of various metals as suitable catalysts, there is still a lack in finding suitable supports for the catalytic system and this area needs to be explored more (Bian *et al.*, 2009b). Strongly coupled graphene based inorganic nanocomposites represent an exciting opportunity for the production innovative functional materials that can be potentially used as suitable heterogeneous catalysts for the synthesis of DMC. Graphene is a unique two-dimensional single layer of carbon in which the atoms are arranged in hexagons (Geim and Novoselov, 2007; Geim, 2009; Rao *et al.*, 2009), which poses excellent physical, chemical and mechanical properties. Graphene has a very high surface area and its surface can be easily modified to allow preparation of nanocomposite materials with novel characteristics (Li and Kaner, 2008; Williams *et al.*, 2008; Dreyer *et al.*, 2010).

Currently, graphene nanocomposites are produced using conventional methods *via* homogenisation by mixing inorganic nanoparticles and grinding, giving little control over the homogeneous dispersion of the nanoparticles. Hydrothermal synthesis of graphene nanocomposite in superheated or supercritical water can offer many advantages over conventional preparative methods including fewer synthetic steps and significantly faster reaction times (Hakuta *et al.*, 1998; Darr and Poliakoff, 1999; Chaudhry *et al.*, 2006; Lester *et al.*, 2006; Goodall *et al.*, 2014; Middelkoop *et al.*, 2014). There are currently few scientific reports utilising hydrothermal routes for graphene nanocomposite particles (Liang *et al.*, 2010; Su *et al.*, 2011; Li *et al.*, 2011b; Perera *et al.*, 2012). However, the current

hydrothermal syntheses are conducted in batch reactors, which are time consuming and give little control over final product properties such as crystallinity and particle size.

Continuous hydrothermal flow synthesis (CHFS) reactors have independent control over reaction variables such as pressure and temperature and hence particle properties (Li *et al.*, 2011b). Generally, the CHFS process involves mixing a flow of supercritical water with a flow of aqueous metal salt(s) to give rapid precipitation and controlled growth of nanoparticles in a continuous manner. The properties of water i.e., diffusivity, density, and dielectric constant change dramatically around the critical temperature (647 K) and pressure (22.1 MPa) leading to its use as an exotic, and tunable reaction solvent/medium. Graphene has a 2D, platelike structure and therefore offers an attractive substrate for deposition of inorganic nanoparticles for highly dispersed composites with novel properties.

Therefore, in this chapter, an innovative approach has been employed for synthesising advanced graphene-inorganic nanocomposite catalyst *via* utilisation of a CHFS reactor. The codes given for various catalysts are shown in Table 4.1. The catalytic activities of the as-synthesised materials have been tested using a new, greener and sustainable process for the direct synthesis of DMC from MeOH and CO<sub>2</sub>. The use of 1,1,1-trimethoxymethane as a dehydrating agent has been evaluated. The optimum reaction conditions for the direct synthesis of DMC have been delineated.

Table 4.1. Names corresponding codes for various catalyst examined for the synthesis of DMC.

Code	Catalyst
CM	Ceria-zirconia oxide/graphene nanocomposite synthesised <i>via</i> wet impregnation route
CM700	Ceria-zirconia oxide/graphene nanocomposite synthesised <i>via</i> wet impregnation route and heat-treated at 973 K
HTR	Ceria-zirconia oxide/graphene nanocomposite synthesised using CHFS route
HTR700	Ceria-zirconia oxide/graphene nanocomposite synthesised using CHFS route and heat-treated at 973 K

## 4.2. EXPERIMENTAL METHOD

### 4.2.1. Materials

Methanol (MeOH), *iso*-propyl alcohol (IPA) and dimethyl carbonate (DMC), 1,1,1-trimethoxymethane (TMM) and zirconium (IV) oxynitrate hydrate (ZrO(NO<sub>3</sub>)<sub>2</sub>.6H<sub>2</sub>O) were all purchased from Sigma Aldrich (UK). Other chemicals were purchased from Fisher Scientific, UK, including hydrochloric acid (HCl), sulfuric acid (H<sub>2</sub>SO<sub>4</sub>), natural graphite powder (NPG), sodium nitrate (NaNO<sub>3</sub>), cerium(III) nitrate hexahydrate (Ce(NO<sub>3</sub>)<sub>3</sub>.6H<sub>2</sub>O), hydrogen peroxide (H<sub>2</sub>O<sub>2</sub>), potassium hydroxide pellets (KOH) and potassium permanganate (KMnO<sub>4</sub>). The liquid CO<sub>2</sub> cylinder (99.9%) equipped with a dip tube was purchased from BOC Ltd, UK.

#### 4.2.2. Catalyst Preparation

##### 4.2.2.1. Preparation of graphene oxide

Natural graphite powder (NGP) was purchased from Sigma Aldrich Ltd and used as a precursor without any treatment. Some modifications were made to the Hummer's method (Hummers and Offeman, 1958) and applied for the synthesis of graphene oxide (GO) from NGP. Figure 4.1 shows the experimental setup for graphene oxide preparation. In a typical reaction, 2.5 g of NGP and 2.5 g of sodium nitrate (NaNO<sub>3</sub>) were added to 115 mL of sulphuric acid (H<sub>2</sub>SO<sub>4</sub>). The mixture was stirred with a magnetic stirrer for about 15 min in an ice bath. 20 g of potassium permanganate (KMnO<sub>4</sub>) were added gradually to the mixture and left for another 15 min with continuous stirring. The resulting mixture was transferred to an oil bath at 313 K and stirred at 600 rpm for 90 min. 200 mL of deionised water was added to the mixture followed by 30 mL of hydrogen peroxide (H<sub>2</sub>O<sub>2</sub>). This was followed by the addition of 200 mL of deionised water. The resulting light brown mixture was heated to 363 K and left for 15 min. The mixture was left to cool down and the product was separated using a centrifuge (5000 rpm, 5 min per cycle). GO was washed successively with 10% hydrochloric acid (HCl) and deionised water to remove any impurities and then dried at 333 K for 24 h. Figure 4.2 shows a representation of graphite powder transformation to graphene oxide. The synthesised GO was then used as a precursor for the synthesis of ceria-zirconia oxide/graphene nanocomposites [Ce–Zr/GO, where nominal atomic ratio of Ce:Zr (1:1)] prepared *via* CHFS and conventional method (wet impregnation) routes as shown in Figure 4.3.

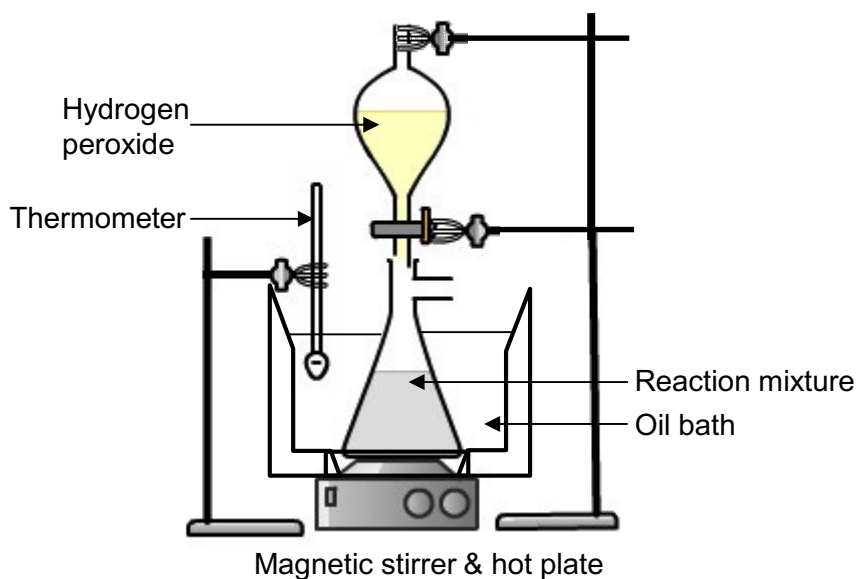


Figure 4.1. Experimental set-up for the preparation of graphene oxide (GO).

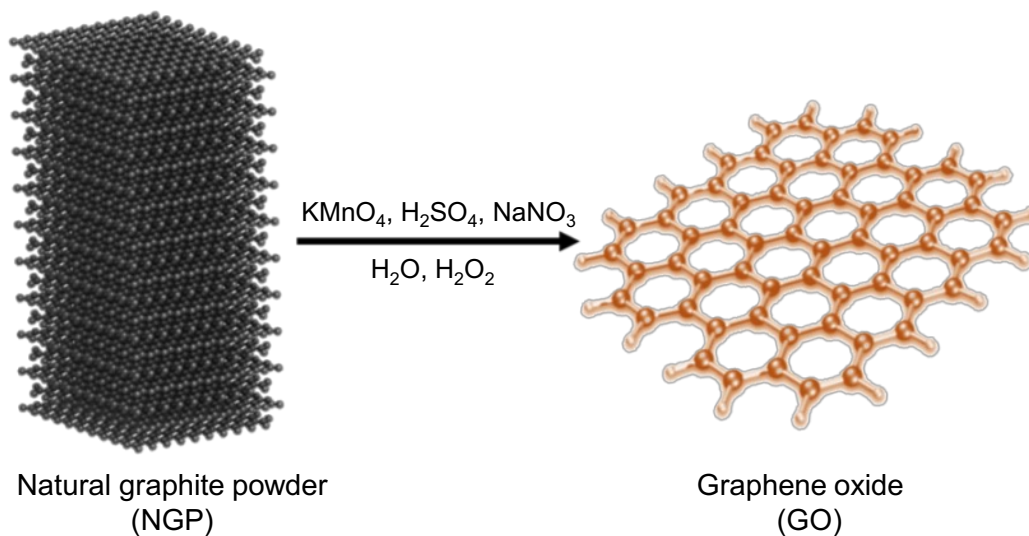


Figure 4.2. A schematic representation of graphite powder transformation to graphene oxide (GO).

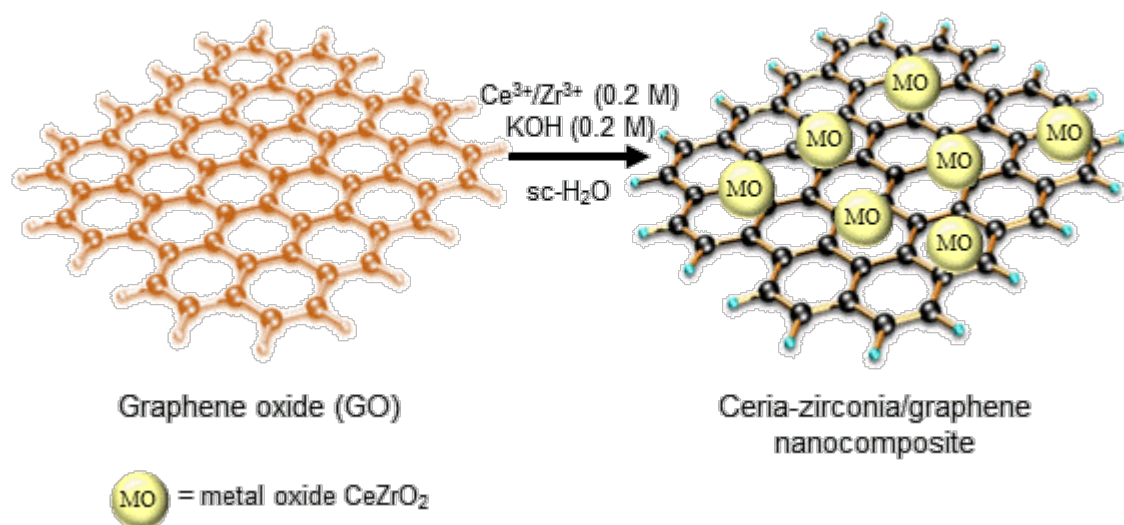


Figure 4.3. A schematic representation of the synthesised Ce–Zr/GO nanocomposite catalyst.

#### 4.2.2.2. Ceria-zirconia oxide/graphene nanocomposite synthesis via conventional method

A control reaction using a traditional wet impregnation method was conducted for the synthesis of Ce–Zr/GO nanocomposite catalyst. Cerium(III) nitrate hexahydrate (Ce(NO<sub>3</sub>)<sub>3</sub>·6H<sub>2</sub>O) and zirconium(IV) oxynitrate hydrate (ZrO(NO<sub>3</sub>)<sub>2</sub>·6H<sub>2</sub>O) were used as metal precursors. 1 g of GO was dispersed in 50 mL of deionised water by ultrasonic vibration for 1 h. The mixture was removed from the ultrasonic bath and 0.1882 g of Ce(NO<sub>3</sub>)<sub>3</sub>·6H<sub>2</sub>O and 0.1 g of ZrO(NO<sub>3</sub>)<sub>2</sub>·6H<sub>2</sub>O were added to the GO suspension and continuously stirred using a magnetic stirrer for 10 min. 6 mL of 8 M sodium hydroxide (NaOH) solution was added dropwise to the mixture while maintaining a vigorous agitation. The mixture was heated at 353 K using an oil bath for 1 h and was then cooled down to room temperature. Ce–Zr/graphene nanocomposite catalyst was separated using a centrifuge (5000 rpm, 30 min per cycle). The prepared catalyst was washed twice with deionised water and dried at 313 K for 24 h. The dried Ce–Zr/graphene nanocomposite catalyst was heat treated at different temperatures (i.e., 773 K, 973 K and 1173 K) under nitrogen for 4 hours. The catalyst was cooled down for 4 hours before it was used for testing. The samples synthesised *via* this method were labelled as CM.

4.2.2.3. Ceria-zirconia oxide/graphene nanocomposite synthesis via CHFS route

CHFS experiments were conducted using a reactor, basic design of which has been reported previously (Chaudhry *et al.*, 2006; Weng *et al.*, 2008; Zhang *et al.*, 2009; Kellici *et al.*, 2014). Briefly, the system consists of three high performance liquid chromatography (HPLC) pumps used for the delivery of aqueous solution of reagents as shown in Figure 4.4. The tubing and fittings were 1/8 inch 316 SS Swagelok, except the counter-current reactor and the cooler, which were constructed using 1/4 inch fittings. Pump 1 (Gilson 307 fitted with 25 mL pump head) was utilised for delivering deionised water through a custom made electrically powered pre-heater (2.5 kW) at a flow rate of 20 mL min<sup>-1</sup>. Pumps 2 and 3 (Varian Pro Star 210 fitted with 5 mL pump head) were employed for pumping pre-sonicated aqueous GO solution premixed with corresponding cerium and zirconium salts at the desired ratios and KOH, respectively, at a flow rate of 5 mL min<sup>-1</sup>. In a typical experiment, each pre-mixed aqueous solution of Ce(NO<sub>3</sub>)<sub>3</sub>·6H<sub>2</sub>O and ZrO(NO<sub>3</sub>)<sub>2</sub>·6H<sub>2</sub>O (with a total metal ion concentration of 0.2 M) and a pre-sonicated (30 min) aqueous solution of GO (4 µg mL<sup>-1</sup>) were pumped to meet a flow of KOH (0.2 M) at a T-junction (see Figure 4.4). The molar ratio of Ce<sup>3+</sup>/Zr<sup>4+</sup> = 1 and GO = 2. This mixture then meet superheated water (723 K, 24.1 MPa) inside an in-house built 1/4 inch counter-current reactor whereupon the formation of Ce–Zr/GO occurs in a continuous manner (Lester *et al.*, 2006). The aqueous suspension was cooled through a vertical cooler and the slurries were collected from the exit of the back pressure regulator. After collection, the particles were centrifuged and washed twice with deionised water.

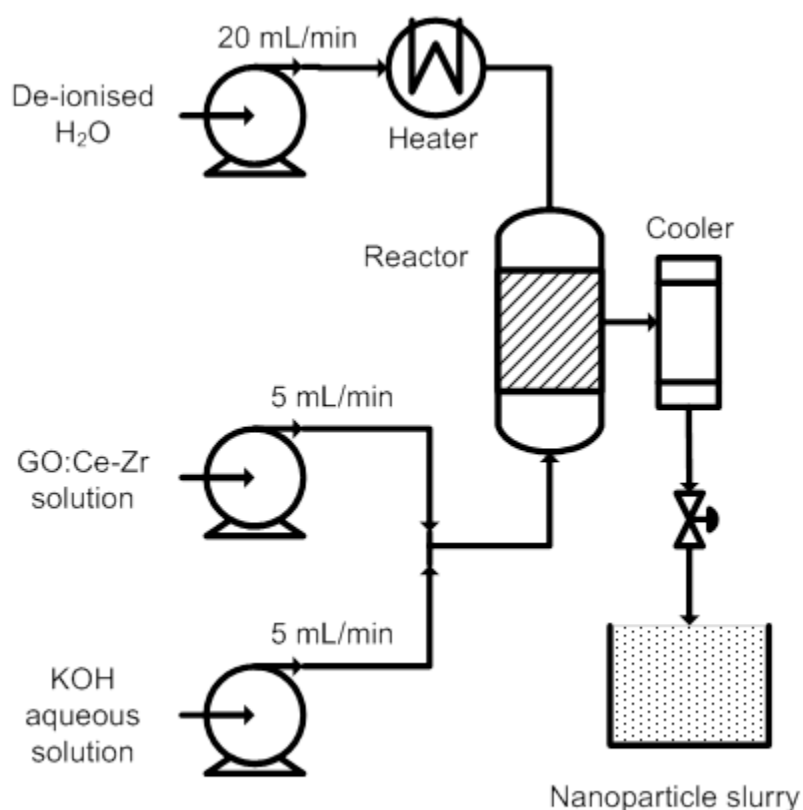


Figure 4.4. A schematic of a CHFS reactor set up used for the synthesis of Ce-Zr/GO nanocomposite catalyst.

#### 4.2.2.4. Ceria-zirconia oxide/graphene nanocomposite heat- treatment

The washed catalysts were frozen in liquid nitrogen and then freeze-dried using a Heto PowerDry PL3000 freezer for 24 h. The dried catalyst was heat-treated for 4 h under nitrogen using a Carbolite tube furnace at various temperatures (773 K–1173 K). The catalyst synthesised using conventional method was identified as CM. The CM catalyst subjected to heat-treatment at temperatures of 773 K, 873 K, 973 K and 1173 K were labelled as CM500, CM600, CM700 and CM900, respectively. The samples synthesised *via* CHFS route were identified as HTR. The HTR catalyst subjected to heat-treatment at temperatures of 773 K, 873 K, 973 K and 1173 K were labelled as HTR500, HTR600, HTR700 and HTR900, respectively. The photographic images of CM, CM700, HTR and HTR700 are shown in Figure 4.5.

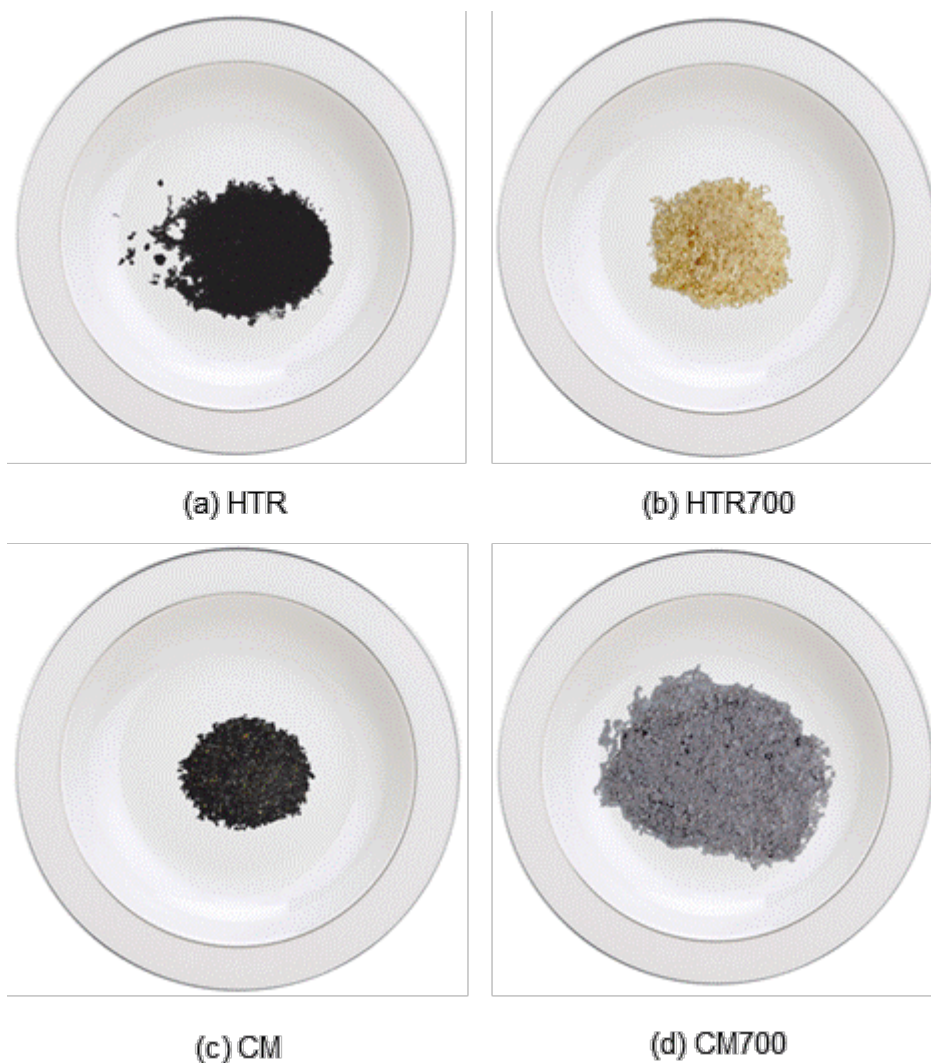


Figure 4.5. Photographic images of Ce–Zr/GO nanocomposite samples: (a) as-prepared sample synthesised using CHFS route labelled as HTR and (b) the corresponding heat-treated (973 K) sample labelled as HTR700; (c) sample CM synthesised *via* wet impregnation route and (d) the corresponding heat treated (973 K) sample labelled as CM700.

#### 4.2.3. Addition Reaction of Methanol and CO<sub>2</sub>

The reaction for direct synthesis of DMC was carried out in a 25 mL stainless steel high pressure reactor (model 4590, Parr Instrument Company, USA) equipped with a stirrer, thermocouple (type J) and a heating mantle and a controller (model 4848). 10 g of methanol were added to a ceria-zirconia/graphene catalyst in a typical process. The reactor was heated to the required temperature and continuously stirred. Supercritical fluid pump (model

SFT-10, Analytix Ltd., U.K) was used to pump CO<sub>2</sub> at a specified pressure from the cylinder to the reactor. CO<sub>2</sub> was injected at a constant pressure for all the optimised reactions. After the reaction, the reactor was cooled down to room temperature using an ice bath. The reactor was depressurised and the reaction mixture was filtered. The products were analysed using a gas chromatography (GC) equipped with a flame ionisation detector (FID) with a capillary column using isopropyl alcohol as an internal standard.

#### 4.2.4. Catalyst Characterisation Techniques

Particle size and morphology of as-prepared and heat treated graphene nanocomposites were investigated using a JEOL 2100FCs with a Schottky Field Emission Gun transmission electron microscope (200 kV accelerating voltage). Samples were collected on carbon-coated copper grids (Holey Carbon Film, 300 mesh Cu, Agar Scientific, Essex, UK) after being briefly dispersed ultrasonically in water. Particle size analysis was performed using ImageJ particle size analysis software. Brunauer-Emmett-Teller (BET) surface area measurements were performed on a Micromeritics Gemini VII analyser (nitrogen adsorption and desorption method). The pore size distribution and pore volume were obtained using the Barrett–Joyner–Halenda (BJH) method. The powders were degassed at 573 K in N<sub>2</sub> (purge gas supplied by BOC, UK) for 5 h, prior to BET analysis. X-ray powder diffraction data were collected on an Analytical X'pert Pro diffractometer with a X'celerator RTMS detector and an X-ray tube with a nickel filtered copper target (CuKα λ = 0.15418 nm) set at 45 kV and 40 mA. The diffractograms were collected over a range from 5 to 70 degrees 2θ with a stepwidth of 0.0334 degrees and a collection time equivalent to 200 seconds per point and an incident beam divergence of 0.25 degrees. XPS measurements were performed using a Kratos Axis ultra DLD photoelectron spectrometer utilising monochromatic Alka source operating at 144 W. Samples were mounted using conductive carbon tape. Survey and narrow scans were performed at constant pass energies of 160 and 40 eV, respectively. The base pressure of the system is ca. 1x10<sup>-9</sup> Torr, rising to ca. 4x10<sup>-9</sup> Torr under analysis of these samples.

#### 4.2.5. Method of Analysis

A Shimadzu gas chromatography (GC) was used for the separation and identification of experimental samples. The GC was equipped with a flame ionisation detector (FID) and a capillary column. Helium was used as the carrier gas and was maintained at a flow rate of 1 mL min<sup>-1</sup>. Oxygen and hydrogen were used as ignition gases. The detector and injector temperatures were maintained at 523 K. A split ratio of 25:1 and injection volume of 0.5 µL were chosen as part of the GC method. A ramp method was used to separate all the compounds present in the sample mixture where the initial temperature of the oven was set at 323 K. The sample was injected by an auto injector for analysis. The oven temperature was programmed at 323 K for 5 min after the sample had been injected. The oven temperature was ramped from 323 K to 523 K at the rate of 50 K min<sup>-1</sup>. The total run time for each sample was 12 min. After each sample run, the oven temperature was cooled down to 313 K so that the following sample could be analysed.

### 4.3. RESULTS AND DISCUSSION

#### 4.3.1. Catalyst Characterisation

In this work, an innovative synthetic approach was employed for synthesising nanoparticle functionalised graphene oxide *via* utilisation of continuous flow of supercritical water in alkaline medium in a single rapid route. The Ce–Zr/GO nanocomposites were made from a 0.2 M (total concentration) pre-mixed aqueous solution of cerium and zirconium (to produce Ce<sup>3+</sup>:Zr<sup>4+</sup> at 50:50 atomic ratio) and GO (synthesised *via* conventional Hummers method) under alkaline conditions (KOH, 0.2 M). For comparison purposes, Ce–Zr/GO nanocomposite catalyst was also synthesised using a traditional wet impregnation method. Transmission Electron Microscopy (TEM) images of the as-prepared and heat treated materials are shown in Figures 4.6–4.9 and the mean particle size values are given in Table 4.1. TEM images for Ce–Zr/GO synthesised using CHFS route (sample labelled as “HTR”) revealed uniform particles exhibiting a mean particle size of 4.0 ± 1.1 nm (Figure 4.6). The TEM images for the corresponding heat treated sample at 973 K (labelled as sample HTR700) showed an increase in particle size with a mean size of 5.8 ± 1.6 nm (Figure 4.7). By contrast, the TEM images (Figure 4.8) of the sample prepared *via* wet impregnation route (labelled as sample CM) exhibited undefined large agglomerated particles and particle size

determination was proved to be challenging. In contrary, the corresponding heat treated (Figure 4.9) Ce–Zr/GO sample revealed the largest mean crystallite size of  $26.0 \pm 8.5$  nm.

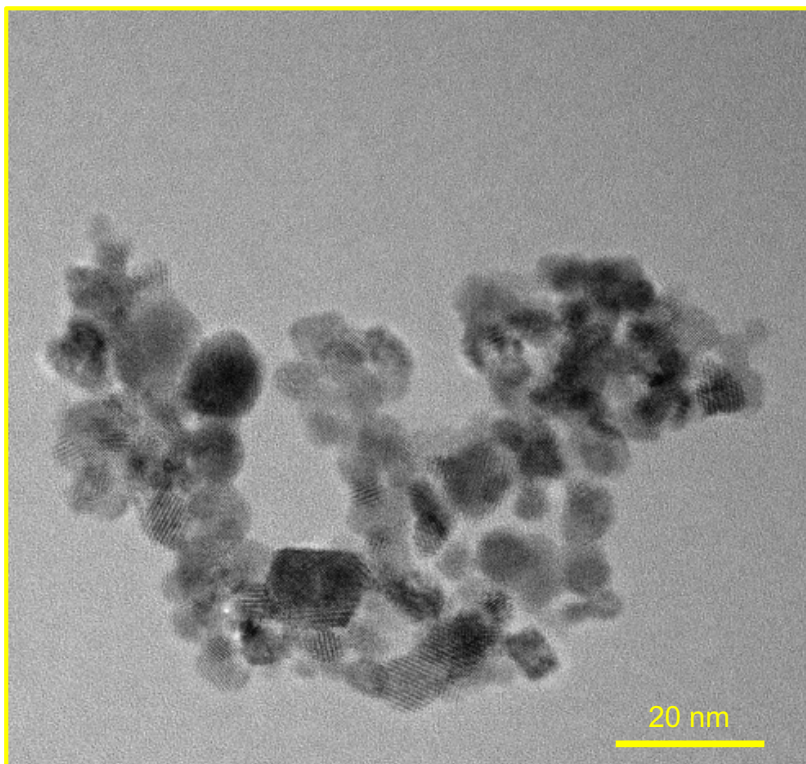


Figure 4.6. Transmission Electron Microscopy (TEM) image of Ce–Zr/GO nanocomposite as-prepared sample synthesised using CHFS route labelled as HTR.

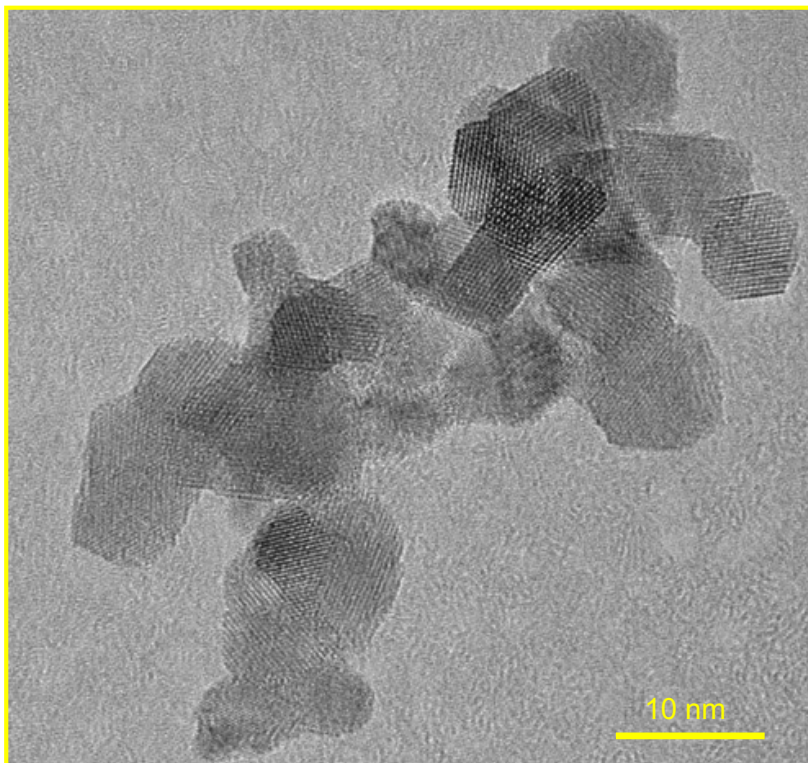


Figure 4.7. Transmission Electron Microscopy (TEM) image of Ce-Zr/GO nanocomposite heat-treated (973 K) sample labelled as HTR700.

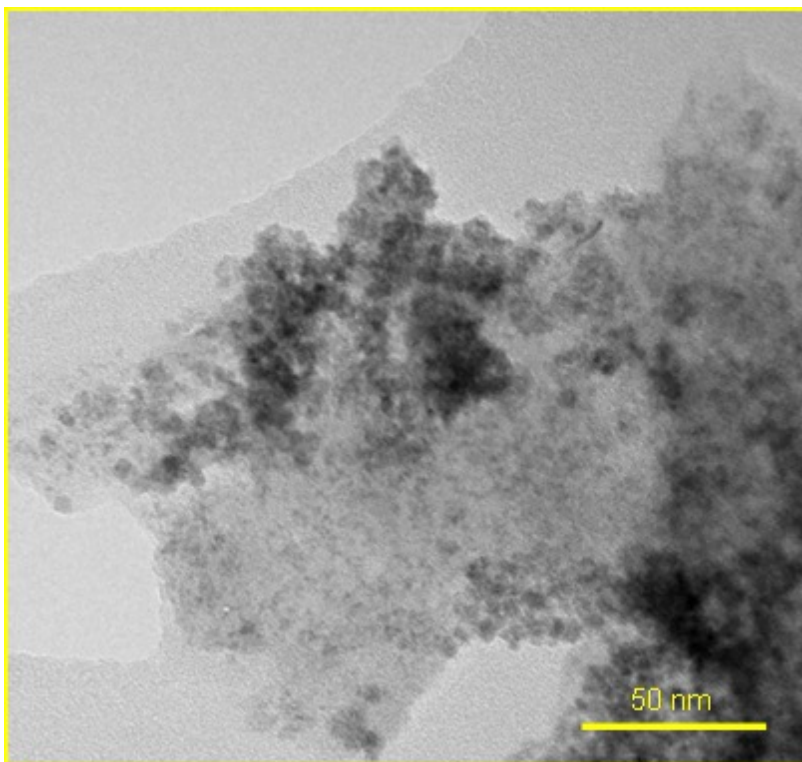


Figure 4.8. Transmission Electron Microscopy (TEM) image of Ce-Zr/GO nanocomposite sample synthesised *via* wet impregnation route labelled as CM.

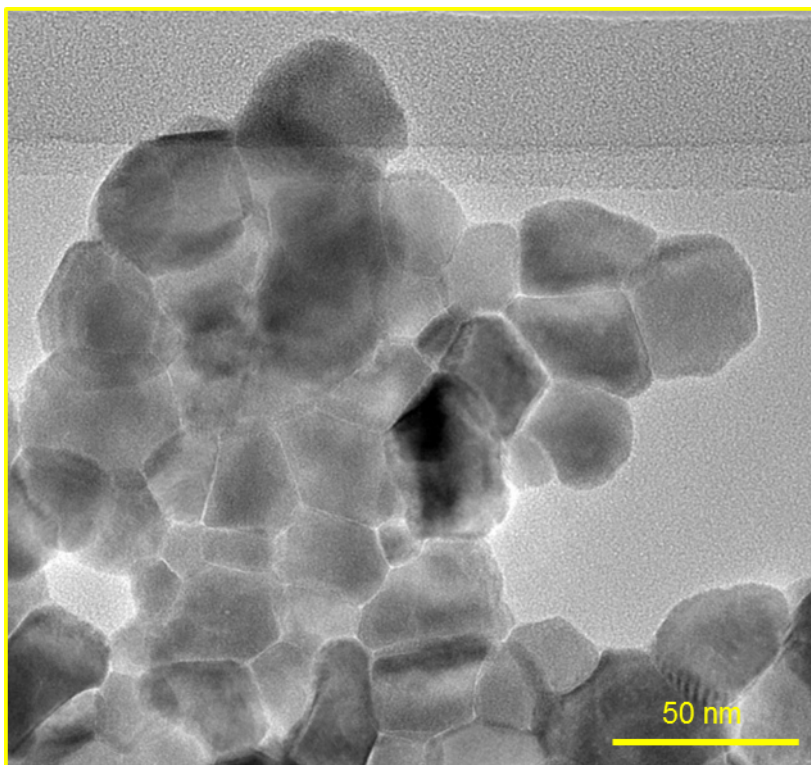


Figure 4.9. Transmission Electron Microscopy (TEM) image of Ce-Zr/GO nanocomposite sample synthesised *via* wet impregnation route, heat-treated (973 K) and labelled as CM700.

Table 4.2. Physical and chemical properties of Ce–Zr/GO nanocomposite catalysts.

Catalyst properties	Catalysts			
	HTR	HTR700	CM	CM700
BET surface area (m <sup>2</sup> g <sup>-1</sup> )	167	106	2	11
BJH adsorption average pore diameter (nm)	4.9	6.7	4.9	7.3
TEM particle size (nm)	4.0 ± 1.1	5.8 ± 1.6	Large agglomerates	26 ± 8.5
Atomic concentration (%) (by XPS analysis)	Ce 3d:8.74 O 1s: 35.43 C 1s: 48.73 Zr 3d: 7.11	Ce 3d:11.74 O 1s: 41.03 C 1s: 38.8 Zr 3d: 8.44	Ce 3d: 0.38 O 1s: 21.33 C 1s: 71.61 Zr 3d: 0.63 Na 1s: 6.04	Ce 3d:5.19 O 1s: 45.85 C 1s: 24.74 Zr 3d: 4.81 Na 1s: 7.92 K 2s: 7.54 Cl 2s: 3.97

The crystallinity of the synthesised and heat treated (973 K) Ce–Zr/GO nanocomposite catalysts synthesised *via* CHFS and conventional wet impregnation route was assessed by X-ray powder diffraction (XRD) and is shown in Figure 4.10. The XRD pattern for sample synthesised *via* CHFS route (HTR sample) gave very broad peaks corresponding to the fluorite structure, suggesting the formation of the solid solution. It has been reported that as the zirconium concentration in the solid solutions increases, the positions of the CeO<sub>2</sub> diffraction peaks shift to higher 2θ values, corresponding to a decrease in the lattice parameter. The observed lattice cell shrinkage is caused by the insertion of smaller Zr<sup>4+</sup> ions into the ceria fluorite, Ce<sup>4+</sup> lattice (Cabanas *et al.*, 2000; 2001, Weng *et al.*, 2009). Furthermore, there is no change in the pattern for the corresponding heat treated sample (HTR700) indicating the thermal stability and high homogeneity of the compound synthesised under CHFS condition. The peak broadness of the observed reflections is reported to be due to the small crystallite size (Cabanas *et al.*, 2000), which is in good agreement with the particle size

data obtained from TEM imaging. In contrast, the as-prepared sample synthesised *via* conventional method (sample CM) revealed an amorphous pattern, which is expected considering the synthetic process utilised for catalyst preparation. The corresponding heat treated sample (CM700) is a mixture of CeO<sub>2</sub> or Ce–Zr/GO, which provides broad peaks along with other unidentified peaks. For all cases, we did not observe peaks corresponding to GO.

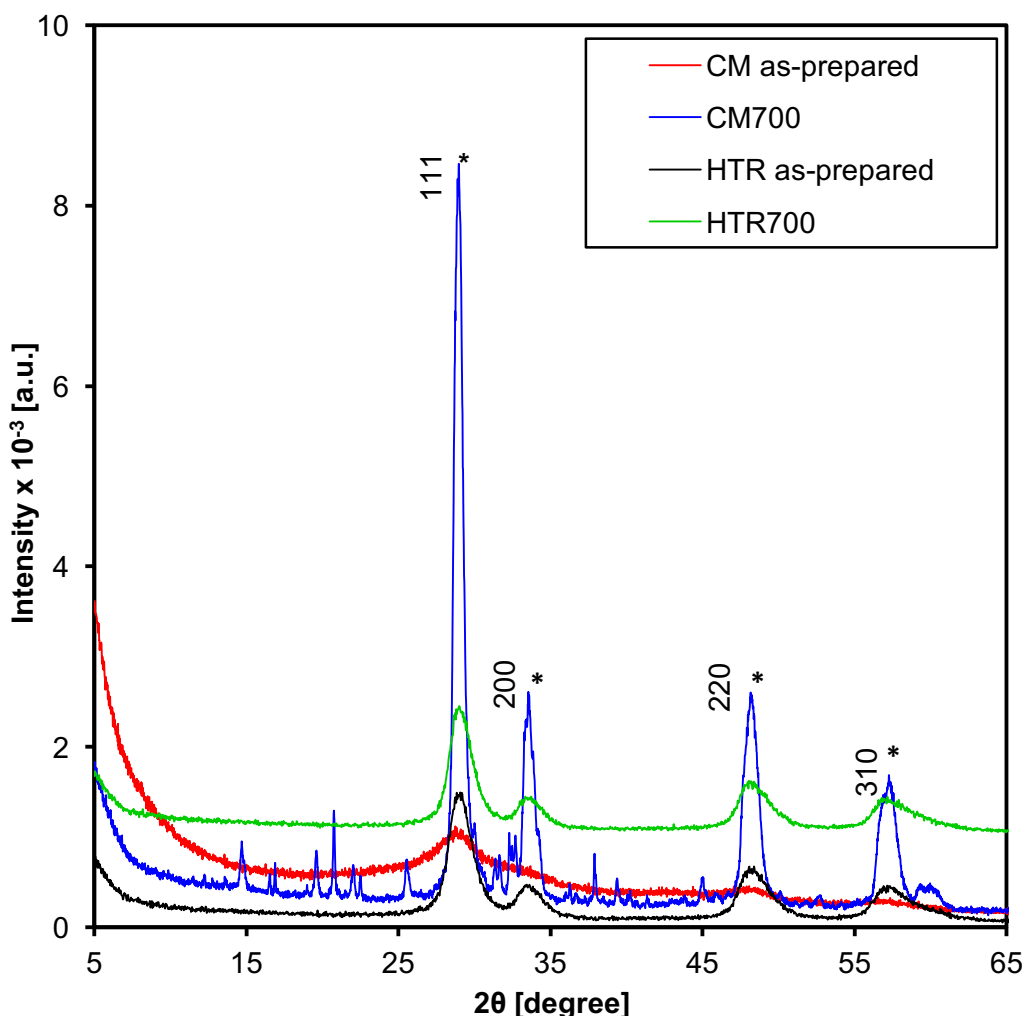


Figure 4.10. X-ray powder diffraction (XRD) patterns of different ceria–zirconia oxide/graphene nanocomposites.

To investigate the changes in the concentration of cerium and zirconium in the lattice, their oxidation states and the chemical states of graphene oxide for all synthesised and heat treated catalysts, X-ray photoelectron spectroscopy (XPS) analysis was employed and the spectra are shown in Figures 4.11–4.13. The

XPS elemental analysis for all catalysts i.e. as-prepared sample *via* CHFS (HTR), corresponding sample heat treated at 973 K (HTR700), the as-prepared sample *via* conventional route (CM) and the corresponding sample heat treated at 973 K (CM700) are given in Table 4.1. Generally, the spectra of all the samples showed strong peaks corresponding to cerium, zirconium, oxygen and carbon. For the conventionally synthesised sample, peaks of sodium were also observed. As previously stated (Kellici *et al.*, 2014) the hydrothermal process is effective in dehydrating/reducing GO. Indeed, the deconvoluted C(1s) XPS spectra (Figure 4.11) of samples made hydrothermally revealed significant reduced peak intensities of the oxygen-containing functional groups (epoxide, carboxyl and hydroxyl), which are associated with GO (starting material). Furthermore, the XPS analysis revealed a complex spectrum for cerium (Figure 4.12) indicating the presence of both Ce(IV) and Ce(III) species as evidenced by the peaks at *ca.* 916 eV (Ce(IV)) (Pirmohamed *et al.*, 2010) and the intensity toward lower binding energy of the Ce(3d<sub>5/2</sub>) peak (*ca.* 880 eV), respectively. The calculation of the exact Ce(III)/Ce(IV) ratio is difficult, however, using the method employed by Preisler *et al.* (2001) we have estimated the Ce(III) content to be approximately 10%. XPS spectrum of the core level of Zr 3d (Figure 4.13) has a strong spin–orbit doublet due to Zr 3d<sub>5/2</sub> at 182.3 eV and Zr 3d<sub>3/2</sub> at 184.7 eV with spin–orbit separation of 2.4 eV, which is in excellent agreement with the reported literature values (Tan *et al.*, 2014) and characteristic of Zr<sup>4+</sup> ions in full oxidation states.

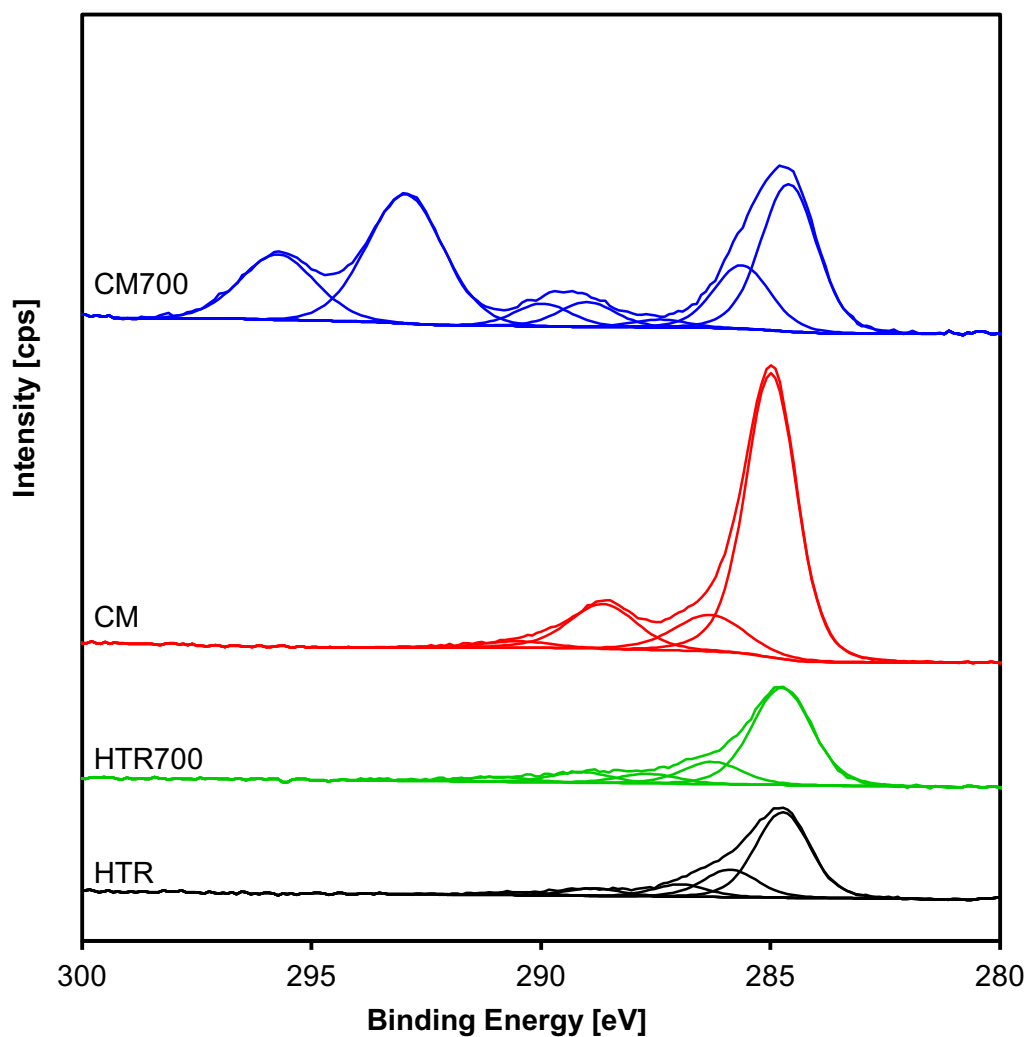


Figure 4.11. X-ray photoelectron spectroscopy (XPS) spectra showing the deconvoluted C(1s) region of Ce-Zr/GO samples synthesised *via* continuous hydrothermal flow reactor and conventional wet impregnation route.

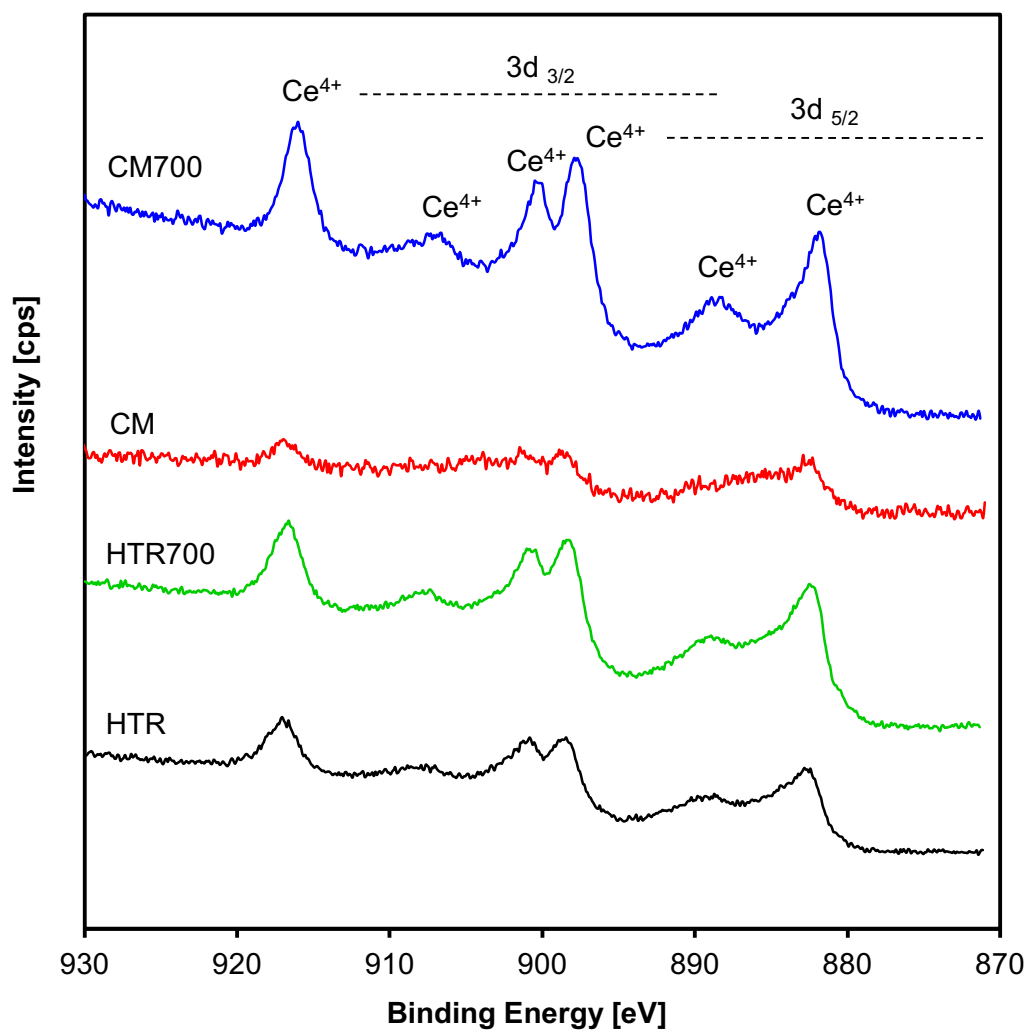


Figure 4.12. X-ray photoelectron spectroscopy (XPS) spectra showing the Ce(3d) region of Ce–Zr/GO samples synthesised *via* continuous hydrothermal flow reactor and conventional wet impregnation route.

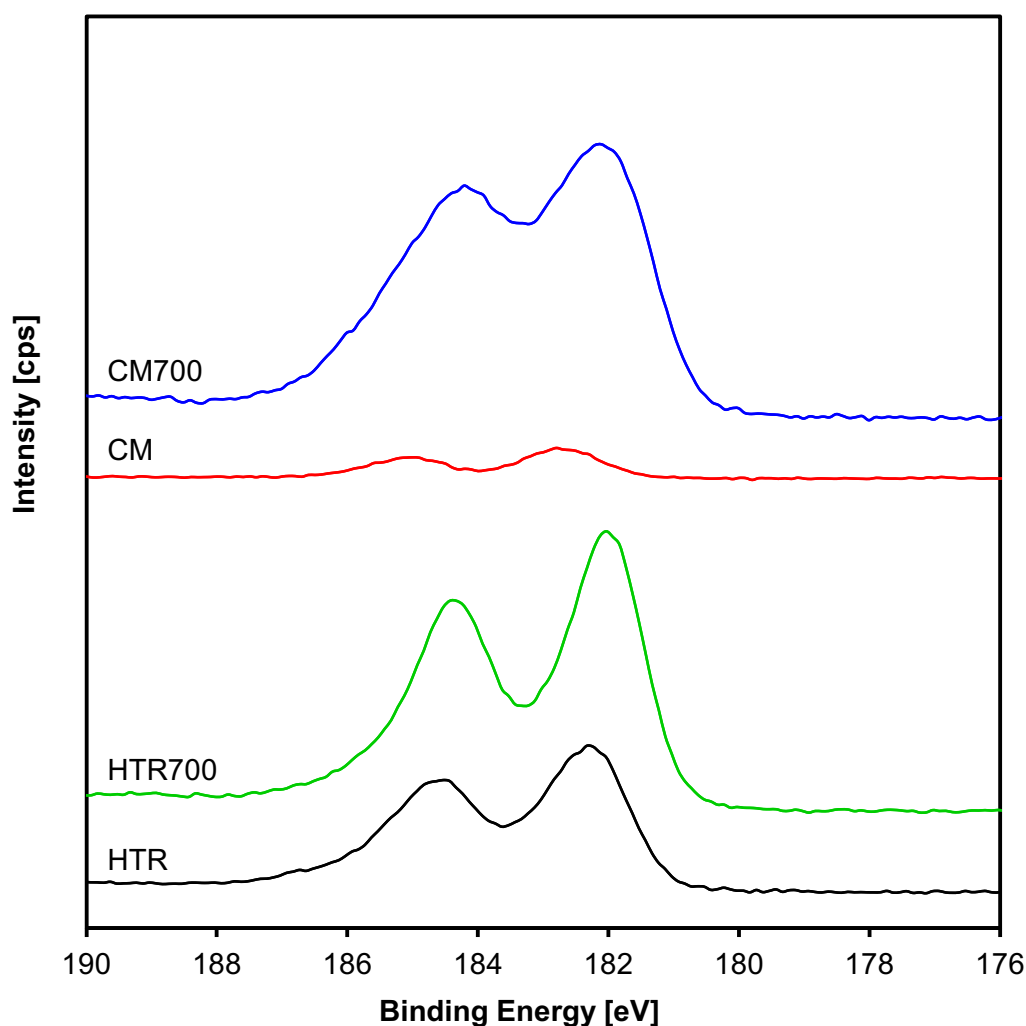


Figure 4.13. X-ray photoelectron spectroscopy (XPS) spectra showing the Zr (3d) region for of Ce-Zr/GO samples synthesised *via* continuous hydrothermal flow reactor and conventional wet impregnation route.

Table 4.1 shows the BET specific surface area (SSA) of all as-prepared and heat treated catalysts synthesised *via* CHFS and wet impregnation route (as control reaction). It is to be noted that sample HTR shows the highest SSA ( $167 \text{ m}^2 \text{ g}^{-1}$ ), which decreased to  $106 \text{ m}^2 \text{ g}^{-1}$  with heat treatment of the catalyst. This is attributed to an increase in the particle size of Ce-Zr/GO as confirmed from TEM data. However, samples synthesised *via* conventional method, exhibited a very low SSA values ( $2 \text{ m}^2 \text{ g}^{-1}$  and  $11 \text{ m}^2 \text{ g}^{-1}$  for CM and CM700, respectively). This is expected, given that the particle size of the CM700 ( $26 \pm 8.5 \text{ nm}$ ) is larger than sample HTR700 ( $5.8 \pm 1.6 \text{ nm}$ ).

It is known that both acidic and basic site on the catalyst surface play an important role on DMC synthesis and greatly influence the activity and selectivity of the desired product (Lilach *et al.*, 2001; Tomishige *et al.*, 2004; Honda *et al.*, 2014). In regards to the GO, it has noted that since carbon atoms do not have empty or full orbitals to act as base centres or Lewis acid, functionalisation is considered as a suitable route for introduction of acidic or basic site (Navalon *et al.*, 2014). Additionally, the acid-base properties of ceria-zirconia solid solutions and their corresponding parent metal oxides have been formerly investigated (Cutrufello *et al.*, 1999). It has been reported that ceria exhibits the lowest strength of acid site, which increases upon addition of zirconia with pure zirconia exhibiting the highest value. In contrary, the ceria rich solid solutions reveal a high basic character. Generally, the introduction of high concentrations of zirconia into ceria lattice, were also associated with complex features on both basicity and acidity in comparison to the pure parent oxide (Cutrufello *et al.*, 1999). Furthermore, it has been reported that weak acidity is favorable in DMC synthesis, since the side product, DME is produced on the strong acid sites.

### 4.3.2. Batch Studies

Addition reactions of carbon dioxide (CO<sub>2</sub>) to methanol (MeOH) were carried out at different reaction conditions in the presence of Ce–Zr/GO nanocomposite as catalysts. All addition reactions were conducted in the presence of 1,1,1-trimethylmethoxymethane (TMM) as a dehydrating agent. The effects of temperature, CO<sub>2</sub> pressure, reaction time, catalyst loading and TMM:MeOH mass ratio on the yield of DMC were studied. Reusability studies were conducted to evaluate the long term stability of Ce–Zr/GO catalyst for the synthesis of DMC.

#### 4.3.2.1. Effect of different catalysts

The performance of various Ce–Zr/GO catalysts was assessed for the effective synthesis of DMC from the reaction of MeOH and CO<sub>2</sub> in the presence of TMM as shown in Figure 4.14. Catalyst activity was indicated by methanol conversion and DMC yield, where two molecules of methanol are incorporated into DMC. CM and HTR represent Ce–Zr/GO catalyst synthesised using conventional method and CHFS method, respectively. The catalysts were heat treated at different temperatures (773 K, 873 K, 973 K and 1173 K) to enhance their catalytic activity. When the catalyst was prepared using CM, the yield of DMC was low

(3.9%) and increased when the catalyst was heat treated to 973 K (22.7%). The activity of the catalyst synthesised using HTR showed a slightly better performance with a DMC yield of 7.9%. This DMC yield further increased to 33% when the catalyst (HTR700) was heat treated at 973 K.

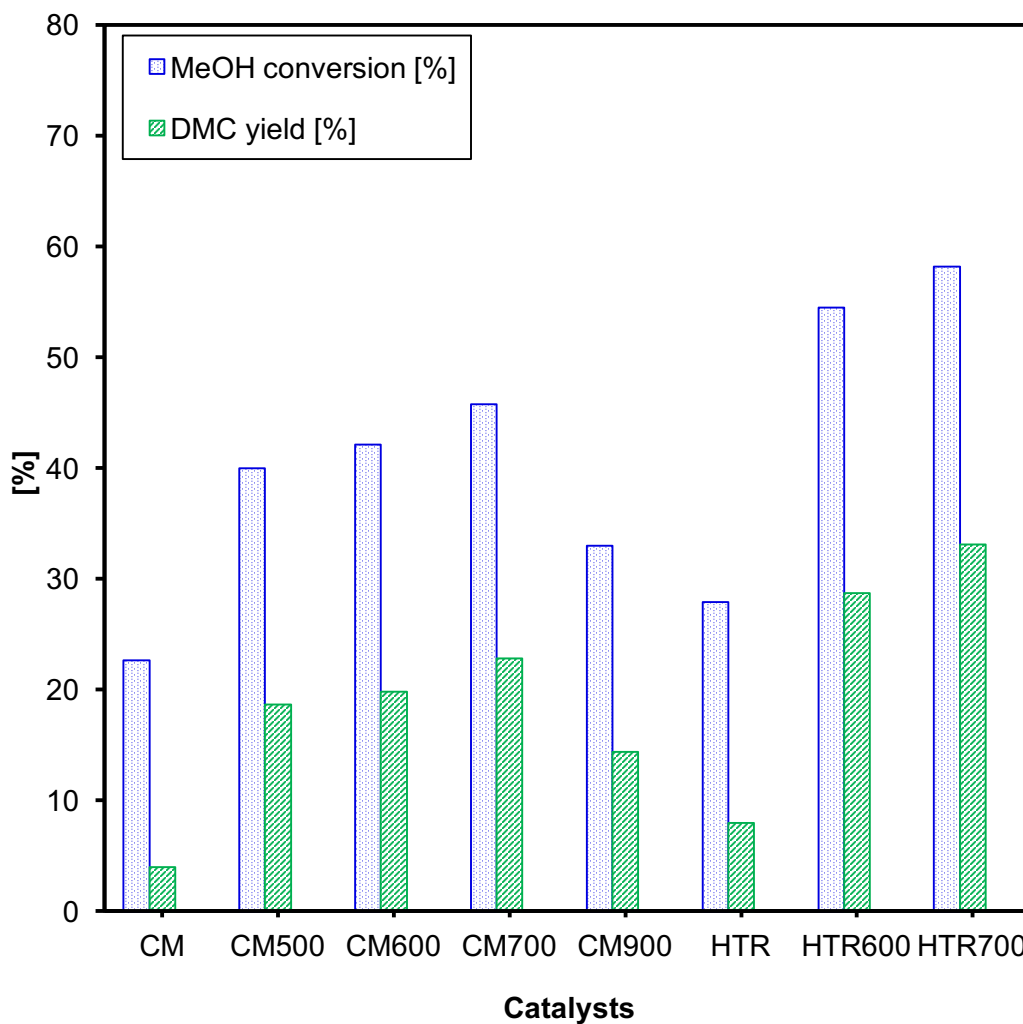


Figure 4.14. Effect of different Ce–Zr/GO nanocomposite catalysts on the direct synthesis of DMC. Experimental conditions: catalyst loading, 10% (w/w); reaction temperature, 383 K; CO<sub>2</sub> pressure, 275 bar; reaction time, 16 h; TMM:MeOH ratio, 1:1 (w/w) and stirring speed, 300 rpm.

The study showed that the catalyst prepared using HTR had a higher catalytic activity to that prepared using CM. The differences in the catalytic performance can be attributed to a series of parameters including smaller particle size, phase

composition, crystallinity and high surface area. From Figure 4.14 it can be seen that Ce–Zr/GO catalyst prepared using CHFS and heat treated at 973 K (HTR700) showed the highest activity with 58% conversion of MeOH and 33% yield of DMC. Based on this study, Ce–Zr/GO HTR700 was found to be the best catalyst for the synthesis of DMC and was used for further studies.

#### 4.3.2.2. Effect of catalyst loading

The effect of catalyst loading (i.e. the percentage ratio of the mass of the catalyst to the mass of the limiting reactant, i.e., MeOH) was investigated using 5%, 10% and 15% catalyst loading for the reaction of MeOH and CO<sub>2</sub> as shown in Figure 4.15. It can be seen that an increase in catalyst loading (w/w) from 5% to 10% had increased MeOH conversion from 53.7% to 58% and the yield of DMC increased from 30.3% to 33%. However, a further increase in catalyst loading to 15% (w/w) has no obvious increase in the MeOH conversion and the yield of DMC. In view of the experimental error of ±3%, it seems that the number of active sites for MeOH and CO<sub>2</sub> to react and produce DMC was sufficient at 10% (w/w) catalyst loading. Therefore, it was not necessary to increase the catalyst loading to 15% (w/w). Hence, it can be concluded that 10% (w/w) catalyst loading is the optimum amount of catalyst required for this reaction.

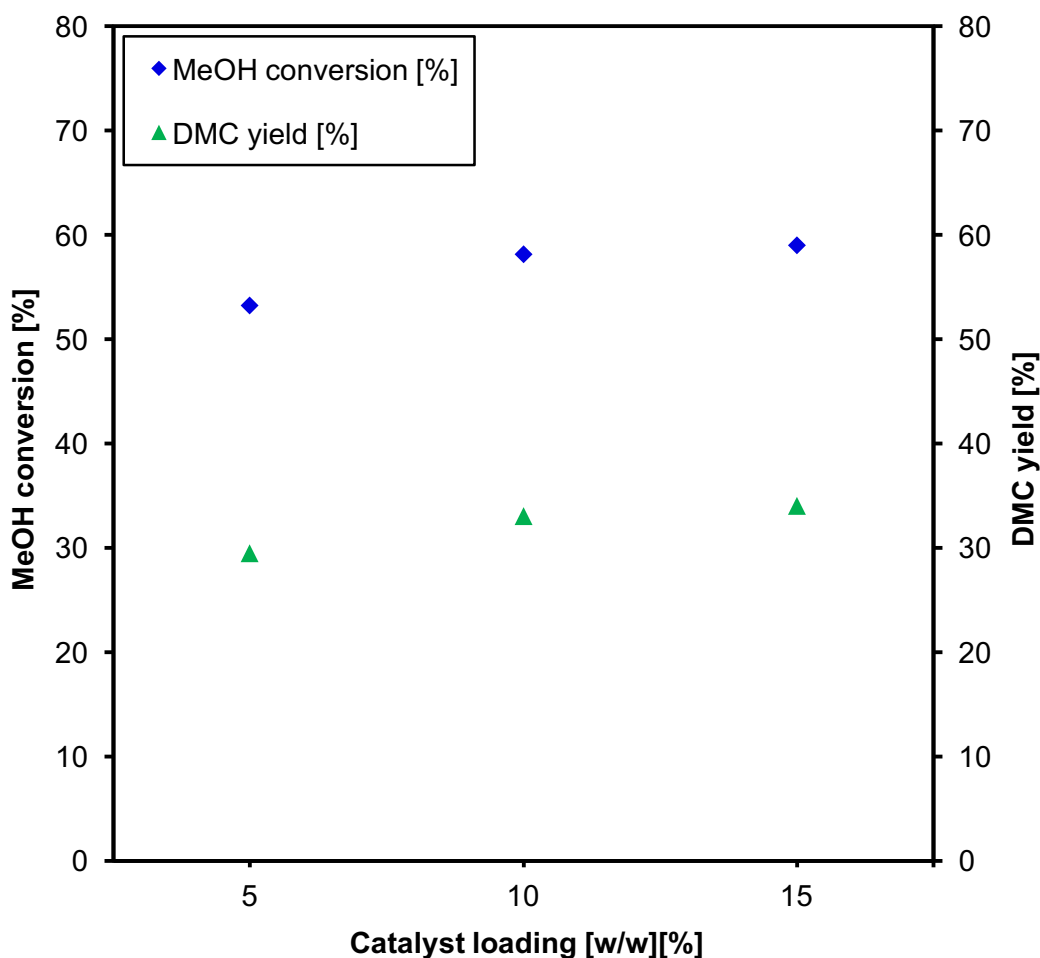


Figure 4.15. Effect of catalyst loading on MeOH conversion and yield of DMC. Experimental conditions: catalyst, Ce–Zr/GO - HTR700; reaction temperature, 383 K; CO<sub>2</sub> pressure, 275 bar; reaction time, 16 h; TMM: MeOH ratio, 1:1 (w/w) and stirring speed, 300 rpm.

#### 4.3.2.3. Effect of reaction temperature

The direct synthesis of DMC *via* the reaction of CO<sub>2</sub> and MeOH was carried out between temperature 373 K and 433 K in order to study the effect of reaction temperature on the yield of DMC. Figure 4.16 presents the variation of MeOH conversion and DMC yield at different reaction temperatures. The conversion of MeOH was 59.5% and the yield of DMC was 31.8% at 393 K after 16 h, whereas at 383 K MeOH conversion was 58% and the yield of DMC reached to 33%. Higher reaction temperatures gave higher conversion of MeOH at a fixed reaction time for the catalysed reaction; however, the yield of DMC was decreased (see

Figure 4.16). At high temperatures, it is thermodynamically favourable for DMC to react with oxygen to form carbon dioxide and water. Other possible by products of DMC decomposition include carbon monoxide, methanol, formaldehyde, formic acid, and their reaction products (Anderson *et al.*, 2005). During analysis, formaldehyde did not appear as a by-product. Other by-products were under the detection limit of the GC-FID used in the analysis. This observation is similar to the work published by Zhang *et al.* (2011).

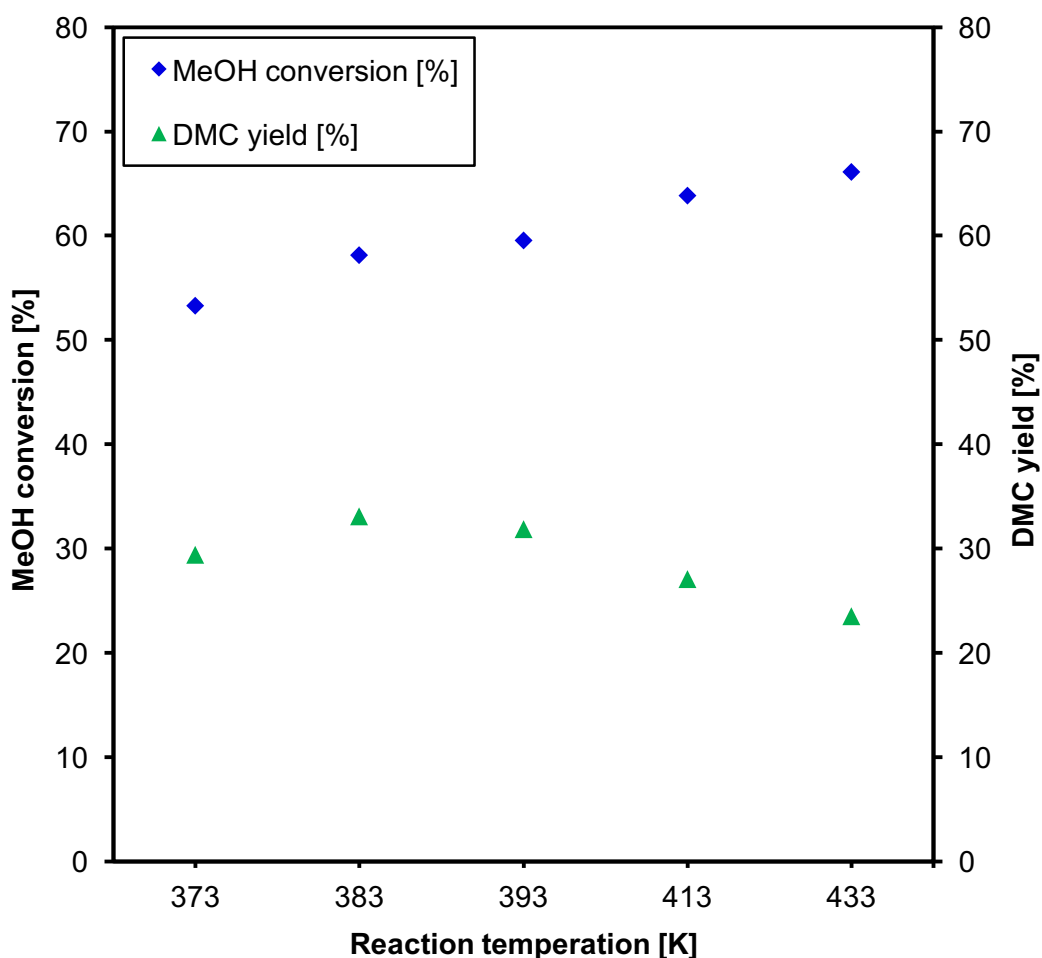


Figure 4.16. Effect of reaction temperature on MeOH conversion and yield of DMC. Experimental conditions: catalyst, Ce–Zr/GO - HTR700; catalyst loading 10% (w/w); CO<sub>2</sub> pressure, 275 bar; reaction time, 16 h; TMM:MeOH ratio, 1:1 (w/w) and stirring speed, 300 rpm.

From this study it can be concluded that the optimum temperature for the endothermic reaction of MeOH and CO<sub>2</sub> using Ce–Zr/GO catalyst is 383 K. Similar reaction temperature for the synthesis of DMC from MeOH and CO<sub>2</sub> have been reported in the literature (Zhao *et al.*, 2000; Bian *et al.*, 2009a, Zhang *et al.*, 2011).

### 4.3.2.4. Effect of CO<sub>2</sub> pressure

The pressure of CO<sub>2</sub> is an important reaction parameter for the addition reaction of MeOH and CO<sub>2</sub>. Near critical or supercritical state CO<sub>2</sub> reaction system can cause an increase in the mass transfer efficiency of the reactants and shift the reaction equilibrium to overcome the thermodynamic limitation of this reaction (Cao *et al.*, 2012). The effect of CO<sub>2</sub> pressure on the MeOH conversion and DMC yield was studied in order to assess the optimum CO<sub>2</sub> pressure for the catalysed reaction. The experiments were conducted in a high pressure reactor at 383 K within a pressure range of 120–290 bar for 16 h and the results are shown in Figure 4.17. It can be seen from Figure 4.17 that an increase in CO<sub>2</sub> pressure increases MeOH conversion and the yield of DMC. At a CO<sub>2</sub> pressure of 200 bar, MeOH conversion and yield of DMC were 47% and 28%, respectively. As the CO<sub>2</sub> pressure was further increased to 275 bar, MeOH conversion and yield of DMC increased to 58% and 33%, respectively. A further increase in pressure to 290 bar showed no significant increase in the methanol conversion or the yield of DMC (see Figure 4.17). Therefore, from this study, it can be concluded that the optimum CO<sub>2</sub> reaction pressure is 275 bar.

This study demonstrates that at an increase in the reaction pressure increases methanol conversion due to an improvement of the physical properties of CO<sub>2</sub>, such as polarity and solubility at supercritical conditions. Supercritical CO<sub>2</sub> have characteristics that affect the activation of the CO<sub>2</sub> molecule in catalytic reactions to the greatest extent (Cao *et al.*, 2002). It has been reported that proper use of supercritical CO<sub>2</sub> in heterogeneous catalysis provides a great enhancement to reaction rates and catalyst reusability (Baiker, 1999; Cao *et al.*, 2002; Du *et al.*, 2005; Wang *et al.*, 2007b). Supercritical CO<sub>2</sub> helps to reduce mass and heat transfer limitations and avoids coke formation and catalyst poisoning (Du *et al.*, 2005). During the reaction between MeOH and CO<sub>2</sub>, there are two phases for the reaction mixture below supercritical conditions, whereas there is only one phase

at supercritical conditions. This favours the catalytic conversion of MeOH and CO<sub>2</sub> and shifts the reaction equilibrium to the product side enhancing the yield of DMC. Zhao *et al.* (2000) had reported that near supercritical conditions, the yield of DMC was 12 times higher than that at non-supercritical conditions.

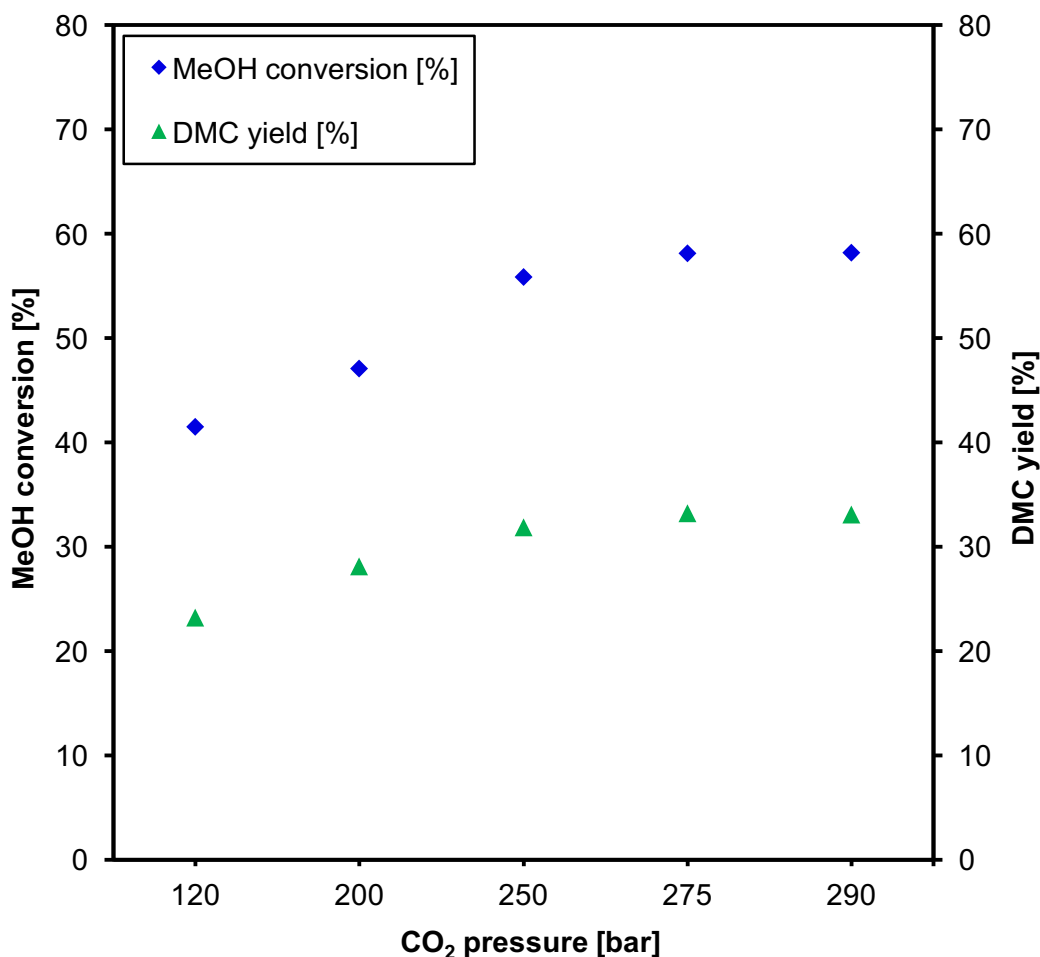


Figure 4.17. Effect of CO<sub>2</sub> pressure on MeOH conversion and yield of DMC. Experimental conditions: catalyst, Ce–Zr/GO - HTR700; catalyst loading 10% (w/w); reaction temperature, 383 K; reaction time, 16 h; TMM:MeOH ratio, 1:1 (w/w) and stirring speed, 300 rpm.

#### 4.3.2.5. Effect of reaction time

The influence of varying the reaction time on the yield of DMC was studied by carrying out a set of addition reactions of MeOH to CO<sub>2</sub> in the presence of the best performed Ce–Zr/GO catalyst (HTR700) and the results are shown in Figure

4.18. A MeOH conversion of 58% and DMC yield of 33% were achieved when the reaction was carried out for 16 h, which marginally increased to 58.2% and 33.1%, respectively when the reaction was carried out for 20 h. These results clearly show that there has been no significant increase in the yield of DMC with prolonged reaction time, indicating that 16 h is the optimum reaction time for this catalysed system.

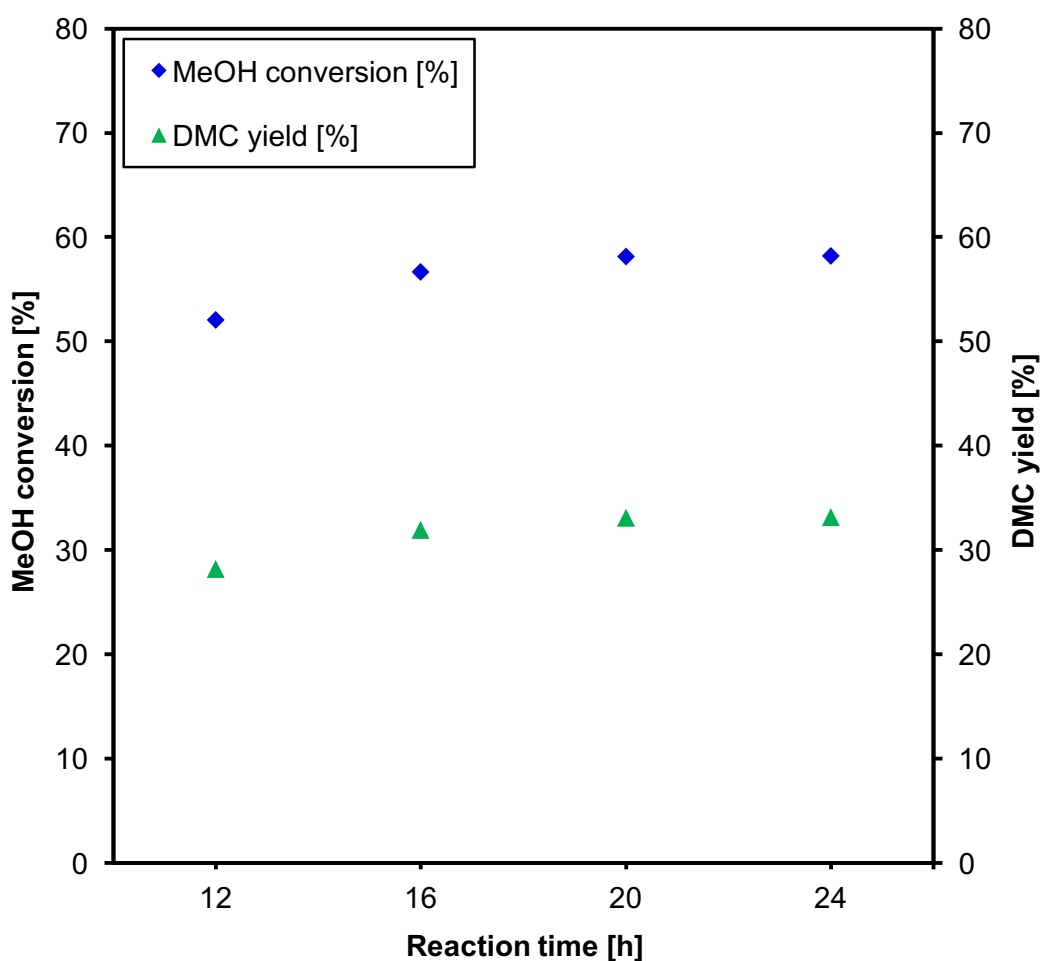


Figure 4.18. Effect of reaction time on MeOH conversion and yield of DMC. Experimental conditions: catalyst, Ce–Zr/GO - HTR700; catalyst loading 10% (w/w); reaction temperature, 383 K; CO<sub>2</sub> pressure, 275 bar; TMM:MeOH ratio, 1:1 (w/w) and stirring speed, 300 rpm.

#### 4.3.2.6. Effect of dehydrating agent

In order to overcome the thermodynamic limitations of the reaction between MeOH and CO<sub>2</sub>, TMM has been added to remove the water produced during the reaction. TMM can also react with CO<sub>2</sub> to produce DMC. Therefore, a blank run was carried out at optimum conditions to that of DMC synthesis for the reaction between TMM and CO<sub>2</sub>. The reaction between TMM and CO<sub>2</sub> in the presence of the catalyst did not produce any DMC, which suggests that this catalyst is not selective for this particular reaction. This result agrees with the work carried out by Zhang *et al.* (2011).

Direct synthesis of DMC was studied using different mass ratio of TMM to MeOH (TMM:MeOH) in the presence of HTR700 catalyst. It can be seen from Figure 4.19 that the methanol conversion and yield of DMC increased from 50% to 58% and 25% to 33%, respectively when TMM:MeOH increased from 0.25:1 to 1:1. There was no further increase in MeOH conversion or yield of DMC when TMM:MeOH increased to 2:1. From this study, it can be concluded that the addition of TMM enhances the conversion of MeOH and DMC yield by shifting the equilibrium to the right and that the optimum TMM:MeOH ratio is 1:1.

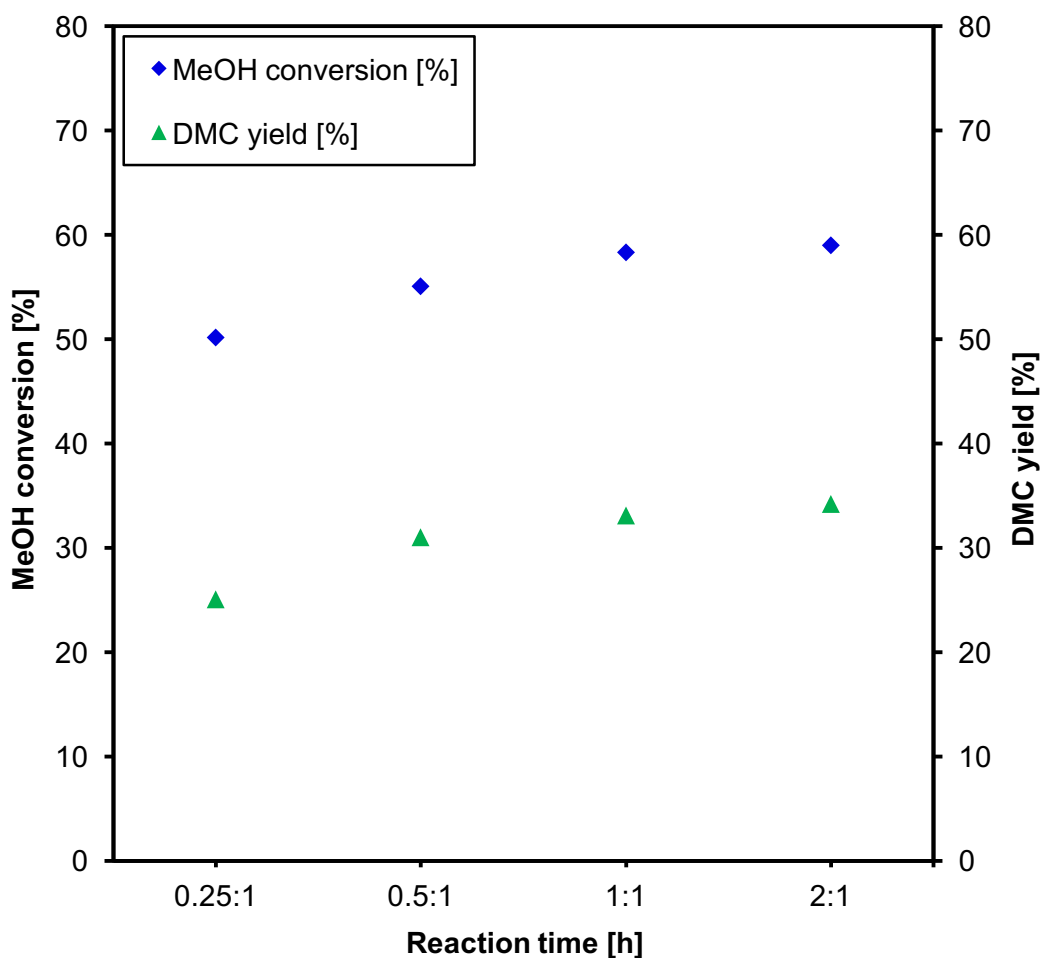


Figure 4.19. Effect of TMM: MeOH (w/w) on MeOH conversion and yield of DMC. Experimental conditions: catalyst, Ce–Zr/GO - HTR700; catalyst loading 10% (w/w); reaction temperature, 383 K; CO<sub>2</sub> pressure, 275 bar and stirring speed, 300 rpm.

#### 4.3.2.7. Effect of mass transfer in heterogeneous catalytic process

Mass transfer limitations can be a major factor that affects MeOH conversion and yield of DMC in heterogeneously catalysed process. External and internal mass transfer resistances are the two different types of mass transfer resistances that exist in heterogeneous catalysed reactions. External mass transfer resistance occurs across the solid-liquid interface due to the stirring of the reaction mixture, whereas internal mass transfer resistance occurs in the intra-particle space due to catalyst's physical and chemical structure, particle size, pore size distribution and porosity. The effect of mass transfer resistance on the addition reaction of

MeOH and CO<sub>2</sub> using Ce–Zr/GO (HTR700) to produce DMC was investigated using a high pressure reactor. The addition reactions were carried out at different stirring speed (300–500 rpm) under otherwise identical conditions as shown in Figure 4.20.

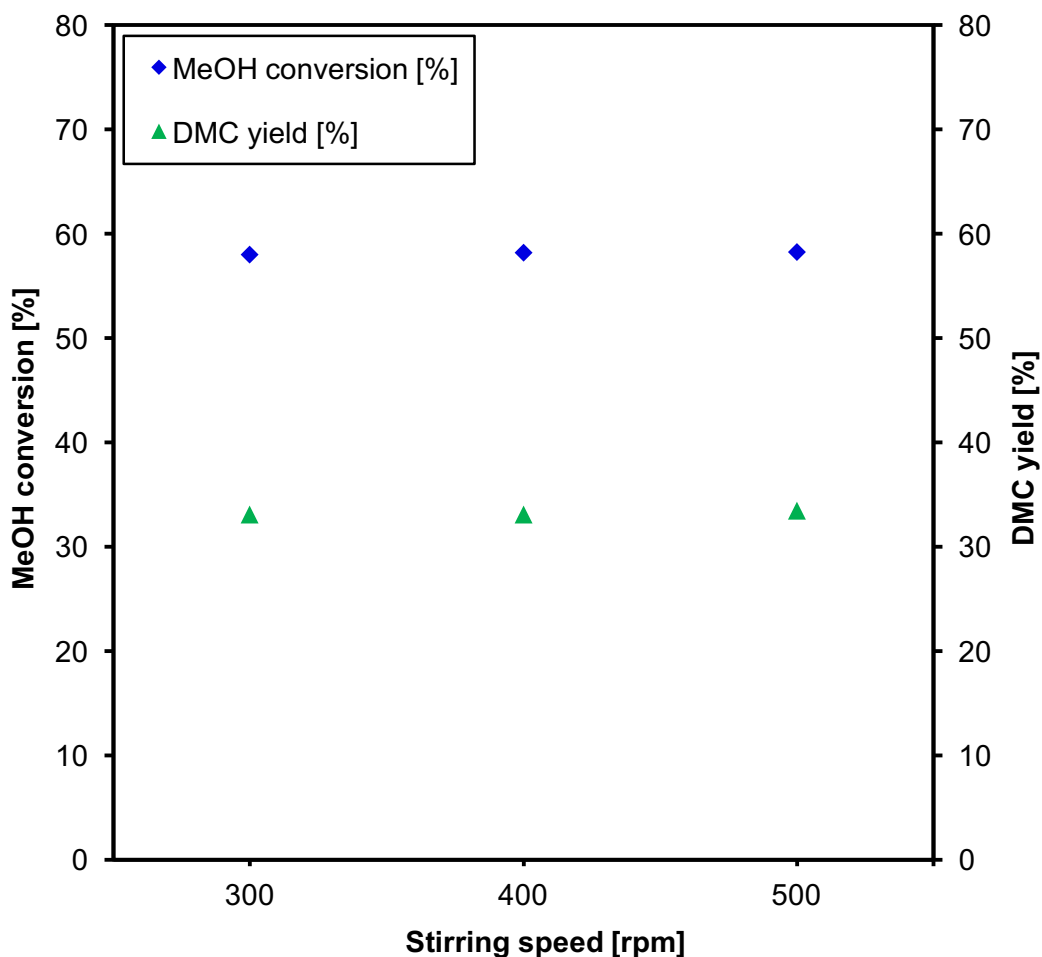


Figure 4.20. Effect of stirring speed on MeOH conversion and yield of DMC. Experimental conditions: catalyst, Ce–Zr/GO - HTR700; catalyst loading 10% (w/w); reaction temperature, 383 K; CO<sub>2</sub> pressure, 275 bar; reaction time, 16 h and TMM:MeOH, 1:1 (w/w).

It can be observed that there is no difference in MeOH conversion and yield of DMC at different stirring speeds, which suggest that there is a homogeneous distribution of catalyst particles in the reaction mixture and hence it can be concluded that external mass transfer resistance is absent in this work. On the

other hand, HTR700 particles are fairly small, uniform and porous (particle size: 5.8 nm and pore diameter 6.7 nm) which eliminates internal mass transfer limitation (Clerici and Kholdeeva, 2013). Therefore, it can be concluded that internal mass transfer resistance is negligible for HTR700 catalysed addition reactions due to the nature of the catalyst particles.

### 4.3.2.8. Reusability studies

The reusability of ceria–zirconia/graphene nanocomposites was studied by carrying out a set of experiments at the optimum reaction condition obtained from the batch studies. The first reaction (labelled as Run 1) was carried out using a fresh batch of catalyst as shown in Figure 4.21. The catalyst was recovered by filtration from the reaction mixture, washed twice with acetone and dried at 333 K for 12 h. The catalyst was then reused for subsequent experiments (labelled as Run 2–Run 6) under the same reaction conditions as shown in Figure 4.21. It can be observed that MeOH conversion and yield of DMC remained comparable even after the 6<sup>th</sup> Run. It is evident that ceria-zirconia/graphene nanocomposites can be easily recovered and reused without any significant reduction in the catalytic performance.

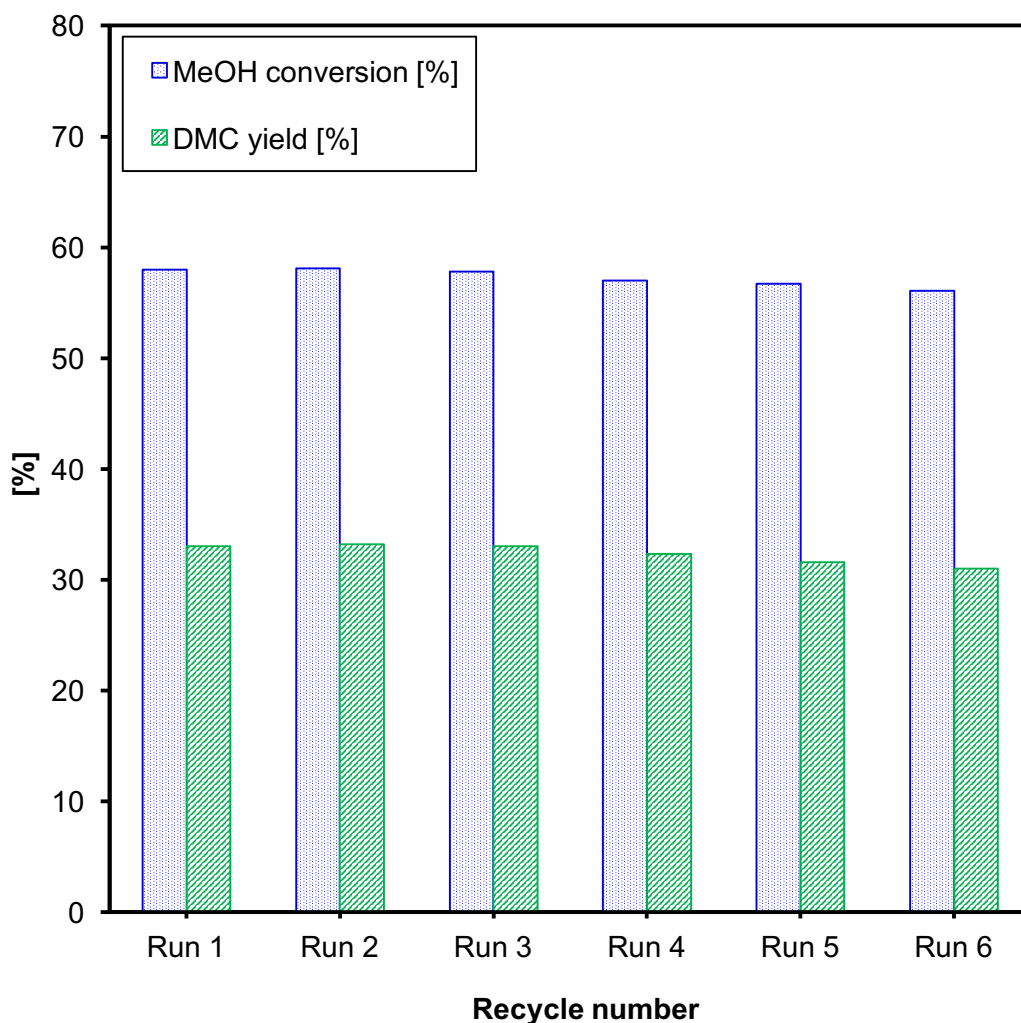


Figure 4.21. Catalyst reusability for synthesis of DMC. Experimental conditions: catalyst, Ce–Zr/GO - HTR700; catalyst loading 10% (w/w); reaction temperature, 383 K; CO<sub>2</sub> pressure, 275 bar; reaction time, 16 h; TMM:MeOH ratio, 1:1 (w/w) and stirring speed, 300 rpm.

#### 4.4. CONCLUSIONS

The preparation of graphene by continuous hydrothermal flow synthesis route allowed simultaneously and homogeneously growing and dispersing metal oxide nanoparticles into graphene substrate in a single step. This single step synthetic approach not only enables control over oxidation state of graphene, but also offers an optimal route for homogeneously producing and depositing highly crystalline nanostructures into graphene oxide. The synthesised Ce–Zr/GO was successfully applied for the direct synthesis of DMC from MeOH and CO<sub>2</sub>. The

effect of various parameters such as the reaction time, reaction temperature, CO<sub>2</sub> pressure, catalyst loading and the addition of dehydrating agent was studied for the optimisation of DMC synthesis. It was found that an increase in CO<sub>2</sub> pressure resulted in an increase in the MeOH conversion and yield of DMC. The experimental results revealed that the use of a dehydrating agent (TMM) to remove residual water produced during the reaction enhances yield of DMC. The highest MeOH conversion of 58% and DMC yield of 33% were obtained at an optimum reaction condition of 383 K, 275 bar, 1:1(w/w) TMM:MeOH and 16 h using 10% (w/w) Ce–Zr/GO nanocomposite catalyst. The catalyst was easily recycled and reused several times without any reduction in its catalytic performance.

# **Chapter 5**

## **Transesterification of Propylene Carbonate (PC) using Commercially Available Catalysts**

## 5. TRANSESTERIFICATION OF PROPYLENE CARBONATE (PC) USING COMMERCIALY AVAILABLE CATALYSTS

### 5.1. INTRODUCTION

DMC can be synthesised *via* the phosgenation or the oxidative carbonylation of methanol in the presence of copper chloride catalyst. However, such synthetic routes involve corrosive and high-risk compounds such as phosgene ( $\text{COCl}_2$ ) and carbon monoxide ( $\text{CO}$ ) (Dharman *et al.*, 2009; Ding *et al.*, 2013). In recent years, the development of greener and more environmentally benign routes for the synthesis of DMC has been explored. Numerous reports have been published describing the interesting possibility of utilising naturally occurring carbon resources such as carbon dioxide ( $\text{CO}_2$ ) for the direct synthesis of DMC from methanol ( $\text{MeOH}$ ) (Saada *et al.*, 2015). Although this synthesis route is very attractive and fulfills the “Sustainable Society” and “Green Chemistry” approach (Delledonne *et al.*, 2001), it suffers from drawback in terms of low yield of DMC due to the inertness of  $\text{CO}_2$  and the thermodynamic limitations due to the equilibrium nature of the reaction.  $\text{CO}_2$  can be applied for a green and sustainable two-step route for the synthesis of DMC, whereby propylene carbonate (PC) can be synthesised *via* the insertion of  $\text{CO}_2$  into propylene oxide (PO) followed by the transesterification of PC and  $\text{MeOH}$  for the synthesis of DMC.

Much effort has been dedicated for the design of new greener catalytic processes for the synthesis of DMC. Several reports have been published describing the efficiency of various catalysts including, alkali metal hydroxide (Han *et al.*, 2001), basic metal oxide (Wang *et al.*, 2006a), double metal cyanide (Srivastava *et al.*, 2006b), anion exchange resin (Dhuri and Mahajani, 2006), hydrotalcite (Watanabe and Tatsumi, 1998; Unnikrishnan and Srinivas, 2012), smectite (Bhanage *et al.*, 2002), mesoporous carbon nitride (Xu *et al.*, 2013c), mesoporous ceria oxide (Xu *et al.*, 2014), tungstate-based catalysts (Sankar *et al.*, 2006), ionic liquids (Kim *et al.*, 2011) and gold nanoparticles (Juarez *et al.*, 2009).

Until recently, ionic liquids have been reported to be the most efficient catalysts proposed for the transesterification of PC and  $\text{MeOH}$  (Kim *et al.*, 2011; Wang *et al.*, 2011a; Xu *et al.*, 2013c; Xu *et al.*, 2014). However, the homogeneous nature

of ionic liquids posed few drawbacks including high cost of separation of products/catalysts from the reaction mixture and challenges in terms of catalyst stability and reusability (Adeleye *et al.*, 2014; Saada *et al.*, 2015). Therefore, the development of solvent-less heterogeneous catalytic process for the synthesis of DMC is highly desirable and a key aspect for the design of greener chemical synthesis. Heterogeneous catalysts offer numerous advantages including the ease of catalyst separation from the reaction mixture, which is more economically viable due to the elimination of complex separation processes. Heterogeneous catalysts have higher stability, longer shelf life and are easier and safer to handle, reuse and dispose compared to the homogenous counterpart (Dai *et al.*, 2009; Adeleye *et al.*, 2014).

In the chapter, several heterogeneous catalysts including ceria and lanthana doped zirconia (Ce–La–Zr–O), ceria doped zirconia (Ce–Zr–O), lanthana doped zirconia (La–Zr–O), lanthanum oxide (La–O) and zirconium oxide (Zr–O) have been characterised and evaluated for the transesterification of propylene carbonate (PC) and methanol (MeOH). The effect of various reaction conditions, such as molar ratio of MeOH:PC, catalyst loading, reaction temperature and reaction time has been extensively studied using the best performed catalyst.

### 5.2. EXPERIMENTAL METHOD

#### 5.2.1. Materials

A number of chemicals used for this research were purchased from Sigma-Aldrich Co. Ltd (UK). These include methanol (MeOH), propylene carbonate (PC), *iso*-propyl alcohol (IPA) and dimethyl carbonate (DMC). Various oxide catalysts were prepared by proprietary processes and supplied by Magnesium Elektron Ltd. (MEL) Chemicals UK, including Ce–La–Zr–O, Ce–Zr–O, La–Zr–O and Zr–O. All chemicals and catalysts were used without any further purification.

#### 5.2.2. Catalytic Reactions

Transesterification reactions of PC with MeOH were carried out in a 100 mL autoclave reactor (model 4590, Parr Instrument Company, USA) equipped with a stirring system, a thermocouple (type J), a heating mantle and a controller (model 4848). In a typical process, different moles of PC and MeOH along with the required amount of the heterogeneous catalyst were charged into the reactor

vessel. The reactor was continuously stirred and heated to the required temperature. The reaction was left for the desired reaction time. After the reaction, the reactor was cooled down to room temperature using an ice bath. The reactor was depressurised and the reaction mixture was filtered. The liquid products were analysed using a gas chromatography (GC) equipped with a flame ionisation detector (FID) with a capillary column using *iso*-propyl alcohol as an internal standard. The effect of various reaction parameters were studied for the optimisation of reaction conditions. The stability of the catalyst was assessed by carrying out catalyst reusability studies on the best performed catalyst at the optimum conditions.

### 5.2.3. Method of Analysis

A Shimadzu gas chromatography (GC–2014) with a split/splitless injector system and flame ionisation detector (FID) was used to analyse the composition of all experimental samples. Helium (99.9%) with a gas flow rate of 1 mL min<sup>-1</sup> passing through a molecular sieve trap was used as the carrier gas for the mobile phase. Separation was carried out on a capillary column with length of 30 m, inner diameter of 320 µm and stationary film thickness of 0.25 µm. Oxygen (99.9%) and hydrogen (99.9%) were used as ignition gases. A temperature program was developed and applied for this process where both the detector and injector temperatures were maintained at 523 K. A split ratio of 25:1 and injection volume of 0.5 µL were chosen as part of the GC method.

A ramp method was used in order to separate all the compounds present in the sample mixture and programmed as follows: the initial temperature of the oven was set at 323 K and the sample was injected by an auto sampler for analysis. The column temperature was then held at 323 K for 5 min after the sample had been injected. Afterwards, a temperature ramp was applied that increased the temperature in a linear fashion at a rate of 50 K min<sup>-1</sup> to a temperature of 523 K. *n*-Pentane was used as a solvent to wash the injection needle after the sample injection. After each sample run, the column temperature was cooled down to 313 K so that the following sample could be analysed.

Internal standardisation technique was used for analysis of samples of the reaction mixture. *Iso-Propyl* alcohol (IPA) was used as an internal standard as discussed in section 3.2.3.1. Calibration curve for MeOH was developed and described in Figure 3.5 (section 3.2.3.1). Figure 5.1 shows the calibration curve for response factor determination of PC using IPA as an internal standard. Figure 5.2 shows a typical chromatogram from Shimadzu gas chromatography (GC–2014). Methanol peak emerged first followed by IPA, DMC and PC. The total time for a single GC run was about 16 min.

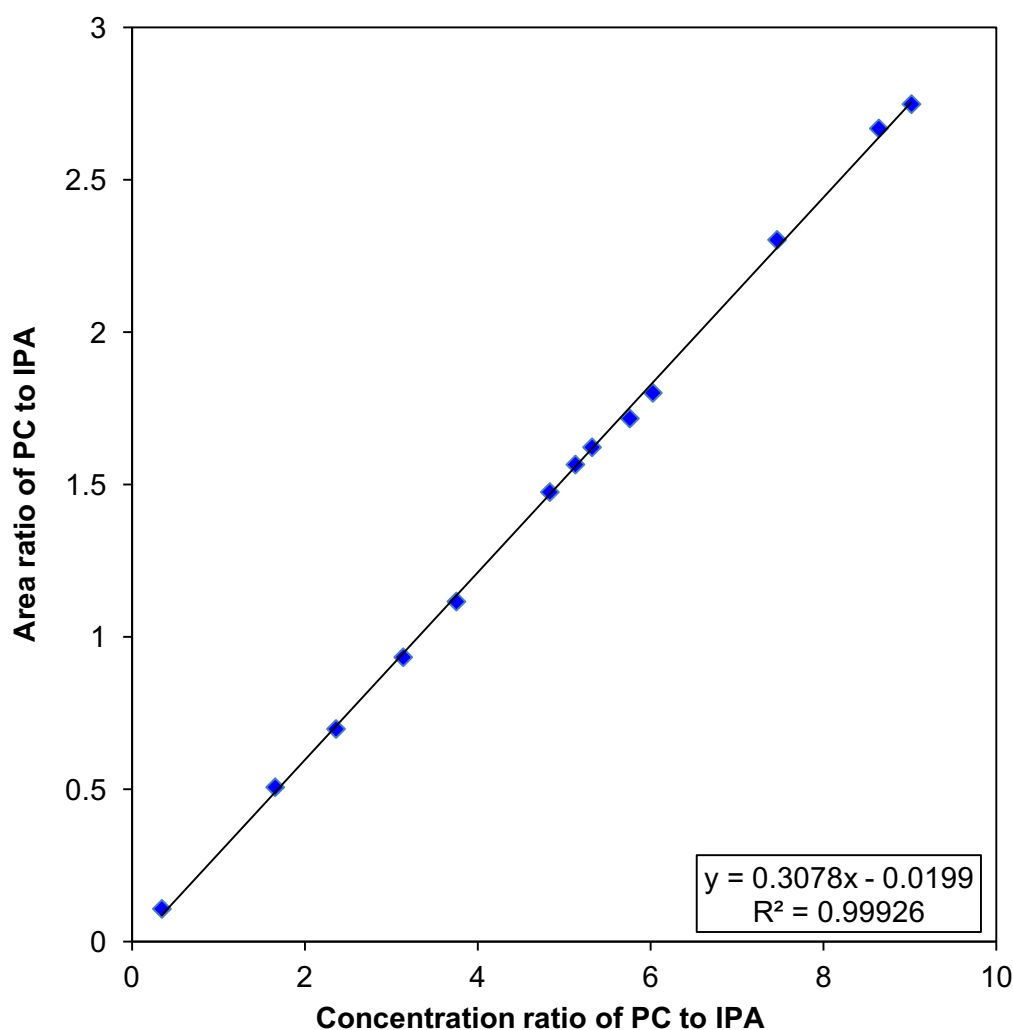


Figure 5.1. Calibration curve for response factor determination of PC using IPA as an internal standard.

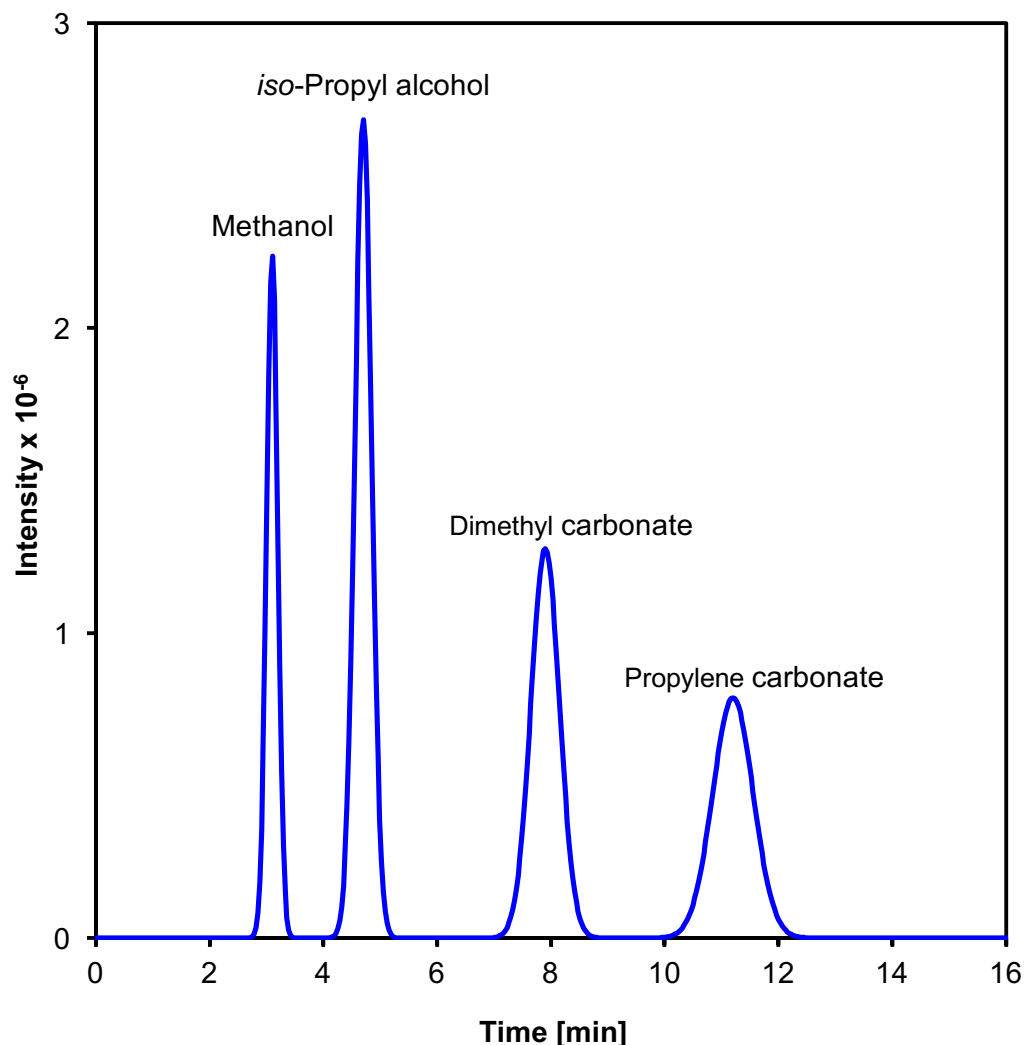


Figure 5.2. A typical chromatogram from Shimadzu-2014 gas chromatograph (GC) for the components present in PC transesterification reaction mixture.

#### 5.2.4. Catalyst Characterisation

Several metal oxide and mixed metal oxide catalysts which include La–O, Zr–O and doped zirconia such as Ce–Zr–O, La–Zr–O and Ce–La–Zr–O have been assessed and analysed based on their catalytic performance towards the synthesis of DMC *via* transesterification of PC with MeOH. These oxide catalysts were prepared by proprietary processes developed by MEL Chemicals Ltd., UK that has been optimised to produce specific particle size distributions and different textural properties (pore volume and pore distribution). Catalyst characterisation techniques and catalyst characterisation results are summarised in Chapter 3, sections 3.2.4 and 3.3.1, respectively.

### 5.3. RESULTS AND DISCUSSION

#### 5.3.1. Reaction Mechanism

DMC can be produced *via* transesterification of propylene carbonate with methanol in the presence of a suitable catalyst as shown in pathway 1 of Figure 5.3. Propylene glycol (PG) is the main co-product which is produced in equimolar quantity to DMC and, therefore, it has been exempted from the discussion. Dimethyl ether (DME) and propylene oxide (PO) are the expected side products from the reaction of PC and MeOH (Williams *et al.*, 2009; Kim *et al.*, 2011, Murugan and Bajaj, 2011; Pyrlík *et al.*, 2012). DME was below the detection limit of the GC–FID used for the analysis of experimental samples and therefore its specific yield was not calculated. This observation is similar to the work published by Zhang *et al.* (2011). PO was not detected as a side product in this study.

A proposed reaction mechanism is shown in Figure 5.4. In the proposed mechanism, M represents a metal atom that consists of an acidic site; O represents an oxygen atom that consists of a basic site. The transesterification reaction of MeOH and PC is initiated by the chemical adsorption of both species on the catalyst surface. MeOH is activated and forms methoxy species bonding on the basic sites of the catalyst (step 1, Figure 5.4). PC is activated by the adsorption on the metallic site of the catalyst. The oxygen atoms from the two methoxy species attack the carbon atom of the carbonyl species to form a chemical bond (O–C) on the metallic site of the catalyst. This finally results in the formation of DMC and PG molecules, which are finally desorbed from the surface of the catalyst.

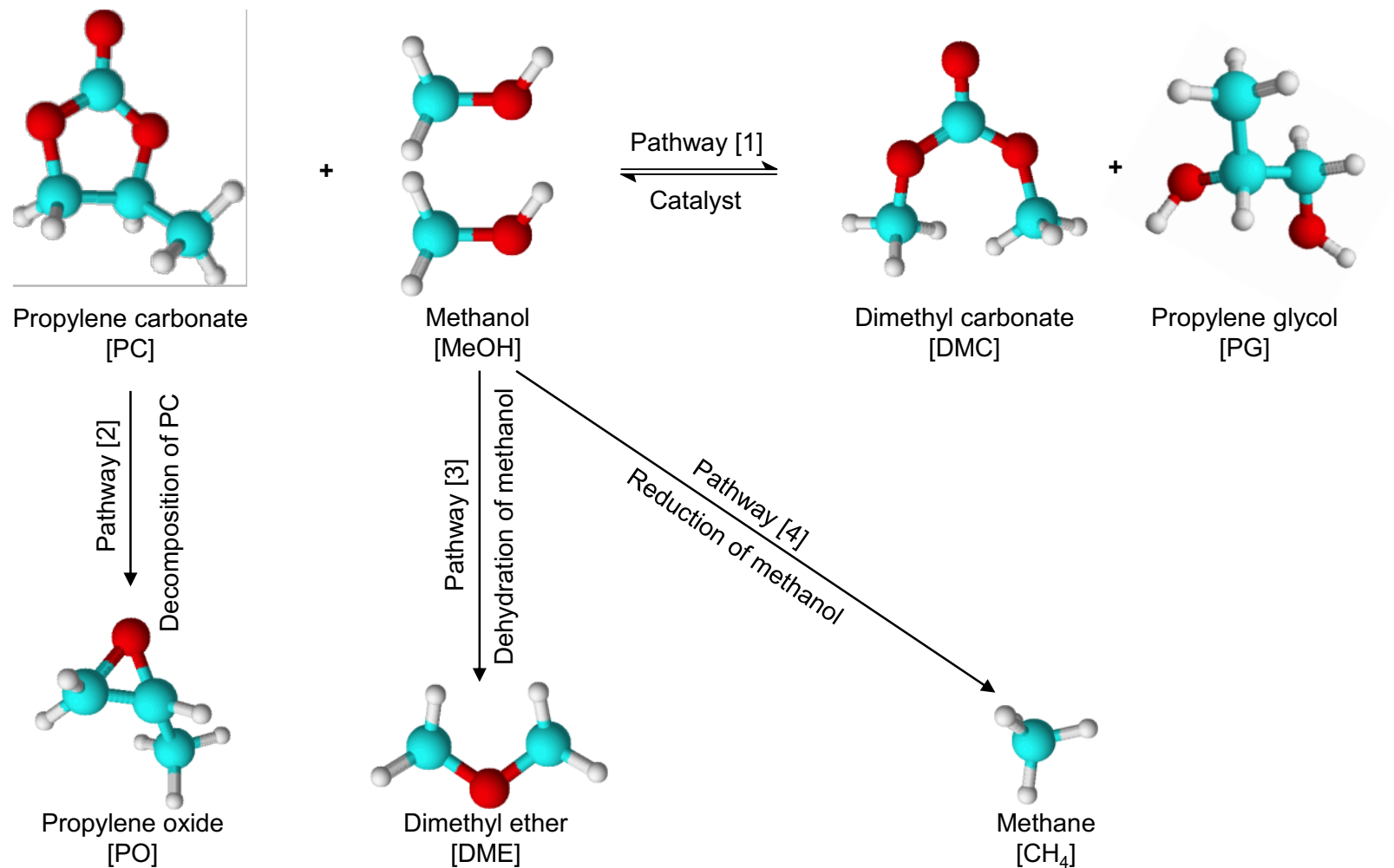
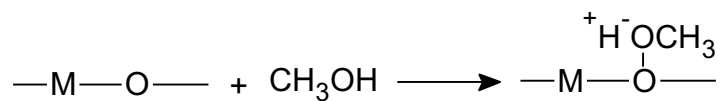
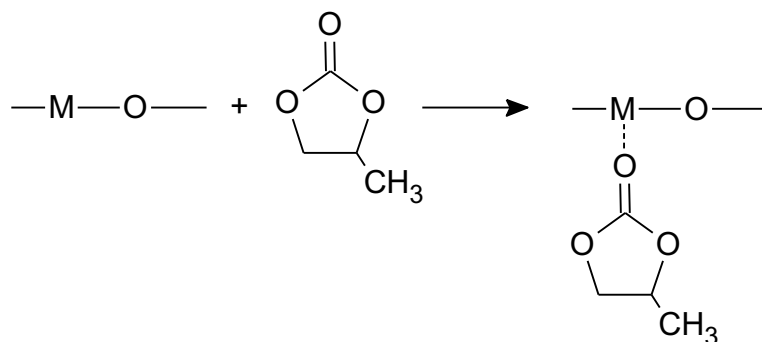


Figure 5.3. Reaction scheme for the synthesis of DMC from PC and MeOH.

Step (I): Adsorption of MeOH onto Ce-La-Zr-O catalyst



Step (II): Adsorption of propylene carbonate onto Ce-La-Zr-O catalyst



Step (III): Surface reaction and product formation

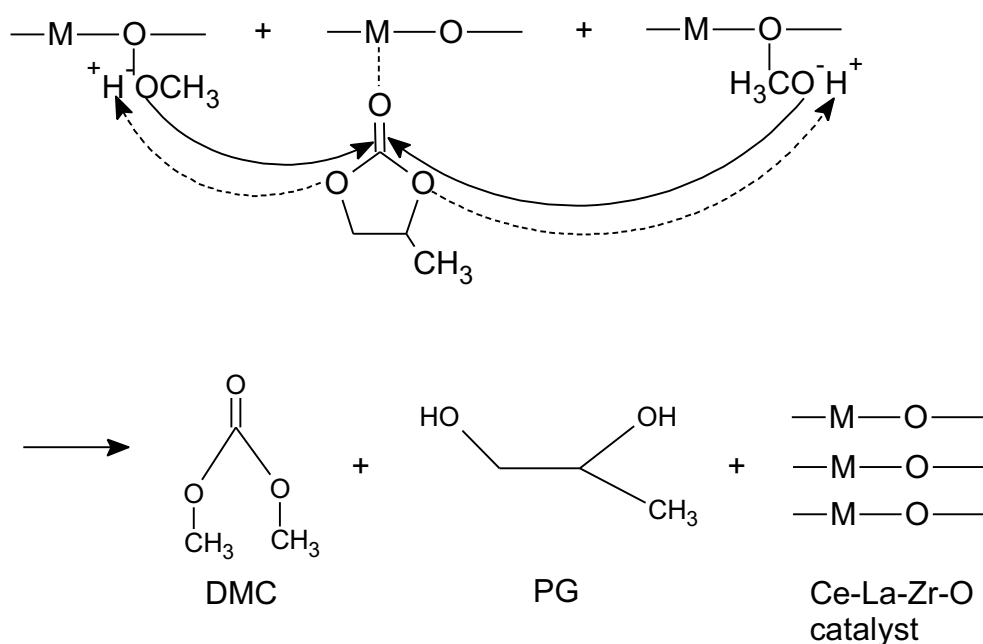


Figure 5.4. Proposed reaction mechanism for the synthesis of DMC from MeOH and CO<sub>2</sub>.

### 5.3.2. Effect of Different Catalysts

At the outset, several heterogeneous catalysts were studied for the synthesis of DMC *via* the transesterification of PC and MeOH. Catalytic performance was indicated by PC conversion and DMC yield. Figure 5.5 shows the effect of different metal oxide and mixed metal oxide catalysts on the conversion of PC and yield of DMC.

La–O catalyst exhibited a PC conversion of ~13.3% and DMC yield of ~7.6%. The performance was very similar to that of Zr–O catalyst, which resulted in a PC conversion and DMC yield of ~16% and ~8.2%, respectively. The catalytic performance of La–O catalyst could be attributed to the lowest particle size (100 nm) and largest pore volume ( $15 \text{ cm}^3\text{g}^{-1}$ ), which provides the reactant molecules with an easy access to the catalyst active sites. The large surface area of Zr–O catalyst ( $310 \text{ m}^2\text{g}^{-1}$ ) explains its good catalytic performance for the synthesis of DMC. Upon the incorporation of La as a dopant into Zr–O to produce La–Zr–O catalyst ( $\text{La}_2\text{O}_3$ :  $10 \pm 1\%$  and  $\text{ZrO}_2$ :  $90 \pm 1\%$ ), a great enhancement to the PC conversion and DMC yield were observed as shown in Figure 5.5. PC conversion and DMC yield reached ~29% and ~24.3%, respectively due to the significant combined effect of both La and Zr in the catalyst.

When ceria was added as a dopant to Zr–O and assessed for its catalytic performance under the same reaction conditions, Ce–Zr–O catalyst ( $\text{CeO}_2$ :  $18 \pm 2\%$  and  $\text{ZrO}_2$ :  $80 \pm 2\%$ ) exhibited a PC conversion of ~23.2% and DMC yield of ~18.6%. The performance of Ce–Zr–O catalyst was remarkably higher than the performance of Zr–O catalyst indicating that the addition of ceria is effective for the synthesis of DMC. Interestingly, when cerium oxide and lanthanum oxide were both incorporated to Zr–O, the performance of the resulting catalyst [i.e. Ce–La–Zr–O ( $\text{CeO}_2$ :  $17 \pm 2\%$ ,  $\text{La}_2\text{O}_3$ :  $5 \pm 1\%$  and  $\text{ZrO}_2$ :  $78 \pm 3\%$ )] improved further giving the highest PC conversion (~45.3%) and DMC yield (~39.7%) when compared to all the other catalysts evaluated in this study. On the basis of the catalyst screening tests, Ce–La–Zr–O was the best performed catalyst for the synthesis of DMC and hence it was used for subsequent studies.

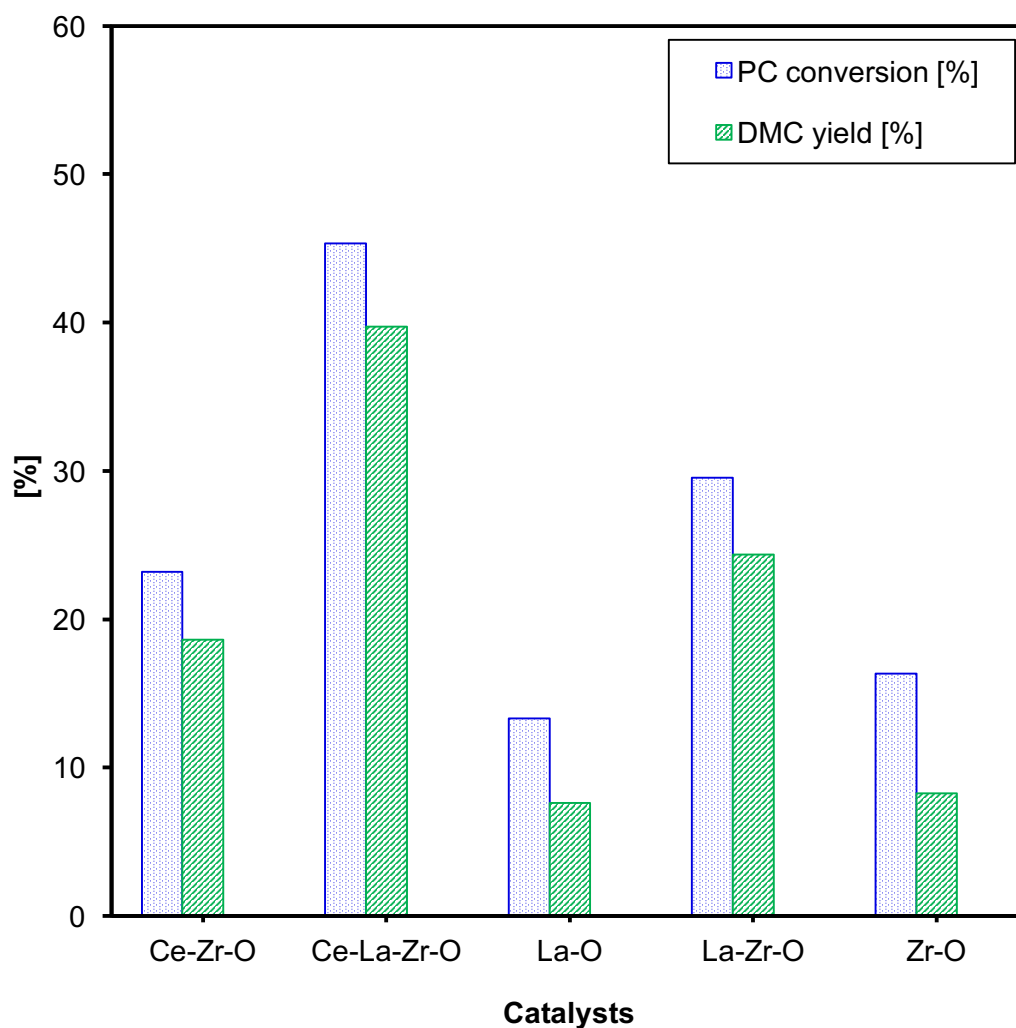


Figure 5.5. Effect of different heterogeneous catalysts for synthesis of DMC. Experimental conditions: MeOH:PC molar ratio, 10:1; catalyst loading, 5% (w/w); reaction temperature, 443 K; reaction time, 6 h and stirring speed, 300 rpm.

### 5.3.3. Effect of Reactant Molar Ratio

A set of transesterification reactions were carried out in the presence of the best performed catalyst (Ce–La–Zr–O) using various molar ratio of methanol to propylene carbonate (MeOH:PC) to evaluate the influence of the reactants molar ratio on the DMC synthesis. The results are presented in Figure 5.6. At low MeOH:PC molar ratio of 2:1, the conversion of PC is as low as 10.7% and the yield of DMC is only ~8.1%. An increase in MeOH:PC molar ratio to 10:1 increases the conversion of PC to ~45.3% and the yield of DMC to 39.7%. DMC yield significantly increases with an increase in the MeOH:PC molar ratio due to

the formation of DMC–MeOH azeotrope caused by the presence of excess MeOH which shifts the equilibrium towards the product side and enhances the synthesis of DMC (Murugan and Bajaj, 2011). PC conversion and DMC yield decreased slightly when MeOH:PC molar ratio was further increased beyond 10:1 indicating that the optimum MeOH:PC molar ratio is 10:1, which agrees with other reported literature (Unnikrishnan and Srinivas, 2012).

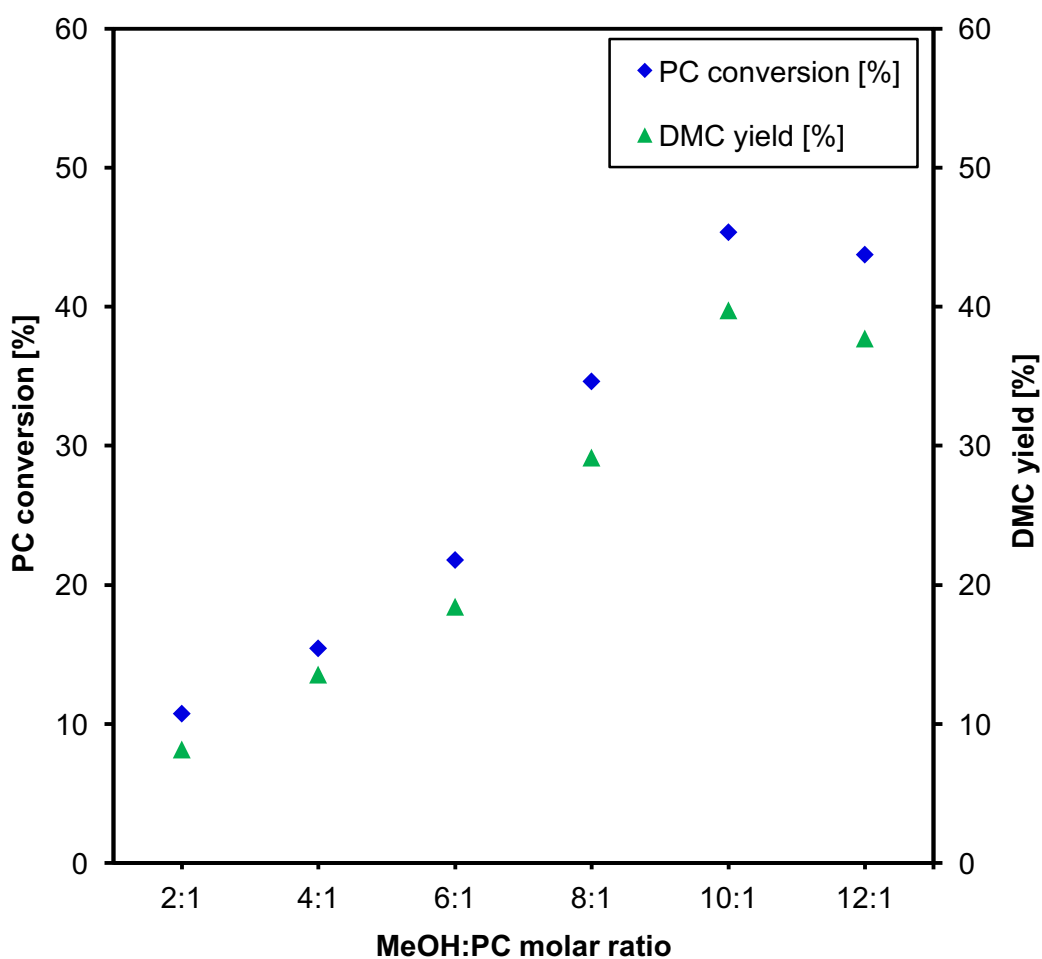


Figure 5.6. Effect of different reactant molar ratio (i.e. MeOH:PC) for synthesis of DMC. Experimental conditions: catalyst, Ce–La–Zr–O; catalyst loading, 5% (w/w); reaction temperature, 443 K; reaction time, 6 h and stirring speed, 300 rpm.

### 5.3.4. Effect of Catalyst Loading

In this study, catalyst loading is defined as the % ratio of the mass of the Ce–La–Zr–O catalyst to the mass of the limiting reactant (PC). The influence of varying the catalyst loading on the yield of DMC was studied by carrying out a set of transesterification reactions of PC and MeOH using different amount of Ce–La–Zr–O. From Figure 5.7, it can be seen that a PC conversion of ~26.5% and DMC yield of ~20.7% were achieved when the reaction was carried out using 2.5% (w/w) catalyst loading. This increased to ~45.3% PC conversion and ~39.7% yield of DMC when catalyst loading increased to 5%. Slightly lower PC conversion and DMC yield were achieved when catalyst loading increased beyond 5% (w/w). This could be attributed to the blockage of the active sites due to the agglomeration of the catalysts and, therefore, it was not necessary to increase the catalyst loading beyond 5% (w/w). In view of the experimental error of  $\pm 2\%$ , it seems that the number of active sites required for PC and MeOH to synthesise DMC was sufficient at 5% (w/w) catalyst loading and hence 5% (w/w) catalyst loading was considered optimum.

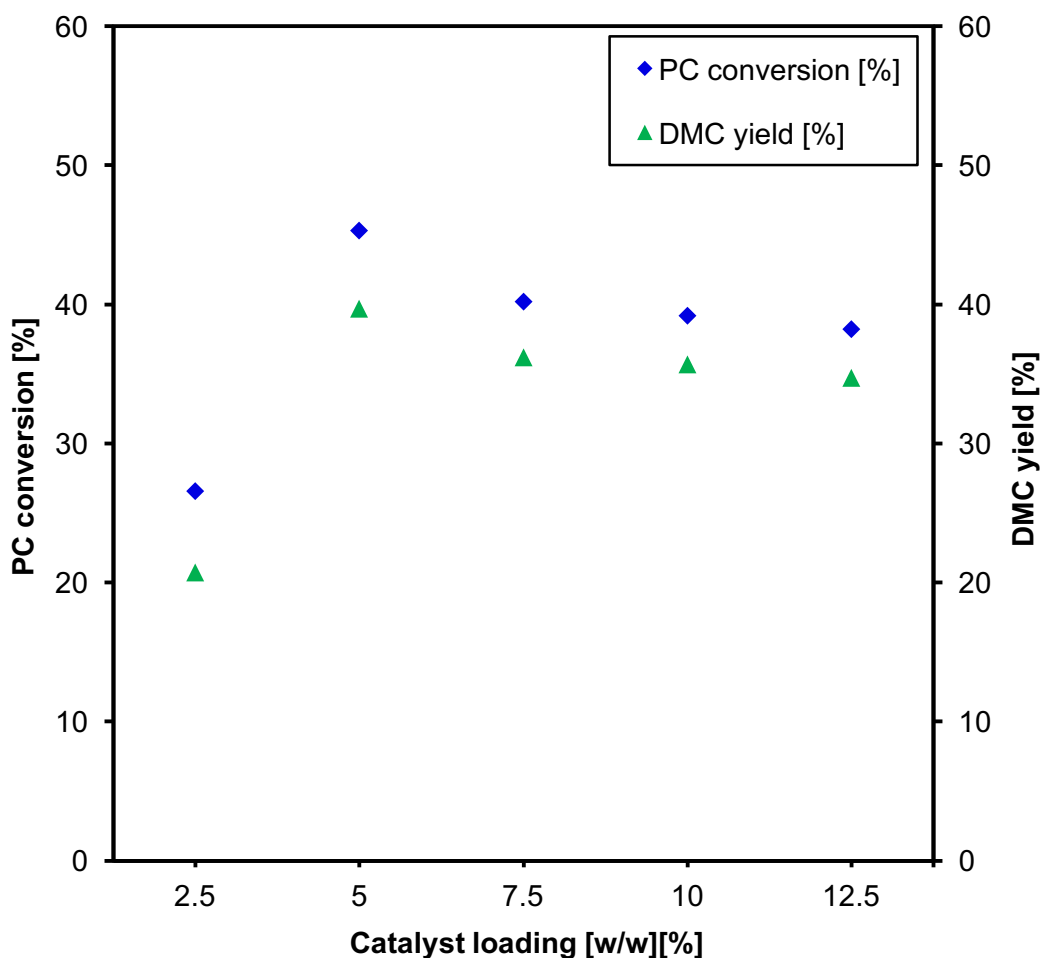


Figure 5.7. Effect of varying catalyst loading on the synthesis of DMC. Experimental conditions: catalyst, Ce–La–Zr–O; MeOH:PC molar ratio, 10:1; reaction temperature, 443 K; reaction time, 6 h and stirring speed, 300 rpm.

### 5.3.5. Effect of Reaction Temperature

In order to evaluate the dependence of the catalytic performance on the reaction temperature, a set of catalytic reactions was conducted within a temperature range of 403 and 463 K for 6 h as shown in Figure 5.8. When the transesterification reaction was carried out at 413 K, the reaction proceeds with moderate PC conversion (~13.7%) and DMC yield (~12%). As the reaction temperature increases from 403 K to 443 K, PC conversion and DMC yield progressively increase in a linear fashion. A maximum PC conversion of ~45.3% and DMC yield of 39.7% were achieved when the reaction was carried out at 443 K. Due to the equilibrium nature of the reaction, higher temperatures can

shift the equilibrium towards the reactant side thus decreasing the yield of DMC (Wei *et al.*, 2003). As the reaction temperature further increased to 453 K and 463 K, the yield of DMC decreased to 34.4% and 32.8%, respectively. Therefore, this study indicates that 443 K is the optimum temperature for the reaction between PC and MeOH, which agrees well with the published literature (Wei *et al.*, 2003, Wang *et al.*, 2006c, Srivastava *et al.*, 2006b).

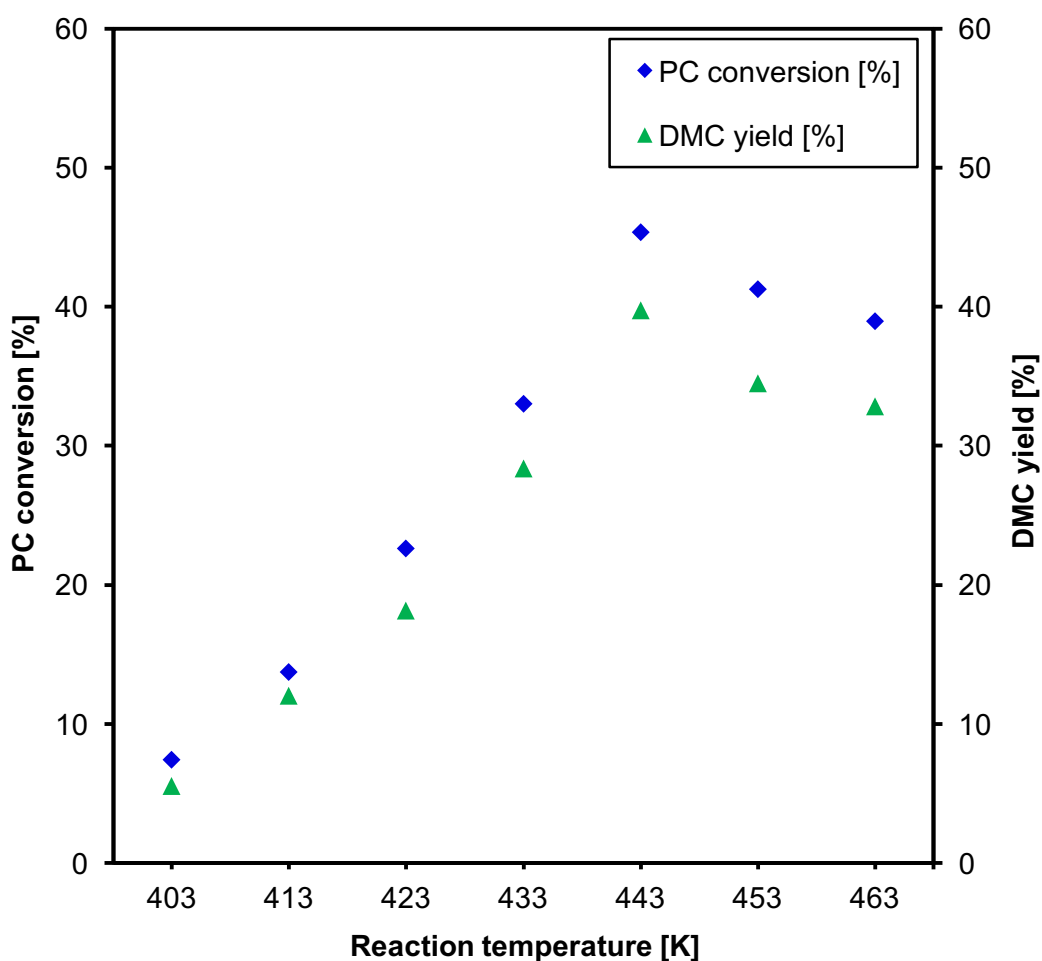


Figure 5.8. Effect of reaction temperature on the synthesis of DMC. Experimental conditions: catalyst, Ce–La–Zr–O; MeOH:PC molar ratio, 10:1; catalyst loading, 5% (w/w); reaction time, 6 h and stirring speed, 300 rpm.

### 5.3.6. Effect of Reaction Time

A series of experiments were carried out at various reaction time to determine the optimum time for the synthesis of DMC using 5% (w/w) Ce–La–Zr–O catalyst to catalyse the reaction. The experiments were carried out at 443 K using MeOH: PC molar ratio of 10:1. Figure 5.9 show that the reaction time exhibits a noticeable relationship with catalytic performance of the transesterification reaction. PC conversion of ~18% and ~14% yield of DMC were observed for only 2 h reaction time, whereas ~45.3% conversion of PC and ~39.7% yield of DMC were obtained for reaction time of 6 h. However, when the reaction was carried out for a longer period, i.e., 10 h, the conversion of PC as well as the yield of DMC started to decline indicating that the reaction had reached equilibrium at 6 h. On the basis of this study, it can be concluded that 6 h is the optimum reaction time for the catalytic system. This phenomenon has been reported for the transesterification of PC with MeOH by other investigators (Sankar *et al.*, 2006; Xu *et al.*, 2013c; Xu *et al.*, 2014).

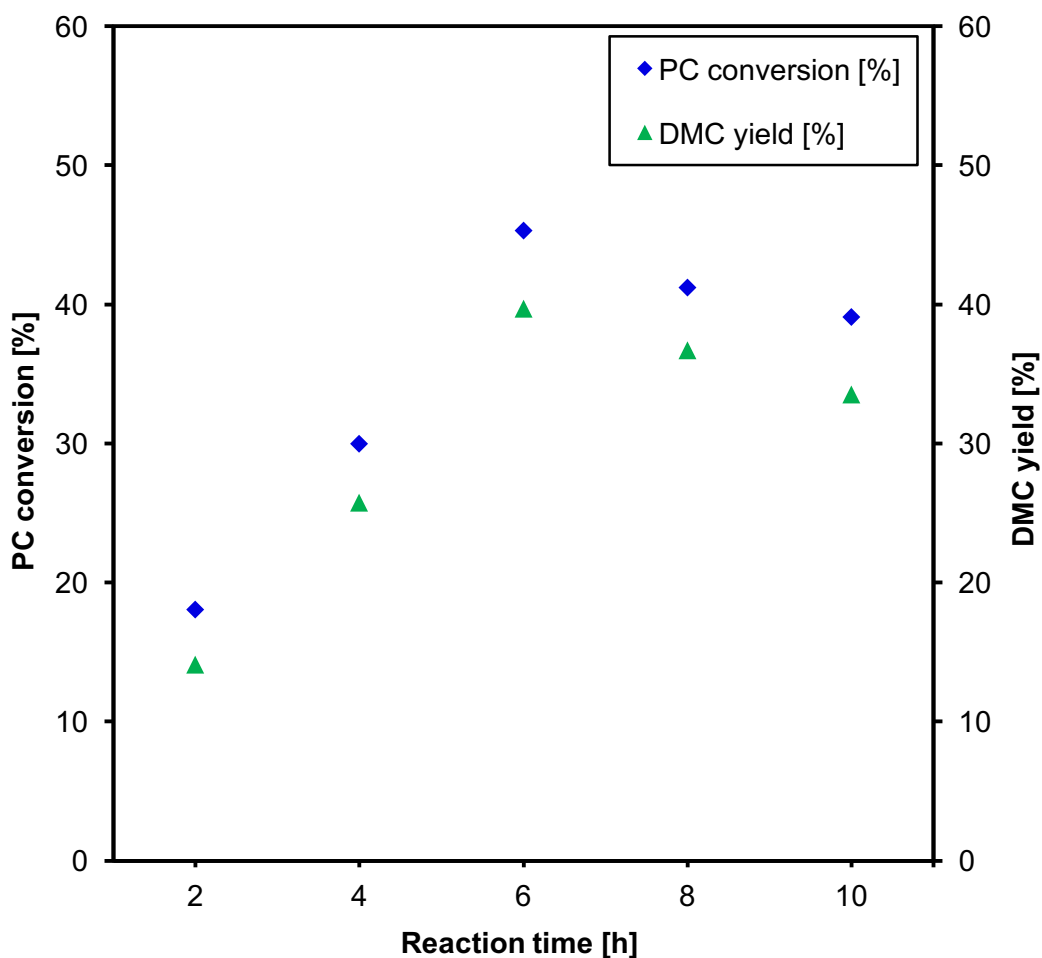


Figure 5.9. Effect of reaction time on the synthesis of DMC. Experimental conditions: catalyst, Ce–La–Zr–O; MeOH:PC molar ratio, 10:1; catalyst loading, 5% (w/w); reaction temperature, 443 K and stirring speed, 300 rpm.

### 5.3.7. Effect of Mass Transfer in Heterogeneous Catalytic Process

Mass transfer limitations can be a major factor that affects PC conversion and yield of DMC in heterogeneously catalysed processes. External and internal mass transfer resistances can exist in heterogeneous catalysed reactions where the former occurs across the solid-liquid interface due to the stirring of the reaction mixture and the latter occurs in the intra-particle space due to catalyst's physical and chemical structure, particle size, pore size distribution and porosity. The effect of mass transfer resistance on the transesterification reaction of PC with MeOH using Ce–La–Zr–O to synthesise DMC was investigated under identical reaction conditions at various stirring speed (300–500 rpm) as shown in

Figure 5.10. It can be observed that there was negligible difference in PC conversion and yield of DMC at different stirring speed, indicating the absence of external mass transfer resistance which can be attributed to the homogeneous distribution of the catalyst particles in the reaction mixture. On the other hand, Ce–La–Zr–O particles are fairly small, uniform and porous (particle size: 1.7 $\mu$ m and pore diameter 21.1 nm) which eliminates mass transfer limitation (Clerici and Kholdeeva, 2013). Therefore, it can be concluded that internal mass transfer resistance is negligible for Ce–La–Zr–O catalysed reaction due to the nature of the catalyst particles. On the basis of this study, all batch experiments were carried out with a stirrer speed of 300 rpm using Ce–La–Zr–O catalyst.

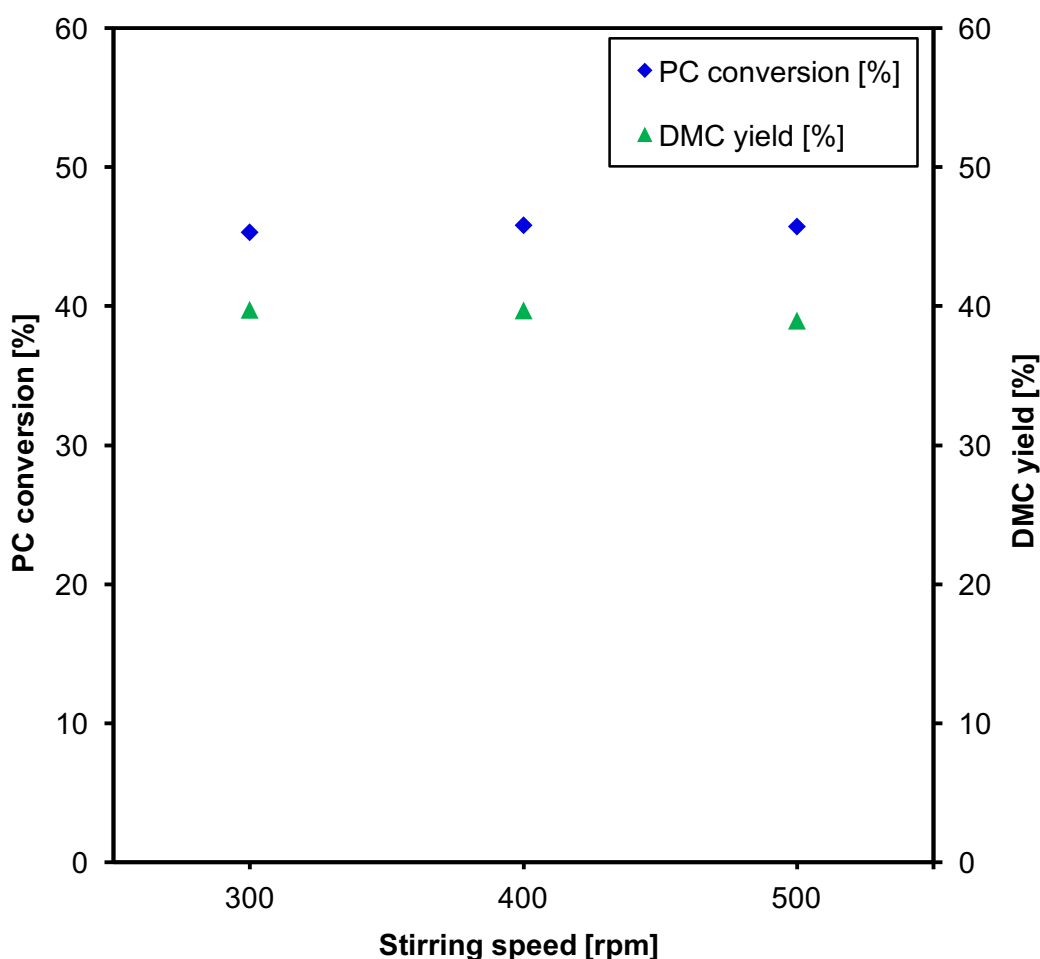


Figure 5.10. Effect of different stirring speed on the synthesis of DMC. Experimental conditions: catalyst, Ce–La–Zr–O; MeOH:PC molar ratio, 10:1; catalyst loading, 5% (w/w); reaction temperature, 443 K and reaction time, 6 h.

#### 5.3.8. Catalyst Reusability

The ease of reusability of Ce–La–Zr–O is an important factor in this heterogeneous catalytic process. The reusability of Ce–La–Zr–O was studied by carrying out a set of experiments at the optimum reaction conditions obtained from the batch studies (i.e., MeOH:PC molar ratio 10:1, 5% catalyst loading (w/w), reaction temperature 443 K and 6 h reaction time). The first reaction was carried out using a fresh catalyst and labelled as Run 1 (see Figure 5.11). The catalyst was recovered by filtration from the reaction mixture, washed twice with acetone and dried at 333 K for 12 h. The catalyst was then reused for subsequent experiments (labelled Run 2–Run 6) under the same optimum reaction conditions (see Figure 5.11). It can be observed that PC conversion and yield of DMC remained similar even after the 6<sup>th</sup> Run indicating that Ce–La–Zr–O catalyst exhibits excellent reusability and stability for the synthesis of DMC. It is evident that Ce–La–Zr–O can be easily recovered and reused without any significant loss in its catalytic performance.

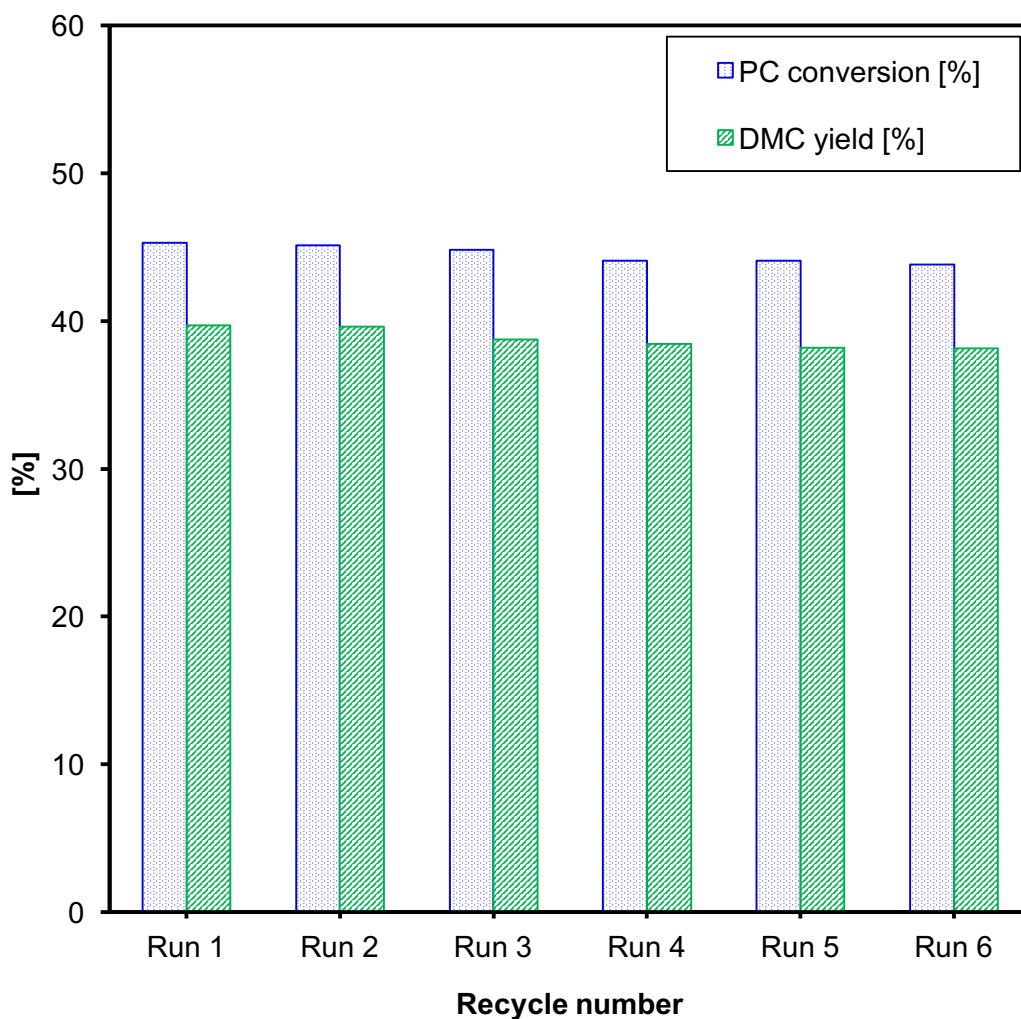


Figure 5.11. Catalyst reusability for the synthesis of DMC. Experimental conditions: catalyst, Ce–La–Zr–O; MeOH:PC molar ratio, 10:1; catalyst loading, 5% (w/w); reaction temperature, 443 K; reaction time, 6 h and stirring speed, 300 rpm.

#### 5.4. CONCLUSIONS

The transesterification of PC with MeOH for the synthesis of DMC was successfully conducted in a high pressure reactor using various heterogeneous catalysts in the absence of any solvent. It was found that an increase in MeOH:PC molar ratio resulted in an increase in the PC conversion and yield of DMC. Ceria lanthana doped zirconia (Ce–La–Zr–O) catalyst was found to be the best performing catalyst for DMC synthesis as compared to other heterogeneous catalysts. The PC conversion of ~45.3% and DMC yield of ~39.7% were obtained

at an optimum reaction condition of 10:1 MeOH: PC molar ratio, 443 K, 6 h and 300 rpm using 5% (w/w) Ce–La–Zr–O catalyst. Reusability studies confirmed that Ce–La–Zr–O could be easily recycled and reused several times without any reduction in its catalytic performance.

# **Chapter 6**

## **Transesterification of Propylene Carbonate (PC) with Methanol (MeOH) using Metal Oxide/ Graphene Nanocomposite Catalysts**

## 6. TRANSESTERIFICATION OF PC WITH MeOH USING METAL OXIDE/GRAPHENE NANOCOMPOSITE CATALYSTS

### 6.1. INTRODUCTION

The synthesis of DMC *via* the transesterification of cyclic carbonates and methanol (MeOH) has gained much interest recently, where cyclic carbonates can be synthesised from their corresponding epoxides and CO<sub>2</sub>, thus making the synthesis of DMC *via* transesterification route more environmentally friendly and desirable in terms of green chemistry and sustainable development.

Much effort has been dedicated for the design of new greener catalytic processes for the synthesis of DMC with ionic liquids being reported to be the most efficient catalysts proposed for the transesterification of propylene carbonate (PC) and MeOH (Kim *et al.*, 2011; Wang *et al.*, 2011a; Xu *et al.*, 2013; Xu *et al.*, 2014). However, there are few drawbacks associated with the homogeneous nature of ionic liquids. Therefore, the development of solvent-less heterogeneous catalytic process for the synthesis of DMC is highly desired and a key aspect for the design of greener chemical synthesis.

The (re)discovery of graphene, a single sheet of hexagonally arrayed sp<sup>2</sup>-bonded carbon atoms, by Geim and Novoselov (Nobel Prize, 2010) introduced a new era in materials science, the epoch of the 2D materials with applications in transformative technologies. Graphene success revealed that it is possible to obtain a stable, one-atom thick 2D material from layered van der Waals solids with fascinating unique physical, chemical and mechanical properties (Geim and Novoselov, 2007; Geim, 2009; Rao *et al.*, 2009). The exciting properties of graphene, such as very high surface area, chemical stability, excellent electrical and thermal conductivity, make graphene a very interesting material for a broad range of potential applications (Li *et al.*, 2008; Williams *et al.*, 2008; Dreyer *et al.*, 2010; Liang *et al.*, 2010) including energy storage and generation (e.g. electrodes for lithium ion batteries, super capacitors, solar and fuel cells), chemical and biochemical sensors, optical devices and high speed electronics, as well as CO<sub>2</sub> conversion technologies (e.g. catalysts and absorbers). However, the 2D material alone does not possess the properties that are required in a range of technological applications. Owing to the flexible yet robust 2D membranes, it is possible to design and construct novel 2D based functional

materials with different properties from parent 2D material. This can be achieved *via* utilising a green, rapid and continuous hydrothermal flow synthesis (CHFS) route for synthesis of 2D-inorganic nanocomposites with superior properties to those currently available (Hakuta *et al.*, 1998; Darr and Poliakoff 1999; Chaudhry *et al.*, 2006; Lester *et al.*, 2006; Goodall *et al.*, 2014; Middelkoop *et al.*, 2014). This will afford advanced functional materials with minimal structural and electronic defects. CHFS reactors offer many advantages as discussed in Chapter 4, section 4.1. It is generally used for syntheses of highly crystalline inorganic nanomaterials, e.g. homogenous and heterogeneous complex metal oxides, zeolites, reduced graphene oxide, biomaterials such as hydroxyapatite at relatively low temperature and at high pressure. The key features of CHFS process are explained in Chapter 4, section 4.1.

In recent years, Response Surface Methodology (RSM) has been employed to evaluate the relationship between multiple process variables in order to optimise a specified response (i.e. output variable) (Zhong *et al.*, 2012; El-Gendy *et al.*, 2014). Applying RSM at experimental stage reduces the number of experimental trials and hence the overall cost of the experiments. RSM is a collection of mathematical and empirical and mathematical techniques based on multivariate statistics which includes experimental design, statistical model and process optimisation (Tahmouzi, 2014). RSM has a track record in helping researchers in modelling and optimisation of the experimental design for various applications in food industry, catalysis and chemical reaction optimisation (Duan *et al.*, 2014). It helps to conclude the most important factors and their direct and interacted effects on the response. A further advantage of using RSM is that it does not require theoretical knowledge or human experience and still could accurately mimic the trends using the design experimental results satisfactorily.

In this study, an innovative approach has been employed for synthesising advanced heterogeneous catalysts such as mixed metal oxides and graphene-inorganic nanocomposite catalyst *via* utilisation of a continuous hydrothermal flow synthesis (CHFS) reactor. The catalytic performance of the synthesised catalysts has been extensively studied for a greener and sustainable process for the synthesis of DMC. RSM using Box-Behnken design (BBD) was carried out for process modelling and optimisation, with an aim to better understand the

relationships between five operating variables (MeOH:PC molar ratio, catalyst loading (w/w), reaction temperature, reaction time and stirring speed) and their impact on PC conversion and yield of DMC. Furthermore, regression analysis was applied to establish validated model used to derive the optimum operating conditions for DMC synthesis.

### 6.2. EXPERIMENTAL METHOD

#### 6.2.1. Materials

Methanol (MeOH), propylene carbonate (PC), *iso*-propyl alcohol (IPA), dimethyl carbonate (DMC), zirconium(IV) oxynitrate hydrate ( $\text{ZrO}(\text{NO}_3)_2 \cdot 6\text{H}_2\text{O}$ ) and tin (II) oxalate ( $\text{SnC}_2\text{O}_4$ , 98%) were purchased from Sigma-Aldrich Co. Ltd (UK). Other chemicals were purchased from Fisher Scientific, UK, including hydrochloric acid (HCl), sulphuric acid ( $\text{H}_2\text{SO}_4$ ), natural graphite powder (NPG), sodium nitrate ( $\text{NaNO}_3$ ), hydrogen peroxide ( $\text{H}_2\text{O}_2$ ), potassium hydroxide pellets (KOH) and potassium permanganate ( $\text{KMnO}_4$ ). In all cases 10 M $\Omega$  deionised water was used. All chemicals were used without any further purification.

#### 6.2.2. Catalyst Preparation

Graphene oxide (GO) was synthesised using Hummer's method shown in Chapter 4, section 4.2.2.1 (Hummers and Offeman, 1958; Zhu *et al.*, 2010; Marcano *et al.*, 2010). The as-prepared GO was then used as a precursor for the synthesis of tin doped zirconium oxide/graphene (Zr–Sn/GO) nanocomposites (see Figure 6.1) (where nominal atomic ratio of Zr:Sn used was 9:1) *via* CHFS design.

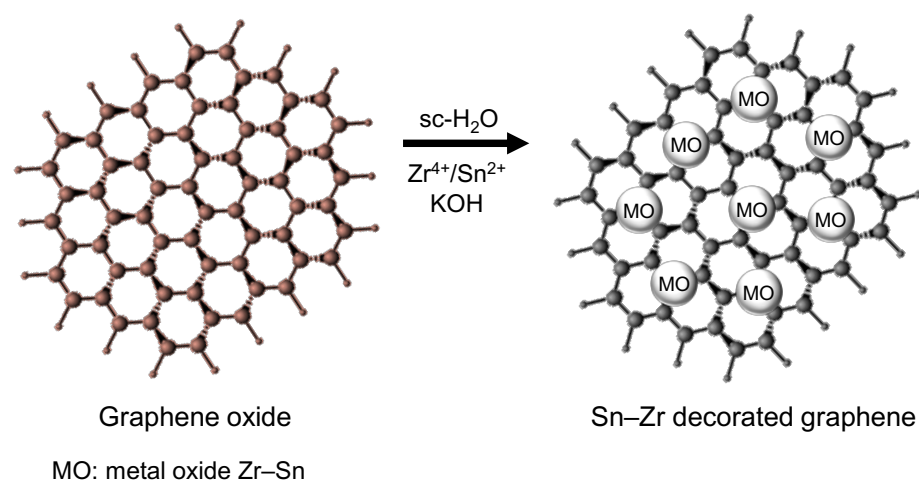


Figure 6.1. A schematic representation of the synthesised tin doped zirconia graphene nanocomposite catalyst.

The CHFS system utilises three high performance liquid chromatography (HPLC) pumps for the delivery of aqueous solution of precursors as shown in Figure 6.2. Pump 1 (Gilson 307 fitted with 25 mL pump head) was used for pumping deionised water through a custom made electrically powered pre-heater (723 K) at a flow rate of  $20 \text{ mL min}^{-1}$ . Pumps 2 and 3 (Varian Pro Star 210 fitted with 5 mL pump head) delivered pre-sonicated aqueous GO solution premixed with corresponding tin and zirconium salts at the desired ratios and KOH, respectively, where both pumps were operated at a flow rate of  $5 \text{ mL min}^{-1}$ . Typically, Zr-Sn/GO nanocomposites were synthesised *via* the following synthetic approach: pre-mixed aqueous solutions of  $ZrO(NO_3)_2 \cdot 6H_2O$  and  $SnC_2O_4$  (with a total metal ion concentration of 0.2 M and molar ratios of 9:1) and a pre-sonicated (60 min) aqueous solution of GO ( $4 \mu\text{g mL}^{-1}$ ) were pumped to meet a flow of KOH (1 M) at a T-junction (see Figure 6.2). The molar ratio used were  $Zr^{4+}/Sn^{2+} = 1$  and GO = 2. This composition then reacted with superheated water (723 K, 24.1 MPa) inside a counter-current reactor whereupon the formation of Zr-Sn/GO nanocomposite occurs in a continuous manner. The aqueous suspension was cooled through the cooler (pipe-in-pipe design) and the slurries were collected from the exit of the back pressure regulator (utilised to maintain a reactor pressure of 24.1 MPa throughout the experiment). After collection, the particles were centrifuged (4500 rpm) and washed twice with deionised water.

Pure tin doped zirconium oxide (Zr–Sn–O) was also synthesised following the same synthetic approach.

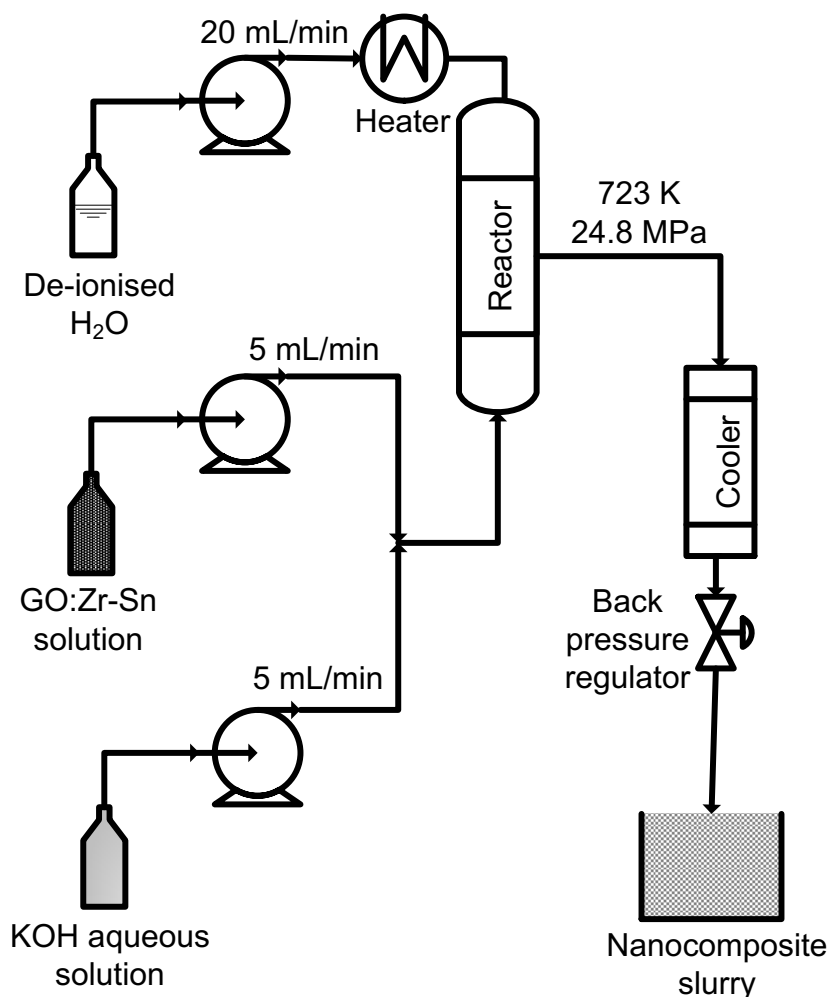


Figure 6.2. A schematic of a CHFS reactor set up used for the synthesis of Zr–Sn/GO nanocomposite catalyst.

### 6.2.3. Tin Doped Zirconia Graphene Nanocomposite Heat-Treatment

The washed catalysts were frozen in liquid nitrogen and then freeze-dried using a Heto PowerDry PL3000 freezer for 24 h. The dried Zr–Sn/GO samples were heat-treated for 4 h under nitrogen using a Carbolite tube furnace at 773 K and 973 K and were labelled as HT500 and HT700, respectively. The photographic images of Zr–Sn–O, Zr–Sn/GO, HT500 and HT700 are shown in Figure 6.3.



Figure 6.3. Photographic images of tin doped zirconia samples: (a) pure tin doped zirconia as-prepared sample synthesised using CHFS route labelled as Zr-Sn-O; (b) tin doped zirconia graphene nanocomposite as-prepared sample synthesised using CHFS route labelled as Zr-Sn/GO; (c) Zr-Sn/GO heat-treated (773 K) sample labelled as HT500 and (d) Zr-Sn/GO heat-treated (973 K) sample labelled as HT700.

#### 6.2.4. Catalyst Characterisation Techniques

Micromeritics Gemini VII analyser (nitrogen adsorption and desorption method) was used to measure the BET surface area of the as prepared samples. The powders were degassed at 423 K in N<sub>2</sub> (purge gas supplied by BOC, UK) for 12 h prior to BET analysis. The particle size and morphology of as-prepared samples

were investigated using a JEOL 2100FCs with a Schottky Field Emission Gun transmission electron microscope (200 kV accelerating Brunauer–Emmett–Teller (BET) surface area measurements of all samples were conducted on a voltage). Samples were collected on carbon-coated copper grids (Holey Carbon Film, 300 mesh Cu, Agar Scientific, Essex, UK) after being briefly dispersed ultrasonically in water. Particle size analysis was performed using ImageJ particle size analysis software. X-ray powder diffraction data were collected on a low background silicon sample holder in Bragg-Brentano geometry on a D8 Bruker diffractometer equipped with primary Gobbel mirrors for parallel Cu Ka X-rays and a Vantec position sensitive linear detector. Collection conditions were: 5-110° in 2θ, 0.04 step size, 450 seconds/step, divergence slits 0.6 mm. XPS measurements were performed using a Kratos Axis ultra DLD photoelectron spectrometer utilising monochromatic Alka source operating at 144 W. Samples were mounted using conductive carbon tape. Survey and narrow scans were performed at constant pass energies of 160 and 40 eV, respectively. The base pressure of the system is ca.  $1 \times 10^{-9}$  Torr, rising to ca.  $4 \times 10^{-9}$  Torr under analysis of these samples. Raman spectra were collected between 50 and 3500  $\text{cm}^{-1}$  using a confocal Labram HR300 Raman spectrometer (Horiba Jobin–Yvon™) of 300 mm focal length equipped with a holographic grating of 1800  $\text{gr.mm}^{-1}$  coupled to a Peltier cooled front illuminated CCD detector, 1024 x 256 pixels in size. Such a configuration allowed reaching a spectral resolution of about 1.4  $\text{cm}^{-1}$  per pixel. The excitation line at 532 nm was produced by a diode-pumped solid state laser (Laser Quantum™) focused on the sample using a Mitutoyo™ 50x long working distance objective (0.42 N.A.). Laser power at the sample was 25 mW. Spectra were corrected from a linear baseline and peak characteristics were obtained by fitting Voigt profiles to the Raman bands using the fitting software Peakfit™.

### 6.2.5. Transesterification of Propylene Carbonate with MeOH

Transesterification reactions of PC with MeOH were carried out in a 25 mL autoclave reactor (model 4590, Parr Instrument Company, USA) equipped with a stirring system, a thermocouple (type J), a heating mantle and a controller (model 4848). In a typical process, different moles of PC and MeOH along with the required amount of the heterogeneous catalyst were charged into the reactor vessel. The reactor was continuously stirred and heated to the required temperature. The reaction was left for the desired reaction time. After the

reaction, the reactor was cooled down to room temperature using an ice bath. The reactor was depressurised and the reaction mixture was filtered. The liquid products were analysed using a gas chromatography (GC) equipped with a flame ionisation detector (FID) with a capillary column using *iso*-propyl alcohol as an internal standard. The effect of various reaction parameters were studied for the optimisation of reaction conditions. The stability of the catalyst was assessed by carrying out catalyst reusability studies on the best performed catalyst at the optimum conditions.

### 6.2.6. Method of Analysis for Transesterification Reactions

The sample collected from the reaction mixture of propylene carbonate and methanol was analysed using a Shimadzu gas chromatography (GC-2014). A ramp method was used in order to separate all the compounds present in the sample mixture. The initial temperature of the oven was set at 323 K and the sample was injected by an auto sampler for analysis. The column temperature was then held at 323 K for 5 min after the sample had been injected. Afterwards, a temperature ramp was applied that increased at a rate of 50 K min<sup>-1</sup> to a temperature of 523 K. *n*-Pentane was used as a solvent to wash the injection needle after the sample injection. The subsequent sample runs were started when the column temperature was cooled back to 323 K. The components mass fractions were directly calculated from the chromatograms *via* internal standard method using IPA as an internal standard.

### 6.2.7. One-Factor-at-a-Time Analysis (OFAT)

PC and MeOH transesterification reactions were carried out as described in section 6.2.5. OFAT analysis was developed to conclude the effective range of the factors in order to start statistical analysis within these ranges. The influence of five single factors (MeOH:PC molar ratio, catalyst loading, reaction temperature, reaction time and stirring rate) were evaluated for effective synthesis of DMC. The OFAT analysis investigated various MeOH: PC molar ratio (2:1, 4:1, 6:1, 8:1, 10:1, 12:1, 14:1), catalyst loading (%)(w/w) (1, 1.5, 2, 2.5, 3, 3.5), reaction temperature (K) (403, 413, 423, 433, 443, 453, 463), reaction time (h) (2, 4, 6, 8, 10) and stirring speed (rpm) (300, 400, 500).

## 6.2.8. Experimental Design

Based on the OFAT method, the effective ranges of the independent factors were observed. The experimental runs were carried out according to five independent variables at 3 levels ( $3^5$ ) factorial design, namely, MeOH:PC molar ratio, catalyst loading, reaction temperature, reaction time and stirring speed, which were labelled as  $X_1$ ,  $X_2$ ,  $X_3$ ,  $X_4$  and  $X_5$ , respectively. Codes were given for the levels of each variable (i.e., -1, 0, 1). The variables and their levels are presented in Table 6.1. Box-Behnken design (BBD) is a method of response surface methodology (RSM) that is used to examine the relationship between of the factors and their direct and combined effect on responses (Khajeh and Sanchooli, 2010). Three levels-five variables BBD model was implemented for this study. The total number of experiments (N) is given by Equation 6.1.

$$N=k^2+k+C_p \quad (6.1)$$

Where,  $k$  is the number of independent factors and  $C_p$  is the replicate number of the center point (Erik and Padmanabhan, 2015). PC conversion and DMC yield were chosen as the responses for this study. The experiments were performed in a randomised order to minimise the influence of unexplained variability in the responses caused by extraneous factors (Bo *et al.*, 2015). Table 6.2 shows the 46 experiments at various conditions and their corresponding responses which were used to develop the model.

Table 6.1. Independent variables and their levels used in the response surface design.

Variables	Code	Levels		
		-1	0	+1
MeOH:PC molar ratio	$X_1$	6	10	14
Catalyst loading (w/w)	$X_2$	1.5	2.5	3.5
Reaction temperature (K)	$X_3$	403	433	463
Reaction time (h)	$X_4$	2	4	6
Stirring speed (rpm)	$X_5$	300	400	500

Table 6.2. Experimental results of the response surface methodology.

Run	A	B	C	D	E	PC	PC	DMC	DMC
						conversion <sup>a</sup>	conversion <sup>b</sup>	yield <sup>a</sup>	yield <sup>b</sup>
						(%)	(%)	(%)	(%)
1	14:1	2.5	433	4	300	73	70.3	70	67.7
2	14	1.5	433	4	400	49	47.6	48	46.7
3	10	2.5	433	2	300	35.5	38	33.7	35.6
4	10	2.5	433	4	400	76.2	76.2	72.2	72.2
5	10	2.5	463	4	500	69.5	67.2	67.3	64.8
6	10	1.5	433	6	400	52	50.1	49.3	47.8
7	10	2.5	433	2	500	35.5	37.9	33.6	36.1
8	10	1.5	463	4	400	44.9	44.4	42.8	42.4
9	6	2.5	433	2	400	14.2	12.6	13.7	12.2
10	10	3.5	403	4	400	14.9	16.5	13.8	14.9
11	6	1.5	433	4	400	25	26.5	23.8	24.8
12	10	2.5	463	2	400	25.6	22.2	24.2	21
13	10	1.5	403	4	400	9.1	8.1	8.6	7.3
14	10	2.5	463	6	400	74	76.3	70.8	72.8
15	10	2.5	403	4	300	21.9	24.7	20.6	23.2
16	10	1.5	433	2	400	20.9	22.9	19.5	21.5
17	10	2.5	433	4	400	76.2	76.2	72.2	72.2
18	10	3.5	433	6	400	74	72.2	70	68.3
19	6	2.5	463	4	400	29	28	26.5	25.9
20	6	2.5	433	4	300	40.9	41.3	38.3	38.9
21	6	3.5	433	4	400	34.1	34.2	32	31.9
22	10	2.5	403	2	400	3.1	2.2	2.2	1.6
23	10	3.5	463	4	400	63.2	65.4	59.9	61.9
24	10	2.5	403	4	500	22	22.8	20.7	21.2
25	10	1.5	433	4	500	52.9	53.7	50.3	51.3
26	14	2.5	433	6	400	72	75.3	71.1	73.8
27	6	2.5	433	6	400	35.1	36.7	33	34
28	10	3.5	433	2	400	28.2	30.2	26.3	28
29	10	2.5	433	4	400	76.2	76.2	72.2	72.1
30	14	2.5	433	2	400	30	30.1	28.8	29

31	10	2.5	463	4	300	65.9	65.5	62.1	61.7
32	14	3.5	433	4	400	72	69.2	69	66.6
33	6	2.5	433	4	500	40.1	42.2	38.4	40
34	10	3.5	433	4	300	69.1	68.5	64.8	64.2
35	10	2.5	403	6	400	12.5	14.2	11.7	13.2
36	10	2.5	433	6	300	75.2	72.6	71.2	68.8
37	10	1.5	433	4	300	52.9	53.5	50.3	50.7
38	10	2.5	433	4	400	76.2	76.2	72.2	72.2
39	14	2.5	403	4	400	12.1	13.4	11.7	13.1
40	10	2.5	433	4	400	76.2	76.2	72.2	72.2
41	10	3.5	433	4	500	68.5	68.1	64.9	64.8
42	14	2.5	463	4	400	68.3	71.5	67.1	70.1
43	14	2.5	433	4	500	70.3	69.3	69.2	67.8
44	6	2.5	403	4	400	3.9	3	3	2
45	10	2.5	433	6	500	75.2	72.6	71.2	69.5
46	10	2.5	433	4	400	76.2	76.2	72.1	72.1

A: MeOH:PC molar ratio; B: Catalyst loading [%][w/w]; C: Reaction temperature [K]; D: Reaction time [h]; E: Stirring speed [rpm]; a: Experimentally obtained; b: Predicted by model

### 6.2.9. Statistical Analysis

A quadratic equation for the model is shown using Equation 6.2:

$$Y = b_0 + \sum_{i=1}^3 b_i X_i + \sum_{i=1}^3 b_{ii} X_i^2 + \sum_{i \neq j=1}^3 b_{ij} X_i X_j \quad (6.2)$$

where  $Y$  is the dependent response,  $b_0$  is the model coefficient constant,  $b_i$ ,  $b_{ii}$ ,  $b_{ij}$  are coefficients for intercept of linear, quadratic, interactive terms respectively, while  $X_i$ ,  $X_j$  are independent variables ( $i \neq j$ ) (Duan *et al.*, 2014). The model was confirmed with the correlation coefficient ( $R^2$ ), adjusted coefficient of determination ( $R^2_{adj}$ ) and the predicted coefficient of determination ( $R^2_{pred}$ ). Analysis of variance (ANOVA) was used to investigate the statistical significance of the regression coefficient by conducting the Fisher's F-test at 95% confident level. The coefficient of determination ( $R^2$ ) is defined as the regression of sum of

squares proportion to the total sum of squares which illustrates the adequacy of a model.  $R^2$  ranges from 0 to 1 and as the value of  $R^2$  approaches 1, it indicates that the model is more accurate. The high adjusted and predicted coefficients of determination also illustrate whether the model adequately fits the data or not (Badwaik *et al.*, 2012). Design Expert 9.0.5 software (Stat-Ease Inc., Minneapolis, MN, USA) was used for the design of experiment, regression and graphical analysis. Statistical significance of the results were presented by  $p < 0.05$  and mean  $\pm$ SE. The fit quality of the polynomial equation was proved by  $R^2$ .

### 6.3. RESULTS AND DISCUSSION

#### 6.3.1. Catalyst Characterisation

An innovative CHFS approach for producing high quality 2D graphene nanocomposites *via* utilisation of continuous hydrothermal flow of superheated water in alkaline medium in a single rapid synthetic route was fostered. Zr–Sn/GO nanocomposites were made from a 0.2 M (total concentration) of pre-mixed aqueous solution of tin oxalate and zinc nitrate (to produce  $\text{Sn}^{4+}$ :  $\text{Zr}^{4+}$  at 10:90 atomic ratio) and GO (produced *via* Hummers method) under alkaline conditions (KOH, 1 M). For comparative purposes, pure Zr–Sn oxide catalyst was also synthesised.

The particle size and morphology of as-prepared samples were investigated by transmission electron microscopy (TEM). TEM images for pure Zr–Sn–O (Figure 6.4) and the corresponding Zr–Sn/GO nanocomposite (Figure 6.5) revealed uniform particles exhibiting a mean particle size of  $4.80 \pm 1.49$  nm and  $5.18 \pm 0.91$  nm, respectively. The TEM image for the graphene oxide (Figure 6.6) revealed a sheet/plate like morphology. The nanocatalyst exhibited moderately high BET surface areas of  $148.39 \text{ m}^2 \text{ g}^{-1}$ ,  $83.32 \text{ m}^2 \text{ g}^{-1}$  and  $139.38 \text{ m}^2 \text{ g}^{-1}$  for pure metal oxide, Zr–Sn/GO and graphene oxide, respectively.

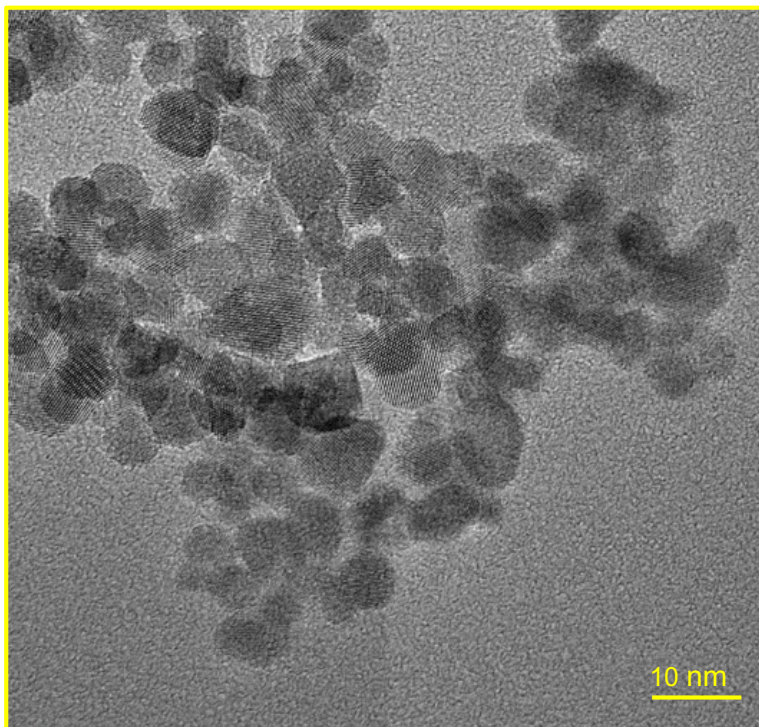


Figure 6.4. Transmission Electron Microscopy (TEM) image of Zr-Sn-O catalyst.

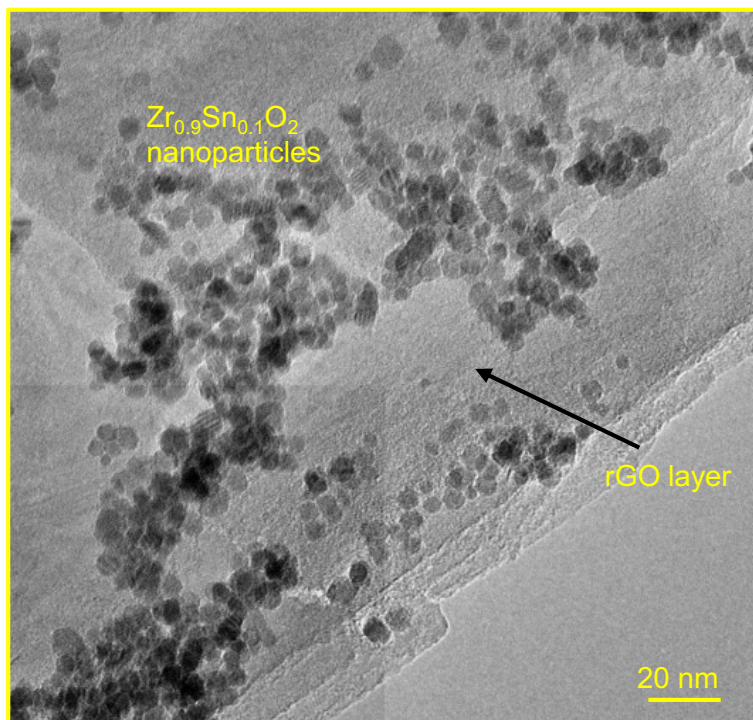


Figure 6.5. Transmission Electron Microscopy (TEM) image of Zr-Sn/GO nanocomposite catalyst.

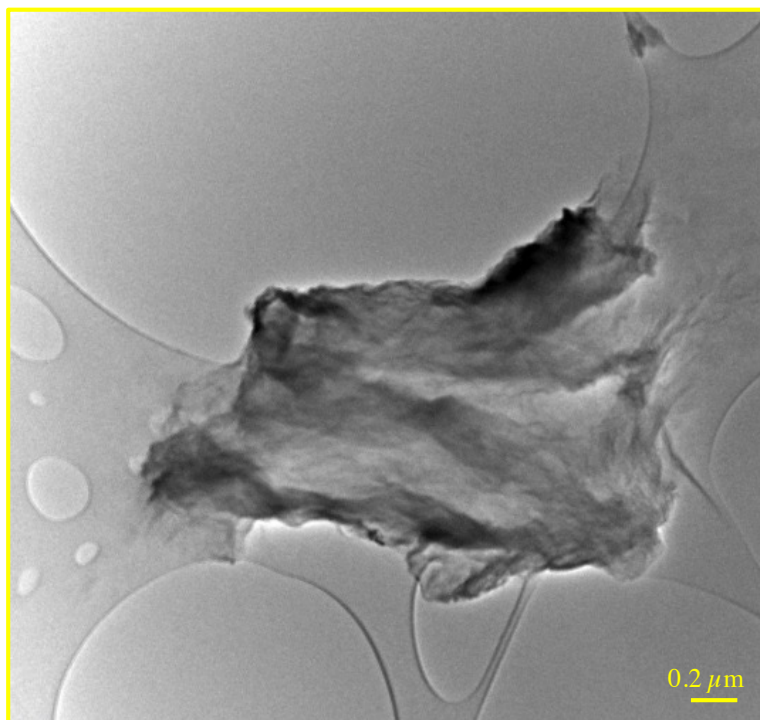


Figure 6.6. Transmission Electron Microscopy (TEM) image of graphene oxide.

The crystallinity of the synthesised nanocomposite catalysts prepared *via* CHFS was assessed by X-ray powder diffraction (XRD) and is shown in Figure 6.7. The XRD pattern for both samples gave peaks corresponding to the zirconium oxide crystal structure.

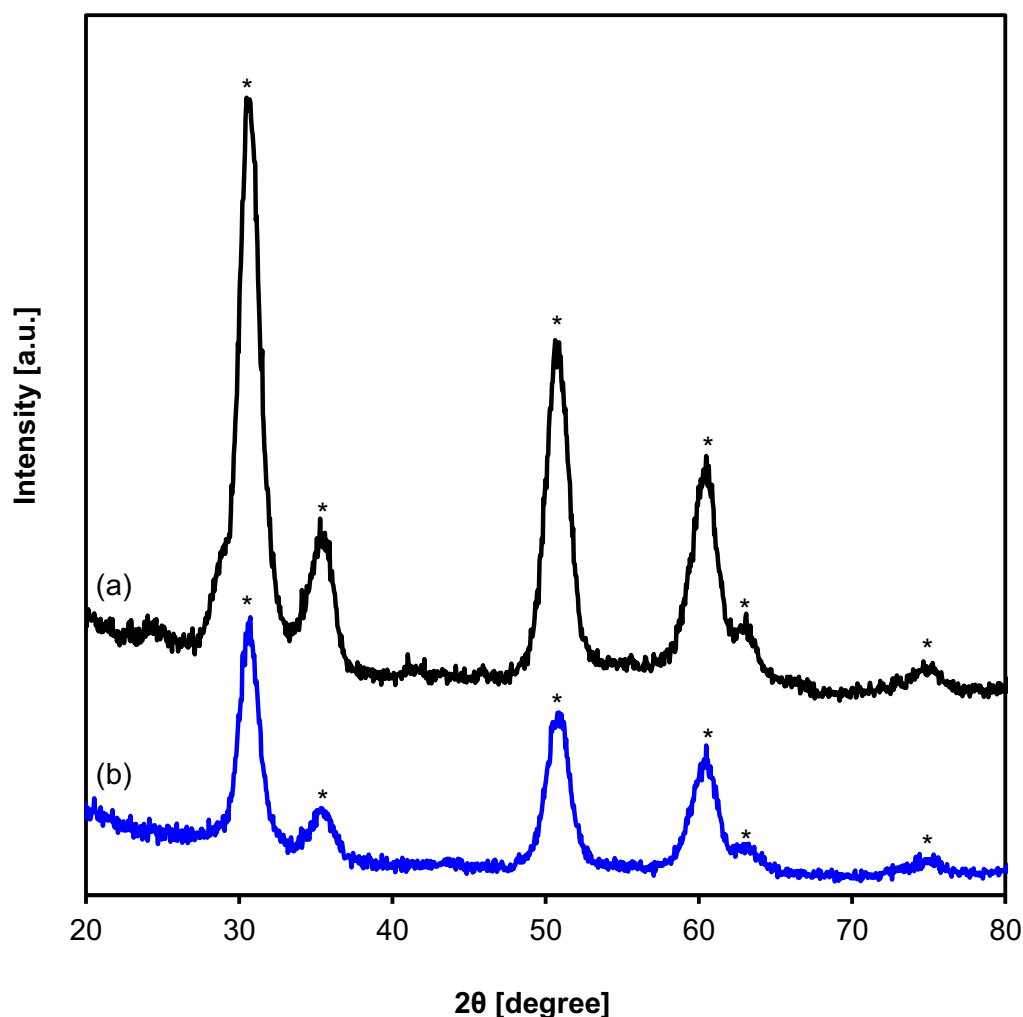


Figure 6.7. X-ray powder diffraction (XRD) patterns of (a) tin doped zirconia graphene (Zr-Sn/GO) and (b) tin doped zirconia (Zr-Sn-O) samples synthesised *via* continuous hydrothermal flow reactor.

\* = reflections assigned to zirconium crystal structure.

To investigate the changes in the concentration of tin and zirconium in the lattice, their oxidation states and the chemical states of graphene oxide for all as prepared catalysts, X-ray photoelectron spectroscopy (XPS) analysis was employed and the spectra of which are shown in Figures 6.8–6.11. The XPS elemental analysis for all the samples showed peaks corresponding to tin (see Figure 6.8), zirconium (see Figure 6.9), oxygen (see Figure 6.10) and carbon (see Figure 6.11). The CHFS approach is effective in dehydrating/reducing GO. Indeed, the deconvoluted C (1s) XPS spectra of Zr-Sn/GO nanocomposite showed considerable reduction in peak intensities of the oxygen-containing

functional groups (carboxyl, epoxide and hydroxyl), which are associated with GO (starting material). Furthermore, the XPS analysis for Sn 3d spectra revealed spin-orbit doublet peaks centred at ca. 487 eV (3d<sub>5/2</sub>) and ca. 495 eV (3d<sub>3/2</sub>) indicating the presence of Sn<sup>4+</sup>, which was confirmed by analysis of the Auger peaks and the corresponding Auger parameter.

XPS spectrum of the Zr 3d core level showed a strong spin-orbit doublet, with the 3d<sub>5/2</sub> peak at 182.3 eV and assigned to Zr<sup>4+</sup>, which is in agreement with reported literature values and characteristic of Zr<sup>4+</sup> ions in their full oxidation state.

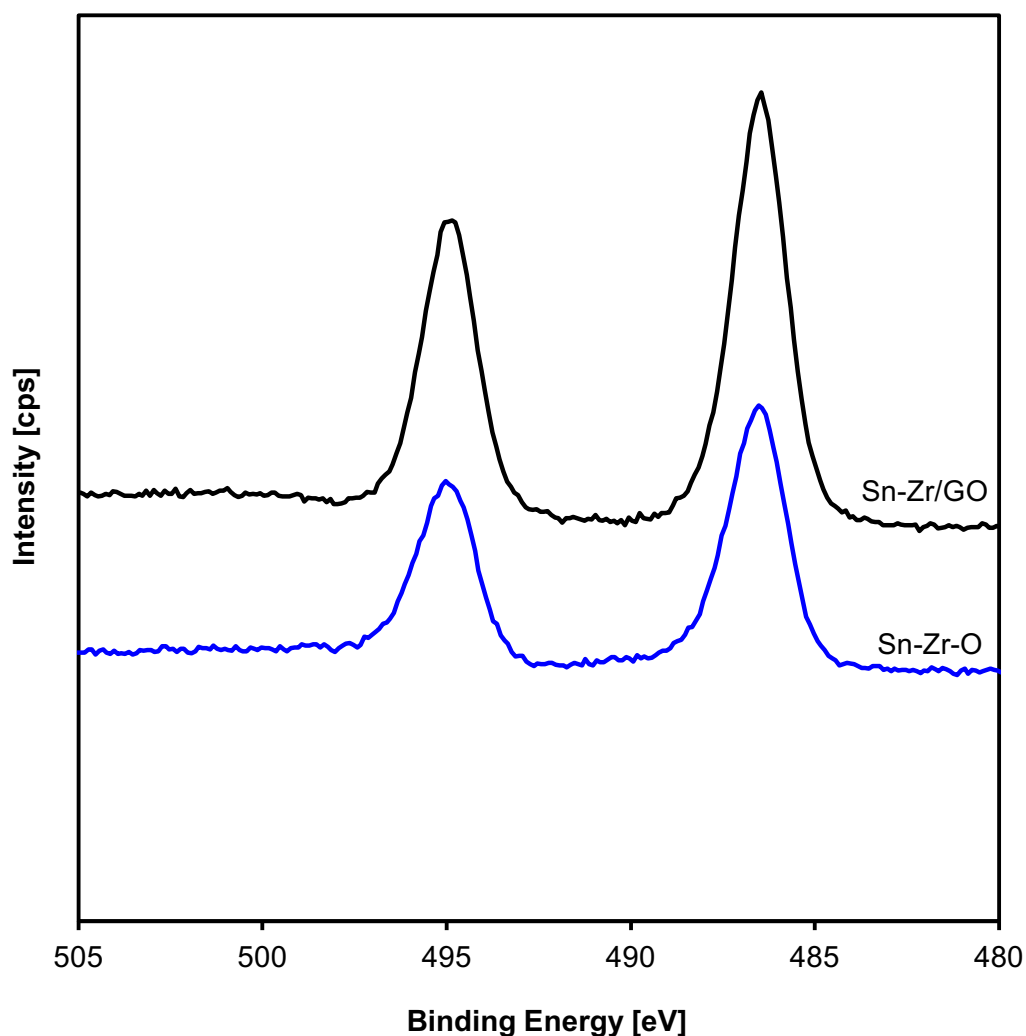


Figure 6.8. X-ray photoelectron spectroscopy (XPS) spectra showing the Sn (3d) region of tin doped zirconia (Zr–Sn–O) and tin doped zirconia graphene (Zr–Sn/GO) samples synthesised *via* continuous hydrothermal flow reactor.

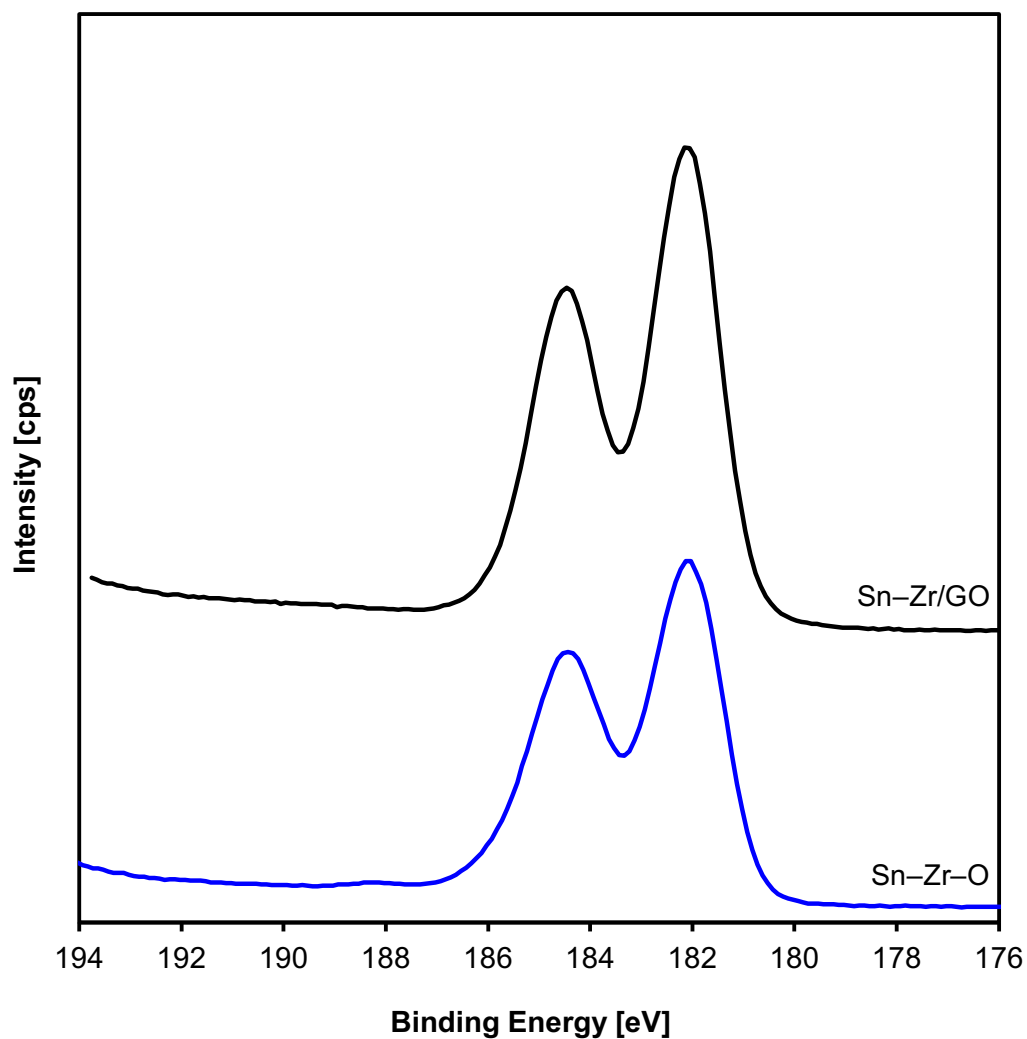


Figure 6.9. X-ray photoelectron spectroscopy (XPS) spectra showing the Zr (3d) region of tin doped zirconia (Zr-Sn-O) and tin doped zirconia graphene (Zr-Sn/GO) samples synthesised *via* continuous hydrothermal flow reactor.

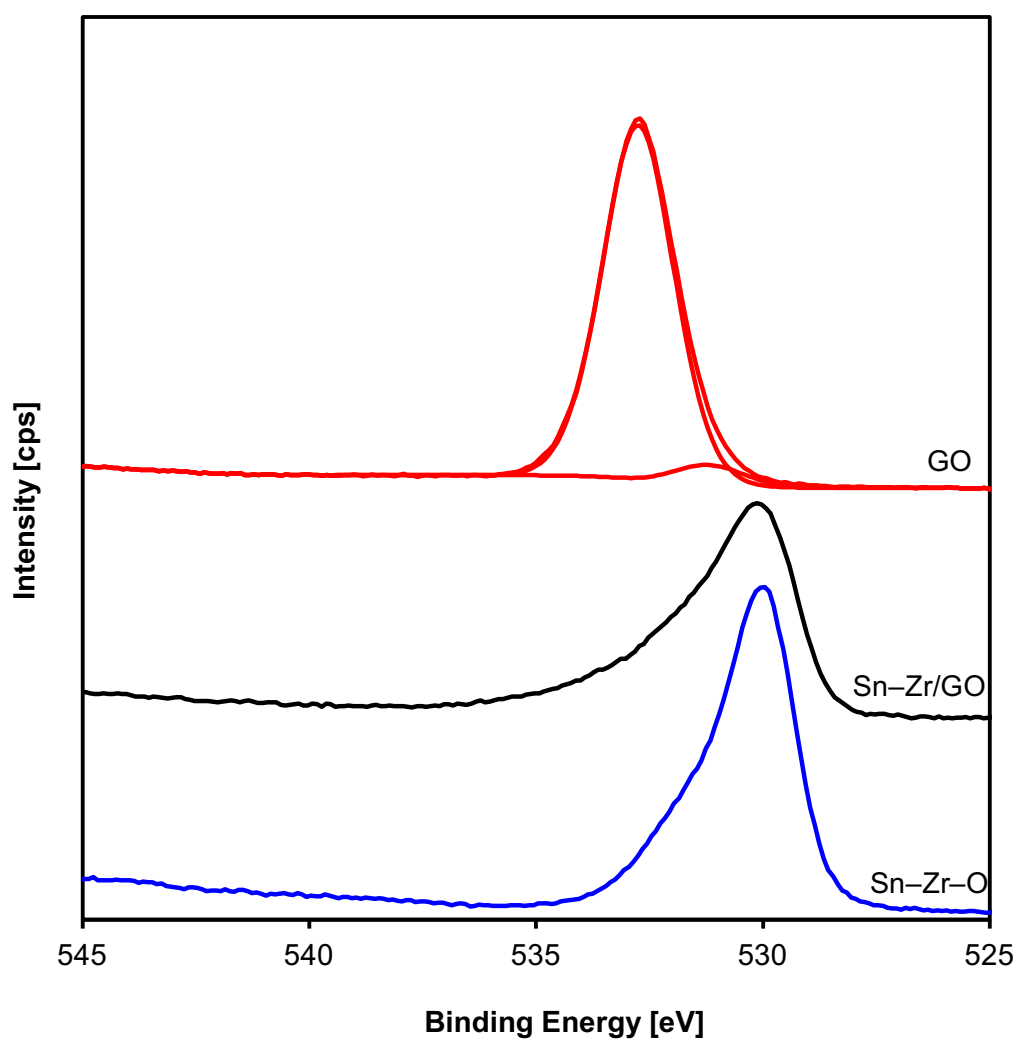


Figure 6.10. X-ray photoelectron spectroscopy (XPS) spectra showing the O (1s) region of graphene oxide (GO), tin doped zirconia (Zr–Sn–O) and tin doped zirconia graphene (Zr–Sn/GO) samples.

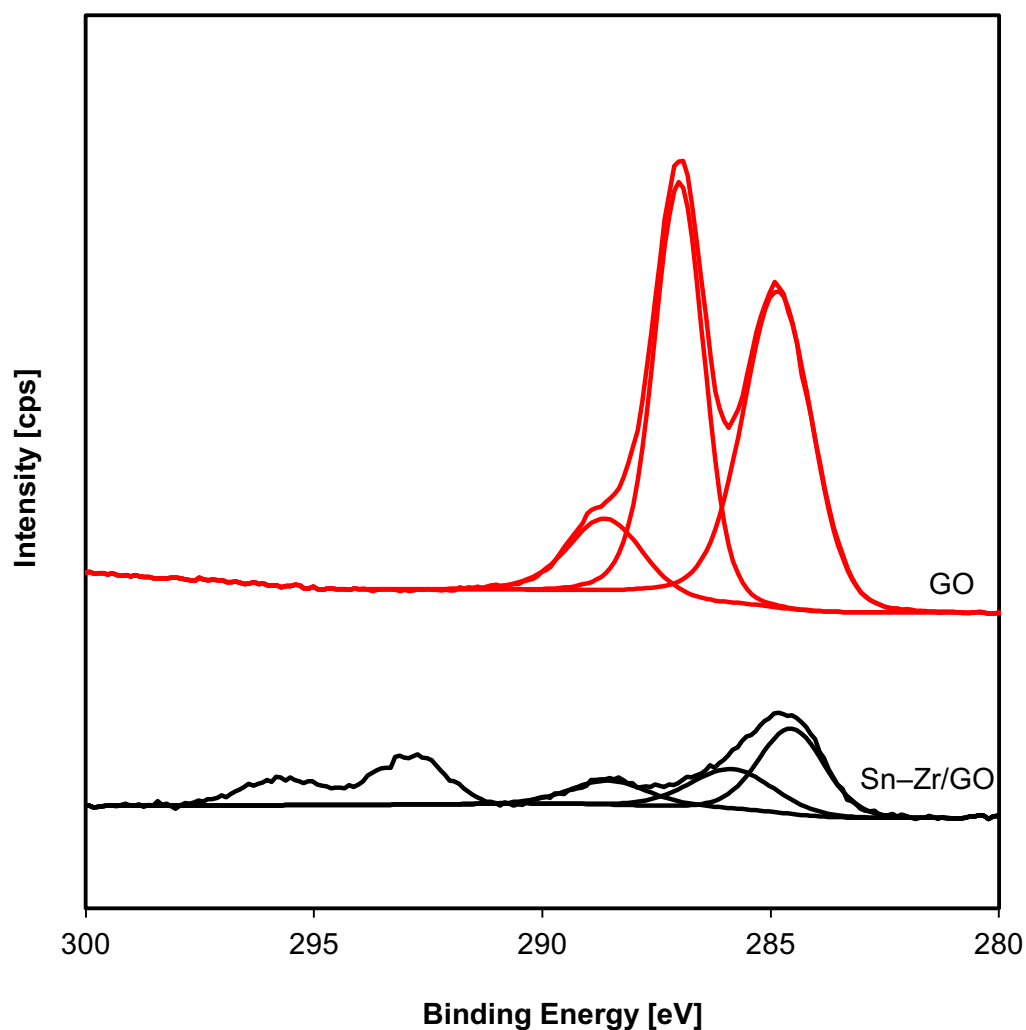


Figure 6.11. X-ray photoelectron spectroscopy (XPS) spectra showing the deconvoluted C(1s) region of graphene oxide (GO) and tin doped zirconia graphene (Zr–Sn/GO) samples.

### 6.3.2. Model Development

Response surface methodology (RSM) is a set of statistical and mathematical techniques that is used for modelling and predicting the direct factors and their interaction that affects the response in order to develop the optimum conditions (Das *et al.*, 2014). The influence of five variables, including, MeOH:PC molar ratio, catalyst loading, reaction temperature, reaction time and stirring speed on the responses (PC conversion and DMC yield) were evaluated using BBD method. Table 6.2 shows the experimental and predicted responses at various process conditions. A quadratic polynomial model was applied to build a

mathematical model in order to combine the relationship between the responses and the independent factors. This was also used to determine the optimum reaction conditions for a maximum PC conversion and DMC yield. The developed quadratic model for the PC conversion and DMC yield are given in Equation 6.3 and 6.4, respectively.

$$\begin{aligned}
 Y_1 = & -5933.96 - 5.71X_1 + 13.24X_2 + 27.19X_3 - 34.89X_4 + 0.037X_5 \\
 & + 0.87X_1X_2 + 0.06X_1X_3 + 0.65X_1X_4 - 0.001X_1X_5 + 0.1X_2X_3 \\
 & + 1.84X_2X_4 - 0.001X_2X_5 + 0.16X_3X_4 + 0.0002X_3X_5 + 1.3^{-17}X_4X_5 \\
 & - 1.15X_1^2 - 13.36X_2^2 - 0.03X_3^2 - 4.75X_4^2 - 0.0001X_5^2
 \end{aligned} \tag{6.3}$$

$$\begin{aligned}
 Y_2 = & -5580.42 - 8.82X_1 + 12.51X_2 + 25.71X_3 - 34.22X_4 + 0.043X_5 \\
 & + 0.8X_1X_2 + 0.06X_1X_3 + 0.71X_1X_4 - 0.0005X_1X_5 + 0.09X_2X_3 \\
 & + 1.74X_2X_4 + 0.0001X_2X_5 + 0.15X_3X_4 + 0.0004X_3X_5 + 0.0001X_4X_5 \\
 & - 1.05X_1^2 - 12.75X_2^2 - 0.03X_3^2 - 4.5X_4^2 - 0.0001X_5^2
 \end{aligned} \tag{6.4}$$

Where,  $X_1$ , MeOH: PC molar ratio;  $X_2$ , catalyst loading (w/w) (%);  $X_3$ , reaction temperature (K);  $X_4$ , reaction time (h);  $X_5$ , stirring rate (rpm);  $Y_1$ , PC conversion (%) and  $Y_2$  yield of DMC (%).

### 6.3.3. Statistical Analysis

Statistical analysis was performed on DMC yield since it is the most important response. The regression model for DMC yield (Equation 6.2) was tested by ANOVA as shown in Table 6.3. The coefficient  $R^2$  is used to define the fitness of the regression model. Adequate precision is defined to measure the signal to noise ratio where its value should be greater than 4 to ensure insufficient noise (Bo *et al*, 2014). The statistical analysis indicated that the developed model is highly significant due to high  $F$ -value (246.3) and very low  $p$ -value (<0.0001).  $R^2$  value was obtained as 0.995 and adequate precision of 42.2 which is extremely larger than the minimum required value of 4. The  $R^2_{pred}$  of 0.9798 is in reasonable agreement with the  $R^2_{adj}$  0.9909 since the difference is less than 0.02. The value of  $R^2_{adj}$  (0.995) shows a difference of 0.5% between the experimentally obtained and model predicted yield of DMC.

Based on the validity analysis of the factors it can be concluded that the independent variables ( $X_1, X_2, X_3, X_4$ ), the interaction variables ( $X_1X_2, X_1X_3, X_1X_4, X_2X_3, X_2X_4, X_3X_4$ ), the quadratic variables ( $X_1^2, X_2^2, X_3^2, X_4^2, X_5^2$ ) are significant factors for the synthesis of DMC. Stirring rate ( $X_5$ ) and its interactions with other variables are insignificant but its quadratic effect ( $X_5^2$ ) is significant. The insignificance of stirring speed ( $X_5$ ) and its interactions indicates a very low effect on the yield of DMC.

Table 6.3. ANOVA for response surface quadratic model analysis of variance.

Source	Sum of squares	Degrees of freedom	Mean square	F value	p-value
Model	25219.9	20	1261.0	246.3	< 0.0001 hs
A	3195.4	1	3195.4	624.2	< 0.0001 hs
B	729.9	1	729.9	142.6	< 0.0001 hs
C	6741.8	1	6741.8	1316.9	< 0.0001 hs
D	4429.9	1	4429.9	865.3	< 0.0001 hs
E	1.3	1	1.3	0.3	0.621 ns
AB	41.2	1	41.2	8.0	0.008 s
AC	255.2	1	255.2	49.8	< 0.0001 hs
AD	131.9	1	131.9	25.8	< 0.0001 hs
AE	0.2	1	0.2	0.0	0.843 ns
BC	35.4	1	35.4	6.9	0.0144 s
BD	48.6	1	48.6	9.5	0.0049 s
BE	0.0	1	0.0	0.0	0.988 ns
CD	344.5	1	344.5	67.3	< 0.0001 hs
CE	6.4	1	6.4	1.3	0.272 ns
DE	0.0	1	0.0	0.0	0.982 ns
A <sup>2</sup>	2489.5	1	2489.5	486.3	< 0.0001 hs
B <sup>2</sup>	1418.9	1	1418.9	277.2	< 0.0001 hs
C <sup>2</sup>	6734.7	1	6734.7	1315.5	< 0.0001 hs
D <sup>2</sup>	2828.6	1	2828.6	552.5	< 0.0001 hs
E <sup>2</sup>	23.8	1	23.8	4.6	0.04 s

A: MeOH:PC molar ratio; B: Catalyst loading [%][w/w]; C: Reaction temperature [K]; D: Reaction time [h]; E: Stirring speed [rpm]; s: significant; ns: not significant; hs: highly significant

## 6.3.4. Model Validation

The results obtained from the ANOVA test indicate that the developed model is suitable to describe the correlations and interactions of the different variables and the yield of DMC. Figure 6.12 shows the experimental vs predicted yield of DMC and illustrates that the model equation is in a good agreement with the experimental data indicating the suitability and accuracy of the model. BBD model was used to predict the effect of various design parameters on DMC synthesis from PC and MeOH. The results are presented in Figures 6.14–6.18. The results confirmed that BBD predicted the experimental results accurately at various reaction conditions.

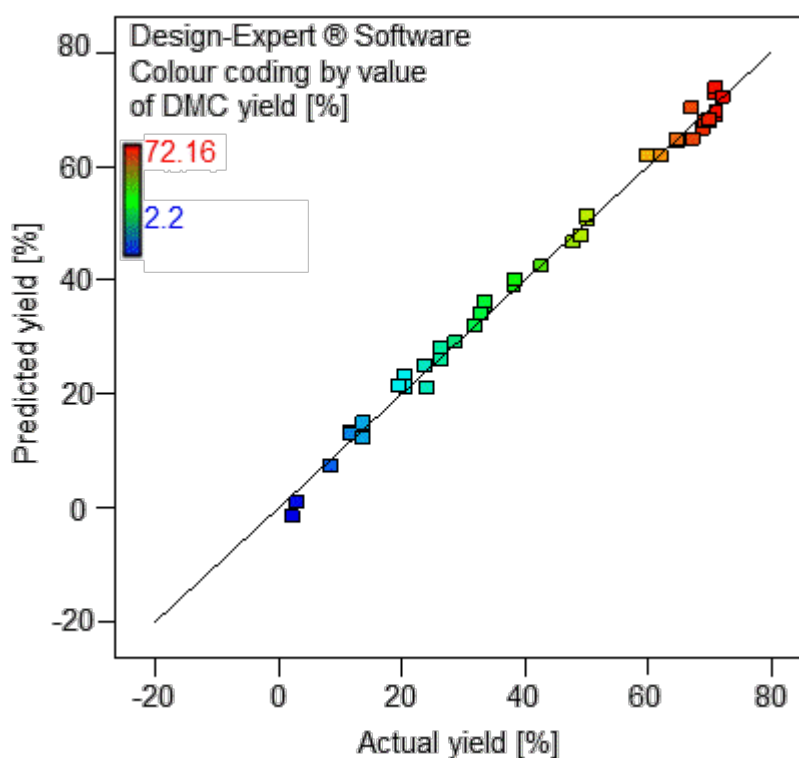


Figure 6.12. Model predicted DMC yield vs experimentally obtained DMC yield.

## 6.3.5. Batch Experimental Results

The reaction scheme for the synthesis of DMC *via* transesterification of propylene carbonate with methanol in the presence of a suitable catalyst is shown in Figure 5.3 (Chapter 5, section 5.3.1). A proposed reaction mechanism is shown in Figure 5.4 (Chapter 5, section 5.3.1). Transesterification reactions of PC and

MeOH were carried out at different reaction conditions in the presence of Zr–Sn/graphene nanocomposite as catalysts. OFAT analysis was carried out to study the effect of reactant molar ratio, catalyst loading, reaction temperature and time on the yield of DMC. Reusability studies were conducted to evaluate the long term stability of Zr–Sn/GO nanocomposite catalyst for the synthesis of DMC.

### 6.3.5.1. Effect of different catalysts

The performance of various different heterogeneous catalysts was assessed for the effective synthesis of DMC from the reaction of PC and MeOH as shown in Figure 6.13, where all experiments were conducted using 10:1 MeOH:PC molar ratio, 10% (w/w) catalyst loading, 433 K, 4 h at 300 rpm. Pure metal of tin doped zirconium oxide (Zr–Sn–O) and tin doped zirconia/ graphene nanocomposite (Zr–Sn/GO) were synthesised using CHFS method. Zr–Sn/GO samples were heat treated at 773 K and 973 K to enhance their catalytic activity and labelled as HT500 and HT700, respectively. When the pure metal oxide was used to catalyse the transesterification reaction, PC conversion and yield of DMC were 45.4% and 38.9%, respectively. Incorporating graphene oxide in the formation on inorganic nanocomposite resulted in high catalytic performance of Zr–Sn/GO, with a PC conversion of 76.2% and DMC yield of 72.1%. The difference in the catalytic performance between Zr–Sn–O and Zr–Sn/GO can be attributed to the phase composition and crystallinity of the catalyst alongside with the defects on the graphene sheet such as holes, acid/basic groups and presence of residual which can provide additional active catalytic sites (Adeleye *et al.*, 2014). HT500 and HT700 were tested at the same reaction condition as Zr–Sn/GO and showed insignificant increase in both PC conversion and yield of DMC ( $\pm 3\%$ ). From energy efficiency view point, the increase in DMC yield is insufficient to carry out the heat treatment. Therefore, on the basis of this study, Zr–Sn/GO was found to be the best catalyst for the synthesis of DMC and was used for further studies.

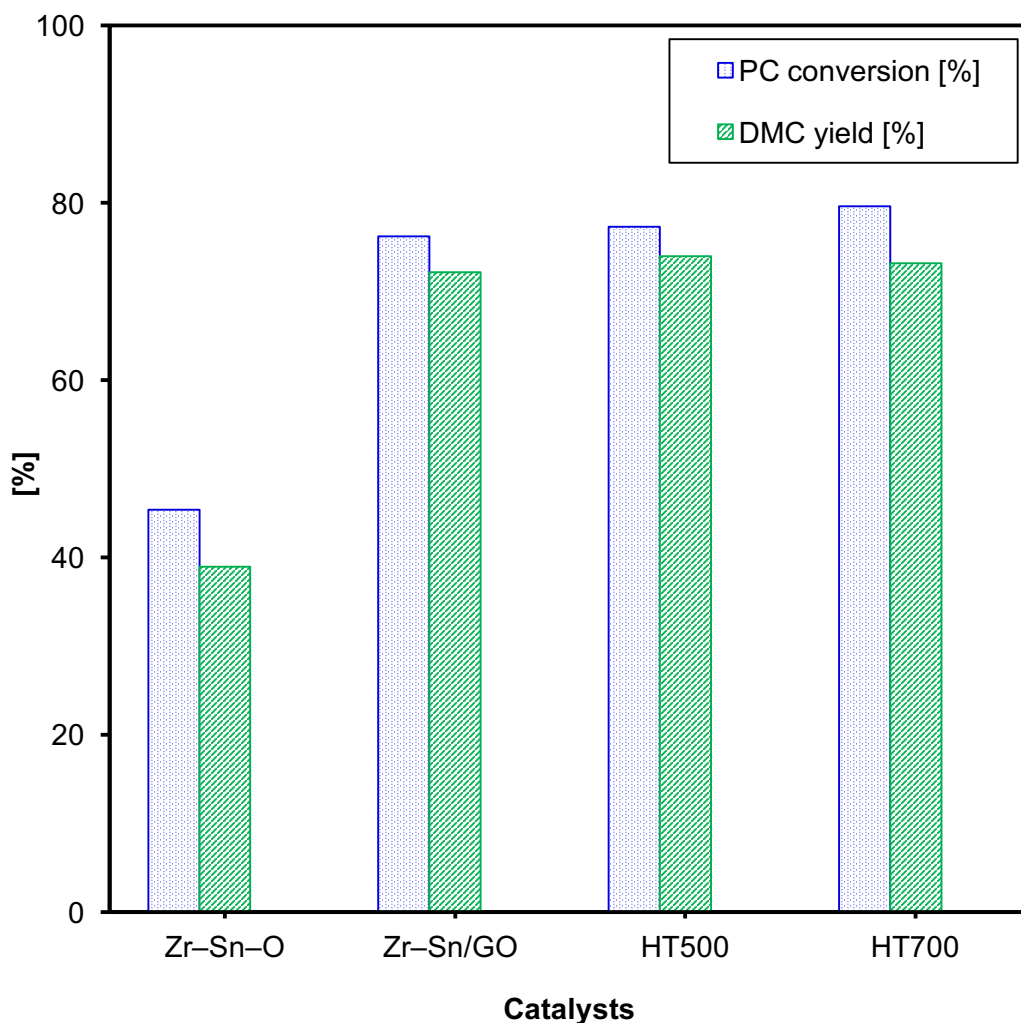


Figure 6.13. Effect of different heterogeneous catalysts for synthesis of DMC. Experimental conditions: MeOH:PC molar ratio, 10:1; catalyst loading, 2.5% (w/w); reaction temperature, 433 K; reaction time, 4 h and stirring speed, 300 rpm.

#### 6.3.5.2. Effect of reactant molar ratio

In order to evaluate the dependence of the catalytic performance on the reaction reactant molar ratio, a set of catalytic reactions was conducted in the presence of Zr-Sn/GO nanocomposite catalyst using various molar ratio of methanol to propylene carbonate (MeOH:PC). The experiments were carried out using 2.5% (w/w) catalyst loading at 433 K for 4 h. The first experiment was carried out (as part of the OFAT) at low MeOH:PC molar ratio (i.e., 2:1) where a PC conversion of ~17.2% and ~13.2% yield of DMC were observed. OFAT analysis showed that the reactant molar ratio almost exhibits a linear relationship with catalytic

performance of the transesterification reaction as ~76.2% conversion of PC and ~72.2% yield of DMC were obtained for higher MeOH:PC molar ratio (i.e., 10:1). The significant increase in the yield of DMC with an increase in the MeOH:PC molar ratio can be attributed to the formation of DMC–MeOH azeotrope due to the presence of excess MeOH which shifts the equilibrium towards the product side and enhances the synthesis of DMC (Murugan and Bajaj, 2011). Figure 6.14 shows the effect of increasing MeOH:PC ratio within the range of 6:1 to 14:1 on the PC conversion and yield of DMC.

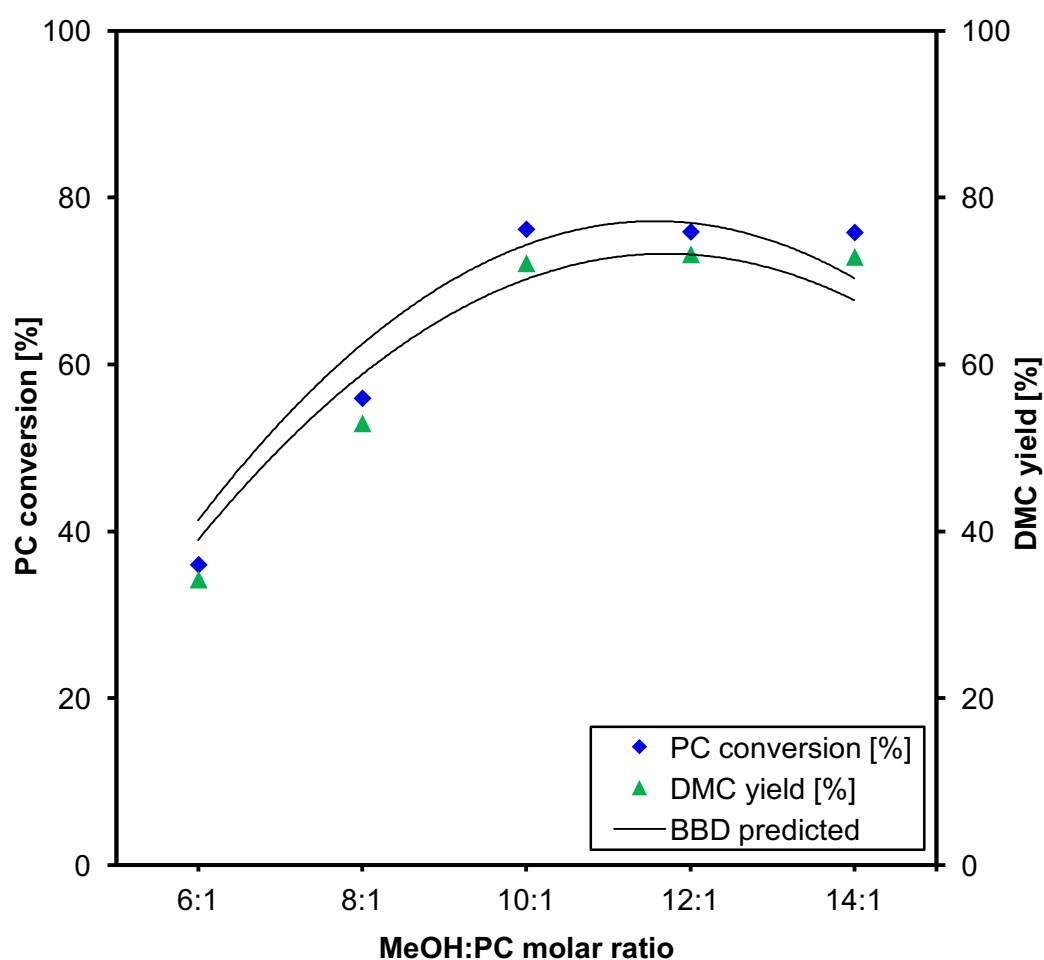


Figure 6.14. Effect of different reactant molar ratio (i.e. MeOH:PC) on the PC conversion and yield of DMC. Experimental conditions: catalyst, Zr–Sn/GO; catalyst loading, 2.5% (w/w); reaction temperature, 433 K; reaction time, 4 h and stirring speed, 300 rpm.

It is evident that when the reactant molar ratio (MeOH:PC) increased to 12:1 and 14:1 (Figure 6.14), there was insignificant change to the yield of DMC when compared to MeOH:PC molar ratio of 10:1. On the basis of this study, it can be concluded that the optimum MeOH:PC ratio is 10:1 for the catalysed system. This is within the range reported in the literature for the transesterification of PC with MeOH by other investigators (Unnikrishnan *et al.*, 2012).

### 6.3.5.3. Effect of catalyst loading

In this study, catalyst loading is defined as the percentage ratio of the mass of the catalyst to the mass of the limiting reactant (PC). The synthesis of DMC *via* the transesterification of PC and MeOH was studied using different amounts of Zr–Sn/GO nanocomposite catalyst at 433 K for 4 h. The results are presented in Figure 6.15. It can be seen that an increase in the catalyst loading increases the PC conversion and yield of DMC. For reactions carried out using 1.0% (w/w) catalyst loading, PC conversion and DMC yield were ~43.8% and ~41.6%, respectively. Further increase in the conversion of PC (~76.2%) and yield of DMC (~72.2) were achieved at 2.5% (w/w) catalyst loading. When the catalyst loading was further increased to 3% (w/w), PC conversion of ~76.5% and DMC yield of ~72.3% were achieved. In view of the experimental error of  $\pm 3\%$ , it seems that the number of active sites required for PC and MeOH to react and produce DMC was sufficient at 2.5% (w/w) catalyst loading. Hence it was not necessary to increase the catalyst loading beyond 2.5% (w/w). Based on this study 2.5% (w/w) of Zr–Sn/GO nanocomposite was chosen as the optimum catalyst loading and was used in all subsequent experiments.

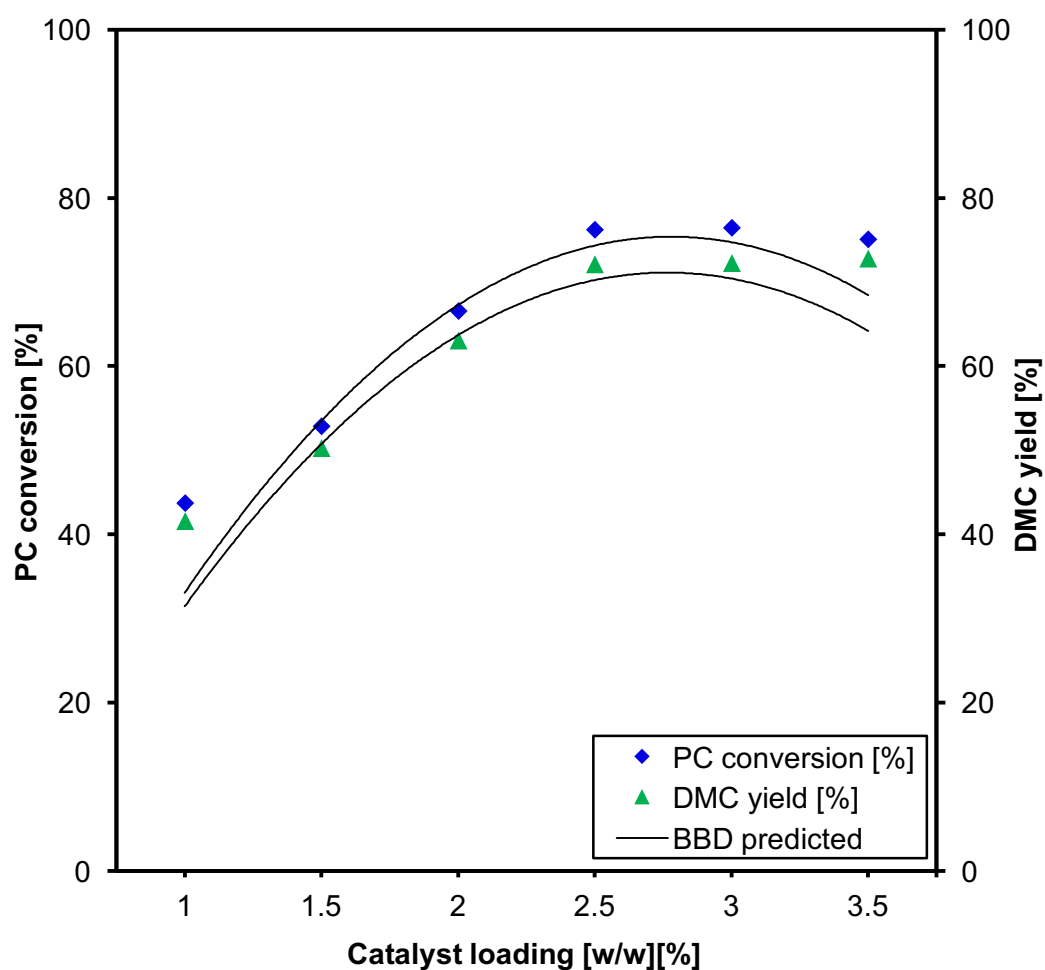


Figure 6.15. Effect of varying catalyst loading on the PC conversion and yield of DMC. Experimental conditions: catalyst, Sn–Zr/GO; MeOH:PC molar ratio, 10:1; reaction temperature, 433 K; reaction time, 4 h and stirring speed, 300 rpm.

#### 6.3.5.4. Effect of reaction temperature

A series of transesterification reaction of PC and MeOH were conducted within a temperature range of 403 K and 463 K to thoroughly investigate the influence of reaction temperature on the synthesis of DMC. The experiments were carried out using MeOH:PC ratio is 10:1 in the presence of 2.5% (w/w) Zr–Sn/GO nanocomposite catalyst for 4 h. Figure 6.16 shows the effect of reaction temperature on the conversion of PC and the yield of DMC. It can be seen from Figure 6.16 that the reaction temperature has a pronounced effect on the efficiency of DMC synthesis.

As the reaction temperature increased from 413 K to 433 K, there was a significant increase in the PC conversion and yield of DMC. At a reaction temperature of 433 K, the conversion of PC and yield of DMC were ~76.2% and ~72.2%, respectively. At reaction temperatures higher than 433 K, a linear decrease in both PC conversion and yield of DMC was observed. This decrease is possibly due to the equilibrium nature of the transesterification reaction where higher reaction temperatures can shift the equilibrium to the reactant side and results in a reduction to the yield of DMC (Wei *et al.*, 2003). Therefore, it can be concluded that 433 K is the optimum reaction temperature and all further OFAT experiments for the synthesis of DMC were performed at a reaction temperature of 433 K. The optimum reaction temperature is within the range of published literature (Wei *et al.*, 2003; Wang *et al.*, 2006b).

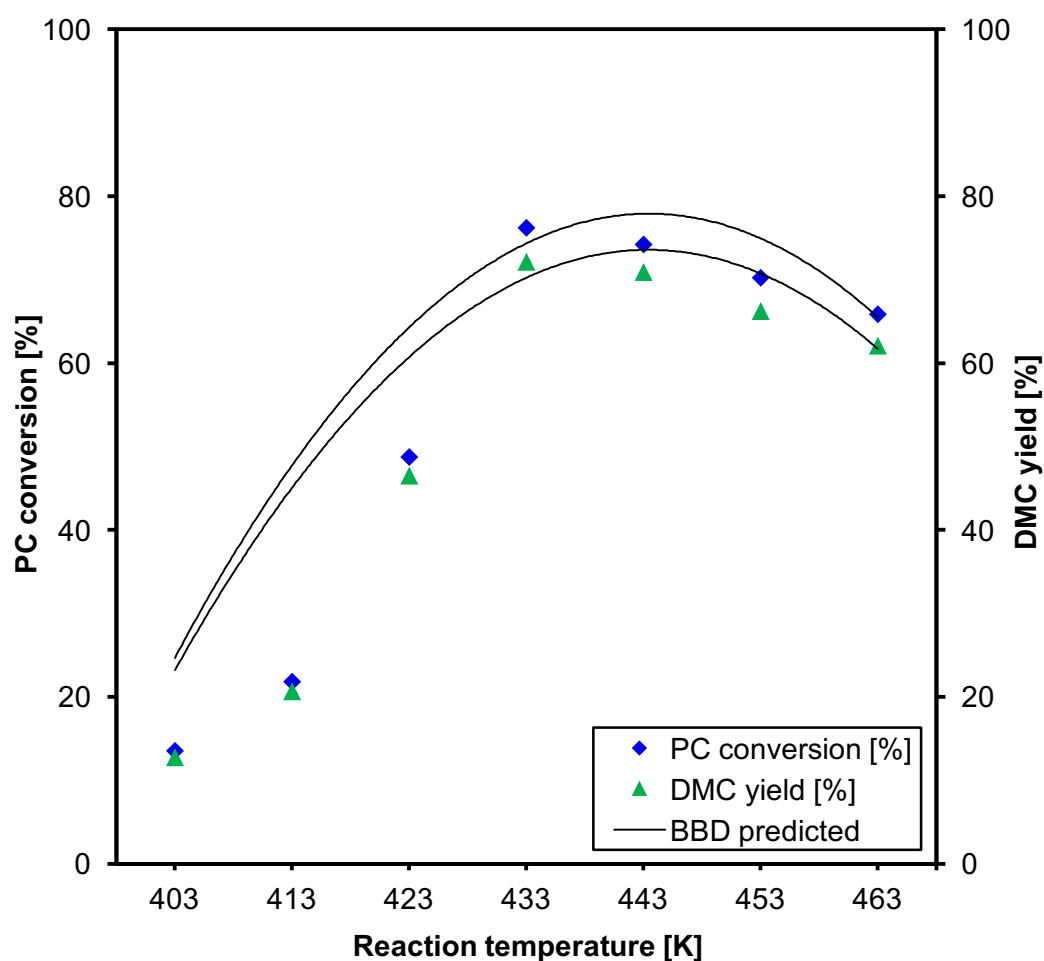


Figure 6.16. Effect of reaction temperature on the PC conversion and yield of DMC. Experimental conditions: catalyst, Sn–Zr/GO; MeOH:PC molar ratio, 10:1; catalyst loading, 2.5% (w/w); reaction time, 4 h and stirring speed, 300 rpm.

#### 6.3.5.5. Effect of reaction time

A set of transesterification reactions were carried out using the best performed catalyst (Zr–Sn/GO) for different time duration (2 h–6 h) to evaluate the influence of the reaction time on the DMC synthesis. The results are presented in Figure 6.17. The reaction proceeds at low reaction time (2 h) and results in a PC conversion of ~30.1% and ~28.8% yield of DMC. An increase in the reaction time significantly increases the conversion of PC to ~76.2% and the yield of DMC to ~72.2%. A similar PC conversion and DMC yield were obtained when the reaction was carried out for 6 h. As the reaction time increased beyond 6 h, PC conversion and DMC yield begin to decline gradually indicating that equilibrium is

reached at 4–6 h. This study indicates that 4 h reaction time is sufficient to reach equilibrium and to achieve the maximum DMC yield and therefore, 4 h was considered as the optimum reaction time for the transesterification of PC.

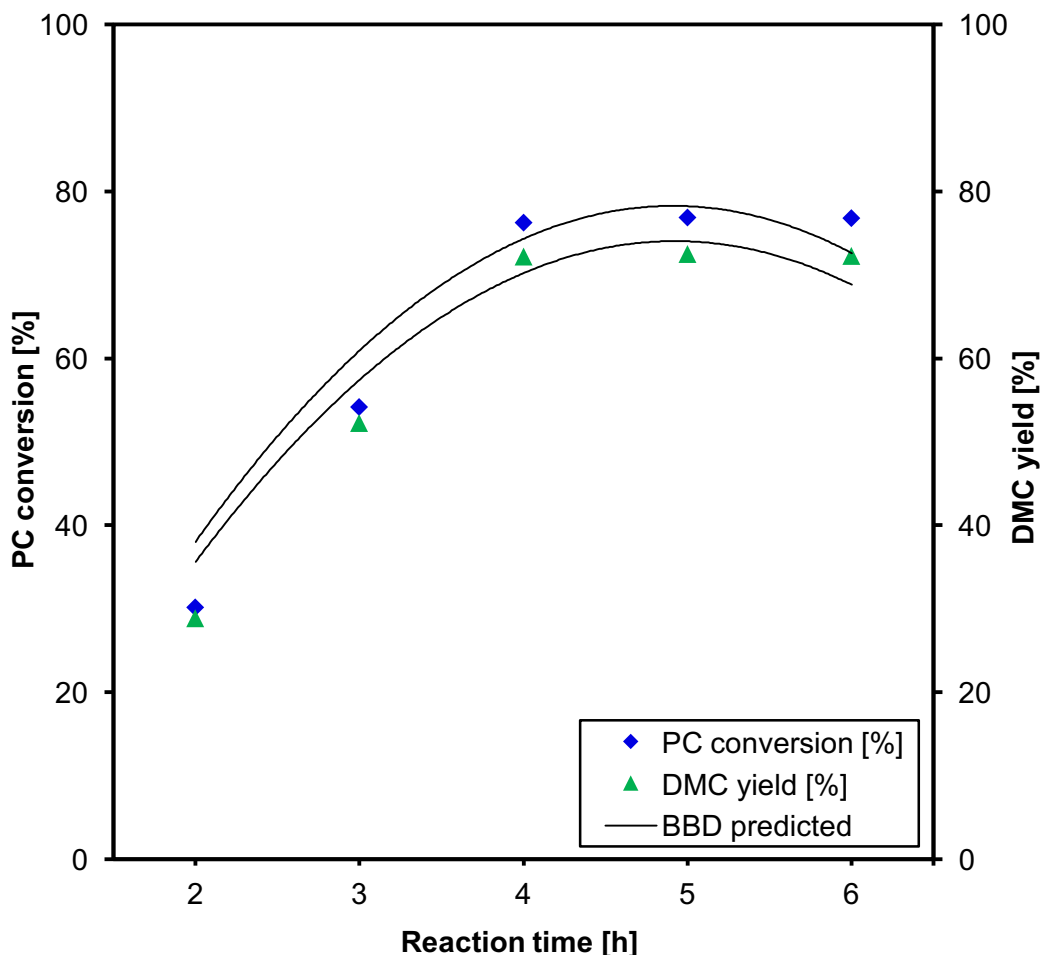


Figure 6.17. Effect of reaction time on the PC conversion and yield of DMC. Experimental conditions: catalyst, Sn–Zr/GO; MeOH:PC molar ratio, 10:1; catalyst loading, 2.5% (w/w); reaction temperature, 433 K and stirring speed, 300 rpm.

#### 6.3.5.6. Effect of mass transfer in heterogeneous catalytic process

The effect of mass transfer resistance on the transesterification reaction of PC and MeOH using Zr–Sn/GO nanocomposite catalyst to produce DMC was investigated at 433 K reaction temperature for 4 h. The reaction of PC and MeOH was conducted at different stirring speed of 300–500 rpm in an autoclave reactor

as shown in Figure 6.18. It was observed that there was no significant change in the conversion of PC and yield of DMC when the stirring speed increased from 300 to 500 rpm. On the other hand, Zr–Sn/GO particles are fairly small, uniform and porous (particle size: 5.18 nm), which eliminates internal mass transfer resistance (Adeleye *et al.*, 2014). These results are in good agreement with the BBD predicted results at various stirring speeds. As external mass transfer resistance is absent, it could be concluded that a good homogenous distribution of Zr–Sn/GO nanocomposite particles was achieved at a low stirring speed of 300 rpm.

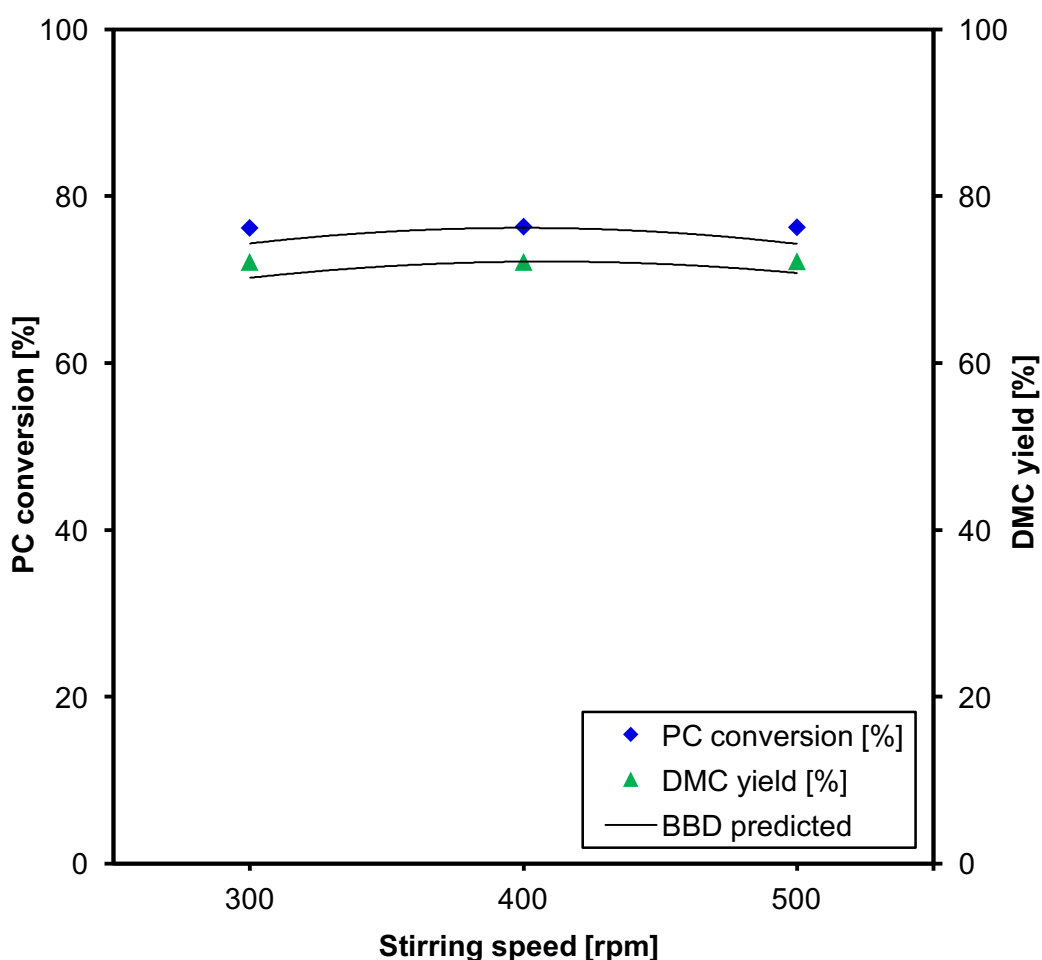


Figure 6.18. Effect of different stirring speed on the PC conversion and yield of DMC. Experimental conditions: catalyst, Sn–Zr/GO; MeOH:PC molar ratio, 10:1; catalyst loading, 5% (w/w); reaction temperature, 443 K and reaction time, 6 h.

#### 6.3.5.7. Catalyst reusability studies

Catalyst reusability studies were carried out to investigate the long term stability of Zr–Sn/GO catalyst for the synthesis of DMC. The experiments were conducted in an autoclave reactor using a 2.5% (w/w) fresh catalyst, MeOH:PC 10:1 molar ratio at a reaction temperature of 433 K and reaction time of 4 h. This was plotted as Run 1 as shown in Figure 6.19. After the first reaction, the catalyst was recovered by filtration from the reaction mixture, washed with acetone and dried in an oven at 333 K for 12 h. The catalyst was then reused for Run 2 under the same optimum reaction conditions (see Figure 6.19). The same procedure was repeated for subsequent Runs (Run 3–Run 6). From Figure 6.19, it can be seen that there is no appreciable change in PC conversion and yield of DMC after 6 Runs. This indicates that Zr–Sn/GO catalyst exhibits excellent reusability and stability for the synthesis of DMC. It is evident that Zr–Sn/GO nanocomposite catalyst can be easily recovered and reused without any significant loss in its catalytic performance.

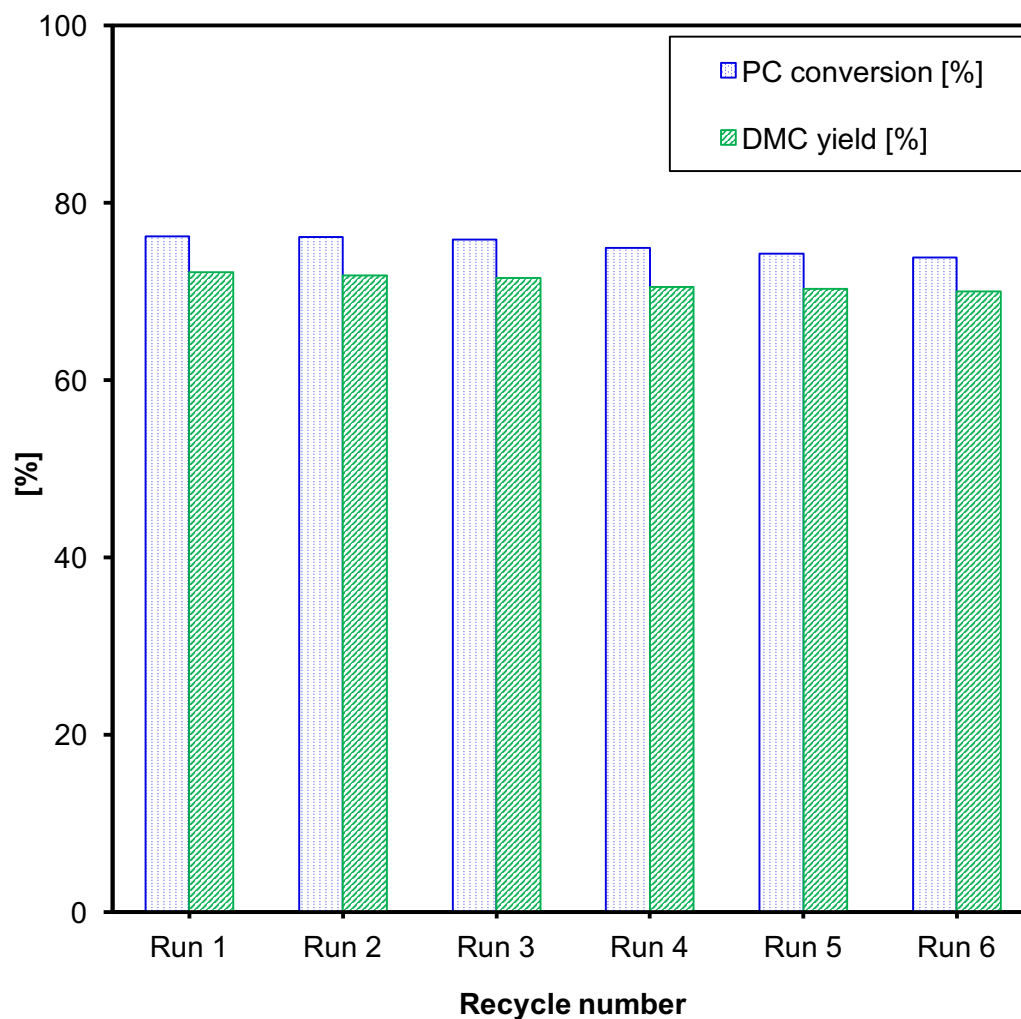


Figure 6.19. Effect of catalyst reusability on the PC conversion and yield of DMC. Experimental conditions: catalyst, Sn–Zr/GO; MeOH:PC molar ratio, 10:1; catalyst loading, 2.5% (w/w); reaction temperature, 433 K; reaction time, 4 h and stirring speed, 300 rpm.

### 6.3.6. Optimisation of DMC synthesis

The aim of the optimisation is to find the reaction conditions that can maximise PC conversion and yield of DMC even further. Batch studies using OFAT analysis showed that 10:1 MeOH:PC molar ratio, 433 K, 4 h and 300 rpm using 2.5% (w/w) Zr–Sn/GO achieves a PC conversion of 76.2% and DMC yield of 72.1%. Evaluating and including the interactions between the various reaction parameters can lead to higher PC conversion and DMC yield. Therefore, applying response surface methodology optimisation using BBD method can be used to

understand the interactions between various reaction parameters and hence to derive maximum responses (i.e., PC conversion and DMC yield). The optimisation process was developed using Design Expert 9.0.5 software. Consequently, the desired target was defined to maximise the yield of DMC and PC conversion with minimising the operational condition levels used in the regression model. The software combines the individual desirability into a single number, and then searches to optimise this function based on the response target. Accordingly, the optimum working conditions were determined.

The maximum predicted responses of 85.1% for PC conversion and 81% DMC yield were achieved at 12.33:1 MeOH: PC molar ratio, 2.9% (w/w) catalyst loading, 446.7 K, 4.08 h and 300 rpm using the BBD model. An additional experiment was then performed to confirm the optimised predicted conditions, where a PC conversion of 82.4% and DMC yield of 78.2% were obtained (within  $\pm 3\%$  experimental error). This demonstrates that the process optimisation using BBD method was accurate.

RSM is also used to determine the interaction between independent variables and the responses which will show the effect of factors interaction on the desired response. Figure 6.20 represents the 3-D graphical representation of the regression model. It shows the effect of MeOH:PC molar ratio and the catalyst loading at fixed reaction temperature, reaction time and stirring speed at their optimum conditions. It is clear that the yield of DMC increases with an increase in MeOH:PC molar ratio and catalyst loading. Maximum yield was observed at a reaction temperature of 446.7 K and catalyst loading of 2.9% (w/w), which indicates the accuracy of the optimisation process that was established. The trend is reversed and the yield of DMC decreases to 20% as MeOH:PC molar ratio and catalyst loading increase beyond 12.3:1 and 2.9% (w/w), respectively.

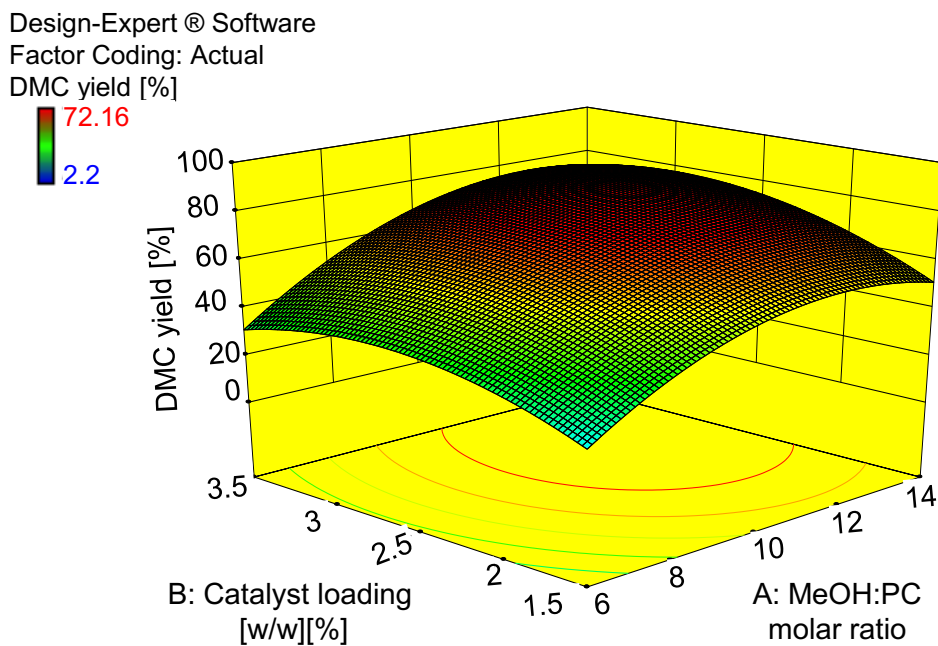


Figure 6.20. Response surface graph: Effect of MeOH:PC molar ratio and catalyst loading (w/w) on DMC yield.

Figure 6.21 shows the effect of varying the stirring speed and reaction temperature at fixed MeOH:PC molar ratio, catalyst loading and reaction time at their optimum conditions. It can be seen that increasing the reaction temperature increases the yield of DMC, however, increasing the stirring speed shows no effect on the yield of DMC. This indicates the insignificance of stirring speed for the synthesis of DMC as concluded by ANOVA. Maximum DMC yield (81%) was observed at a reaction temperature of 446.7 K (Figure 6.21). A decrease in the yield of DMC to 22% is obtained as the temperature increases beyond 446.7 K.

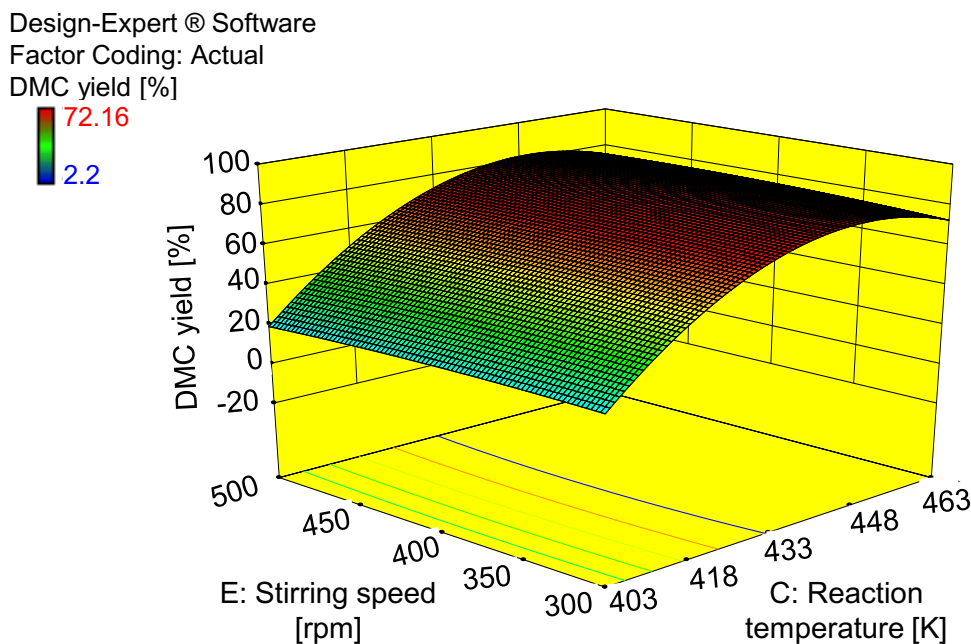


Figure 6.21. Response surface graph: Effect of reaction temperature and stirring speed on DMC yield.

The interaction between reaction time and catalyst loading was studied at the optimum MeOH:PC molar ratio, reaction temperature and stirring speed as shown in Figure 6.22. It is evident that an increase in the reaction time and catalyst loading increases the yield of DMC. DMC yield of 81% is observed at 4.08 h reaction time and 2.9% (w/w) catalyst loading, which agrees with the results obtained from optimisation process and further verifies its accuracy. Figure 6.22 also shows that long reaction time (i.e. higher than 4.08 h) and larger amounts of catalyst (i.e. more than 2.9 % (w/w)) reduces the yield of DMC to as low as 9%.

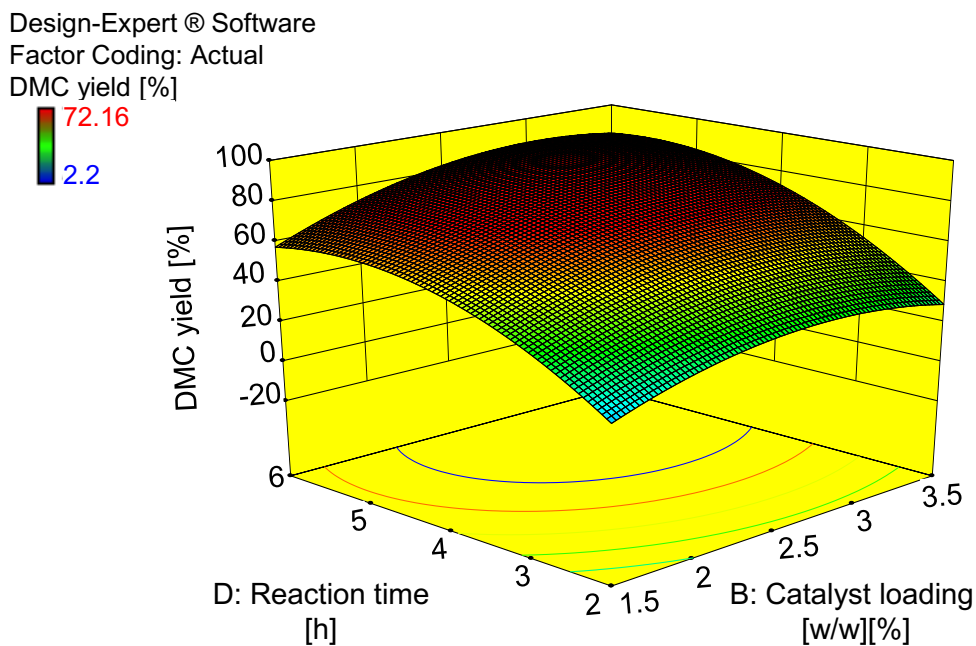


Figure 6.22. Response surface graph: Effect of catalyst loading (w/w) and reaction time on DMC yield.

#### 6.4. CONCLUSIONS

The preparation of graphene by continuous hydrothermal flow synthesis route allowed simultaneously and homogeneously growing and dispersing metal oxide nanoparticles into graphene substrate in a single step. This single step synthetic approach not only enables control over oxidation state of graphene, but also offers an optimal route for homogeneously producing and depositing highly crystalline nanostructures into graphene oxide. The synthesised Zr–Sn/GO nanocomposite was successfully applied for the synthesis of DMC from PC and MeOH in the absence of a solvent. Tin doped zirconia/graphene nanocomposite catalyst was found to be the best performed catalyst for DMC synthesis as compared to other heterogeneous catalysts.

RSM using BBD method was conducted to study and optimise the interactive effects of five process variables: MeOH:PC molar ratio, catalyst loading, reaction temperature, reaction time and stirring speed on the yield of DMC. A modified quadratic model equation was concluded by analysing the experimental data. The model concluded the highest PC conversion and DMC yield of ~85.1% and ~81%, respectively were obtained at an optimum reaction condition of

12.3:1 MeOH: PC molar ratio, 446.7 K, 4.08 h and 300 rpm using 2.9% (w/w) of Zr–Sn/GO. Experimental results at optimum predicted reaction conditions verified the model predicted response where 82.4% PC conversion and 78.2% yield of DMC were obtained. Statistical analysis of the data showed that the MeOH:PC molar ratio, catalyst loading, reaction temperature and time are highly significant variables while stirring speed is an insignificant variable for the synthesis of DMC. Catalyst reusability studies confirmed very high stability of Zr–Sn/GO catalyst and it could be reused several times without any significant reduction in its catalytic performance.

# **Chapter 7**

## **Conclusions and Recommendations for Future Works**

## 7. CONCLUSIONS AND RECOMMENDATIONS FOR FUTURE WORKS

### 7.1. CONCLUSIONS

In this work, the direct synthesis of dimethyl carbonate (DMC) from methanol (MeOH) and carbon dioxide (CO<sub>2</sub>) has been studied. The transesterification of propylene carbonate (PC) and MeOH have also been studied as an alternative route for the synthesis of DMC. Batch studies for both routes have been conducted in a high pressure reactor to evaluate the effect of various reaction conditions on the synthesis of DMC. A detailed literature review about DMC synthesis has been presented to provide a broad overview on the different routes and main types of catalysts employed for the synthesis of DMC.

Various commercial and novel metal oxide and mixed metal oxides have been extensively studied as heterogeneous catalysts for the synthesis of DMC. Graphene oxide represents an exciting and new class of functional materials due to its unique physical, chemical and mechanical properties including a very high surface area and easy surface modifications, which allow preparation of nanocomposite materials with novel properties and characteristics. Therefore, in this work, a green, rapid and continuous hydrothermal flow synthesis (CHFS) route has been used to produce highly stable and active novel and innovative graphene-inorganic nanocomposites catalysts which were assessed for the synthesis of DMC.

Detailed catalyst characterisation have been performed using various analytical techniques such as scanning electron microscopy (SEM), transmission electron microscopy (TEM), powder X-ray diffraction (XRD), X-ray photoelectron spectroscopy (XPS), Raman spectroscopy and Brunauer-Emmett-Teller (BET) surface area measurement in order to investigate the effect of the catalyst morphology, particle size, surface area and composition on the catalytic performance of the catalyst.

Ceria-zirconia oxide/graphene (Ce–Zr/GO) nanocomposite catalyst synthesised using CHFS reactor and heat-treated at 973 K (HTR700) exhibited BET surface area of 106 m<sup>2</sup>g<sup>-1</sup> and particle size of 5.8 nm. HTR700 showed the highest catalytic activity for the synthesis of DMC from the addition reaction of MeOH and CO<sub>2</sub>. The experimental results revealed that the use of a dehydrating agent

(TMM) to remove residual water produced during the reaction enhances the yield of DMC. The highest MeOH conversion of 58% and DMC yield of 33% were obtained at optimum reaction conditions of 373 K, 275 bar, 1:1(w/w) TMM:MeOH and 16 h using 10% (w/w) Ce–Zr/GO nanocomposite catalyst.

Tin doped zirconia graphene oxide (Zr–Sn/GO) nanocomposite catalyst synthesised using a CHFS reactor exhibited BET surface area of  $83.32 \text{ m}^2\text{g}^{-1}$  and particle size of 5.18 nm. Zr–Sn/GO showed the highest catalytic activity for the synthesis of DMC *via* the transesterification of PC with MeOH. Response surface methodology (RSM) using Box-Behnken design (BBD) method was conducted to study and optimise the interactive effects of five process variables: MeOH:PC molar ratio, catalyst loading, reaction temperature, reaction time and stirring speed on the yield of DMC. A modified quadratic model equation was concluded by analysing the experimental data. The model predicted the highest PC conversion and DMC yield of ~85.1% and ~81%, respectively at an optimum reaction condition of 12.3:1 MeOH: PC molar ratio, 446.7 K, 4.08 h and 300 rpm using 2.9% (w/w) Zr–Sn/GO. Experimental results at optimum predicted reaction conditions verified the model predicted response where 82.4% PC conversion and 78.2% yield of DMC were obtained. Statistical analysis of the data showed that the MeOH:PC molar ratio, catalyst loading, reaction temperature and time are highly significant variables, whilst stirring speed is an insignificant variable for the synthesis of DMC.

The efficiency and long term stability of HTR700 and Sn–Zr/GO catalysts have been assessed for the synthesis of DMC in a high pressure reactor. A series of experiments were carried out by reusing the recycled catalyst several times. The catalysts could be easily separated from the reaction mixture using simple filtration. The recycled catalyst showed no significant reduction in their catalytic performance after several runs.

### **7.2. RECOMMENDATION FOR FUTURE WORK**

#### **7.2.1. Development of New Innovative Catalysts with Higher Catalytic Performance**

Heterogeneous catalysts are preferred in the process industry over homogeneous catalysts because of its advantages over the latter. These

advantages include the ease of catalyst separation from the reaction mixture, which is more economically viable due to the elimination of complex separation processes. Therefore, the development of new innovative heterogeneous catalysts that possess high efficiency and selectivity for the synthesis of DMC and various other organic carbonates is highly desirable. The performance of various mixed metal oxides with a variation in the percentage composition of the catalyst components is required to determine the optimum percentage ratio of each component in order to optimise the catalytic performance. New approaches for the use and application of advanced materials as suitable catalyst supports such as activated carbon and carbon nanotubes could be used in order to increase the surface area of the catalyst and enhance its performance.

### 7.2.2. Extensive Catalyst Characterisation

The performance of the heterogeneous catalysts can be partly attributed to the effect of the bifunctional action of acidic and basic sites of the catalysts. The acidic-basic sites of metal oxide/mixed metal oxides derived from the formation of metal-oxygen bonds provide a platform for the activation of CO<sub>2</sub> and the production of DMC. Therefore, it is vital to investigate the redox properties of heterogeneous catalysts to identify appropriate opportunities for improving the design of new catalysts. Temperature-programmed reduction (TPR) and NH<sub>3</sub> temperature-programmed desorption (TPD) could be used as powerful methods to determine the redox properties and the surface acidity of the heterogeneous catalysts. The influence of incorporating various metals together to prepare mixed metal oxide catalysts, the composition of various components of the catalysts and the use of different catalyst supports on the redox properties and acidic-basic surface properties of the catalysts can aid in the design of catalysts with higher catalytic activity.

### 7.2.3. Utilisation of Waste CO<sub>2</sub> for the Synthesis of DMC

The utilisation of waste CO<sub>2</sub> captured from industries and power plants in the synthesis of valuable products is a challenging task for researchers due to the low concentration of CO<sub>2</sub>. Heterogeneous catalysts have low tolerance for the impurities in flue gas such as water vapour, sulphur dioxide and nitrogen dioxide. Using real carbon dioxide emissions to synthesise organic carbonates such as DMC offers technological advancement towards the reduction of CO<sub>2</sub> emission

levels along with economical benefits such as reducing costs associated with carbon capture, storage and purification. Hence, various heterogeneous catalysts can be evaluated for the synthesis of DMC using simulated flue gas.

### 7.2.4. Investigating Different Routes for the Synthesis of DMC

Different routes for the synthesis of DMC could be evaluated using HTR700 and Zr–Sn/GO nanocomposite catalysts. Batch studies for the synthesis of DMC from other alcohols such as ethanol or cyclic carbonates such as ethylene carbonate and CO<sub>2</sub> could be studied and compared to the current process. One pot synthesis of DMC from CO<sub>2</sub>, alcohols and epoxides could be investigated using HTR700 and Zr–Sn/GO nanocomposite catalysts. Modifications to the catalyst (i.e., the incorporation of different metal oxides, the optimum percentage ratio of each component of the catalyst and catalyst heat treatment) could be carried out to enhance the catalytic performance of the proposed catalyst.

### 7.2.5. Syntheses of Other Organic Carbonates

The syntheses of industrially important organic carbonates such as ethylene carbonate, styrene carbonate, diphenyl carbonate, diethyl carbonate, butylene carbonate, 4-vinyl-1-cyclohexene carbonate and (chloromethyl)ethylene carbonate using CO<sub>2</sub> as a raw material could be investigated using HTR700 and Sn–Zr/GO nanocomposite catalysts.

### 7.2.6. Continuous Flow Synthesis of DMC

HTR700 has shown a significant catalytic performance for the direct synthesis from MeOH and CO<sub>2</sub> using a high pressure reactor. Similarly Zr–Sn/GO nanocomposite catalyst has shown a remarkable performance for the synthesis of DMC *via* the transesterification of PC using an autoclave reactor. It would be important to investigate the catalytic performance of both catalysts in a high pressure continuous flow reactor to compare the efficiency of catalysts for the continuous synthesis of DMC.

### 7.2.7. Aspen HYSYS Simulation

Aspen HYSYS can be used to simulate the two process routes for the synthesis of DMC proposed in this research work. The reaction equilibrium for each reaction pathway could be calculated using Aspen Plus software where all

necessary model parameters are available. Mass and energy balance could be easily obtained from HYSYS and therefore, the net energy consumption per unit mass of DMC product could be calculated. A comparison between the conventional route for synthesis of DMC and the proposed routes in this research can then be made.

### 7.2.8. Economic Feasibility Study of the Current Process

This research has been focused on the experimental and technical challenges associated with the utilisation of highly stable CO<sub>2</sub> and the synthesis of DMC using heterogeneous catalysts in the absence of co-catalysts and solvents. The research has provided a step forward towards the greener synthesis of DMC and the utilisation of CO<sub>2</sub>. However, a comprehensive assessment for the economical and environmental benefits of the current method is required. A comparison could then be made to the conventional methods to evaluate the feasibility of the proposed processes. Life cycle assessment (LCA) could be used to provide a systematic evaluation of the environmental aspects of the proposed catalytic processes for the synthesis of DMC.

# **Chapter 8**

## **References**

## 8. REFERENCES

Abimanyu, H., Kim, C. S., Ahn, B. S. and Yoo, K. S. (2007) Synthesis of dimethyl carbonate by transesterification with various MgO-CeO<sub>2</sub> mixed oxide catalysts, *Catalysis Letters*, 118 (1–2), 30–35.

Adeleye, A. I., Patel, D., Niyogi, D. and Saha, B. (2014) Efficient and greener synthesis of propylene carbonate from carbon dioxide and propylene oxide. *Industrial and Engineering Chemistry Research*, 53 (49), 18647–18657.

Adeleye, A. I., Kellici, S., Heil, T., Morgan, D., Vickers, M. and Saha, B. (2015) Greener synthesis of propylene carbonate using graphene-inorganic nanocomposite catalysts. *Catalysis Today*, 256 (2), 23–27.

Adeleye, A. I. (Supervisor–Saha B) (2015) Heterogeneous catalytic conversion of carbon dioxide to value added chemicals. PhD Thesis, London South Bank University, London, UK.

Allaoui, L. A. and Aouissi, A. (2006) Effect of the Brønsted acidity on the behavior of CO<sub>2</sub> methanol reaction, *Journal of Molecular Catalysis A: Chemical*, 259 (1–2), 281–285.

Alvaro, M., Baleizao, C., Das, D., Carbonell, E. and Garcia, H. (2004) CO<sub>2</sub> fixation using recoverable chromium salen catalysts: use of ionic liquids as cosolvent or high-surface-area silicates as supports, *Journal of Catalysis*, 228 (1), 254–258.

Alvaro, M., Baleizao, C., Carbonell, E., El Ghouli, M., Garcia, H. and Gigante, B. (2005) Polymer-bound aluminium salen complex as reusable catalysts for CO<sub>2</sub> insertion into epoxides, *Tetrahedron*, 61 (51), 12131–12139.

Almusaiteer, K. (2009) Synthesis of dimethyl carbonate (DMC) from methanol and CO<sub>2</sub> over Rh-supported catalysts, *Catalysis Communications*, 10 (7), 1127–1131.

Anderson, S. A. and Root, T. W. (2004) Investigation of the effect of carbon monoxide on the oxidative carbonylation of methanol to dimethyl carbonate over  $\text{Cu}^+\text{X}$  and  $\text{Cu}^+\text{ZSM-5}$  zeolites, *Journal of Molecular Catalysis A: Chemical*, 220 (2), 247–255.

Anderson, S. A., Manthata, S. and Root, T. (2005) The decomposition of dimethyl carbonate over copper zeolite catalysts, *Applied Catalysis A: General*, 280 (2) 117–124.

Arakawa, H., Aresta, M., Armor, J. N., Barteau, M. A., Beckman, E. J. Bell, A. T., Bercaw, J. E., Creutz, C., Dinjus, E., Dixon, D. A., Domen, K., DuBois, D. L., Eckert, J., Fujita, E., Gibson, D. H., Goddard, W. A., Goodman, D. W., Keller, J., Kubas, G. J., Kung, H. H., Lyons, J. E., . Manzer, L. E., Marks, T. J., Morokuma, K., Nicholas, K. M., Periana, R., Que, L., Rostrup-Nielsen, J., Sachtler, W. M. H., Schmidt L. D., Sen, A., Somorjai, G. A., Stair, P. C., Stults, B. R. and Tumas, W. (2001) Catalysis research of relevance to carbon management: Progress, challenges, and opportunities, *Chemical Reviews*, 101 (4), 953–996.

Aresta, M. and Quaranta, E. (1991) Mechanistic studies on the role of carbon dioxide in the synthesis of methylcarbamates from amines and dimethylcarbonate in the presence of  $\text{CO}_2$ , *Tetrahedron*, 47 (45), 9489–9502.

Aresta, M. and Quaranta, E. (1992) Roles of the macrocyclic polyether in the synthesis of n-alkylcarbonate esters from primary amines,  $\text{CO}_2$  and alkyl-halides in the presence of crown-ethers, *Tetrahedron*, 48 (8), 1515–1530.

Aresta, M. and Quaranta, E. (1997) Carbon dioxide: A substitute for phosgene, *Chemtech*, 27 (3), 32–40.

Aresta, M., Dibenedetto, A., Gianfrate, L. and Pastore, C. (2003a) Nb(V) compounds as epoxides carboxylation catalysts: The role of the solvent, *Journal of Molecular Catalysis A-Chemical*, 204, 245–252.

Aresta, M., Dibenedetto, A. and Pastore, C. (2003b) Synthesis and characterization of  $\text{Nb}(\text{OR})_4[\text{OC}(\text{O})\text{OR}]$  (R = Me, Et, allyl) and their reaction

with the parent alcohol to afford organic carbonates, *Inorganic Chemistry*, 42 (10), 3256–3261.

Aresta, M., Dibenedetto, A., Devita, C., Bourova, O. A. and Chupakhin, O. N. (2004) New catalysts for the conversion of urea into carbamates and carbonates with C1 and C2 alcohols, *Studies in Surface Science and Catalysis*, 153, 213–220.

Aresta, M. and Dibenedetto, A. (2007) Utilisation of CO<sub>2</sub> as a chemical feedstock: opportunities and challenges, *Dalton Transactions*, (28), 2975–2992.

Aresta, M., Dibenedetto, A., Nocito, F. and Pastore, C. (2008a) Comparison of the behaviour of supported homogeneous catalysts in the synthesis of dimethylcarbonate from methanol and carbon dioxide: Polystyrene-grafted tin-metallorganic species versus silesquioxanes linked Nb-methoxo species, *Inorganica Chimica Acta*, 361 (11), 3215–3220.

Aresta, M., Dibenedetto, A., Pastore, C., Corrado, C., Aresta, B., Cometa, S. and De Giglio, E. (2008b) Cerium(IV)oxide modification by inclusion of a hetero-atom: A strategy for producing efficient and robust nano-catalysts for methanol carboxylation, *Catalysis Today*, 137 (1), 125–131.

Aresta, M., Dibenedetto, A., Nocito, F., Angelini, A., Gabriele, B. and De Negri, S. (2010) Synthesis and characterisation of a novel polystyrene-tethered niobium methoxo species. Its application in the CO<sub>2</sub>-based carboxylation of methanol to afford dimethyl carbonate, *Applied Catalysis A: General*, 387 (1–2), 113–118.

Ashley, A. E., Thompson, A. L. and O'Hare, D. (2009) Non-metal-mediated homogeneous hydrogenation of CO<sub>2</sub> to CH<sub>3</sub>OH, *Angewandte Chemie International Edition*, 48 (52), 9839–9843.

Aymes, D., Ballivet-Tkatchenko, D., Jeyalakshmi, K., Saviot, L. and Vasireddy, S. (2009) A comparative study of methanol carbonation on unsupported SnO<sub>2</sub> and ZrO<sub>2</sub>, *Catalysis Today*, 147 (2), 62–67.

Baba, T., Fujiwara, M., Oosaku, A., Kobayashi, A., Deleon, R. G. and Ono, Y. (2002) Catalytic synthesis of *n*-alkyl carbamates by methoxycarbonylation of alkylamines with dimethyl carbonate using  $\text{Pb}(\text{NO}_3)_2$ , *Applied Catalysis A: General*, 227 (1–2), 1–6.

Badwaik, L. S., Prasad, K. and Deka, S. C. (2012) Optimization of extraction conditions by response surface methodology for preparing partially defatted peanut, *International Food Research Journal*, 19 (1), 341–346.

Bai, S. and Shen, X. (2012) Graphene-inorganic nanocomposites, *RSC Advances*, 2 (1), 64–98.

Baiker, A. (1999) Supercritical Fluids in Heterogeneous Catalysis, *Chemistry Reviews*, 99 (2), 453–474.

Baleizao, C., Gigante, B., Sabater, M. J., Garcia, H. and Coma, A. (2002) On the activity of chiral chromium salen complexes covalently bound to solid silicates for the enantioselective epoxide ring opening, *Applied Catalysis A: General*, 228 (1–2), 279–288.

Ballivet-Tkatchenko, D., Douteau, D. and Stutzmann, S. (2000) Reactivity of carbon dioxide with *n*-butyl(phenoxy)-, (alkoxy)-, and (oxo)stannanes: Insight into dimethyl carbonate synthesis, *Organometallics*, 19 (22), 4563–4567.

Ballivet-Tkatchenko, D., Jerphagnon, T., Ligabue, R., Plasseraud, L. and Poinot, D. (2003) The role of distannoxanes in the synthesis of dimethyl carbonate from carbon dioxide, *Applied Catalysis A: General*, 255 (1), 93–99.

Ballivet-Tkatchenko, D., Chambrey, S., Keiski, R., Ligabue, R., Plasseraud, L., Richard, P. and Turunen, H. (2006) Direct synthesis of dimethyl carbonate with supercritical carbon dioxide: Characterisation of a key organotin oxide intermediate, *Catalysis Today*, 115 (1–4), 80–87.

Ballivet-Tkatchenko, D., Bernard, F., Demoisson, F., Plasseraud, L. and Sanapureddy, S. R. (2011a) Tin-based mesoporous silica for the conversion of CO<sub>2</sub> into dimethyl carbonate, *ChemSusChem*, 4 (9), 1316–1322.

Ballivet-Tkatchenko, D., dos Santos, J. H. Z., Philippot, K. and Vasireddy, S. (2011b) Carbon dioxide conversion to dimethyl carbonate: The effect of silica as support for SnO<sub>2</sub> and ZrO<sub>2</sub> catalysts, *Comptes Rendus Chimie*, 14 (7–8), 780–785.

Bansode, A. and Urakawa, A. (2014) Continuous DMC synthesis from CO<sub>2</sub> and methanol over a CeO<sub>2</sub> catalyst in a fixed bed reactor in the presence of a dehydrating agent, *ACS Catalysis*, 4 (11), 3877–3880.

Barbarini, A., Maggi, R., Mazzacani, A., Mori, G., Sartori, G. and Satorio, R. (2003) Cycloaddition of CO<sub>2</sub> to epoxides over both homogeneous and silica-supported guanidine catalysts, *Tetrahedron Letters*, 44 (14), 2931–2934.

Barberis, P., Méjean, T-M. and Quintard, P. (1997) On Raman spectroscopy of zirconium oxide films, *Journal of Nuclear Material*, 246 (2–3), 232–243.

Beckman, E. J. (2004) Supercritical and near-critical CO<sub>2</sub> in green chemical synthesis and processing, *The Journal of Supercritical Fluids*, 28 (2–3), 121–191.

Bernini, R., Crisante, F. and Ginnasi, M.C. (2011) A convenient and safe O-methylation of flavonoids with dimethyl carbonate (DMC), *Molecules*, 16 (2), 1418–1425.

Bhanage, B., Fujita, S., Ikushima, Y. and Arai, M. (2001) Synthesis of dimethyl carbonate and glycols from carbon dioxide, epoxides, and methanol using heterogeneous basic metal oxide catalysts with high activity and selectivity, *Applied Catalysis A-General*, 219 (1–2), 259–266.

Bhanage, B. M., Fujita, S. I., He, Y. F., Ikushima, Y., Shirai, M., Torii, K. and Arai, M. (2002) Concurrent synthesis of dimethyl carbonate and ethylene glycol via

transesterification of ethylene carbonate and methanol using smectite catalysts containing Mg and/or Ni, *Catalysis Letters*, 83 (3–4), 137–141.

Bhanage, B., Fujita, S., Ikushima, Y., Torii, K. and Arai, M. (2003a) Synthesis of dimethyl carbonate and glycols from carbon dioxide epoxides, and methanol using heterogeneous Mg containing smectite catalysts: effect of reaction variables on activity and selectivity performance, *Green Chemistry*, 5 (1), 71–75.

Bhanage, B. M., Fujita, S., Ikushima, Y. and Arai, M. (2003b) Transesterification of urea and ethylene glycol to ethylene carbonate as an important step for urea based dimethyl carbonate synthesis, *Green Chemistry*, 5 (4), 429–432.

Bhattacharya, A. K. and Nolan, J. T. (1987) Preparation of organic carbonates. European Patent 4636572.

Bian, J., Xiao, M., Wang, S., Lu, Y. and Meng, Y. (2009a) Direct synthesis of DMC from CH<sub>3</sub>OH and CO<sub>2</sub> over V-doped Cu-Ni/AC catalysts, *Catalysis Communications*, 10 (8), 1142–1145.

Bian, J., Xiao, M., Wang, S. J., Lu, Y. X. and Meng, Y. Z. (2009b) Novel application of thermally expanded graphite as the support of catalysts for direct synthesis of DMC from CH<sub>3</sub>OH and CO<sub>2</sub>, *Journal of Colloid and Interface Science*, 334 (1), 50–57.

Bian, J., Xiao, M., Wang, S. J., Wang, S. J., Lu, Y. X. and Meng, Y. Z. (2009c) Highly effective synthesis of dimethyl carbonate from methanol and carbon dioxide using a novel copper-nickel/graphite bimetallic nanocomposite catalyst, *Chemical Engineering Journal*, 147 (2–3) 287–296.

Bian, J., Xiao, M., Wang, S. J., Lu, Y. X. and Meng, Y. Z. (2009d) Highly effective direct synthesis of DMC from CH<sub>3</sub>OH and CO<sub>2</sub> using novel Cu-Ni/C bimetallic composite catalysts, *Chinese Chemical Letters*, 20 (3) 352–355.

Bo, R., Ma, X., Feng, Y., Zhu, Q., Huang, Y., Liu, Z., Liu, C., Gao, Z., Hu, Y. and Wang, D. (2015) Optimization on conditions of *Lycium barbarum* polysaccharides

liposome by RSM and its effects on the peritoneal macrophages function, *Carbohydrate Polymers*, 117, 215–222.

Bomben, A., Marques, C. A., Selva, M. and Tundo, P. (1995) A new synthesis of 2-aryloxypropionic acids derivatives via selective mono-C-methylation of methyl aryloxyacetates and aryloxyacetonitriles with dimethyl carbonate, *Tetrahedron*, 51(42), 11573–11580.

Bond, G. C. (1987) *Heterogeneous Catalysis: Principle and Applications*. Second Edition, Clarendon Press, Oxford, UK.

Bruno, T. J., Wolk, A., Naydich, A. and Huber, M. L. (2009) Composition-explicit distillation curves for mixtures of diesel fuel with dimethyl carbonate and diethyl carbonate, *Energy and Fuels*, 23 (8), 3989–3997.

Bu, Z., Qin, G. and Cao, S. (2007) A ruthenium complex exhibiting high catalytic efficiency for the formation of propylene carbonate from carbon dioxide, *Journal of Molecular Catalysis A-Chemical*, 277 (1–2), 35–39.

Cabanas, A., Darr, J. A., Lester, E. and Poliakoff, M. (2000) A continuous and clean one-step synthesis of nano-particulate  $Ce_{1-x}Zr_xO_2$  solid solutions in near-critical water, *Chemical Communications*, (11), 901–902.

Cabanas, A., Darr, J. A., Lester, E. and Poliakoff, M. (2001) Continuous hydrothermal synthesis of inorganic materials in a near-critical water flow reactor; the one-step synthesis of nano-particulate  $Ce_{1-x}Zr_xO_2$  ( $x=0-1$ ) solid solutions, *Journal of Materials Chemistry*, 11 (2), 561–568.

Cai, Q. H., Jin, C., Lu, B., Tangbo, H. J. and Shan, Y. K. (2005) Synthesis of dimethyl carbonate from methanol and carbon dioxide using potassium methoxide as catalyst under mild conditions, *Catalysis Letters*, 103 (3–4), 225–228.

Caló, V., Nacci, A., Monopoli, A. and Fanizzi, A. (2002) Cyclic carbonate formation from carbon dioxide and oxiranes in tetrabutylammonium halides as solvents and catalysts, *Organic Letters*, 4 (15), 2561–2563.

Cao, F. H., Fang, D. Y., Liu, D. H. and Ying, W. Y. (2002) Catalytic esterification of carbon dioxide and methanol for the preparation of dimethyl carbonate, *Fuel Chemistry Division Preprints*, 74 (1), 295–297.

Cao, Y., Cheng, H., Ma, L., Liu, F. and Liu, Z. (2012) Research progress in the direct synthesis of dimethyl carbonate from CO<sub>2</sub> and methanol, *Catalysis Surveys from Asia*, 16 (3), 138–147.

Carnaroglio, D., Martina, K., Palmisano, G., Penoni, A., Domini, C. and Cravotto, G. (2013) One-pot sequential synthesis of isocyanates and urea derivatives via a microwave-assisted staudinger–aza-wittig reaction, *Beilstein Journal of Organic Chemistry*, (9), 2378–2386.

Casadei, M. A., Cesa, S. and Rossi, L. (2000) Electrogenerated base-promoted synthesis of organic carbonates from alcohols and carbon dioxide, *European Journal of Organic Chemistry*, (13), 2445–2448.

Centi, G. and Perathoner, S. (2003) Catalysis and sustainable (green) chemistry, *Catalysis Today*, 77 (4), 287–297.

Chakraborty, S., Zhang, J., Krause, J. A. and Guan, H. R. (2010) An efficient nickel catalyst for the reduction of carbon dioxide with a borane, *Journal of the American Chemical Society*, 132 (26), 8872–8873.

Chaudhry, A. A., Haque, S., Kellici, S., Boldrin, P., Rehman, I., Khalid, f., A. and Darr, J. A. (2006) Instant nano-hydroxyapatite: A continuous and rapid hydrothermal synthesis, *Chemical Communications*, (21), 2286–2288.

Chen, S. W., Kawthekar, R. B. and Kim, G. J. (2007) Efficient catalytic synthesis of optically active cyclic carbonates via coupling reaction of epoxides and carbon dioxide, *Tetrahedron Letters*, 48 (2), 297–300.

Chen, H., Wang, S., Xiao, M., Han, D., Lu, Y. and Meng, Y. (2012) Direct synthesis of dimethyl carbonate from CO<sub>2</sub> and CH<sub>3</sub>OH using 0.4 nm molecular sieve supported Cu-Ni bimetal catalyst, *Chinese Journal of Chemical Engineering*, 20 (5), 906–913.

Cho, T., Tamura, T., Cho, T. and Suzuki, K. (1996) Process for preparing dialkyl carbonates. U.S. Patent 5534649.

Choi, J.C., He, L.N., Yasuda, H. and Sakakura, T. (2002) Selective and high yield synthesis of dimethyl carbonate directly from carbon dioxide and methanol, *Green Chemistry*, 4 (3), 230–234.

Choi, J.C., Kohno, K., Ohshima, Y., Yasuda, H. and Sakakura, T. (2008) Tin- or titanium-catalyzed dimethyl carbonate synthesis from carbon dioxide and methanol: Large promotion by a small amount of triflate salts, *Catalysis Communications*, 9 (7), 1630–1633.

Chu, G. H., Park, J. B. and Cheong, M. (2002) Synthesis of dimethyl carbonate from carbon dioxide over polymer-supported iodide catalysts, *Inorganica Chimica Acta*, 307 (1–2), 131–133.

Clements, J. H. (2003) Reactive applications of cyclic alkylene carbonates, *Industrial and Engineering Chemistry Research*, 42 (4), 663–674.

Clerici, M. G. and Kholdeeva, O. A. (2013) Liquid Phase Oxidation via heterogeneous catalysis: Organic synthesis and industrial applications, John Wiley & Sons: Hoboken, USA.

Coates, G. W. and Moore, D. R. (2004) Discrete metal-based catalysts for the copolymerization CO<sub>2</sub> and epoxides: Discovery, reactivity, optimization, and mechanism, *Angewandte Chemie International Edition*, 43 (48), 6618–6639.

Coker, A., (2012) Dimethyl carbonate 2012S12 Report, *Nexant*, 43 (48), 1–3.

Creutz, C. and Fujita, E. (2000) Carbon Dioxide as a Feedstock, carbon management: Implications for R&D in the chemical sciences and technology: A workshop report to the chemical sciences roundtable, The National Academies Press, Washington, D.C.

Cui, H., Wang, T., Wang, F., Gu, C., Wang, P. and Dai, Y. (2003) One-pot synthesis of dimethyl carbonate using ethylene oxide, methanol and carbon dioxide in supercritical conditions, *Industrial and Engineering Chemistry Research*, 42 (17), 3865–3870.

Cui, H., Wang, T., Wang, F., Gu, C., Wang, P. and Dai, Y. (2004a) Kinetic study on the one-pot synthesis of dimethyl carbonate in supercritical CO<sub>2</sub> conditions, *Industrial and Engineering Chemistry Research*, 43 (24), 7732–7739.

Cui, H., Wang, T., Wang, F. J., Gu, C., Wang, P. and Dai, Y. (2004b) Transesterification of ethylene carbonate with methanol in supercritical carbon dioxide, *The Journal of Supercritical Fluids*, 30 (1), 63–69.

Cutrufello, M. G., Ferino, I., Solinas, V., Primavera, A., Trovarelli, A., Auroux, A. and Picciau, C. (1999) Acid-base properties and catalytic activity of nanophase ceria-zirconia catalysts for 4-methylpentan-2-ol dehydration, *Physical Chemistry Chemical Physics*, 1 (14), 3369–3375.

Dai, H., Hafner, J., Rinzler, A., Colbert, D. and Smalley, R. (1996) Nanotubes as nanoprobe in scanning probe microscopy, *Nature*, 384 (6605), 147–150.

Dai, W. L., Luo, S., Yin, S. L. and Au, C. T. (2009) The direct transformation of carbon dioxide to organic carbonates over heterogeneous catalysts, *Applied Catalysis A-General*, 366 (1), 2–12.

Darensbourg, D. J. and Holtcamp, M. W. (1996) Catalysts for the reactions of epoxides and carbon dioxide, *Coordination Chemistry Reviews*, 153, 155–174.

Darensbourg, D. J., Lewis, S. J., Rodgers, J. L. and Yarbrough, J. C. (2003) Carbon dioxide/epoxide coupling reactions utilizing lewis base adducts of zinc

halides as catalysts. Cyclic carbonate versus polycarbonate production, *Inorganic Chemistry*, 42 (2), 581–589.

Darensbourg, D. J., Fang, C. C. and Rodgers, J. L. (2004) Catalytic coupling of carbon dioxide and 2,3-epoxy-1,2,3,4-tetrahydronaphthalene in the presence of a (Salen)(CrCl)-Cl-III derivative, *Organometallics*, 23 (4), 924–927.

Darensbourg, D. J. (2007) Making plastics from carbon dioxide: Salen metal complexes as catalysts for the production of polycarbonates from epoxides and CO<sub>2</sub>, *Chemical Reviews*, 107 (6), 2388–2410.

Darensbourg, D. J. (2010) Chemistry of carbon dioxide relevant to its utilisation: A personal perspective, *Inorganic Chemistry*, 49 (23), 10765–10780.

Darr, J. A. and Poliakoff, M. (1999) New directions in inorganic and metal-organic coordination chemistry in supercritical fluids, *Chemical Reviews*, 99 (2), 495–542.

Das, A., Vimala, R. and Das, N. (2014) Biosorption of Zn(II) onto pleurotus platypus: 5-level Box–Behnken design, equilibrium, kinetic and regeneration studies, *Ecological Engineering*, 64, 136–141.

Davis, R. J., Duskocil, E. J. and Bordawekar (2000) Structure/function relationships for basic zeolite catalysts containing occluded alkali species, *Catalysis Today*, 62 (2–3), 241–247.

De Filippis, P., Scarsella, M., Borgianni, C. and Pochetti, F. (2006) Production of dimethyl carbonate via alkylene carbonate transesterification catalyzed by basic salts, *Energy and Fuels*, 20 (1), 17–20.

De Pasquale, .R.J. (1973) Unusual catalysis with nickel(0) complexes, *Journal of the Chemical Society, Chemical Communications* (5), 157–158.

Delledonne, D., Rivetti, F. and Romano, U. (1995) Oxidative carbonylation of methanol to dimethyl carbonate (DMC): A new catalytic system, *Journal of Organometallic Chemistry*, 488 (1–2), C15–C19.

Delledonne, D., Rivetti, F. and Romano, U. (2001) Developments in the production and application of dimethylcarbonate, *Applied Catalysis A: General*, 221 (1–2), 241–251.

Dharman, M. M., Ju, H. Y., Shim, H. L., Lee, M. K., Kim, Y. H. and Park, D. W. (2009) Significant influence of microwave dielectric heating on ionic liquid catalyzed transesterification of ethylene carbonate with methanol, *Journal of Molecular Catalysis A: Chemical*, 303 (1–2), 96–101.

Dhuri, S. M. and Mahajani, V. V. (2006) Studies in transesterification of ethylene carbonate to dimethyl carbonate over amberlyst A-21 catalyst, *Journal of Chemical Technology and Biotechnology*, 81 (1), 62–69.

Dibenedetto, A., Pastore, C. and Aresta, M. (2006) Direct carboxylation of alcohols to organic carbonates: Comparison of the group 5 element alkoxides catalytic activity: An insight into the reaction mechanism and its key steps, *Catalysis Today*, 115 (1–4), 88–94.

Dienes, Y., Leitner, W., Müller, M. G. J., Offermans, W. K., Reier, T., Reinholdt, A., Weirich, T. E. and Müller, T. E. (2012) Hybrid sol-gel double metal cyanide catalysts for the copolymerisation of styrene oxide and CO<sub>2</sub>, *Green Chemistry*, 14 (4), 1168–1177.

Ding, Y. J., Kong, A. K., Zhang, H. Q., Shen, H. H., Sun, Z. D., Huang, S. P. D. and Shan, Y. K. (2013) A novel synthetic approach for preparing dimethyl carbonate from dimethoxymethane and O-2 over Cu-MCM-48, *Applied Catalysis A: General*, 455, 58–64.

Diwekar, U. (2005) Green process design, industrial ecology, and sustainability: A systems analysis perspective, *Resources, Conservation and Recycling*, 44 (3), 215–235.

Dlugokencky, Ed. and Tans, P. (2015) Trends in atmospheric carbon dioxide. U.S. Department of Commerce, National oceanic & atmospheric administration (NOAA) research, earth system research laboratory (ESRL).

Global monitoring division - global greenhouse gas reference network. Available at: <http://www.esrl.noaa.gov/gmd/ccgg/trends/global.html> Accessed on 12 August 2015.

Doskocil, E. J., Bordawekar, S. V., Kaye, B. G. and Davis, R. J. (1999) UV-vis spectroscopy of iodine adsorbed on alkali-metal-modified zeolite catalysts for addition of carbon dioxide to ethylene oxide, *Journal of Physical Chemistry B*, 103 (30), 6277–6282.

Doskocil, E. J. (2004) Ion-exchanged ETS-10 catalysts for the cycloaddition of carbon dioxide to propylene oxide, *Microporous and Mesoporous Materials*, 76 (1–3), 177–183.

Doskocil, E. J. (2005) Effect of water and alkali modifications on ETS-10 for the cycloaddition of CO<sub>2</sub> to propylene oxide, *Journal of Physical Chemistry B*, 109 (6), 2315–2320.

Dreyer, D. R., Park, A., Bielawski, C. W. and Ruoff, R. S. (2010) The chemistry of graphene oxide, *Chemical Society Reviews*, 39 (1), 228–240.

Du, Y., Cai, F., Kong, D. L. and He, L. N. (2005) Organic solvent-free process for the synthesis of propylene carbonate from supercritical carbon dioxide and propylene oxide catalyzed by insoluble ion exchange resins, *Green Chemistry*, 7 (7), 518–523.

Duan, X., Zhang, Z., Srinivasakannan, C., Wang, F. and Liang, J. (2014) Regeneration of spent catalyst from vinyl acetate synthesis as porous carbon: Process optimization using RSM, *Chemical Engineering Research and Design*, 92 (7), 1249–1256.

Duranleau, R. G., Nieh, E. C. Y. and Knifton, J. F. (1987) Process for production of ethylene glycol and dimethyl carbonate. U.S. Patent 4691041.

Eghbali, N. and Li, C. (2007) Conversion of carbon dioxide and olefins into cyclic carbonates in water, *Green Chemistry*, 9 (3), 213–215.

El-Gendy, N. S., Deriase, S. F. and Osman, D. I. (2014) The Optimization of bio-diesel production from waste frying oil using response surface methodology and the investigation of correlations for changes in basic properties of bio-petro-diesel blends, *Energy Sources, Part A: Recovery, Utilization and Environmental Effects*, 36 (5), 457–470.

Fan, B., Li, H., Fan, W., Zhang, J. and Li, R. (2010) Organotin compounds immobilized on mesoporous silicas as heterogeneous catalysts for direct synthesis of dimethyl carbonate from methanol and carbon dioxide, *Applied Catalysis A: General*, 372 (1), 94–102.

Fang, S. and Fujimoto, K. (1996) Direct synthesis of dimethyl carbonate from carbon dioxide and methanol catalyzed by base, *Applied Catalysis A: General*, 142 (1), L1–L3.

Fournaison, L., Delahaye, A. and Chatti, I. (2004) CO<sub>2</sub> hydrates in refrigeration processes, *Industrial Engineering Chemical Research*, 43 (20), 6521–6526.

Fu, Y. and Ono. Y. (1994) Synthesis of methyl *n*-phenyl carbamate by methoxycarbonylation of aniline with dimethyl carbonate using PB compounds as catalysts, *Journal of Molecular Catalysis*, 91 (3), 399–405.

Fu, Y., Baba, T. and Ono. Y. (1998) Vapor-phase reactions of catechol with dimethyl carbonate. Part II. Selective synthesis of guaiacol over alumina loaded with alkali hydroxide, *Applied Catalysis A: General*, 166 (2), 425–430.

Fujihara, T., Xu, T. H., Semba, K., Teraro, J. and Tsuji, Y. (2011) Copper-catalyzed hydrocarboxylation of alkynes using carbon dioxide and hydrosilanes, *Angewandte Chemie International Edition*, 50 (2), 523–527.

Fujita, S. I., Bhanage, B. M., Ikushima, Y. and Arai, M. (2001) Synthesis of dimethyl carbonate from carbon dioxide and methanol in the presence of methyl iodide and base catalysts under mild conditions: effect of reaction conditions and reaction mechanism, *Green Chemistry*, 3 (2), 87–91.

Fujita, S. I., Bhanage, B. M., Ikushima, Y., Shirai, M, Torii, K and Arai, M. (2002) Chemical fixation of carbon dioxide to propylene carbonate using smectite catalysts with high activity and selectivity, *Catalysis Letters*, 79 (1–4), 95–98.

Fujita, S. I., Bhanage, B. M., Aoki, D., Ochiai, Y., Iwasa, N. and Arai, M. (2006) Mesoporous smectites incorporated with alkali metal cations as solid base catalysts, *Applied Catalysis A: General*, 313 (2), 151–159.

Fujita, S., Nishiura, M. and Arai, M. (2010) Synthesis of styrene carbonate from carbon dioxide and styrene oxide with various zinc halide-based ionic liquids, *Catalysis Letters*, 135 (3–4), 263–268.

Gale, J., Bradshaw. J., Chen, Z., Garg, A., Gomez, D., Rogner. H., Simbeck. D., Williams. R., Toth, F., van Vuuren. D., (2006). Sources of CO<sub>2</sub>. IPCC. Available at: [https://www.ipcc.ch/pdf/special-reports/srccls/srccls\\_chapter2.pdf](https://www.ipcc.ch/pdf/special-reports/srccls/srccls_chapter2.pdf) Accessed on 12 August 2015.

Geim, A. K. and Novoselov, K. S. (2007) The rise of graphene, *Nature Materials*, 6, 183–191.

Geim, A. K. (2009) Graphene: status and prospects, *Science*, 324, 1530–1534.

Gibbins, J. and Chalmers, H. (2008) Carbon capture and storage, *Energy Policy*, 36 (12), 4317–4322.

Glasnov, T. N., Holbrey, J. D., Kappe, C. O., Seddon, K. R. and Yan, T. (2012) Methylation using dimethylcarbonate catalysed by ionic liquids under continuous flow conditions, *Green Chemistry*, 14, 3071–3076.

Gongying, W., Tao, H., Meiguang L., Chuang, S. S. C. (2000) Oxidative carbonylation of methanol to dimethylcarbonate over copper complex catalysts, *Journal of Natural Gas Chemistry*, 9 (1), 8–17.

Goodall, J. B. M., Kellici, S., Illsley, D., Lines, R., Knowles, J. C. and Darr, J. A. (2014) Optical and photocatalytic behaviours of nanoparticles in the Ti-Zn-O binary system, *RSC Advances*, 4 (60), 31799–31809.

Grabow, L. C. and Mavrikakis, M. (2011) Mechanism of methanol synthesis on Cu through CO<sub>2</sub> and CO hydrogenation, *ACS Catalysis*, 1 (4), 365–384.

Hakuta, Y., Adschiri, T., Suzuki, T., Chida, T., Seino, K. and Arai, K. (1998) Flow method for rapidly producing barium hexaferrite particles in supercritical water, *Journal of the American Ceramic Society*, 81 (9), 2461–2464.

Han, M. S., Lee, B. G., Ahn, B. S., Park, K. Y. and Hong, S. I. (2001) Kinetics of dimethyl carbonate synthesis from ethylene carbonate and methanol using alkali-metal compounds as catalysts, *Reaction Kinetics and Catalysis Letters*, 73 (1), 33–38.

Hepworth, J. D., Waring, D. R. and Waring, M. J. (2002) *Aromatic Chemistry*, The Royal Society of Chemistry, Cambridge, UK.

Hitzler, M. G., Smail, F. R., Poliakoff, M. and Ross, S. K. (1998) Friedel-Crafts alkylation in supercritical fluids: continuous, selective and clean, *Chemical Communications*, (3), 359–360.

Hoffman, W. (1982) A convenient preparation of carbonates from alcohols and carbon-dioxide, *Journal of Organic Chemistry*, 47 (26), 5209–5210.

Honda, M., Suzuki, A., Noorjahan, B., Fujimoto, K. I., Suzuki, K. and Tomishige, K. (2009) Low pressure CO<sub>2</sub> to dimethyl carbonate by the reaction with methanol promoted by acetonitrile hydration, *Chemical Communications*, (30), 4596–4598.

Honda, M., Kuno, S., Begum, N., Fujimoto, K. I., Suzuki, K., Nakagawa, Y. and Tomishige, K. (2010) Catalytic synthesis of dialkyl carbonate from low pressure CO<sub>2</sub> and alcohols combined with acetonitrile hydration catalyzed by CeO<sub>2</sub>, *Applied Catalysis A: General*, 384 (1–2), 165–170.

Honda, M., Kuno, S., Sonehara, S., Fujimoto, K. I., Suzuki, K., Nakagawa, Y. and Tomishige, K. (2011) Tandem carboxylation-hydration reaction system from methanol, CO<sub>2</sub> and benzonitrile to dimethyl carbonate and benzamide catalyzed by CeO<sub>2</sub>, *ChemCatChem*, 3 (2), 365–370.

Honda, M., Tamaura, M., Nakagawa, Y. and Tomishige, K. (2014) Catalytic CO<sub>2</sub> conversion to organic carbonates with alcohols in combination with dehydration system, *Catalysis Science and Technology*, 4 (9), 2830–2845.

Hong, S. T., Park, H. S., Lim, J. S., Lee, Y. W., Anpo, M. and Kim, J. D. (2006) Synthesis of dimethyl carbonate from methanol and supercritical carbon dioxide, *Research on Chemical Intermediates*, 32 (8), 737–747.

Hou, Z. S., Han, B. X., Liu, Z. M., Jiang, T. and Yang, G. Y. (2002) Synthesis of dimethyl carbonate using CO<sub>2</sub> and methanol: Enhancing the conversion by controlling the phase behavior, *Green Chemistry*, 4 (5), 467–471.

Hu, C., Liu, H., Dong, W., Zhang, W., Bao, G., Lao, C. and Wang Z. L. (2007) La(OH)<sub>3</sub> and La<sub>2</sub>O<sub>3</sub> nanobelts-Synthesis and physical properties, *Advanced Materials*, 19 (3), 470–474.

Huang, J. W. and Shi, M. (2003) Chemical fixation of carbon dioxide by NaI/PPh<sub>3</sub>/PhOH, *Journal of Organic Chemistry*, 68 (17), 6705–6709.

Huang, D. G., Makhlynets, O. V., Tan, L. L., Lee, S. C., Rybak-Akimova, E. V. and Holm, R. H. (2011) Kinetics and mechanistic analysis of an extremely rapid carbon dioxide fixation reaction, *Proceedings of the National Academy of Sciences of the United States of America*, 108 (4), 1222–1227.

Hummers, W. S. and Offeman, R. E. (1958) Preparation of graphitic oxide, *Journal of the American Chemical Society*, 80 (6), 1339–1339.

Ikeda, Y., Sakaihorii, T., Tomishige, K. and Fujimoto, K. (2000) Promoting effect of phosphoric acid on zirconia catalysts in selective synthesis of dimethyl carbonate from methanol and carbon dioxide, *Catalysis Letters*, 66 (1-2), 59–62.

Ikeda, Y., Asadullah, M., Fujimoto, K. and Tomishige, K. (2001) Structure of the active sites on H<sub>3</sub>PO<sub>4</sub>/ZrO<sub>2</sub> catalysts for dimethyl carbonate synthesis from methanol and carbon dioxide, *Journal of Physical Chemistry B*, 105 (43), 10653–10658.

Jagtap, S. R., Raje, V. P., Samant, S. D. and Bhanage, B. M. (2007) Silica supported polyvinyl pyridine as a highly active heterogeneous base catalyst for the synthesis of cyclic carbonates from carbon dioxide and epoxides, *Journal of Molecular Catalysis A: Chemical*, 266 (1–2), 69–74.

Jagtap, S. R., Bhor, M. D. and Bhanage, B. M. (2008) Synthesis of dimethyl carbonate via transesterification of ethylene carbonate with methanol using poly-4-vinyl pyridine as a novel base catalyst, *Catalysis Communications*, 9 (9), 1928–1931.

Jiang, C. J., Guo, Y. H., Wang, C. G., Hu, C. W., Wu, Y. and Wang, E. B. (2003) Synthesis of dimethyl carbonate from methanol and carbon dioxide in the presence of polyoxometalates under mild conditions, *Applied Catalysis A: General*, 256 (1–2), 203–212.

Jiang, J. L., Gao, F. X., Hua, R. M. and Qui, X. Q. (2005) Re(CO)<sub>5</sub>Br-catalyzed coupling of epoxides with CO<sub>2</sub> affording cyclic carbonates under solvent-free conditions, *Journal of Organic Chemistry*, 70 (1), 381–383.

Jiang, J. L. and Hua, R. M. (2006) Efficient DMF-catalyzed coupling of epoxides with CO<sub>2</sub> under solvent-free conditions to afford cyclic carbonates, *Tetrahedron Letters*, 36 (21), 3141–3148.

Jin, L. L., Jing, H. W., Chang, T., Bu, X. L., Wang, L., and Liu, Z. L. (2007) Metal porphyrin/phenyltrimethylammonium tribromide: High efficient catalysts for coupling reaction of CO<sub>2</sub> and epoxides, *Journal of Molecular Catalysis A: Chemical*, 261 (2), 262–266.

Jing, H. W., Chang, T., Jin, L., Wu, M. and Qiu, W. Y. (2007) Ruthenium Salen/phenyltrimethylammonium tribromide catalyzed coupling reaction of carbon dioxide and epoxides, *Catalysis Communications*, 8 (11), 1630–1634.

Joó, F. (2007) Activation of carbon dioxide, in *Physical Inorganic Chemistry: Reactions, Processes, and Applications*, Wiley-VCH: Weinheim, Germany, 259–259.

Ju, H. Y., Manju, M. D., Park, D. W., Choe, Y. and Park, S. W. (2007) Performance of ionic liquid as catalysts in the synthesis of dimethyl carbonate from ethylene carbonate and methanol, *Reaction Kinetics and Catalysis Letters*, 90 (1), 3–9.

Juarez, R., Corma, A. and Garcia, H. (2009) Gold nanoparticles promote the catalytic activity of ceria for the transalkylation of propylene carbonate to dimethyl carbonate, *Green Chemistry*, 11 (7), 949–952.

Jung, K. T. and Bell, A. T. (2001) An *in situ* infrared study of dimethyl carbonate synthesis from carbon dioxide and methanol over zirconia, *Journal of Catalysis*, 204 (2), 339–347.

Jutz, F., Grunwaldt, J. D. and Baiker, A. (2008) Mn(III)(salen)-catalyzed synthesis of cyclic organic carbonates from propylene and styrene oxide in "supercritical" CO<sub>2</sub>, *Journal of Molecular Catalysis A: Chemical*, 279 (1), 94–103.

Kawanami, H. and Ikushima, Y. (2000) Chemical fixation of carbon dioxide to styrene carbonate under supercritical conditions with DMF in the absence of any additional catalysts, *Chemical Communications*, (21), 2089–2090.

Kellici, S., Acord, J., Ball, J., Reehal, J., Morgan, D., and Saha, B. (2014) A single rapid route for the synthesis of reduced graphene oxide with antibacterial activities, *RSC Advances*, 4 (29), 14858–14861.

Khajeh, M. and Sanchooli, E. (2010) Optimization of microwave-assisted extraction procedure for zinc and iron determination in celery by Box–Behnken Design, *Food Analytical Methods*, 3 (2), 75–79.

Kim, H. S., Kim, J. J., Kwon, H. N., Chung, M. J., Lee, B. G. and Jang, H. G. (2002) Well-defined highly active heterogeneous catalyst system for the coupling reactions of carbon dioxide and epoxides, *Journal of Catalysis*, 205 (1), 226–229.

Kim, H. S., Kim, J. J., Kim, H. and Jang, H. G. (2003) Imidazolium zinc tetrahalide-catalyzed coupling reaction of CO<sub>2</sub> and ethylene oxide or propylene oxide, *Journal of Catalysis*, 220 (1), 44–46.

Kim, H. S., Bae, J. Y., Lee, J. S., Kwon, O. S., Jelliarko, P., Lee, S. D. and Lee, S. H. (2005) Phosphine-bound zinc halide complexes for the coupling reaction of ethylene oxide and carbon dioxide, *Journal of Catalysis*, 232 (1), 80–84.

Kim, D. W., Lim, D. O., Cho, D. H., Koh, J. C. and Park, D. W. (2011) Production of dimethyl carbonate from ethylene carbonate and methanol using immobilized ionic liquids on MCM-41, *Catalysis Today*, 164, 556–560.

King, S. T. (1996) Reaction mechanism of oxidative carbonylation of methanol to dimethyl carbonate in Cu–Y zeolite, *Journal of Catalysis*, 161 (2), 530–538.

Knifton, J. F. (1987) Process for cosynthesis of ethylene glycol and dimethyl carbonate. U.S. Patent 4661609.

Knifton, J. F. and Duranleau, R. G. (1991) Ethylene glycol-dimethyl carbonate cogeneration, *Journal of Molecular Catalysis*, 67 (3), 389–399.

Knifton, J. F. (1993) Process for cogeneration of ethylene glycol and dimethyl carbonate. U.S. Patent 5214182.

Kohno, K., Choi, J. C., Ohshima, Y., Yili, A., Yasuda, H. and Sakakura, T. (2008) Reaction of dibutyltin oxide with methanol under CO<sub>2</sub> pressure relevant to catalytic dimethyl carbonate synthesis, *Journal of Organometallic Chemistry*, 693 (7), 1389–1392.

Komoto, I. and Kobayashi, S. (2002) 1-dodecyloxy-4-perfluoroalkylbenzene as a novel efficient additive in aldol reactions and friedel–crafts alkylation in supercritical carbon dioxide, *Organic Letters*, 4 (7), 1115–1118.

Kong, L., Zhong, S. H. and Yin, L. (2005) Photocatalytic reaction for synthesis of dimethyl carbonate from CO<sub>2</sub> and CH<sub>3</sub>OH over Cu/NiO-MoO<sub>3</sub>/SiO<sub>2</sub> catalyst, *Chinese Journal of Catalysis*, 26 (10), 917–922.

Kong, L. L., Zhong, S. H., Liu, Y. and Xiao, X. F. (2006) Study on photo-catalytic synthesis of dimethyl carbonate from CO<sub>2</sub> and CH<sub>3</sub>OH over Cu/NiO-V<sub>2</sub>O<sub>5</sub>/SiO<sub>2</sub> catalyst, *Acta Chimica Sinica*, 64 (5), 409–414.

Kossev, K., Koseva, N. and Troev, K. (2003) Calcium chloride as co-catalyst of onium halides in the cycloaddition of carbon dioxide to oxiranes, *Journal of Molecular Catalysis A: Chemical*, 194 (1–2), 29–37.

Kricsfalussy, Z., Waldmann, H. and Traenckner, H. J. (1998) Oxycarbonylation of methanol to dimethyl carbonate using molten salts as catalyst, *Industrial and Engineering Chemistry Research*, 37 (3), 865–866.

La, K. W. and Song, I. K. (2006) Direct synthesis of dimethyl carbonate from CH<sub>3</sub>OH and CO<sub>2</sub> by H<sub>3</sub>PW<sub>12</sub>O<sub>40</sub>/Ce<sub>x</sub>Ti<sub>1-x</sub>O<sub>2</sub> catalyst, *Reaction Kinetics and Catalysis Letters*, 89 (2), 303–309.

La, K. W., Jung, J. C., Kim, H., Baeck, S. H. and Song, I. K. (2007) Effect of acid-base properties of H<sub>3</sub>PW<sub>12</sub>O<sub>40</sub>/Ce<sub>x</sub>Ti<sub>1-x</sub>O<sub>2</sub> catalysts on the direct synthesis of dimethyl carbonate from methanol and carbon dioxide: A TPD study of H<sub>3</sub>PW<sub>12</sub>O<sub>40</sub>/Ce<sub>x</sub>Ti<sub>1-x</sub>O<sub>2</sub> catalysts, *Journal of Molecular Catalysis A: Chemical*, 269 (1–2), 41–45.

Laitar, D. S., Muller, P. and Sadighi, J. P. (2005) Efficient homogeneous catalysis in the reduction of CO<sub>2</sub> to CO, *Journal of the American Chemical Society*, 127 (49), 17196–17197.

Leino, E., Mäki-Arvela, P., Etsä, V., Murzin, D. Y., Salmi, T. and Mikkola, J. P. (2010) Conventional synthesis methods of short-chain dialkylcarbonates and novel production technology via direct route from alcohol and waste CO<sub>2</sub>, *Applied Catalysis A: General*, 383 (1–2), 1–13.

Leitner, W. (2002) Supercritical carbon dioxide as a green reaction medium for catalysis, *Accounts of Chemical Research*, 35 (9), 746–756.

Lester, E., Blood, P., Denyer, J., Giddings, D., Azzopardi, B. and Poliakoff, M. (2006) Reaction engineering: The supercritical water, hydrothermal synthesis of nano-particles, *Journal of Supercritical Fluids*, 37(2), 209–214.

Li, Z., Xie, K. and Slade, R. C. T. (2001) High selective catalyst CuCl/MCM-41 for oxidative carbonylation of methanol to dimethyl carbonate, *Applied Catalysis A: General*, 205 (1–2), 85–92.

Li, C. F. and Zhong, S. H. (2003) Study on application of membrane reactor in direct synthesis DMC from CO<sub>2</sub> and CH<sub>3</sub>OH over Cu-KF/MgSiO catalyst, *Catalysis Today*, 82 (1–4), 83–90.

Li, F. W., Xiao, L. F., Xia, C. G. and Hu, B. (2004) Chemical fixation of CO<sub>2</sub> with highly efficient ZnCl<sub>2</sub>/[BMIm]Br catalyst system, *Tetrahedron Letters*, 45 (45), 8307–8310.

Li, Y., Zhao, X. Q. and Wang, Y. J. (2005) Synthesis of dimethyl carbonate from methanol, propylene oxide and carbon dioxide over KOH/4A molecular sieve catalyst, *Applied Catalysis A: General*, 279 (1–2), 205–208.

Li, D. and Kaner, R. B. (2008) Materials science: Graphene-based materials, *Science*, 320 (5880), 1170–1171.

Li, S. H., Yuan, W. M. and Ma, S. M. (2011a) Highly regio- and stereoselective three-component nickel-catalyzed syn-hydrocarboxylation of alkynes with diethyl zinc and carbon dioxide, *Angewandte Chemie International Edition*, 50 (11), 2578–2582.

Li, N., Zheng, M., Chang, X., Ji, G., Lu, H., Xue, L., Pan, L. and Cao, J. (2011b) Preparation of magnetic CoFe<sub>2</sub>O<sub>4</sub>-functionalized graphene sheets via a facile hydrothermal method and their adsorption properties, *Journal of Solid State Chemistry*, 184 (4), 953–958.

Liang, Y., Wang, H., Casalongue, H. S., Chen, Z. and Dai, H. (2010) TiO<sub>2</sub> nanocrystals grown on graphene as advanced photocatalytic hybrid materials, *Nano Research*, 3 (10), 701–705.

Lilach, Y., Danziger, I. M. and Asscher, M. (2001) Second order isothermal desorption kinetics, *Catalysis Letters*, 76 (1–2), 35–39.

Lin, T., Kellici, S., Gong, K., Thompson, K., Evans, J. R. G., Wang, X. and Darr, J. A. (2010) Rapid automated materials synthesis instrument: Exploring the composition and heat-treatment of nanoprecursors toward low temperature red phosphors, *Journal of Combinatorial Chemistry*, 12 (3), 383–392.

Liu, L., Yao, Z, Liu B. and Dong, L. (2010) Correlation of structural characteristics with catalytic performance of CuO/Ce<sub>x</sub>Zr<sub>1-x</sub>O<sub>2</sub> catalysts for NO reduction by CO, *Journal of Catalysis*, 275 (1), 45–60.

Loosen, P. C., Tundo, P. and Selva, M. (1996) A process for the alpha-monoalkylation of arylacetonitriles, arylacetoesters and arylacetic acids. European Patent 525506.

Lu, X. B., Wang, H. and He, R. (2002) Aluminum phthalocyanine complex covalently bonded to MCM-41 silica as heterogeneous catalyst for the synthesis of cyclic carbonates, *Journal of Molecular Catalysis A: Chemical*, 186 (1–2), 33–42.

Lu, X., Zhang, Y., Liang, B., Li, X. and Wang, H. (2004) Chemical fixation of carbon dioxide to cyclic carbonates under extremely mild conditions with highly active bifunctional catalysts, *Journal of Molecular Catalysis A: Chemical*, 210 (1–2), 31–34.

Marcano, D. C., Kosynkin, D. V., Berlin, J. M., Sinitskii, A., Sun, Z., Slesarev, A., Alemany, L. B., Lu, W., Tour, J. M., (2010) Improved synthesis of graphene oxide, *ACS NANO*, 4 (8), 4806–4814.

Matsuo, T. and Kawaguchi, H. (2006) From carbon dioxide to methane: Homogeneous reduction of carbon dioxide with hydrosilanes catalyzed by zirconium-borane complexes, *Journal of the American Chemical Society*, 128 (38), 12362–12363.

McGhee, W., Riley, D., Christ, M. and Christ, K. (1993) Palladium-catalyzed generation of O-allylic urethanes and carbonates from amines/alcohols, carbon dioxide and allylic chlorides, *Organometallics*, 12 (4), 1429–1433.

McGhee, W., Riley, D., Christ, K., Pan, Y. and Parnas, B. (1995) Carbon dioxide as a phosgene replacement-Synthesis and mechanistic studies of urethanes from amines, CO<sub>2</sub>, and alkyl chlorides, *The Journal of Organic Chemistry*, 60 (9), 2820–2830.

Menard, G. and Stephen, D. W. (2010) Room temperature reduction of CO<sub>2</sub> to methanol by Al-based frustrated lewis pairs and ammonia borane, *Journal of the American chemical Society*, 132 (6), 1796–1797.

Middelkoop, V., Tighe, C. J., Kellici, S., Gruar, R. I., Perkins, J. M., Jacques, S. D. M., Barnes, P. and Darr, J. A. (2014) Imaging the continuous hydrothermal flow synthesis of nanoparticulate CeO<sub>2</sub> at different supercritical water temperatures using in situ angle-dispersive diffraction, *The Journal of Supercritical Fluids*, 87, 118–128.

Mikkelsen, M., Jørgensen, M. and Krebs, F. C. (2010) The teraton challenge. A review of fixation and transformation of carbon dioxide, *Energy and Environmental Science*, 3 (1), 43–81.

Mo, W., Xiong, H., Li, T., Guo, X. and Li, G. (2006) The catalytic performance and corrosion inhibition of CuCl/Schiff base system in homogeneous oxidative carbonylation of methanol, *Journal of Molecular Catalysis A: Chemical*, 247 (1–2), 227–232.

Mori, K., Mitani, Y., Hara, T., Mizugaki, T., Ebitani, K. and Kaneda, K. (2005) A single-site hydroxyapatite-bound zinc catalyst for highly efficient chemical fixation of carbon dioxide with epoxides, *Chemical Communications*, (26), 3331–3333.

Morris, G. E., Oakley, D., Pippard, D. and Smith, D. (1987) Copper catalysed reactions of di-*t*-butyl peroxide: Oxidative carbonylation of alcohols to give dialkyl carbonates, oxalates, or succinates, *Journal of the Chemical Society, Chemical Communications*, (6), 410–411.

Murugan, C., Sharma, S. K., Jasra, R. V. and Bajaj, H. C. (2010) Hydrotalcite catalyzed cycloaddition of carbon dioxide to propylene oxide in the presence of N, N-dimethylformamide, *Indian Journal of Chemistry Section A, Inorganic Bio-Inorganic Physical Theoretical and Analytical Chemistry*, 49 (3), 288–294.

Murugan, C. and Bajaj, H. C. (2011) Synthesis of diethyl carbonate from dimethyl carbonate and ethanol using  $\text{KF}/\text{Al}_2\text{O}_3$  as an efficient solid base catalyst, *Fuel Processing Technology*, 92 (1), 77–82.

Navalon, S., Dhakshinamoorthy, A., Alvaro, M. and Garcia, H. (2014) Carbocatalysis by graphene-based materials, *Chemical Reviews*, 114 (12), 6179–6212.

NOAA, (2008) Carbon Dioxide, Methane Rise Sharply in 2007. Available at: [http://www.noaaneews.noaa.gov/stories2008/20080423\\_methane.html](http://www.noaaneews.noaa.gov/stories2008/20080423_methane.html) Accessed on 12 August 2015.

NOAA, (2014) Trends in atmospheric carbon dioxide. Available at: <http://www.esrl.noaa.gov/gmd/ccgg/trends/weekly.html>, Accessed on 12 August 2015.

Omae, I. (2006) Aspects of carbon dioxide utilisation, *Catalysis Today*, 115 (1–4), 33–52.

Omae, I. (2012) Recent developments in carbon dioxide utilisation for the production of organic chemicals, *Coordination Chemistry Reviews*, 256 (13–14), 1384–1405.

Pacheco, M. A. and Marshall, C. L. (1997) Review of dimethyl carbonate (DMC) manufacture and its characteristics as a fuel additive, *Energy and Fuels*, 11 (1), 2–29.

Paddock, R. L. and Nguyen, S. T. (2001) Chemical CO<sub>2</sub> fixation: Cr(III) salen complexes as highly efficient catalysts for the coupling of CO<sub>2</sub> and epoxides, *Journal of the American Chemical Society*, 123 (46), 11498–11499.

Paddock, R. L., Hiyama, Y., McKay, J. M. and Nguyen, S. T. (2004) Co(III) porphyrin/DMAP: An efficient catalyst system for the synthesis of cyclic carbonates from CO<sub>2</sub> and epoxides, *Tetrahedron Letters*, 45 (9), 2023–2026.

Park, J. H., Jeon, J. Y., Lee, J. J., Jang, Y., Varghese, J. K. and Lee, B. Y. (2013) Preparation of high-molecular-weight aliphatic polycarbonates by condensation polymerization of diols and dimethyl carbonate, *Macromolecules*, 46 (9), 3301–3308.

Patel, D., Kellici, S. and Saha, B. (2014) Green process engineering as the key to future processes, *Processes*, 2, 311–332.

Peng, J. J. and Deng, Y. Q. (2001) Cycloaddition of carbon dioxide to propylene oxide catalyzed by ionic liquids, *New Journal of Chemistry*, 25 (4), 639–641.

Perera, S. D., Mariano, R. G., Vu, K., Nour, N., Seitz, O., Chabal, Y. and Balkus, K. J. (2012) Hydrothermal synthesis of graphene-TiO<sub>2</sub> nanotube composites with enhanced photocatalytic activity, *ACS Catalysis*, 2 (6), 949–956.

Pescarmona, P. P. and Taherimehr, M. (2012) Challenges in the catalytic synthesis of cyclic and polymeric carbonates from epoxides and CO<sub>2</sub>. *Catalysis Science and Technology*, 2, 2169–2187.

Pirmohamed, T., Dowding, J. M., Singh, S., Wasserman, B., Heckert, E., Karakoti, A. S., King, J. E. S., Seal, S. and Self, W. T. (2010) Nanoceria exhibit redox state-dependent catalase mimetic activity, *Chemical Communications*, 46 (16), 2736–2738.

Preisler, E. J., Marsh, O. J., Beach, R. A. and McGill, T. C. (2001) Stability of cerium oxide on silicon studied by X-ray photoelectron spectroscopy, *Journal of Vacuum Science and Technology: B*, 19 (4), 1611–1618.

Pyrlik, A., Hoelderich, W. F., Muller, K., Arlt, W., Strautmann, J. and Kruse, D. (2012) Dimethyl carbonate via transesterification of propylene carbonate with methanol over ion exchange resins, *Applied Catalysis B: Environmental*, 125, 486–491.

Ramin, M., Jutz, F., Grunwaldt, J. D. and Baiker, A. (2005) Solventless synthesis of propylene carbonate catalysed by chromium-salen complexes: Bridging homogeneous and heterogeneous catalysis, *Journal of Molecular Catalysis A: Chemical*, 242 (1–2), 32–39.

Ramin, M., van Vegten, N., Grunwaldt, J. D. and Baiker, A. (2006) Simple preparation routes towards novel Zn-based catalysts for the solventless synthesis of propylene carbonate using dense carbon dioxide, *Journal of Molecular Catalysis A: Chemical*, 258 (1–2), 165–171.

Rao, C. N. R., Sood, A. K., Subrahmanyam, K. S. and Govindaraj, A. (2009) Graphene: The new two-dimensional nanomaterial, *Angewandte Chemie International Edition*, 48 (42), 7752–7777.

Razali, N. A. M., Lee, K. T., Bhatia, S. and Mohamed, A. R. (2012) Heterogeneous catalysts for production of chemicals using carbon dioxide as raw material: A review, *Renewable and Sustainable Energy Reviews*, 16 (7), 4951–4964.

Richter, M., Fait, M. J. G., Eckelt, R., Schneider, M., Radnik, J., Heidemann, D. and Fricke, R. (2007) Gas-phase carbonylation of methanol to dimethyl

carbonate on chloride-free Cu-precipitated zeolite Y at normal pressure, *Journal of Catalysis*, 245 (1), 11–24.

Riduan, S. N., Zhang, Y. and Ying, J. Y. (2009) Conversion of carbon dioxide into methanol with silanes over N-Heterocyclic carbene catalysts, *Angewandte Chemie International Edition*, 48 (18), 3322–3325.

Riduan, S. N. and Zhang, Y. (2010) Recent developments in carbon dioxide utilisation under mild conditions, *Dalton Transactions*, 39 (14), 3347–3357.

Rivetti, F. and Romano, U., (1992) Procedure for the production of alkyl carbonates. European Patent 534545.

Rivetti, F. Anastas, P.T. and Tundo, P. (2000) *Green Chemistry: Challenging Perspective*, Oxford University Press, Oxford, UK.

Rudnick, L. R. (2013) Synthetic, mineral oils and bio-based lubricants, *Chemistry and Technology*, 2<sup>nd</sup> Edition, CRC Press, New York, U.S.

Ryu, J. Y. and Gelbein, A. P. (2002) Process and catalyst for making dialkyl carbonates. U.S. Patent 6392078.

Saada, R., Kellici, K., Heil, T., Morgan, D. and Saha, S. (2015) Greener synthesis of dimethyl carbonate using a novel ceria–zirconia oxide/graphene nanocomposite catalyst, *Applied Catalysis B: Environmental*, 168, 353–362.

Saito, M. (1998) R&D activities in Japan on methanol synthesis from CO<sub>2</sub> and H<sub>2</sub>. *Catalysis Surveys from Japan*, 2 (2), 175–184.

Sakai, T., Tsutsumi, Y. and Ema, T. (2008) Highly active and robust organic-inorganic hybrid catalyst for the synthesis of cyclic carbonates from carbon dioxide and epoxides, *Green Chemistry*, 10 (3), 337–341.

Sakakura, T., Choi, J., Saito, P., Masuda, T., Sako, T. and Oriyama, T. (1999) Metal-catalyzed dimethyl carbonate synthesis from carbon dioxide and acetals, *The Journal of Organic Chemistry*, 64 (12), 4506–4508.

Sakakura, T., Choi, J., Saito, Y. and Sako, T. (2000) Synthesis of dimethyl carbonate from carbon dioxide: catalysis and mechanism, *Polyhedron*, 19 (5), 573–576.

Sakakura, T., Choi, J. and Yasuda, H. (2007) Transformation of carbon dioxide, *Chemical Reviews*, 107 (6), 2365–2387.

Sakakura, T. and Kohno, K. (2009) The synthesis of organic carbonates from carbon dioxide, *Chemical Communications*, (11), 1312–1330.

Saleh, R. Y., Michaelson, R. C., Suci, E. N. and Kuhlmann, B. (1996) Process for manufacturing dialkyl carbonate from urea and alcohol. U.S. Patent 5565603.

Salvatore, R.N., Shin, S.I., Nagle, A. S. and Jung, K. W. (2001) Efficient carbamate synthesis via a three-component coupling of an amine, CO<sub>2</sub> and alkyl halides in the presence of Cs<sub>2</sub>CO<sub>3</sub> and tetrabutylammonium iodide, *The Journal of Organic Chemistry*, 66 (3), 1035–1037.

Samseth, J., (2012). Closing and decommissioning nuclear power reactors. Available at: [http://www.unep.org/yearbook/2012/pdfs/UYB\\_2012\\_CH\\_3.pdf](http://www.unep.org/yearbook/2012/pdfs/UYB_2012_CH_3.pdf) Accessed on 12 August 2015.

Sankar, M., Tarte, N. H. and Manikandan, P. (2004) Effective catalytic system of zinc-substituted polyoxometalate for cycloaddition of CO<sub>2</sub> to epoxides, *Applied Catalysis A: General*, 276 (1–2), 217–222.

Sankar, M., Nair, C. M., Murty, K. V. G. K. and Manikandan, P. (2006) Transesterification of cyclic carbonates with methanol at ambient conditions over tungstate-based solid catalysts, *Applied Catalysis A: General*, 312, 108–114.

Sato, Y., Kagotani, M., Yamamoto, T. and Souma, Y. (1999) Novel effective poly(2,2'-bipyridine-5,5'-diyl)-CuCl<sub>2</sub> catalyst for synthesis of dimethyl carbonate (DMC) by oxidative carbonylation of methanol, *Applied Catalysis A: General*, 185 (2), 219–226.

Sato, Y. and Souma, Y. (2000) Novel type of heterogenized  $\text{CuCl}_2$  catalytic systems for oxidative carbonylation of methanol, *Catalysis Surveys from Japan*, 4 (1), 65–74.

Selva, M., Marques, C. A. and Tundo, P. (1994) Selective mono-methylation of arylacetonitriles and methyl arylacetates by dimethyl carbonate, *Journal of the Chemical Society, Perkin Transactions 1*, (10), 1323–1328.

Selva, M., Bomben, A. and Tundo, P. (1997) Selective mono-N-methylation of primary aromatic amines by dimethylcarbonate over faujasite X- and Y-type zeolites, *Journal of the Chemical Society, Perkin Transactions 1*, (7), 1041–1046.

Shaikh, A. and Sivaram, S. (1996) Organic carbonates, *Chemical Reviews*, 96 (3), 951–976.

Shen, Y. M., Duan, W. L. and Shi, M. (2003) Chemical fixation of carbon dioxide catalyzed by binaphthyldiamino Zn, Cu, and Co salen-type complexes, *Journal of Organic Chemistry*, 68 (4), 1559–1562.

Shi, F., Deng, Y. Q., Sima, T. L., Peng, J. J., Gu, Y. L. and Qiao, B. T. (2003) Alternatives to phosgene and carbon monoxide: Synthesis of symmetric urea derivatives with carbon dioxide in ionic liquids, *Angewandte Chemie International Edition*, 42 (28), 3257–3260.

Shieh, W. C., Dell, S. and Repic, O. (2001) 1,8-Diazabicyclo [5.4.0]undec-7-ene (DBU) and microwave-accelerated green chemistry in methylation of phenols, indoles, and benzimidazoles with dimethyl carbonate, *Organic Letters*, 3 (26), 4279–4281.

Shiels, R. A. and Jones, C. W. (2007) Homogeneous and heterogeneous 4-(*N,N*-dialkylamino)pyridines as effective single component catalysts in the synthesis of propylene carbonate, *Journal of Molecular Catalysis A-Chemical*, 261 (2), 160–166.

Shilov, A. E. and Shul'pin, G. B. (1997) Activation of C–H bonds by metal complexes, *Chemical Reviews*, 97 (8), 2879–2932.

Sima, T., Guo, S., Shi, F. and Deng, Y. (2002) The syntheses of carbamates from reactions of primary and secondary aliphatic amines with dimethyl carbonate in ionic liquids, *Tetrahedron Letters*, 43 (45), 8145–8147.

Sneeden, R. P. A. (2011) Carbon dioxide utilisation: Electrochemical conversion of CO<sub>2</sub> – Opportunities and challenges, *Research and Innovation in DNV*, (7) 1–18.

Song, C., Gaffney, A. M., Fujimoto, K. (2002) CO<sub>2</sub> conversion and utilisation, *American Chemical Society ACS Symposium*, Washington, DC,(809) 420–421.

Song, C. (2006) Global challenges and strategies for control, conversion and utilisation of CO<sub>2</sub> for sustainable development involving energy, catalysis, adsorption and chemical processing, *Catalysis Today*, 115 (1–4), 2–32.

Srinivas, D. and Ratnasamy, P. (2007) Spectroscopic and catalytic properties of SBA-15 molecular sieves functionalized with acidic and basic moieties, *Microporous and Mesoporous Materials*, 105 (1–2), 170–180.

Srivastava, R., Srinivas, D. and Ratnasamy, P. (2003) Synthesis of polycarbonate precursors over titanosilicate molecular sieves, *Catalysis Letters*, 91 (1-2), 133–139.

Srivastava, R., Manju, M. D., Srinivas, D. and Ratnasamy, P. (2004) Phosgene-free synthesis of carbamates over zeolite-based catalysts, *Catalysis Letters*, 97 (1-2), 41-47.

Srivastava, R., Srinivas, D. and Ratnasamy, P. (2005a) CO<sub>2</sub> activation and synthesis of cyclic carbonates and alkyl/aryl carbamates over adenine-modified Ti-SBA-15 solid catalysts, *Journal of Catalysis*, 233 (1), 1–15.

Srivastava, R., Bennur, T. H. and Srinivas, D. (2005b) Factors affecting activation and utilisation of carbon dioxide in cyclic carbonates synthesis over Cu and Mn peraza macrocyclic complexes, *Journal of Molecular Catalysis A: Chemical*, 226 (2), 199–205.

Srivastava, R., Srinivas, D. and Ratnasamy, P. (2006a) Syntheses of polycarbonate and polyurethane precursors utilizing CO<sub>2</sub> over highly efficient, solid as-synthesised MCM-41 catalyst, *Tetrahedron Letters*, 47 (25), 4213-4217.

Srivastava, R., Srinivas, D. and Ratnasamy, P. (2006b) Fe-Zn double-metal cyanide complexes as novel, solid transesterification catalysts, *Journal of Catalysis*, 241 (1), 34–44.

Srivastava, R., Srinivas, D. and Ratnasamy, P. (2006c) Sites for CO<sub>2</sub> activation over amine-functionalized mesoporous Ti(Al)-SBA-15 catalysts, *Microporous and Mesoporous Materials*, 90 (1–3), 314–326.

Stephen, D. W. and Erker, G. (2010) Frustrated lewis pairs: Metal-free hydrogen activation and more, *Angewandte Chemie International Edition*, 49 (1), 46–76.

Stoica, G., Abelló, S. and Pérez-Ramírez, J. (2009) Synthesis of dimethyl carbonate by transesterification of ethylene carbonate over activated dawsonites, *ChemSusChem*, 2 (4), 301–304.

Su, J., Cao, M., Ren, L. and Hu, C. (2011) Fe<sub>3</sub>O<sub>4</sub>-graphene nanocomposites with improved lithium storage and magnetism properties, *Journal of Physical Chemistry C*, 115 (30), 14469–14477.

Suciu, E. N., Kuhlmann, B., Knudsen, G. A. and Michaelson, R. C. (1998) Investigation of dialkyltin compounds as catalysts for the synthesis of dialkyl carbonates from alkyl carbamates, *Journal of Organometallic Chemistry*, 556 (1–2), 41–54.

Sun, J., Fujita, S., Bhanage, B. and Arai, M. (2004a) One-pot synthesis of styrene carbonate from styrene in tetrabutylammonium bromide, *Catalysis Today*, 93–5 383–388.

Sun, J. M., Fujita, S., Zhao, F. Y. and Arai, M. (2004b) Synthesis of styrene carbonate from styrene oxide and carbon dioxide in the presence of zinc bromide and ionic liquid under mild conditions, *Green Chemistry*, 6 (12), 613–616.

Sun, J. J., Yang, B. L. and Lin, H. Y. (2004c) A semi-continuous process for the synthesis of methyl carbamate from urea and methanol, *Chemical Engineering and Technology*, 27 (4), 435–439.

Sun, J., Fujita, S., Zhao, F. and Arai, M. (2005) A highly efficient catalyst system of  $ZnBr_2/n-Bu_4NI$  for the synthesis of styrene carbonate from styrene oxide and supercritical carbon dioxide, *Applied Catalysis A: General*, 287 (2), 221–226.

Sun, J., Wang, L., Zhang, S. J., Li, Z. X., Zhang, X. P., Dai, W. B. and Mori, R. H. (2006)  $ZnCl_2$ /phosphonium halide: An efficient Lewis acid/base catalyst for the synthesis of cyclic carbonate, *Journal of Molecular Catalysis A: Chemical*, 256 (1–2), 295–300.

Sun, J., Zhang, S. J., Cheng, W. G. and Ren, J. Y. (2008) Hydroxyl-functionalized ionic liquid: a novel efficient catalyst for chemical fixation of  $CO_2$  to cyclic carbonate, *Tetrahedron Letters*, 49 (22), 3588–3591.

Sun, J., Ren, J. Y., Zhang, S. J. and Cheng, W. G. (2009) Water as an efficient medium for the synthesis of cyclic carbonate, *Tetrahedron Letters*, 50 (4), 423–426.

Sweileh, B. A., Al-Hiari, Y. M., Kialani, M. H. and Mohammad, H. A. (2010) Synthesis and characterisation of polycarbonates by melt phase interchange reactions of alkylene and arylene diacetates with alkylene and arylene diphenyl dicarbonates, *Molecules*, (15), 3661–3682.

Takahashi, T., Watahiki, T., Kitazume, S., Yasuda, H. and Sakakura, T. (2006) Synergistic hybrid catalyst for cyclic carbonate synthesis: Remarkable acceleration caused by immobilization of homogeneous catalyst on silica, *Chemical Communications*, (15), 1664–1666.

Takaya J., Sasano, K. and Iwasawa, N. (2011) Efficient one-to-one coupling of easily available 1,3-Dienes with carbon dioxide, *Organic Letters*, 13 (7), 1698–1701.

Tahmouzi, S. (2014) Optimization of polysaccharides from zagros oak leaf using RSM: Antioxidant and antimicrobial activities, *Carbohydrate Polymers*, 106, 238–246.

Tan, Z. A., Li, S. S., Wang, F. Z., Qian, D. P., Lin, J., Hou, J. H. and Li, Y. F. (2014) High performance polymer solar cells with as-prepared zirconium acetylacetonate film as cathode buffer layer, *Scientific Reports*, 4, 4691–4691.

Tasaki, K., Goldberg, A., Lian, J. J., Walker, M., Timmons, A. and Harris, S. J. (2009) Solubility of lithium salts formed on the lithium-ion battery negative electrode surface in organic solvents, *Journal of The Electrical Society*, 156, (12), A1019–A1027.

Timofeeva, M. N., Ayupov, A. B., Volodin, A. M., Pak, Y. R., Volkova, G. G. and Echevskii, G. V. (2005) Surface acid sites of  $H_3PW_{12}O_{40}$  as studied by the adsorption of stable nitroxyl radicals, *Kinetics and Catalysis*, 46 (1), 123–127.

Tominaga, K., Sasaki, Y., Kawai, M., Watanabe, T. and Saito, M. (1993) Ruthenium complex catalysed hydrogenation of carbon dioxide to carbon monoxide, methanol and methane, *Journal of the Chemical Society-Chemical Communications*, (7), 629–631.

Tomishige, K., Sakai, T., Sakai, S. and Fujimoto, K. (1999) Dimethyl carbonate synthesis by oxidative carbonylation on activated carbon supported  $CuCl_2$  catalysts: catalytic properties and structural change, *Applied Catalysis A: General*, 181 (1), 95–102.

Tomishige, K., Ikeda, Y., Sakaihorii, T. and Fujimoto, K. (2000) Catalytic properties and structure of zirconia catalysts for direct synthesis of dimethyl carbonate from methanol and carbon dioxide, *Journal of Catalysis*, 192 (2), 355–362.

Tomishige, K., Furusawa, Y., Ikeda, Y., Asadullah, M. and Fujimoto, K. (2001) CeO<sub>2</sub>-ZrO<sub>2</sub> solid solution catalyst for selective synthesis of dimethyl carbonate from methanol and carbon dioxide, *Catalysis Letters*, 76 (1–2), 71–74.

Tomishige, K. and Kunimori, K. (2002) Catalytic and direct synthesis of dimethyl carbonate starting from carbon dioxide using CeO<sub>2</sub>-ZrO<sub>2</sub> solid solution heterogeneous catalyst: Effect of H<sub>2</sub>O removal from the reaction system, *Applied Catalysis A: General*, 237 (1–2), 103–109.

Tomishige, K., Yasuda, H., Yoshida, Y., Nurunnabi, M., Li, B. T. and Kunimori, K. (2004) Catalytic performance and properties of ceria based catalysts for cyclic carbonate synthesis from glycol and carbon dioxide, *Green Chemistry*, 6 (4), 206–214.

Tu, M. and Davis, R. J. (2001) Cycloaddition of CO<sub>2</sub> to epoxides over solid base catalysts, *Journal of Catalysis*, 199 (1), 85–91.

Tundo, P. (1991) *Continuous Flow Methods in Organic Synthesis*, Ellis Horwood, Chichester, UK.

Tundo, P. and Esposito, V. (2008) *Green Chemical Reactions*, Springer, Dordrecht, The Netherlands.

Udayakumar, S., Park, S. W., Park, D. W. and Choi, B. S. (2008) Immobilization of ionic liquid on hybrid MCM-41 system for the chemical fixation of carbon dioxide on cyclic carbonate, *Catalysis Communications*, 9 (7), 1563–1570.

Ulusoy, M., Kilic, A., Durgun, M., Tasci, Z. and Cetinkaya, B. (2011) Silicon containing new salicylaldehyde Pd(II) and Co(II) metal complexes as efficient

catalysts in transformation of carbon dioxide (CO<sub>2</sub>) to cyclic carbonates, *Journal of Organometallic Chemistry*, 696 (7), 1372–1379.

Unnikrishnan, P. and Srinivas, D. (2012) Calcined, rare earth modified hydrotalcite as a solid, reusable catalyst for dimethyl carbonate synthesis, *Industrial and Engineering Chemistry Research*, 51 (18), 6356–6363.

Ushikoshi, K., Mori, K., Watanabe, T., Takeuchi, M. and Saito, M. (1998) A 50 kg/day class test plant for methanol synthesis from CO<sub>2</sub> and H<sub>2</sub>, *Studies in Surface Science and Catalysis*, 114, 357–362.

Wang, M., Zhao, N., Wei, W. and Sun, Y. (2004) Synthesis of dimethyl carbonate from urea and methanol over metal oxides, *Studies in Surface Science and Catalysis*, 153, 197–200.

Wang, H., Wang, M. H. Liu, S. G., Zhao, N., Wei, W. and Sun, Y. H. (2006a) Influence of preparation methods on the structure and performance of CaO-ZrO<sub>2</sub> catalyst for the synthesis of dimethyl carbonate via transesterification, *Journal of Molecular Catalysis A: Chemical*, 258 (1–2), 308–312.

Wang, J. Q., Kong, D. L., Chen, J. Y., Cai, F. and He, L. N. (2006b) Synthesis of cyclic carbonates from epoxides and carbon dioxide over silica-supported quaternary ammonium salts under supercritical conditions, *Journal of Molecular Catalysis A: Chemical*, 249 (1–2), 143–148.

Wang, H., Wang, M. H., Zhang, W. Y., Zhao, N., Wei, W. and Sun, Y. H. (2006c) Synthesis of dimethyl carbonate from propylene carbonate and methanol using CaO-ZrO<sub>2</sub> solid solutions as highly stable catalysts, *Catalysis Today*, 115 (1–4), 107–110.

Wang, X. J., Xiao, M., Wang, S. J., Lu, Y. X. and Meng, Y. Z. (2007a) Direct synthesis of dimethyl carbonate from carbon dioxide and methanol using supported copper (Ni, V, O) catalyst with photo-assistance, *Journal of Molecular Catalysis A: Chemical*, 278 (1–2), 92–96.

Wang, X. J., Xiao, M., Wang, S. J., Lu, Y. X. and Meng, Y. Z. (2007b) Solventless synthesis of cyclic carbonates from carbon dioxide and epoxides catalyzed by silica-supported ionic liquids under supercritical conditions, *Catalysis Communications*, 8 (2), 167–172.

Wang, H., Lu, B., Wang, X., Zhang, J. and Cai, Q. (2009) Highly selective synthesis of dimethyl carbonate from urea and methanol catalyzed by ionic liquids, *Fuel Processing Technology*, 90 (10), 1198–1201.

Wang, X. Y., Liu, S. Q., Huang, K. L., Feng, Q. J., Ye, D. L., Liu, B., Liu, J. L. and Jin, G. H. (2010) Fixation of CO<sub>2</sub> by electrocatalytic reduction to synthesis of dimethyl carbonate in ionic liquid using effective silver-coated nanoporous copper composites, *Chinese Chemical Letters*, 21 (8), 987–990.

Wang, L., Wang, Y., Liu, S., Lu, L., Ma, X. and Deng, Y. (2011a) Efficient synthesis of dimethyl carbonate via transesterification of ethylene carbonate with methanol over binary zinc-yttrium oxides, *Catalysis Communications*, 16 (1), 45–49.

Wang, J. Q., Sun, J., Shi, C. Y., Cheng, W. G., Zhang, X. P. and Zhang, S. J. (2011b) Synthesis of dimethyl carbonate from CO<sub>2</sub> and ethylene oxide catalyzed by K<sub>2</sub>CO<sub>3</sub>-based binary salts in the presence of H<sub>2</sub>O, *Green Chemistry*, 13 (11), 3213–3217.

Watanabe, Y. and Tatsumi, T. (1998) Hydrotalcite-type materials as catalysts for the synthesis of dimethyl carbonate from ethylene carbonate and methanol, *Microporous and Mesoporous Materials*, 22 (1–3), 399–407.

Wei, T., Wang, M., Wei, W., Sun, Y. and Sun, Y. (2003) Effect of base strength and basicity on catalytic behavior of solid bases for synthesis of dimethyl carbonate from propylene carbonate and methanol, *Fuel Processing Technology*, 83 (1–3), 175–182.

Weng, X., Boldrin, P., Abrahams, I., Skinner, S. J., Kellici, S. and Darr, J. A. (2008) Direct syntheses of La<sub>(n+1)</sub>Ni<sub>(n)</sub>O<sub>(3n+1)</sub> phases (n = 1, 2, 3 and

infinity) from nanosized co-crystallites, *Journal of Solid State Chemistry*, 181 (5), 1123–1132.

Weng, X., Perston, B., Wang, X. Z., Abrahams, I., Lin, T., Yang, S. F., Evans, J. R. G., Morgan, D. J., Carley, A. F. and Bowker, M. (2009) Synthesis and characterization of doped nano-sized ceria-zirconia solid solutions, *Applied Catalysis B: Environmental*, 90 (3–4), 405–415.

Whipple, D. T. Kenis, P. J. A. (2010) Prospects of CO<sub>2</sub> utilisation via direct heterogeneous electrochemical reduction, *Journal of Physical Chemistry Letters*, (1), 3451–3458.

Wigley, T. M. L. (1998) The Kyoto Protocol: CO<sub>2</sub>, CH<sub>4</sub> and climate implications, *Geophysical Research Letters*, 25 (13), 2285–2288.

Williams, G., Seger, B. and Kamat, P. V. (2008) TiO<sub>2</sub>-graphene nanocomposites: UV-assisted photocatalytic reduction of graphene Oxide, *ACS Nano*, 2 (7), 1487–1491.

Williams, D. B. G., Sibiya, M. S., van Heerden, P. S., Kirk, M. and Harris, R. (2009) Verkade super base-catalysed transesterification of propylene carbonate with methanol to co-produce dimethyl carbonate and propylene glycol, *Journal of Molecular Catalysis A: Chemical*, 304, 147–152.

Wong, W. L., Cheung, K. C., Chan, P. H., Zhou, Z. Y., Lee, K. H. and Wong, K. Y. (2007) A tricarbonyl rhenium(I) complex with a pendant pyrrolidinium moiety as a robust and recyclable catalyst for chemical fixation of carbon dioxide in ionic liquid, *Chemical Communications*, (21), 2175–2177.

Wu, X. L., Xiao, M., Meng, Y. Z. and Lu, Y. X. (2005) Direct synthesis of dimethyl carbonate on H<sub>3</sub>PO<sub>4</sub> modified V<sub>2</sub>O<sub>5</sub>, *Journal of Molecular Catalysis A: Chemical*, 238 (1–2), 158–162.

Wu, X. L., Meng, Y. Z., Xiao, M. and Lu, Y. X. (2006) Direct synthesis of dimethyl carbonate (DMC) using Cu-Ni/VSO as catalyst, *Journal of Molecular Catalysis A: Chemical*, 249 (1–2), 93–97.

Wu, S. S., Zhang, X. W., Dai, W. L., Yin, S. F. Li, W. S., Ren, Y. Q. and Au, C. T. (2008) ZnBr<sub>2</sub>-Ph<sub>4</sub>PI as highly efficient catalyst for cyclic carbonates synthesis from terminal epoxides and carbon dioxide, *Applied Catalysis A: General*, 341 (1–2), 106–111.

Xiang, X. F., Guo, L., Wu, X., Ma, X. and Xia, Y. (2012) Urea formation from carbondioxide and ammonia at atmospheric pressure, *Environmental Chemistry Letters*, 10 (3), 295–300.

Xiao, L. F., Li, F. W. and Xia, C. G. (2005) An easily recoverable and efficient natural biopolymer-supported zinc chloride catalyst system for the chemical fixation of carbon dioxide to cyclic carbonate, *Applied Catalysis A: General*, 279 (1–2), 125–129.

Xiao, L. F., Li, F. W., Peng, H. H. and Xia, C. G. (2006) Immobilized ionic liquid/zinc chloride: Heterogeneous catalyst for synthesis of cyclic carbonates from carbon dioxide and epoxides, *Journal of Molecular Catalysis A: Chemical*, 253 (1–2), 265–269.

Xie, S. B. and Bell, A. T. (2000) An *in situ* Raman study of dimethyl carbonate synthesis from carbon dioxide and methanol over zirconia, *Catalysis Letters*, 70 (3–4), 137–143.

Xie, Y., Zhang, Z. F., Jiang, T., He, J. L., Han, B. X., Wu, T. B. and Ding, K. L. (2007) CO<sub>2</sub> cycloaddition reactions catalyzed by an ionic liquid grafted onto a highly cross-linked polymer matrix, *Angewandte Chemie International Edition*, 46 (38), 7255–7258.

Xu, W. H., Ji, S. G., Quan, W. and Yu, J. Q. (2013a) One-Pot Synthesis of Dimethyl Carbonate over Basic Zeolite Catalysts, *Modern Research in Catalysis*, (2), 22–27.

Xu, J., Feng, E. and Song, J. (2013b) Renaissance of aliphatic polycarbonates: New techniques and biomedical applications, *Journal of Applied Polymer Science*, 131 (5), 39822–39823.

Xu, J., Long, K. Z., Chen, T., Xue, B., Li, Y. X. and Cao, Y. (2013c) Mesoporous graphitic carbon nitride as a new base catalyst for the efficient synthesis of dimethyl carbonate by transesterification, *Catalysis Science and Technology*, 3 (12), 3192–3199.

Xu, J., Long, K. Z., Wu, F., Xue, B., Li, Y. X. and Cao, Y. (2014) Efficient synthesis of dimethyl carbonate via transesterification of ethylene carbonate over a new mesoporous ceria catalyst, *Catalysis Science and Technology*, 484, 1–7.

Yagi, O. and Shimizu, S. (1993) Synthesis of pure tetramethylammonium hydroxide solution free from chloride-ion by the electrolysis of hydrogen carbonate, *Chemistry Letters*, (12), 2041–2044.

Yamaguchi, K., Ebitani, K., Yoshida, T., Yoshida, H. and Kaneda, K. (1999) Mg-Al mixed oxides as highly active acid-base catalysts for cycloaddition of carbon dioxide to epoxides, *Journal of the American Chemical Society*, 121 (18), 4526–4527.

Yang, Z. Z., He, L. N., Dou, X. Y. and Chanfreau, S. (2010) Dimethyl carbonate synthesis catalyzed by DABCO-derived basic ionic liquids via transesterification of ethylene carbonate with methanol, *Tetrahedron Letters*, 51 (21), 2931–2934.

Yano, T., Matsui, H., Koike, T., Ishiguro, H., Fujihara, H., Yoshihara, M. and Maeshima, T. (1997) Magnesium oxide-catalysed reaction of carbon dioxide with an epoxide with retention of stereochemistry, *Chemical Communications*, (12), 1129–1130.

Yasuda, H., He, L. and Sakakura, T. (2002) Cyclic carbonate synthesis from supercritical carbon dioxide and epoxide over lanthanide oxychloride, *Journal of Catalysis*, 209 (2), 547–550.

Yasuda, H., He, L. N. and Sakakura, T. (2003) Cyclic carbonate synthesis from carbon dioxide and epoxide catalyzed by samarium oxychloride supported on zirconia, *Studies in surface Science and Catalysis*, 145, 259–262.

Yasuda, H., He, L., Takahashi, T. and Sakakura, T. (2006) Non-halogen catalysts for propylene carbonate synthesis from CO<sub>2</sub> under supercritical conditions, *Applied Catalysis A-General*, 298 177–180.

Yoshida, M., Hara, N. and Okuyama, S. (2000) Catalytic production of urethanes from amines and alkyl halides in supercritical carbon dioxide, *Chemical Communications*, (2), 151–152.

Yoshida, Y., Arai, Y., Kado, S., Kunimori, K. and Tomishige, K. (2006) Direct synthesis of organic carbonates from the reaction of CO<sub>2</sub> with methanol and ethanol over CeO<sub>2</sub> catalysts, *Catalysis Today*, 115 (1–4), 95–101.

Yoshida, J. I., Kim, H. and Nagaki, A. (2009) Electrochemical activation of carbon dioxide for synthesis of dimethyl carbonate in an ionic liquid, *Electrochimica Acta*, 54 (10), 2912–2915.

Yuan, D., Yan, C. H., Lu, B., Wang, H., Zhong, C. and Cai, Q. (2009) Electrochemical activation of carbon dioxide for synthesis of dimethyl carbonate in an ionic liquid, *Electrochimica Acta*, 54 (10), 2912–2915.

Zevenhoven, R., Eloneva, S. and Teir, S. (2006) Chemical fixation of CO<sub>2</sub> in carbonates: Routes to valuable products and long-term storage, *Catalysis Today*, 115 (1–4), 73–79.

Zhang, X., Zhao, N., Wei, W. and Sun, Y. (2006) Chemical fixation of carbon dioxide to propylene carbonate over amine-functionalized silica catalysts, *Catalysis Today*, 115 (1–4), 102–106.

Zhang, L., Niu, D. F., Zhang, K., Zhang, G., Luo, Y. and Lu, J. (2008) Electrochemical activation of CO<sub>2</sub> in ionic liquid (BMIMBF<sub>4</sub>): synthesis of organic carbonates under mild conditions, *Green Chemistry*, (10) 2, 202–206.

Zhang, Z., Brown, S., Goodall, J. B. M., Weng, X., Thompson, K., Gong, K., Kellici, S., Clark, R. J. H., Evans, J. R. G. and Darr, J. A. (2009) Direct continuous hydrothermal synthesis of high surface area nanosized titania, *Journal of Alloys and Compounds*, 476 (1–2), 451–456.

Zhang, Z. F., Liu, Z. W., Lu, J. and Liu, Z. T. (2011) Synthesis of dimethyl carbonate from carbon dioxide and methanol over  $Ce_xZr_{1-x}O_2$  and [EMIM]Br/ $Ce_{0.5}Zr_{0.5}O_2$ , *Industrial and Engineering Chemistry Research*, 50 (4), 1981–1988.

Zhang, Y. G. and Riduan, S.N. (2011) Catalytic hydrocarboxylation of alkenes and alkynes with  $CO_2$ , *Angewandte Chemie International Edition*, 50 (28), 6210–6212.

Zhao, T. S., Han, Y. Z. and Sun, Y. H. (2000) Novel reaction route for dimethyl carbonate synthesis from  $CO_2$  and methanol, *Fuel Processing Technology*, 62 (2–3), 187–194.

Zhao, X., Zhang, Y. and Wang, Y. (2004) Synthesis of propylene carbonate from urea and 1,2-propylene glycol over a zinc acetate catalyst, *Industrial and Engineering Chemistry Research*, 43 (5), 4038–4042.

Zhao, Y., Tian, H. S., Qi, X. H., Han, Z. N., Zhuang, Y. Y. and He, L. N. (2007) Quaternary ammonium salt-functionalized chitosan: An easily recyclable catalyst for efficient synthesis of cyclic carbonates from epoxides and carbon dioxide, *Journal of Molecular Catalysis A: Chemical*, 271 (1–2), 284–289.

Zhong, S. H., Wang, J. W., Xiao, X. F. and Li, H. S. (2000). Dimethyl carbonate synthesis from carbon dioxide and methanol over Ni-Cu/MoSiO(VSiO) catalysts, *Studies in Surface Science and Catalysis*, Elsevier, 130, 1565–1570.

Zhong, K., Lin, W. J., Wang, Q. and Zhou, S. (2012) Extraction and radicals scavenging activity of polysaccharides with microwave extraction from mung bean hulls, *International Journal of Biological Macromolecules*, 51 (4), 612–617.

Zhou, Y. X., Hu, S. Q., Ma, X. M., Liang, S. G., Jiang, T. and Han, B. X. (2008) Synthesis of cyclic carbonates from carbon dioxide and epoxides over betaine-based catalysts, *Journal of Molecular Catalysis A: Chemical*, 284 (1–2), 52–57.

Zhu, H. Chen, L. B. and Jiang, Y. Y. (1996) Synthesis of propylene glycol and dimethyl carbonate using polymer-supported catalysts, *Chinese Chemical Letters*, 7 (6), 519–522.

Zhu, A. L., Jiang, T., Han, B. X., Zhang, J. C., Xie, Y. and Ma X. M. (2007) Supported choline chloride/urea as a heterogeneous catalyst for chemical fixation of carbon dioxide to cyclic carbonates, *Green chemistry*, 9 (2), 169–172.

Zhu, Y., Murali, S., Cai, W. W., Li, X., Suk, J. W., Potts, J. R. and Ruoff, R. S. (2010). Graphene and graphene oxide: synthesis, properties, and applications, *Advanced Materials*, 22 (35), 3906–3924.

# **Chapter 9**

## **Appendix**

## 9. APPENDIX

### 9.1. RESEARCH PUBLICATIONS

#### 9.1.1. Journal Papers

- ❖ **Saada, R.**, Kellici, S., Heil, T., Morgan, D. and Saha, B. (2015) “Greener synthesis of dimethyl carbonate using a novel ceria-zirconiaoxide/graphene nanocomposite catalyst”, *Applied Catalysis B: Environmental*, (168–169), 353–362. (Full paper is attached to the thesis)
  
- ❖ **Saada, R.**, Adeleye, A. I. and Saha, B. (2015) “Synthesis of dimethyl carbonate from carbon dioxide and methanol using heterogeneous catalysts”, *Industrial and Engineering Chemistry Research*, manuscript in preparation.
  
- ❖ **Saada, R.** and Saha, B. (2015) “Synthesis of dimethyl carbonate from propylene carbonate and methanol using heterogeneous catalysis”, *Chemical Engineering Research and Design*, manuscript in preparation.
  
- ❖ **Saada, R.**, Kellici, S., Omar AboElazayem; Heil, T., Morgan, D., and Saha, B. (2015) “Greener and efficient synthesis of dimethyl carbonate using a novel tin-zirconia oxide/graphene nanocomposite catalyst”, *Applied Catalysis B : environmental*, manuscript in preparation.

#### 9.1.2. Conference Papers

- ❖ **Saada, R.**, Kellici, S. and Saha, B. (2015) “Synthesis of dimethyl carbonate from methanol using novel metal oxide/graphene nanocomposite catalysts”, *10<sup>th</sup> European Congress of Chemical Engineering*, Nice, France. Abstract accepted.
  
- ❖ **Saada, R.**, Kellici, S. and Saha, B. (2015) “CO<sub>2</sub> Utilisation using novel Ce–Zr oxide/graphene nanocomposite catalysts”, *ChemEngDayUK*, Sheffield, UK.
  
- ❖ **Saada, R.**, Kellici, S. and Saha, B. (2014) “Utilisation of CO<sub>2</sub> using advanced graphene-based nanocomposite material for greener synthesis of DMC”, *Emerging Separation Technology, IChemE Research Event*, London, UK.

- ❖ **Saada, R.**, Kellici, S. and Saha, B. (2014) “Greener synthesis of DMC from CO<sub>2</sub> using a novel ceria-zirconia/graphene catalyst”, *Fluid Separation, IChemE Research Event, London,UK*.
- ❖ **Saada, R.**, Patel, D., Kellici, S. and Saha, B. (2014) “Greener synthesis of dimethyl carbonate using a novel ceria–zirconia/graphene catalyst”, *ChemEngDayUK, Manchester, UK*.

## 9.2. NEWS AND AWARDS

- ❖ I have been awarded the first prize for “Technical Excellence & Outstanding Presentation” at a research event organised by IChemE held at AstraZeneca, Macclesfield. A copy of the certificate and news are attached to the thesis.
- ❖ A press request from Adam Duckett, editor of tce, IChemE during ChemEngDayUK2015. A copy of the article is attached to the thesis.

## 9.3. RISK ASSESSMENT

A copy of the risk assessment form for DMC synthesis is attached on pages 265–270. A copy of the risk assessment form for catalyst preparation is attached to the thesis.

## 9.4. TRAINING SESSIONS

9.4.1. Postgraduate Certificate in Research Skills Key Skills Development Programme Training

Attended the following courses . The certificates of attendance are attached to the thesis.

- ❖ Key Skills in the Research Environment – 5 November 2012.
- ❖ The Student-Supervisor Relationship – 07 November 2012.
- ❖ Thesis Submission, Viva and Career Management – 25 April 2013.
- ❖ Academic Publication – 26 April 2013.
- ❖ Conference Presentation 2013.
- ❖ Thesis Submission and Viva – 26 June 2013.
- ❖ Intellectual Property – 25 February 2014.

9.4.2. Additional Training Sessions

- ❖ Health and Safety Induction – 8 June 2012.
- ❖ Career Management – 25 April 2013.
- ❖ Development Plan and Portfolio – April 2013.
- ❖ After your research degree-Looking ahead – 30 April 2014.
- ❖ Understanding LinkedIn-Briefing – 6 May 2014.
- ❖ Introduction to the Moodle Virtual Learning Environment – 8 May 2014.
- ❖ LinkedIn Practical Session (Basic) – 14 May 2014.
- ❖ Introduction to QuizSlides/ExamSlides – 21 May 2014.
- ❖ ACHIEVE Workshop (HEA) – 20 March 2015.



# Institution of Chemical Engineers

This certificate is awarded to

**Rim Saada**

Winner of the '*What's New in Fluid Separations? 2014*' event on

20 June 2014

for her presentation on

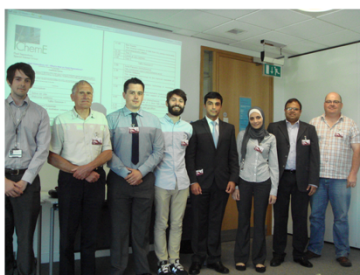
**Greener synthesis of DMC from CO<sub>2</sub> using a novel ceria-zirconia/graphene catalyst**

Signed: IChemE Training and Events Co-ordinator

**IChemE** ADVANCING  
CHEMICAL  
ENGINEERING  
WORLDWIDE

## PhD Chemical Engineering student scoops top prize

17 July 2014



### LSBU PhD Chemical Engineering student scoops top prize for outstanding work and technical excellence at prestigious IChemE research event

An LSBU third year PhD student has been awarded first prize for her technical excellence and outstanding presentation in the field of Fluid Separation Processes at an event organised by the Institution of Chemical Engineers (IChemE).

Rim Saada, who is currently in the third year of her PhD in Chemical Engineering under the supervision of Professor Basu Saha in the Centre for Green Process Engineering at the Applied Science Department, received the award at the annual research event entitled "What's New in Fluid Separations" organised by the IChemE Fluid Separations Special Interest Group (FSSIG) at AstraZeneca, Macclesfield.

The topic of Rim's presentation was entitled: **Greener synthesis of DMC from CO<sub>2</sub> using a novel ceria-zirconia/graphene catalyst.**

Carbon dioxide (CO<sub>2</sub>) is the most important anthropogenic greenhouse gas and therefore it is considered as the main contributor for global warming. However, CO<sub>2</sub> is recognised as an abundant, cheap, recyclable and non-toxic carbon source and thus its utilisation for the production of value added chemicals is extremely beneficial for the chemical industry.

Dimethyl carbonate (DMC) is a non-toxic, biodegradable and valuable chemical of great commercial interest. DMC has versatile chemical properties that make it a good precursor material for the production of polycarbonates and a potential gasoline additive due to its high oxygen content. Her research focused on the direct synthesis of dimethyl carbonate from methanol and carbon dioxide using a novel ceria-zirconia/graphene as a catalyst.

Bev Julien, Pro Vice chancellor at LSBU, said: "Coming from AstraZeneca myself, I am well aware of the standards which they look for and expect - recognition from this peer group and IChemE is a real tribute to Rim's ability and the quality of the work which she is doing."

The event brought together individuals and organisations from across the country to discover the exciting and diverse separation processes research currently underway in the UK. Ten young researchers (Post-docs, PhD students and industrial researchers) from the UK Universities and industry presented their research, including Rim. A panel of judges, from both industry and academia, evaluated the presentations and gave feedback at the end of the event.

The best contributions received prizes, from a total prize allocation of £1000. Rim received £400 as the overall winner of the event.

Find out more about [Engineering, Science and the Built Environment](#) at LSBU.

[ShareThis](#) 227 [Share](#) 51 [Tweet](#) 11 [Email](#) 0



Top of page

### Latest news

[View all news...](#)

[Survey proves more graduates in work](#)  
27 August 2015

[Clearing: significant gender gap in expectations](#)  
11 August 2015

[LSBU wins green technology grant of €150,000 to research cargo air fire suppression techniques](#)  
5 August 2015

[LSBU nominated for...](#)

### Upcoming events

[View all events...](#)

**2** September 2015  
[Clearing Drop-In Session](#)

**5** September 2015  
[International Conference on Health, Healthcare and Eco-civilisation](#)

# An academic exercise

**Adam Duckett** talks to up-and-coming researchers about their impression of ChemEngDayUK and the positive impact experts say they can make

**E**xplain how your research makes a difference' was the challenge thrust upon the 350 delegates attending this year's ChemEngDayUK, hosted by the University of Sheffield in early April.

The event, now in its third year, sees chemical engineering academics - dominated by postgrads - and educators from across the UK meet to share their research through poster presentations and lectures.

"I ask you to stand up, speak out, and tell the world why you are making a difference - because each one of you is," said IChemE president Geoff Maitland in his opening address.

It's election season in the UK right now, so many readers would be forgiven for feeling fatigued by what sounds like another trite call

to arms. But this was not just another hollow message: delegates were invited to describe the difference they are making in a single short message and pose for a Polaroid-style photo that was then pinned to a board among the 200 poster presentations.

Standing there scanning all the photos, you get a true appreciation of the breadth of the problems that our discipline's researchers are trying to overcome, the scene lending real weight to Maitland's message that they are "the future of chemical engineering, bringing the new ideas and the new processes and concepts to practical implementation."

This view was repeated by expert speakers at the event who said that those embarking on their early research careers have an array of world-scale issues to address (see *Make a big difference*).

## relaxed researchers

What is striking is how different the conference felt to the other chemical engineering conferences I've attended.

UCL's deputy head of education Eva Sorensen, summed it up like this: "The ChemEngDayUK conference is an ideal first conference for a fresh PhD student.

The relaxed atmosphere during the poster

sessions takes the pressure out of presenting research work for the first time, and provides an excellent opportunity for networking with academics and students at other UK institutions. The step to an oral presentation at an international conference is therefore much smaller and far less intimidating."

The students I spoke to admitted feeling a little anxious at putting their research on view for experts to wander by and critique.

Tatiana Grebennikova, a first-year PhD student at the University of Manchester, said: "To be honest, I was a little bit worried in the morning before my presentation. You know, everyone wants to be a good presenter but it's usually hard to predict the reaction to your research. However after my first conversation I understood that actually my poster was quite interesting to others and I felt a relief; after that I presented with confidence."

University of Sheffield's Chris Porter, who is completing the final year of his PhD, agrees: "It can be nerve-racking but generally I'm quite enthused about discussing my work with other people."

## an outside perspective

Rim Saada, a final-year PhD student at London South Bank University who attended

**"I ask you to stand up, speak out, and tell the world why you are making a difference - because each one of you is,"**  
**Geoff Maitland,**  
**IChemE president**



## Make a big difference

"We face huge challenges that need to be addressed over decades not just a few years," said Geoff Maitland in his opening address. "The people who are going to commercialise existing research and make the research breakthroughs of the future are in this room today."

Given that they will be reading this article too, tce asked experts speaking at the conference to tell up-and-coming researchers where they can make the biggest difference in their own sectors:

**John McGagh, former head of technology and innovation at Rio Tinto:**

"Water use in the mining sector will continue to increase as populations increase and we build more cities to house them. Water use in the sector is already unsustainable in some areas. Research that finds ways to move from conventional wet ore processing methods to dry processing methods would make a huge difference to the future sustainability and profitability of the sector."

**Chris Tighe, department of chemical engineering, Imperial College London:**

"Society demands products which the chemical industry supplies, but often does not like the way they are made. For example, the viscose process has long been used to make textile fibre and packaging film from wood pulp. Carbon disulphide and caustic soda are employed to render the cellulose soluble; sulphuric acid is added to precipitate it in the desired form. Although these aggressive streams are recycled, there is a lot of exciting research still to be done to invent and scale-up new processes utilising stable ionic liquids and supercritical fluids, or even some hitherto undiscovered solvent."

**Constantijn Sanders, group leader of powder science and encapsulation, Nestle:**

"One billion people do not eat enough, even more are eating too much, while losses along the food chain can be as high as one third of production. Meanwhile, the chemical industry is set to use more plant resources to boost efficiency and reduce CO<sub>2</sub> emissions. These plants come from the same soils as our food. In the interests of sustainable agriculture, we must maintain healthy soils and ensure the efficient use of plants that grow from them. Engineers can help to optimise efficiency by understanding the mass balances of all nutrients and environmental indicators. There is a need to link farmers, food companies and the chemical industry to optimise the use of plants to produce food, fuel and chemicals."

last year's conference in Manchester describes it as an "uplifting" experience. "I benefited a lot last year. I managed to talk to people about my research and get some excellent feedback. They opened my eyes to look at my research from a different perspective. It was great to have someone looking at my research from an outsider point of view."

Many cited the chance to network as a key reason to attend - and for Saada, this already looks to have paved the way for further research opportunities. "I am hoping to arrange some collaboration with an academic I have met to improve my study further at a post-doc level," she adds.

Dimitris Karampalis, a first-year PhD student at the University of Birmingham says the most beneficial aspect of the conference was attending two "very inspirational" lectures.

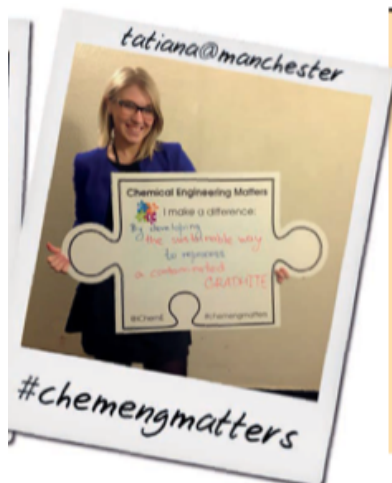
"Ray Allen [chairman of the curriculum committee at University of Sheffield] talked about the history of chemical engineering in the UK and tried to link it with some predictions for the future, while Jeroen van der Veer [former CEO of Shell] described in the simplest way the bond of the industry and academia."

"ChemEngDayUK should be the event in which all chemical engineers in the UK participate," Karampalis adds. "It's an event dedicated to us. I will definitely advise others to attend."

Porter sums it up: "You should never pass up an opportunity to discuss your work with others. There is no telling who you might meet and who will be interested in what you have to say."

If you want to share your research at the next ChemEngDayUK, it's being hosted at the University of Bath from 31 March 2016. [tce](#)

[aduckett@ichema](mailto:aduckett@ichema), [@adam\\_tce](https://twitter.com/adam_tce)



## Maximise your impact at a conference

### 1. Talk to someone new

The biggest mistake you can make at a conference is talking to those you came with. To make an impression, network and make new contacts.

### 2. Ask questions

Ask questions during the conference sessions. Planning a question will focus your listening. Asking a question breaks the ice with the presenter, and you can continue the discussion after the session.

### 3. Try something new

Attend a session that is different or unusual. You may learn something that sows the seeds of a new collaboration.

### 4. Go to the social events

These are as important as the conference itself. They offer the opportunity to talk in a relaxed setting and extend the energy of the conference. Don't be afraid to relax, mingle and let the conversation flow.

### 5. Follow up post conference

You'll have collected lots of business cards and social media contacts. Don't forget to reach out to these people, and thank them for their ideas.

\*adapted from IChemE's ChemEng365 blogpost <http://bit.ly/11HEWpN>

## Risk Assessment

### General Health and Safety Risk Assessment Guidance

Risk Assessment is a process by which the risks of work activities are assessed and controlled. Both the Health and Safety at Work Act and the Management of Health and Safety at Work Regulations require the employer to produce risk assessments.

This document is intended to remove some of the burden of risk assessment by providing a structure for the process. The task of risk assessment may be delegated to a person who possesses the necessary skills to carry it out, however, Heads of Department remain responsible for the findings and implementation of the assessment.

In order to carry out a risk assessment the terms “risk” and “hazard” must be understood. Hazard is the potential to do harm and a risk is the chance of that hazard being realised. In order to prevent foreseeable risks occurring adequate controls must be put in place. The process is as follows;

- Heads of Department must identify the foreseeable hazards posed by work activities, working environment and the materials used.
- Identify who and how many people will be affected. Consider the experience, age, disabilities, medical condition and expertise of those involved.
- The location of the work to be identified and stated.
- Adequate controls must be put into place and implemented under the authority of the Head of Department to prevent or reduce risk to individuals.
- The assessment must be signed and dated by the person responsible for generating the risk and a review date agreed. This safe system of work will need to be monitored to ensure that controls are effective.
- The amount of time put into a risk assessment should be proportional to the degree of risk.

An assessment should be carried out for each task e.g. moving chairs to a different location, using dangerous substances or machinery.

Risk assessments are working documents and should remain available to people to consult in the course of their everyday activities.

### Risk Assessment Form

**Task;** Clearly identify the work covered by the assessment. Include a brief description of the work involved.

Addition reaction of carbon dioxide (CO<sub>2</sub>) to methanol (MeOH) in an autoclave reactor. A sample of dimethyl carbonate (desired product) and any undesired products will be analysed using Gas Chromatography (GC).

**Note:**

- 1) First experiment will be carried out using Lanthana doped zirconia will be used as a catalyst.
- 2) Other catalysts will be used including, ceria lanthana doped zirconia, ceria doped zirconia and zirconium oxide.

Different reaction conditions may be used. Temperature range (25°C-200°C). Pressure Range 5 bar- 120 bar. Reaction time: 2h – 96 h.

The following procedure will be followed:

- 1) Accurately measure the calculated amount of the catalyst and MeOH.
- 2) Transfer the catalyst and MeOH into the reactor vessel.
- 3) Close and tighten the reactor vessel. Ensure that equal pressure is applied to all sides of the reactor lid using a spanner.
- 4) Transfer the reactor vessel into the heating mantle.
- 5) Connect the stirring system and the thermocouple to the reactor.
- 6) Ensure CO<sub>2</sub> cylinder valves are closed. Connect CO<sub>2</sub> cylinder to the reactor vessel.
- 7) Switch on the power supply system.
- 8) Using the reactor controller, set the temperature to the required reaction temperature. Set the stirrer motor at 600 rpm on the reactor controller.
- 9) Allow enough time for the reactor vessel to reach the required temperature i.e. achieved the steady state.
- 10) Check the pressure in the reactor vessel. Add CO<sub>2</sub> to the reactor to the required pressure. Close CO<sub>2</sub> reactor inlet valve and remove the CO<sub>2</sub> connection to the reactor.
- 11) The reaction is left for the required time.

12) Stop the stirring system. Switch off the heating system and the electricity supply.

13) Disconnect stirrer motor. Cool the reactor to room temperature.

14) Open the reactor and filter its contents. Collect the filtrate and take a sample to analyse it using GC. Use isopropyl alcohol as an internal standard.

**Location;** Where the task is to be carried out. Where this includes multiple locations these must also be stated.

E217 ( Experimental work) , M211( GC analysis)

**People involved;** Individual names or if larger group are involved a general description. (e.g. staff, students, visitors, contractors or specific individuals.)

Rim Saada

**Hazards;** A list of all those substances or actions which are hazardous. (e.g. working at computers, laboratory work, electricity, manual handling etc.)

Hazardous chemicals used are: MeOH, CO<sub>2</sub>, DMC, isopropyl alcohol, lanthana doped zirconia, ceria lanthana doped zirconia, ceria doped zirconia and zirconium oxide.

Hazards: Tripping over, chemical spillage, bottles slipping while carrying. Harm by contact with skin/ eyes, through inhalation and if swallowed.

Reaction running overnight. Touching the hot reactor. Temperature increase in the reactor. Pressure build up inside the reactor. Power cut to the reactor or fume cupboard. Reactor Leakage. Mechanical failure of the stirring system.

**MeOH:** R11(Highly flammable) R23/24/25 ( Toxic by inhalation, in contact with skin and if swallowed) R39 ( Toxic: danger of serious irreversible effects through inhalation, in contact with skin and if swallowed) Likelihood: 1 points; Hazard potential 2 points;

Risk :**Low**

**Isopropyl alcohol:** R11(Highly flammable) R36 (Irritating to eyes) R67 (Vapours may cause drowsiness and dizziness) Likelihood: 1 points; Hazard potential 2 points; Risk: **Low**

**CO<sub>2</sub>:** No R-phrases

**DMC:** R11(Highly flammable) Likelihood:1 points; Hazard potential 2 points; Risk: **Low**

**Lanthana doped zirconia:** No R-phrases

**Ceria lanthana doped zirconia:** No R-phrases

**Ceria doped zirconia:** No R-phrases

**Zirconium oxide:** No R-phrases

**Risk Assessment;** An assessment of the likelihood of injury resulting from the hazards.

The student is at risk if the substances come in contact with skin, if inhaled or swallowed. This is avoided by using proper protective equipment while conducting the experiments. Protective equipment used will include: safety goggles (EN166), gloves resistant to solvents (EN374), respiratory protection (ABEK EN 14387), lab coat, separate bin for chlorinated waste and carriers to carry out the chemical bottles to avoid spillage.

The experiments will be conducted in a fume cupboard including weighing the chemicals and washing the equipment.

A 'Hot surface' sign is placed next to the reactor to inform other students that the reactor is hot. The temperature inside the reactor will be checked every 1hr using the thermo couple. Reaction will be stopped if temperature is increased by 25 °C. Pressure inside the reactor will be noted every 1hr and will be monitored. Reaction will be terminated in case of power loss, or mechanical failure to the stirring system.

**Controls Measures;** Put in place to prevent the risk occurring.(e.g. training, supervision, the use of less toxic materials, the use of guards, regular maintenance, providing more space etc.)

All equipment (reactor, cylinder, pump, scales) must be PAT tested. Safety procedure will be followed during the reaction.

Personal Precautions: The addition reaction is being conducted in a fume cupboard. Breathing vapors, gas and mist is avoided by adequate ventilation. Personal protection equipment is used while handling the chemicals. A “Hot surface” sign is placed next to the reactor to inform other students that the reactor should not be touched. Reactor will be cooled using ice, heat resistant gloves will be used to prevent burning. Chemicals will be handled with a safety practice.

Storage Precautions: Chemicals will be stored in a cool place (E217). Containers will be tightly closed in a dry and well ventilated place. Bottles will be kept upright to prevent any leakage. Chemicals will be stored away from sources of ignition and away from oxidising agents/ strong acids and strong bases.

Spillage and Disposal: the chemicals are handled inside the fume cupboard at all time so in case of spillage, the fume cupboard will be closed and the student will leave it to evaporate. Chemicals will not be let down the drain. Separate individual bin for unchlorinated waste inside the fume cupboard will be used. Carriers to carry out the chemical bottles to avoid spillage.

- This risk assessment will be reviewed in May, July and then on request.
- Assistance will be sought from Isaac if unable to do any part of the experiment.
- Also, the student will seek assistance from lab technicians if required.
- The lab work does not require carrying any heavy materials/equipment. The student will ask someone to assist if carrying heavy material is required.

- Minimal quantities on the chemicals are used. The chemicals have been reviewed to reduce toxicity.
- All MSDS are checked carefully. None contain any of the following risk phrases; R45, R46, R47, R49.
- The reactor is safe to operate at high pressures as it is equipped with a safety rupture disc.
- The student will only carry out of Hours experiments if someone else is available
- In case of any dizziness, the student will leave the laboratory and seek assistance.
- The student will contact her supervisor and health and safety officer if there are any concerns regarding safety in the laboratory.
- A risk assessment form for pregnant students have been completed.

**Residual Risk;** This is the risk remaining after the controls above are applied

The likelihood of any incidents occurring is reduced to a minimum by putting in place the listed control measures mentioned earlier and thus the overall risk is reduced.

I, the undersigned state that there is **no significant risk / the risks will be controlled by the methods stated on this form** (delete as appropriate). This assessment will be reviewed in one year, if the work should change or an unforeseen hazard arises.

Name:..... Date;.....

Signed;..... Position;.....

### Risk Assessment Form

**Task;** Clearly identify the work covered by the assessment. Include a brief description of the work involved.

Preparation of Ce–Zr/graphene nanocomposite catalyst by traditional wet impregnation method. Cerium (III) nitrate, hexahydrate ( $\text{Ce}(\text{NO}_3)_3 \cdot 6\text{H}_2\text{O}$ ) and zirconium (IV) oxynitrate hydrate ( $\text{ZrO}(\text{NO}_3)_2 \cdot x\text{H}_2\text{O}$ ) were used as metal precursors.

**Note:**

Step1: Preparation of grapheme oxide (GO).

Step 2: Doping the GO with ceria-zirconia (Ce-Zr)

Preparation of GO:

- 1) Accurately measure 2.5 g of natural graphite powder (NGP) and 2.5 g of sodium nitrate ( $\text{NaNO}_3$ ) and transfer into a conical flask.
- 2) Accurately measure 115 mL of sulphuric acid ( $\text{H}_2\text{SO}_4$ ) and transfer it to the flask.
- 3) Using a magnetic stirrer, allow the mixture to continuously stir for about 15 mins in an ice bath.
- 4) Accurately measure 20 g of potassium permanganate ( $\text{KMnO}_4$ ). Add  $\text{KMnO}_4$  gradually to the mixture and leave for another 15 min with continuous stirring.
- 5) Transfer the resulting mixture to an oil bath at  $40^\circ\text{C}$  and continuous stirring at 600 rpm for 90 min.
- 6) Add 200 mL of deionised water was to the mixture followed by 30 mL of hydrogen peroxide ( $\text{H}_2\text{O}_2$ ).
- 7) Again, add 200 mL of deionised water. Heat the resulting mixture to  $90^\circ\text{C}$  and leave for 15 min.
- 8) Leave the mixture was left to cool down and the separated the product using centrifuge (5000 rpm, 5 min per cycle).
- 9) Wash GO was successively with 10% hydrochloric acid (HCl) and deionised water to remove any impurities. Dry GO was at  $60^\circ\text{C}$  for 24 h before doping it with ceria-zirconia (Ce-Zr).

Doping GO with ceria-zirconia (Ce-Zr):

- 1) Measure GO (1 g) was disperse it in 50 mL of deionised water by ultrasonic vibration for 1 h.
- 2) Remove the mixture from the ultrasonic bath.
- 3) Accurately weigh 0.1882 g of  $\text{Ce}(\text{NO}_3)_3 \cdot 6\text{H}_2\text{O}$  and 0.1 g of  $\text{ZrO}(\text{NO}_3)_2 \cdot x\text{H}_2\text{O}$  and add to the GO suspension while continuously stirring using a magnetic stirrer for 10 min.
- 4) Add 6 mL of 8 M sodium hydroxide (NaOH) solution dropwise to the mixture while maintaining vigorous agitation.
- 5) Heat the mixture at  $80^\circ\text{C}$  using oil bath for 1 h and then cool down to room temperature.
- 6) Separate Ce–Zr/graphene nanocomposite catalyst using centrifuge (5000rpm, 30 min per cycle).
- 7) Wash the prepared catalyst twice with deionised water and dry at  $40^\circ\text{C}$  for 24 h.
- 8) Heat treat the dried Ce–Zr/graphene nanocomposite catalyst at the required temperature (i.e.,  $500^\circ\text{C}$ ,  $700^\circ\text{C}$ ,  $900^\circ\text{C}$ ) using a furnace under nitrogen for 4 hours.
- 9) Cool the catalyst was down for 4 hours before testing it.

**Location;** Where the task is to be carried out. Where this includes multiple locations these must also be stated.

E217

**People involved;** Individual names or if larger group are involved a general description. (e.g. staff, students, visitors, contractors or specific individuals.)

Rim Saada

**Hazards;** A list of all those substances or actions which are hazardous. (e.g. working at computers, laboratory work, electricity, manual handling etc.)

Hazardous chemicals used are: natural graphite powder (NGP), sodium nitrate ( $\text{NaNO}_3$ ), sulphuric acid ( $\text{H}_2\text{SO}_4$ ), potassium permanganate ( $\text{KMnO}_4$ ), hydrogen peroxide ( $\text{H}_2\text{O}_2$ ), hydrochloric acid (HCl), Cerium (III) nitrate, hexahydrate ( $\text{Ce}(\text{NO}_3)_3 \cdot 6\text{H}_2\text{O}$ ), zirconium (IV) oxynitrate hydrate ( $\text{ZrO}(\text{NO}_3)_2 \cdot x\text{H}_2\text{O}$ ), sodium hydroxide (NaOH).

Hazards: Tripping over, chemical spillage, bottles slipping while carrying. Harm by contact with skin/ eyes, through inhalation and if swallowed.

**NGP:** R36/R37 (Irritating to eyes and respiratory system). Likelihood: 1 points; Hazard potential 2 points; Risk :**Low**

**NaNO<sub>3</sub>:** R8 (Contact with combustible material may cause fire), R22 ( Harmful if swallowed), R36/37/38 (Irritating to eyes, respiratory system and skin) ). Likelihood: 1 points; Hazard potential 2 points; Risk :**Low**

**H<sub>2</sub>SO<sub>4</sub>:** R35 (Causes severe burns). Likelihood: 1 points; Hazard potential 2 points; Risk :**Low**

**KMnO<sub>4</sub>:** R8 (Contact with combustible material may cause fire), R22 (Harmful if swallowed),

R50/53 (Very toxic to aquatic organisms, may cause long-term adverse effects in the aquatic

Environment). Likelihood: 1 points; Hazard potential 3 points; Risk :**Low**

**H<sub>2</sub>O<sub>2</sub>:** R22 (Harmful if swallowed), R41 (Risk of serious damage to eyes). Likelihood: 1 points; Hazard potential 2 points; Risk :**Low**

**HCl:** R34 (Causes burns), R37 (Irritating to respiratory system). Likelihood: 1 points; Hazard potential 3 points; Risk :**Low**

**Ce(NO<sub>3</sub>)<sub>3</sub>·6H<sub>2</sub>O:** R8 (Contact with combustible material may cause fire), R36/38 (Irritating to eyes and skin), R52/53 (Harmful to aquatic organisms, may cause long-term adverse effects in the aquatic environment). Likelihood: 1 points; Hazard potential 2 points; Risk :**Low**

**ZrO(NO<sub>3</sub>)<sub>2</sub>·xH<sub>2</sub>O:** R8 ( Contact with combustible material may cause fire), R34 (Causes burns).

Likelihood: 1 points; Hazard potential 2 points; Risk :**Low**

**Risk Assessment;** An assessment of the likelihood of injury resulting from the hazards.

The student is at risk if the substances come in contact with skin, if inhaled or swallowed. This is avoided by using proper protective equipment while conducting the experiments. Protective equipment used will include: safety goggles (EN166), gloves resistant to solvents (EN374), respiratory protection (ABEK EN 14387), lab coat, separate bin for chlorinated waste and carriers to carry out the chemical bottles to avoid spillage.

The experiments will be conducted in a fume cupboard including weighing the chemicals and washing the equipment.

A 'Hot surface' sign is placed next to the reactor to inform other students that the reactor is hot. The temperature inside the reactor will be checked every 1hr using the thermo couple. Reaction will be stopped if temperature is increased by 25 °C. Pressure inside the reactor will be noted every 1hr and will be monitored. Reaction will be terminated in case of power loss, or mechanical failure to the stirring system.

**Controls Measures;** Put in place to prevent the risk occurring.(e.g. training, supervision, the use of less toxic materials, the use of guards, regular maintenance, providing more space etc.)

All equipment must be PAT tested. Safety procedure will be followed during the reaction.

Personal Precautions: The reaction is being conducted in a fume cupboard. Breathing vapors, gas and mist is avoided by adequate ventilation. Personal protection equipment is used while handling the chemicals. Chemicals will be handled with a safety practice.

Storage Precautions: Chemicals will be stored in a cool place (E217). Containers will be tightly closed in a dry and well ventilated place. Bottles will be kept upright to prevent any leakage. Chemicals will be stored away from

sources of ignition and away from oxidising agents/ strong acids and strong bases.

Spillage and Disposal: the chemicals are handled inside the fume cupboard at all time so in case of spillage, the fume cupboard will be closed and the student will leave it to evaporate. Chemicals will not be let down the drain. Separate individual bin for unchlorinated waste inside the fume cupboard will be used. Carriers to carry out the chemical bottles to avoid spillage.

**Residual Risk;** This is the risk remaining after the controls above are applied

The likelihood of any incidents occurring is reduced to a minimum by putting in place the listed control measures mentioned earlier and thus the overall risk is reduced.

I, the undersigned state that there is **no significant risk / the risks will be controlled by the methods stated on this form** (delete as appropriate). This assessment will be reviewed in one year, if the work should change or an unforeseen hazard arises.

Name:..... Date;.....

Signed;..... Position;.....

**London South Bank**  
University

PG Certificate in Research Skills

Postgraduate Training Session

## **CERTIFICATE OF ATTENDANCE**

THIS IS TO CERTIFY THAT

**RIM SAADA**

ATTENDED A COURSE OF INSTRUCTION

**Key Skills in the Research Environment**

ON 5 NOVEMBER 2012



PROFESSOR PETER DOYLE  
PG CERTIFICATE COORDINATOR  
LONDON SOUTH BANK UNIVERSITY

**London South Bank**  
University

PG Certificate in Research Skills

Postgraduate Training Session

## **CERTIFICATE OF ATTENDANCE**

THIS IS TO CERTIFY THAT

**RIM SAADA**

ATTENDED A COURSE OF INSTRUCTION

**The Student–Supervisor Relationship**

ON 7 NOVEMBER 2012



PROFESSOR PETER DOYLE  
PG CERTIFICATE COORDINATOR  
LONDON SOUTH BANK UNIVERSITY

**London South Bank**  
University

Postgraduate Certificate in Research Skills  
Key Skills Development Programme Training Session

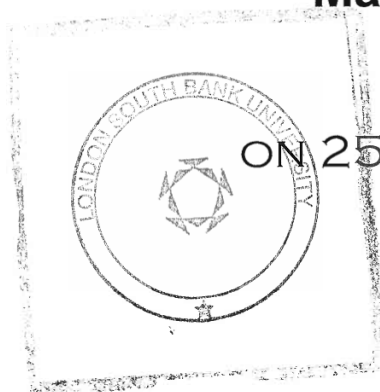
## **CERTIFICATE OF ATTENDANCE**

THIS IS TO CERTIFY THAT

**RIM SAADA**

ATTENDED A COURSE OF INSTRUCTION

**Thesis Submission, Viva and Career  
Management**



ON 25 APRIL 2013

PROFESSOR PETER DOYLE  
POSTGRADUATE SKILLS COORDINATOR  
LONDON SOUTH BANK UNIVERSITY

**London South Bank**  
University

Postgraduate Certificate in Research Skills  
Key Skills Development Programme Training Session

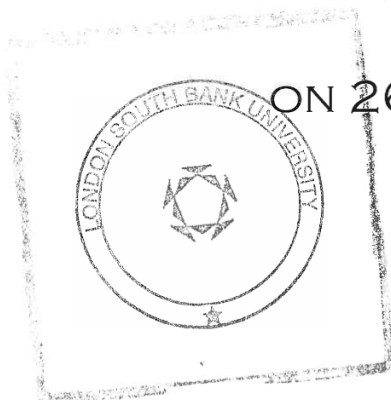
## **CERTIFICATE OF ATTENDANCE**

THIS IS TO CERTIFY THAT

**RIM SAADA**

ATTENDED A COURSE OF INSTRUCTION

### **Academic Publication**



ON 26 APRIL 2013

PROFESSOR PETER DOYLE  
POSTGRADUATE SKILLS COORDINATOR  
LONDON SOUTH BANK UNIVERSITY

**London South Bank**  
University

Postgraduate Certificate in Research Skills  
Key Skills Development Programme Training Session

## **CERTIFICATE OF ATTENDANCE**

THIS IS TO CERTIFY THAT

**RIM SAADA**

ATTENDED A COURSE OF INSTRUCTION

### **Conference Presentation**



ON 24 JUNE 2013

PROFESSOR PETER DOYLE  
POSTGRADUATE SKILLS COORDINATOR  
LONDON SOUTH BANK UNIVERSITY

**London South Bank**  
University

Postgraduate Certificate in Research Skills  
Key Skills Development Programme Training Session

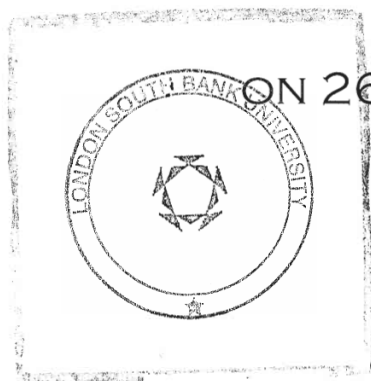
## **CERTIFICATE OF ATTENDANCE**

THIS IS TO CERTIFY THAT

**RIM SAADA**

ATTENDED A COURSE OF INSTRUCTION

**Thesis Submission and Viva**



ON 26 JUNE 2013

PROFESSOR PETER DOYLE  
POSTGRADUATE SKILLS COORDINATOR  
LONDON SOUTH BANK UNIVERSITY

**London South Bank  
University**

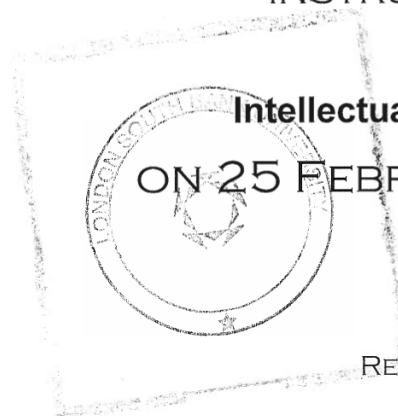
RESEARCHER DEVELOPMENT

## **CERTIFICATE OF ATTENDANCE**

THIS IS TO CERTIFY THAT

**Rim SAADA**

ATTENDED A COURSE OF  
INSTRUCTION



**Intellectual Property**  
ON 25 FEBRUARY 2014

CHUNG LAM  
RESEARCH SUPPORT OFFICER